

# Redox regulation of the tumor suppressor p53

Tao Shi  
石涛

ISBN: 978-90-393-7417-7

DOI: 10.33540/966

© Tao Shi, Utrecht, 2021

All rights are reserved. No part of this thesis may be reproduced or transmitted in any form or by means without the prior permission of the author. The copy right of articles that have been published has been transferred the respective journals.

Cover design and thesis layout by: Tao Shi

Print by: Ridderprint, [www.ridderprint.nl](http://www.ridderprint.nl)

# **Redox regulation of the tumor suppressor p53**

## **Redox-regulatie van de tumor suppressor p53**

(met een samenvatting in het Nederlands)

### **Proefschrift**

ter verkrijging van de graad van doctor aan de  
Universiteit Utrecht  
op gezag van de  
rector magnificus, prof.dr. H.R.B.M. Kummeling,  
ingevolge het besluit van het college voor promoties  
in het openbaar te verdedigen op

maandag 6 december 2021 des ochtends te 10.15 uur

door

**Tao Shi**

geboren op 22 april 1992  
te Gansu, China

**Promotor:**

Prof. dr. ir. B.M.T. Burgering

**Copromotor:**

Dr. T.B. Dansen

The research in this thesis was financially supported by Chinese Scholarship Council (CSC) to Tao Shi; Dutch Cancer Society research grant (KWF UU 2014-6902) to T.B. Dansen. B.M.T. Burgering is part of the Oncode Institute.

# Table of contents

<b>Chapter 1</b>	
General introduction	7
<b>Chapter 2</b>	
ROS induced p53 activation: DNA damage, redox signaling or both?	33
<b>Chapter 3</b>	
DNA damage and oxidant stress activate p53 through differential upstream signaling pathways	69
<b>Chapter 4</b>	
p53 forms redox-dependent protein-protein interactions through cysteine 277	103
<b>Chapter 5</b>	
Evaluation and optimization of two thiol-labeling approaches	137
<b>Chapter 6</b>	
Monitoring the activity of multiple transcription factors simultaneously through fluorescence-based transcriptional reporters	157
<b>Chapter 7</b>	
Summarizing discussion	175
<b>Appendices</b>	185
Nederlandse Samenvatting	
Acknowledgement	
Publications	
<i>Curriculum Vitae</i>	



# ***Chapter 1***

## **General introduction**

Signal transduction is the process by which an (extracellular) chemical or physical signal is transmitted to evoke an appropriate cellular response. This process involves a signal-specific cascade of molecular events, most notably post-translational modification by for instance kinases. In this way each signal leads to activation of specific transcriptional programs resulting in cell growth, differentiation and programmed cell death. Proper signal transduction is the basis for normal cell growth and function. Dysregulated signal transduction can lead to disease onset, including cancer. One could argue that every Hallmark of Cancer as proposed by Hanahan & Weinberg [1] can be explained as the result of altered signal transduction. For example, the hallmark "sustained proliferative signaling" can be the result of mutations in the epidermal growth factor receptor (EGFR) signaling pathway. Indeed, gene duplications or activating mutations in the coding or regulatory regions can be found in cancer cells in the EGFR gene itself and various genes whose products act downstream of the EGFR signaling like Ras, MEK, ERK and c-Myc. Mutations in genes that contribute to tumor initiation and growth are called oncogenes [1, 2]. On the other hand, tumor suppressor genes inhibit cell proliferation and growth or activate cell death. Activation of tumor suppressor-dependent signaling pathways occurs in response to various signals including oncogenic transformation and is essential to prevent oncogenic transformation. Inactivation of tumor suppressors, such as impairment of regulatory signaling pathways, loss-of-function (LOF) mutations or complete loss of the tumor suppressor gene, contributes to cancer development and is also required for cancer progression. For cancer to fully develop both activation of an oncogene as well as loss of multiple tumor suppressors is thought to be required. Taken together, signal transduction regulates the activity of both oncogenes and tumor suppressors. It is therefore crucial to understand the molecular mechanisms involved in signal transduction to be able to better detect and treat cancer onset and development.

## **The p53 tumor suppressor**

### **p53 overview**

The p53 protein, encoded by the TP53 gene, was originally identified as an oncogenic protein based on several observations. Firstly, p53 was discovered to interact with the large T antigen, a product from the simian virus 40 (SV40) oncogene, in transformed cells. Secondly, overexpression of a p53 encoding construct promoted cell growth, but later on the construct was turned out to encode mutant p53 isolated from a tumor cell line (reviewed in [3]). Subsequent experiments with overexpression of wild-type p53 prevented cellular transformation, provide the first evidence that the p53 protein functions as a tumor suppressor [4, 5]. The tumor suppressive function of p53 has been attributed to its roles in DNA damage repair, cell cycle arrest, senescence and apoptosis, which collectively prevent that mutations are passed on to daughter cells and thereby lower the risk of oncogenic transformation. p53 also plays important roles in maintaining redox homeostasis (e.g., upregulation of antioxidant genes) and metabolic adaptation (e.g., activation in response to nutrient depletion), which are essential for supporting cell survival. These functions may protect normal cells from da-



mage and thereby also lower the risk of oncogenic transformation. However, maintenance of the redox balance and flexibility in metabolite choice also is beneficial for tumor cells and evidence accumulates that these p53 functions may in some cases actually contribute to cancer cell survival [6, 7]. So historically p53 went from an oncogene to a tumor suppressor to a bit of both, depending on the context.

The p53 tumor suppressive function is lost in most cancers due to four principal mechanisms: complete loss of p53 expression, inactivating or oncogenic mutations in the TP53 gene, impaired signaling upstream of p53 or loss or mutation of p53 target genes. When p53 is still expressed in cancer, it might be possible to reactivate it, for instance by restoring or boosting upstream signaling or using chemicals aimed at refolding mutant p53. Several anti-cancer therapies relying on p53 reactivation have been investigated and show promising treatment efficacy but also have limitations, like drug resistance or selective pressure to lose p53 altogether [8]. Most of these therapies are based on stimulation of activating or blockage of inhibitory signal transduction pathways upstream of p53 (see below). These include for instance DNA damaging agents or irradiation or inhibitors of p53 degradation like the Nutlins. In this thesis we focus on the regulation of p53 by redox signaling: an upcoming and exciting form of signal transduction mediated by the reversible oxidation of cysteines. A deeper understanding of this relatively recently discovered regulatory network could potentially yield ideas for the development of novel anti-cancer therapies aimed at reactivation of p53.

## p53 regulation

Under basal conditions the p53 protein is kept at a low level through the continuous MDM2-mediated ubiquitinylation and subsequent proteasomal break-down [9, 10]. Signaling upstream of p53 triggered by diverse stresses lead to a suite of post-translational modifications (PTMs) that prevent binding and ubiquitinylation by MDM2, leading to the rapid stabilization and activation of the p53 protein (**Fig. 1**). For example, DNA damage response kinases ATM and ATR-induced p53 phosphorylation on multiple serines (e.g., S15 and 37), play an important role in p53 activation in response to DNA damage [11, 12]. The stress-activated protein kinases (SAPK) JNK and p38MAPK-mediated phosphorylation on for instance S15 is important for p53 activation by ROS but also DNA damage [13, 14]. Additionally, AMP-activated protein kinase (AMPK)-dependent phosphorylation (e.g., also on S15) is essential for p53 activation upon nutrient depletion [15]. p53 induces differential transcriptional programs depending on the cellular context (Stimuli, PTMs, cell type, etc.) and subsequent biological outcomes to tackle specific stresses. For example, p21-dependent transient cell cycle arrest buys time for cells to repair damaged DNA before they re-enter the cell cycle [16, 17]. Alternatively, p21 can mediate a permanent cell cycle arrest (senescence) or PUMA/NOXA induces apoptosis upon irreparable DNA damage to prevent cells pass on DNA mutations down the lineage and hence prevent tumor formation [18-20]. p21-induced cell cycle arrest also helps cell survival upon nutrition depletion by reducing nutrient consumption [6]. Upregulation of antioxidant genes like Glutathione peroxidase (*GPX1*) and Glutaredoxin 3 (*GRX3*) are

involved in ROS clearance and support cell survival [21, 22]. On the other hand, activation of the pro-oxidant genes PIG3 and PIG6 induce ROS-dependent cell death [23, 24].

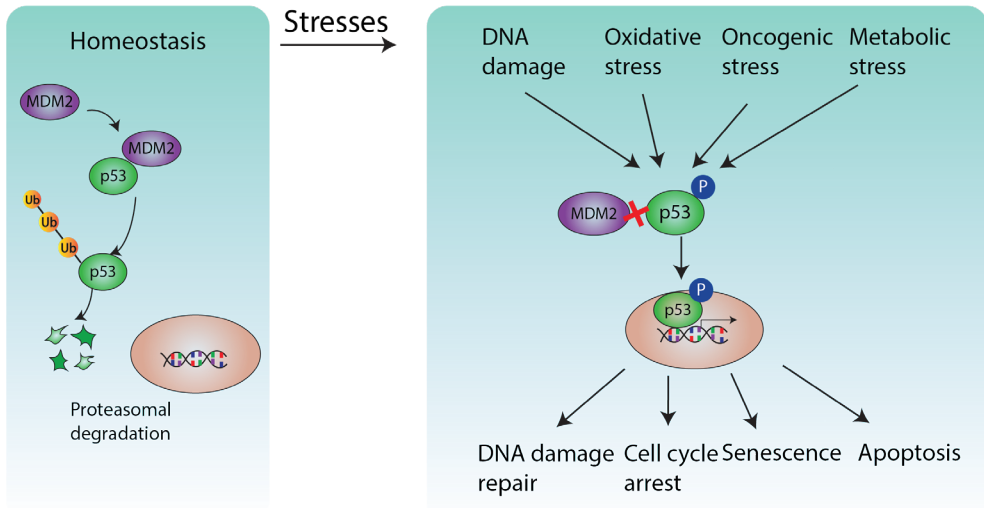


**Figure 1. Scheme of p53 regulation.**

Under normal conditions, p53 is continuously ubiquitinated by MDM2 and subsequently degraded by the proteasome. Upon cellular stresses, like DNA damage and oxidative stress, p53 undergoes different types of post-translational modifications (PTMs), for instance phosphorylation at multiple serine sites. These phosphorylation events prevent the binding and ubiquitination by MDM2, resulting in p53 stabilization and activation. By activating differential target genes, p53 triggers a variety of cellular response, including DNA damage repair, cell cycle arrest and apoptosis, which are essential for its tumor-suppressive function.

## Redox signaling: an emerging and exciting form of signal transduction

### Endogenous H<sub>2</sub>O<sub>2</sub> production

Redox signaling is initiated with the generation of reactive oxygen species (ROS), particularly in the form of hydrogen peroxide (H<sub>2</sub>O<sub>2</sub>). H<sub>2</sub>O<sub>2</sub> and other forms of ROS like superoxide (O<sub>2</sub><sup>-</sup>) are different derivatives of molecular oxygen and generated from different subcellular sources. Mitochondria are considered the most significant contributors of endogenous H<sub>2</sub>O<sub>2</sub> production, where O<sub>2</sub><sup>-</sup> generated in the electron transport chain is dismutated to H<sub>2</sub>O<sub>2</sub> catalyzed by superoxide dismutases (SODs) [25]. H<sub>2</sub>O<sub>2</sub> is also generated from O<sub>2</sub><sup>-</sup> produced by NADPH oxidases (NOXs) on the plasma membrane in response to growth factor receptor signaling [26]. NOXs can also produce H<sub>2</sub>O<sub>2</sub> in the nucleus or endoplasmic reticulum (ER) (e.g., NOX4)[27, 28]. Other enzymes like Lipoxygenase, cytochrome P450 monooxygenase and xanthine oxidase produce O<sub>2</sub><sup>-</sup> that is converted to H<sub>2</sub>O<sub>2</sub> in the cytoplasm [29]. Additionally, oxidases involved in the metabolism of D-amino acids, various fatty acids and glycola-

te generate  $H_2O_2$  inside the peroxisome [30] (Fig. 2). For an extensive review on subcellular sources of ROS see [31].

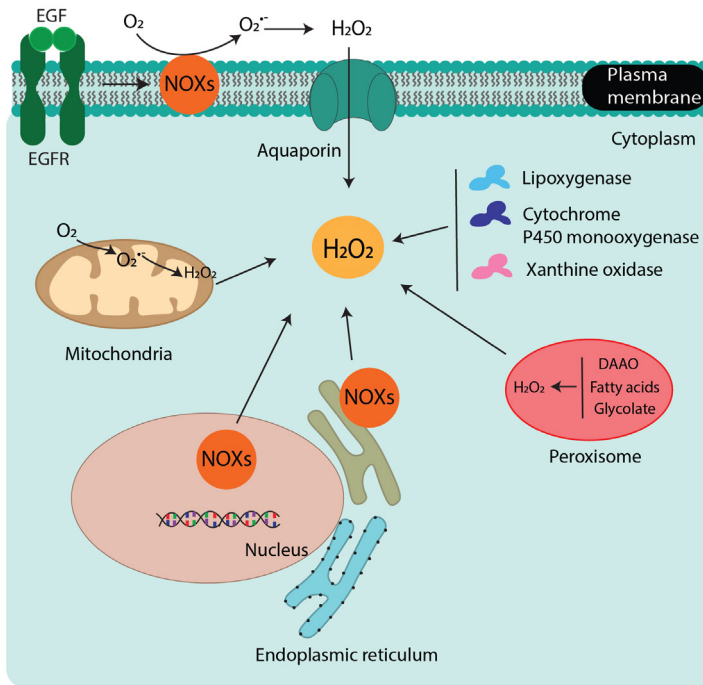


**Figure 2. Endogenous  $H_2O_2$  production.**

Mitochondria are considered the most significant contributors of endogenous  $H_2O_2$  production, where  $O_2^{\cdot-}$  generated in the electron transport chain is dismutated to  $H_2O_2$  catalyzed by superoxide dismutases (SODs).  $H_2O_2$  is also generated from  $O_2^{\cdot-}$  produced by NADPH oxidases (NOXs) on the plasma membrane in response to growth factor receptor signaling.  $H_2O_2$  then enters cells through the Aquaporin channel. NOXs (e.g., NOX4) can also produce  $H_2O_2$  in the nucleus or endoplasmic reticulum (ER). Other enzymes like Lipoxigenase, cytochrome P450 monooxygenase and xanthine oxidase produce  $O_2^{\cdot-}$  that is converted to  $H_2O_2$  in the cytoplasm. Additionally, oxidases involved in the metabolism of D-amino acids, various fatty acids and glycolate generate  $H_2O_2$  inside the peroxisome. Note that the arrows pointing from the various organelles to ' $H_2O_2$ ' in the center of the figure are meant to indicate that these contribute to endogenous  $H_2O_2$  production, and not necessarily to cytosolic  $H_2O_2$ . There is evidence that the diffusion of  $H_2O_2$  is actually quite limited, and that it is largely confined to the site of production due to the efficient scavenging system [32, 33]. This creates  $H_2O_2$ -gradients in the cell that could contribute to specificity in Redox signaling [31, 34, 35]. NOXs, NADPH oxidases; EGF, epidermal growth factor; EGFR, EGF receptor.

## Redox signaling

Redox signaling depends on a range of cysteine modifications. At low levels of  $H_2O_2$ , reactive cysteinyl thiols undergo reversible oxidation to sulfenic acid (-SOH) and subsequent intra- and intermolecular disulfide bonds (-S-S-) which are constantly reduced by the thio-

doxin (Trx/TrxR) system that depends on NADPH. With  $H_2O_2$  level increases, some cysteinyl thiols (particularly in Peroxiredoxins) could undergo overoxidation ending up in the form of sulfinic acid ( $-SO_2H$ ) and sulfonic acid ( $-SO_3H$ ). The sulfinic acid ( $-SO_2H$ ) can still be able to be recycled by sulfiredoxin1 (SRX1) at the expense of ATP, but with a relatively low cycling rate, whereas sulfonic acid ( $-SO_3H$ ) is no longer reducible. Therefore, these two forms are termed 'irreversible thiol oxidation' (**Fig. 3**). Reversible, rather than irreversible cysteine oxidation, leads to a transient change of protein state and therefore is more relevant for redox signal transduction.

Compared with other ROS like superoxide ( $O_2^{\cdot-}$ ) and hydroxyl radicals ( $\cdot OH$ ),  $H_2O_2$  is less reactive and relatively stable. Its reactivity with most cysteinyl thiols is actually quite low but may increase dramatically depending on the target protein structure or microenvironment. This means that at low levels  $H_2O_2$  likely reacts mostly with the cysteines in the active sites of dedicated  $H_2O_2$  scavenging enzymes like the Peroxiredoxins.

Peroxiredoxins (PRDXs) are a family of peroxidase enzymes that are essential for scavenging  $H_2O_2$  and protecting cells and tissues from oxidative damage. However, in recent years, rather than being merely a scavenger of  $H_2O_2$ , PRDXs have been proposed to be a mediator of  $H_2O_2$ -dependent redox signaling through a so-called "redox relay" model [36, 37]. This model explains how redox signaling can take place at low physiological levels of  $H_2O_2$  despite the low intrinsic reactivity of most thiols found to be targeted by redox signaling. The extremely high reactivity of the PRDXs with  $H_2O_2$  assures their oxidation already at low physiological  $H_2O_2$  levels. Oxidized PRDXs then transfer the oxidizing equivalents to target proteins that have a lower intrinsic reactivity toward  $H_2O_2$ . One of the redox-relay examples is mediated by PRDX2 and the target the transcription factor STAT3 [38]. More potential targets of all five human PRDXs have been identified by our lab very recently, showing that PRDXs relay redox signaling in an isoform-specific fashion [39]. The relay model implies that redox signaling already occurs at very low  $H_2O_2$  levels. In parallel, the 'floodgate' model has been proposed, which hypothesizes that oxidation of low reactive thiols occurs only upon accumulation of  $H_2O_2$  due to inactivating over-oxidation of PRDXs. In the floodgate model redox signaling therefore occurs only above a certain (local)  $H_2O_2$  threshold and would therefore be taking place likely in parallel with oxidative damage. More information about these two models is discussed in **Chapter 2**.

### **The roles of redox signaling in physiology and pathology**

Redox signaling has been found to play essential roles in various biological processes, including cell proliferation, differentiation, regeneration, migration, and the immune response. However, an overload of  $H_2O_2$  and the concurrent damage as well as the prolonged offset of redox homeostasis are also associated with various pathological processes, like age-related diseases and cancer [29, 31] (**Fig. 3**).



thioredoxin reductase 1; SOD2, superoxide dismutase 2; GPX1, Glutathione peroxidase 1; PRDXs, Peroxiredoxins; GRX3, glutaredoxin 3; PIG3/6, the p53-inducible genes; NRF2, E2-related factor 2; HIFs, Hypoxia-inducible factors; FOXOs, Forkhead box O proteins.

*Cellular proliferation, differentiation and regeneration* Several studies have found that ROS (and hence redox signaling) are required for cellular proliferation [29]. Tyrosine kinase (e.g., EGFR, PDGFR and insulin receptor) activation triggers superoxide production by NOXs in the plasma membrane. After spontaneous or enzyme-catalyzed dismutation, the formed  $H_2O_2$  can be taken up by the cell through Aquaporin [40], where it will subsequently inactivate protein tyrosine phosphatases like PTP1B through oxidation of its catalytic cysteine [41]. It is thought that only the simultaneous activation of the tyrosine kinase receptor and the inactivation of the tyrosine phosphatase bring about a strong enough proliferative signal. In line with this,  $H_2O_2$  has long been known as an insulin-mimetic [42]. Furthermore, sulfenylation of EGFR increases its activity [43]. The dynamics of  $H_2O_2$  levels and cellular redox enzymes during embryo development and tissue homeostasis indicate that redox signaling is closely associated with cell differentiation [35, 44]. In *Drosophila*, a more oxidized state is observed in early embryos as compared to mature oocytes [45]. Consistently, low catalase protein levels are identified during embryo development and high levels in mature tissues, which is conserved among *Drosophila*, zebrafish, and mice [44]. Redox signaling also has been associated with adult tissue homeostasis by regulating stem cell renewal and differentiation. In most cases, stem cells maintain a low basal level of  $H_2O_2$  but an increased level with differentiation [46-49]. The  $H_2O_2$  level increases during the process of wound repair and cell regeneration. The increased  $H_2O_2$  not only promotes proliferation of endothelial cells and fibroblast, but also functions in the immune system to kill pathogens and bacteria, all together facilitating wound healing by remodeling the extracellular matrix [50, 51].

*Aging and cancer* The widespread sense that ROS or oxidative stress is associated with aging is mainly based on the free radical theory of aging [52]. In this theory, the free radicals derived from molecular oxygen were proposed to be reactive and toxic to all kinds of macromolecules, which eventually cause aging and aging-associated degenerative disease. Indeed, ROS like hydroxyl radicals ( $\cdot OH$ ) is a larger contributor to oxidative DNA damage. Unrepaired DNA damage ultimately induces genomic instability, a hallmark of aging [53]. The hallmarks of aging also include telomere attrition, epigenetic alterations, proteostasis loss, mitochondria dysfunction, deregulated nutrient sensing, stem cell exhaustion, and cellular senescence and death [53], which are also correlated with the negative side of oxidants. However, it was shown that in mice increased ROS ( $O_2^{\cdot -}$ ) caused by SOD depletion did not necessarily accelerate aging [54], and a similar observation was observed in *C.elegans* [55, 56]. Notably, the latter paper showed that the conversion of  $O_2^{\cdot -}$  to  $H_2O_2$  by SODs is required for lifespan extension induced by low levels of the redox cycler paraquat. This observation shows that 1) ROS does not necessarily induce aging and 2) that  $H_2O_2$  and not  $O_2^{\cdot -}$  mediates the biological effects in redox signaling. Altogether, low levels of  $H_2O_2$  have positive effects

on lifespan extension, whereas excess oxidants correlate with aging-associated features.

Cancer cells are characterized by the increased production of ROS (e.g.,  $H_2O_2$ ) through, for instance, the increased activity of NOX enzymes and metabolic reprogramming [57], which in turn supports the malignancy by for instance sustaining proliferation, resisting cell death, and promoting invasion and metastasis [58, 59]. However, prolonged elevated ROS production would lead to severe oxidative stress and eventually induce tumor cell death. To survive and thrive cancer cells therefore also need to boost their anti-oxidation defense for instance by increasing the NRF2-dependent detoxification [60], and promoting the production of NADPH as a benefit of the Warburg effect [61]. Nevertheless, this remodeled redox balance with both high levels of oxidants and antioxidants in cancer cells seems to be more easily disturbed. This is the rationale behind many redox-dependent treatments that aim to either enhance pro-oxidant production or weaken reductive capacity have been developed and showed promising anti-cancer potential [59, 62]. However, it is often not entirely clear which downstream redox-sensitive proteins these drugs target and whether or what type of redox/cysteine modifications contribute to their therapeutic potential.

## p53 regulation by redox signaling

### Cysteine oxidation

Reversible cysteine modifications, such as sulfenic acid (-SOH) and disulfide(-S-S), play essential roles in modulating protein activity [29, 31]. p53 has previously been shown to be reversibly oxidized on cysteines (predominantly C182 and C277) in response to oxidants like  $H_2O_2$  and diamide (a thiol-directed oxidizing agent) [63, 64]. However, it is unclear whether or how reversible cysteine oxidation would contribute to the regulation of p53 activity. While C277-dependent oxidation has been proposed to be implicated in the selective transcriptional activation of specific p53 response element variants that are either similar to those found in the *CDKN1A* or the *GADD45a* promoter [65, 66], the exact mechanism is not entirely clear (described in **Chapter 2**).

### Upstream redox signaling

JNK and p38MAPK are two important kinases mediating p53 activation in response to ROS [67]. While multiple potential mechanisms underlying how JNK and p38MAPK are activated by ROS have been proposed [68], one of these depends on the reversible cysteine oxidation on their upstream kinase ASK-1 [69]. Cysteine oxidation of ASK-1 leads to its disulfide-dependent dimerization and activation, which in turn phosphorylates and activates JNK and p38MAPK, followed by p53 phosphorylation and activation [70]. Besides ASK-1, JNK and p38MAPK have also been shown to be subject to cysteine oxidation-dependent regulation of their kinase activity [71, 72], implying that downstream p53 activation could also be a result of redox control of JNK and p38MAPK through direct cysteine oxidation. Nevertheless, given these observations it suggests that p53 activation in response to ROS depends on both upstream redox signaling (e.g., cysteine oxidation of ASK-1) and following canonical

kinase signaling (phosphorylation of SAPK and p53),

### **Crosstalk between canonical kinase and redox signaling to p53**

p53 activation in response to  $H_2O_2$  has long been known to occur and is generally attributed to the ATM/ATR dependent response triggered by  $H_2O_2$  induced DNA damage [73, 74]. Indeed, exogenously-added  $H_2O_2$  triggers activation of both the ATM and ATR pathways, suggesting that  $H_2O_2$  induces both DNA single-strand breaks (SSB) and double-strand breaks (DSB) [75]. However, as described above  $H_2O_2$  also acts as a second messenger in redox signaling and induces redox signaling-dependent SAPK activation [76]. Furthermore, treatment with genotoxic agents like chemotherapeutic drugs and UV irradiation have been linked to the generation of ROS, resulting in the simultaneous activation of SAPK signaling and the DDR [14, 77, 78]. These observations imply that downstream p53 activation in response to compounds like  $H_2O_2$  and chemotherapeutic drugs could be a result of several parallel signaling pathways, including canonical kinase cascades (ATM and ATR) and redox signaling targeting the upstream proteins (e.g., ASK-1) and (or) p53 itself. However, it remains unclear which signaling pathways (canonical kinase signaling vs. redox signaling) are involved in p53 activation in response to which signaling pathways (DNA damage, redox signaling, or both) and to what extent. An overview of the literature on the differential upstream signaling pathways to mediate p53 activation, and how these play a potential role in current and future anti-cancer therapies has been outlined in **Chapter 2**.

## **Tools to detect redox signaling**

### **Fluorescent-based $H_2O_2$ probes**

The recent improvements in fluorescence-based  $H_2O_2$  probes have enabled researchers to monitor low, physiological levels of cellular  $H_2O_2$ . This has contributed greatly in uncovering potential the roles of redox signaling in physiological and pathological processes [32, 35, 79]. Historically, small molecule-based fluorescent  $H_2O_2$  probes were used, for example the cell-permeable 2'-7'-dichlorofluorescein diacetate ( $H_2DCF$ -DA) dye, which generates a bright green fluorescent signal upon oxidation by  $H_2O_2$  (**Fig. 4A**). The main problem with these dyes is that they are not specific for the detection of  $H_2O_2$ .  $H_2DCF$ -DA, or rather its intracellularly de-esterified form  $H_2DCF$ , also reacts with a range of other ROS species and oxidants such as  $\cdot OH$  and  $^1O_2$  [80].

The recent versions of genetically encoded probes have a high specificity for oxidation by  $H_2O_2$ , and have several other advantages, including high sensitivity, reversibility, ratiometric detection, possibilities for subcellular localization, and real-time detection in live cells. Genetically encoded  $H_2O_2$  sensors like roGFP-Orp1 and HyPer and their derivatives are characterized by an  $H_2O_2$  reactive protein (domain) fused with a fluorescent protein variant that has been mutated to exhibit different excitation properties in the reduced and oxidized states. roGFP-Orp1 is a fusion of the redox-sensitive green fluorescent protein 2 and a yeast peroxidase, Orp1 [81]. Upon exposure to  $H_2O_2$ , Orp1 is oxidized to form a disulfide bond



between C36 and C82 which will be transferred to roGFP2 in a similar fashion as described earlier in this chapter for the PRDX-based redox relay. Oxidized roGFP2 will show an increased emission upon excitation at 405 nm and a decreased signal when excited at 488 nm, allowing the ratiometric measurement of  $\text{H}_2\text{O}_2$  (**Fig. 4B**). The oxidation of roGFP2-Orp1 is specifically induced by  $\text{H}_2\text{O}_2$ , and not by other oxidants such as GSSG [81]. But since oxidation

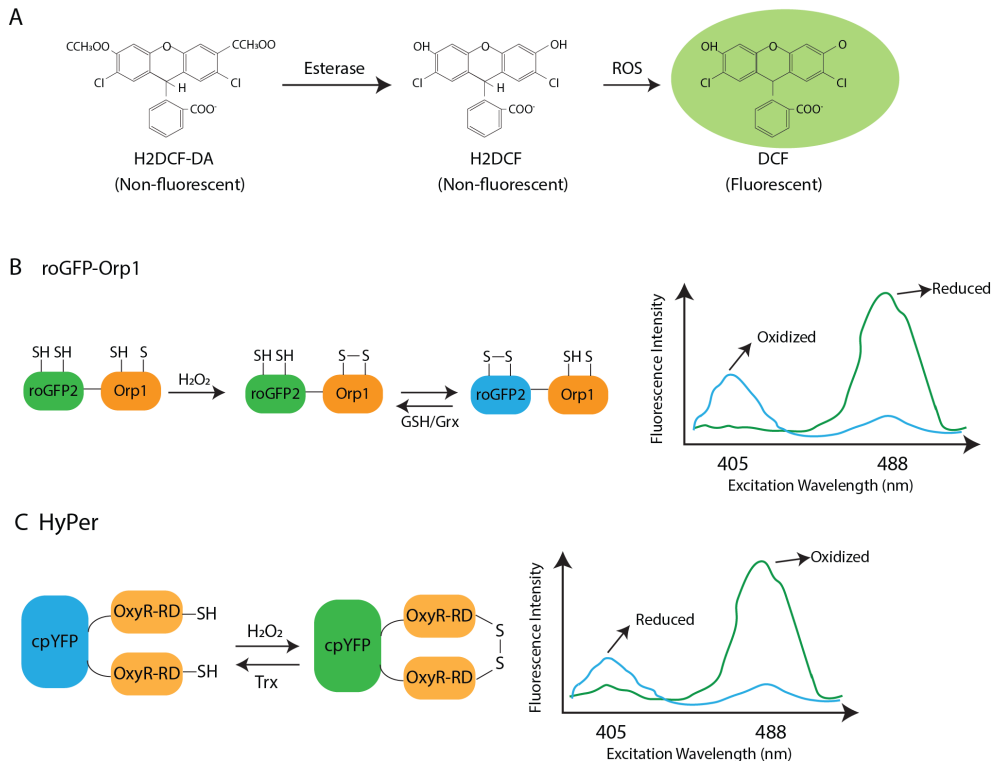


**Figure 4. Fluorescence-based  $\text{H}_2\text{O}_2$  probes.**

**(A)** 2'-7'-dichlorofluorescein diacetate (H2DCF-DA) is a cell-permeable and non-fluorescent dye. After being taken up by cells, H2DCF-DA undergoes hydrolysis catalyzed by Esterase to yield H2DCF (non-fluorescent). H2DCF reacts with ROS (e.g.,  $\text{H}_2\text{O}_2$ ,  $\cdot\text{OH}$  and  $^1\text{O}_2$ ), generating the product DCF which shows a bright green fluorescent signal. **(B)** The roGFP2-Orp1 probe is a fusion of the redox-sensitive green fluorescent protein 2 and a yeast peroxidase, Orp1. Upon exposure to  $\text{H}_2\text{O}_2$ , Orp1 is oxidized to form a disulfide bond which will be transferred to roGFP2. Oxidized roGFP2 will show an increased emission upon the excitation at 405 nm (oxidized) and a decreased signal when excited at 488 nm (reduced), allowing the ratiometric measurement of  $\text{H}_2\text{O}_2$ . **(C)** The HyPer probe is developed based on a circularly permuted yellow fluorescent protein (cpYFP) integrated into the regulatory domain of the *E. Coli* OxyR protein, which is a bacterial  $\text{H}_2\text{O}_2$  sensor. Upon exposure to  $\text{H}_2\text{O}_2$ , OxyR forms a disulfide bond, which results in a conformational change in HyPer that alters its excitation characteristics. This allows for the ratiometric measurement of  $\text{H}_2\text{O}_2$  by comparing the HyPer emission signal at 515 nm upon excitation at 488 nm (oxidized) and 405 nm (reduced). The newest generation of the HyPer probe, HyPer7, uses the regulatory domain of the *N. meningitidis* OxyR protein, is more sensitive to small  $\text{H}_2\text{O}_2$  changes and not affected by pH changes unlike earlier versions of HyPer.

of the probe is reversible, it reports in fact on the combined rates of oxidation by  $\text{H}_2\text{O}_2$  and reduction by the glutathione system. Although the roGFP-Orp1 has been used to visualize physiological  $\text{H}_2\text{O}_2$  production in *Drosophila* larvae and tissues [82, 83], its reaction rate with  $\text{H}_2\text{O}_2$  is much lower when compared with the recently developed 2-Cys PRDX-based probes, roGFP-Tsa2 $\Delta$ C<sub>R</sub> and roGFP-Tsa2 $\Delta$ C<sub>P</sub> $\Delta$ C<sub>R</sub> [35, 79].

The original HyPer probe is developed based on a circularly permuted yellow fluorescent protein (cpYFP) integrated into the regulatory domain of *E. Coli* OxyR protein, which is a bacterial  $\text{H}_2\text{O}_2$  sensor [84]. Upon exposure to  $\text{H}_2\text{O}_2$ , OxyR forms a disulfide bond between C199 and C208, which results in a change in the HyPer conformation resulting in altered excitation characteristics. Like roGFP2, this allows for the ratiometric measurement of  $\text{H}_2\text{O}_2$  by comparing the HyPer emission at 515 nm upon excitation at 488 nm (oxidized) and 405 nm (reduced) (**Fig. 4C**). Different versions of HyPer probes (Hyper 2, 3 and 7) aimed to improve the sensitivity and dynamics have been developed by Belousov's lab [32, 85, 86], and have been applied into several biological systems, including *C. elegans* [87] and zebrafish [88]. HyPer7, (currently) the latest version of the HyPer probes, consists of a *Neisseria meningitidis* OxyR protein and a modified cpYFP with a number of point mutations. Unlike roGFP2, the reduction of HyPer is mainly dependent on the thioredoxin system, and its rapid reduction seems to somewhat hamper its sensitivity to very low  $\text{H}_2\text{O}_2$  levels [89]. Besides its higher sensitivity towards oxidation by  $\text{H}_2\text{O}_2$ , a major improvement over previous versions of the HyPer probe is its insensitivity to pH changes [32].

### **Chemical probes to monitor cysteinyl thiol redox state**

Reversible cysteine oxidation is the linchpin in redox signaling in response to  $\text{H}_2\text{O}_2$ . Like phosphoproteomics used to understand kinase-based signaling, redox proteomics aims to map what proteins undergo cysteine oxidation in response to certain oxidants. Most redox proteomics protocols make use of different cysteine-reactive alkylators that are applied before and after the reduction of cysteines. Pitfalls include post-lysis oxidation and reduction and the loss of the type of oxidative PTMs. Recent technological advances using novel chemical thiol labeling probes and Mass spectrometry (MS) have allowed to identify the redox state of thousands of cysteinyl thiols and in some cases also specific forms of oxidative PTMs (OxiPTMs) [90, 91], in a proteome-wide manner and various biological settings. Redox proteomics therefore is a powerful tool, which has greatly facilitated deciphering the mechanisms underlying redox signaling and the downstream cellular and organismal responses.

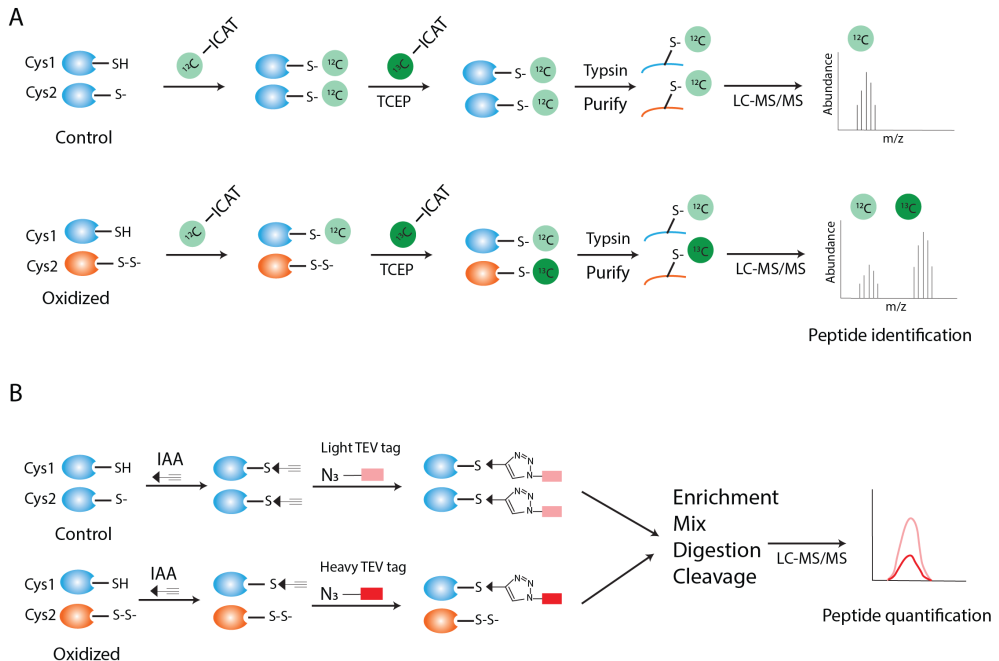
Due to the intrinsic nucleophilicity of (deprotonated) cysteines, chemical probes designed to monitor thiol redox state generally rely on an electrophilic group that can react with reduced thiols (or more specific thiolate anions). To date, several chemical thiol labeling methods have been developed and applied in redox biology research, each with its own advantages and limitations. A widely-used chemical reagent in proteomics is the isotope-coded affinity tags (ICAT), which for redox proteomics (OxiCAT) [92] that consists of a thiol-reactive group (e.g., iodoacetamide), a biotin moiety for streptavidin-based enrichment. OxiCAT enables

differential labeling of reduced and oxidized thiols in the same sample, in which for instance the light-OxiCAT reagent ( $^{12}\text{C}$ ) is used to label reduced thiols, and heavy-OxiCAT ( $^{13}\text{C}$ ) is used to label the reversibly oxidized thiols after reduction [92-95] (**Fig. 5A**). This enables the quantitative measurement of the ratio of reversibly oxidized and reduced for every cysteine covered in the proteomics approach, which can amount to ratios of thousands of unique cysteines. However, the high price of the reagents limits their application as a routine technique in most labs. Alternatively, a biotinylated iodoacetamide (BIAM)-based approach is being used [96, 97]. A major drawback of using this BIAM-switch assay however is the inefficient elution of biotinylated proteins or peptides from streptavidin beads, which can result in a low yield of labeled cysteines. Furthermore, the bulky structure of both ICAT and BIAM reagents limits their accessibility to buried cysteines, particularly in native conditions. Therefore, quite harsh denaturing methods are often required in sample preparation, which may increase artifacts during sample preparation and background noise in the MS analysis.

Alternatively, the method termed isotopic tandem orthogonal proteolysis activity-based protein profiling (isoTOP-ABPP) is based on a smaller cysteine reactive probe IAAyne (iodoacetamide alkyne) and a cleavable biotin linker containing a biotin group, a cleavage site, and an azide moiety, which has been used to evaluate cysteine reactivity in native conditions [98] (**Fig. 5B**). The evaluation of cysteine reactivity makes use of sub-stoichiometric amounts of a label, with the rationale that the most reactive cysteines are labeled already at low amounts of probe. The ratio of labeling of a cysteine at two concentrations of a label (low and high) is a measure for its reactivity. The method can also be adapted to measure to what extent cysteines are oxidized, similar to the OxiCAT method. To this end reduced cysteines are first blocked by an unlabeled alkylator (e.g., NEM), after which the reversibly oxidized cysteines are reduced. IAAyne is used to label the previously oxidized but now free thiols through its iodoacetamide moiety, followed by conjugation with the biotin-azide linker through a 'click-chemistry' alkyne-azide reaction catalyzed by Copper (I) (CuAAC). The biotinylated proteins (peptides) are enriched using streptavidin beads and subsequently cleaved off through the cleavable site recognized by tobacco etch virus protease (TEV) [98]. This probe has been used to identify and quantify the reactivity of over 1000 cysteine sites in mouse tissue samples [98]. Using the isotopically-labeled biotin linkers enables the comparison of two samples in a single MS run. Similar methods based on the IAAyne reagent but with a different biotin-linker, such as the photo-cleavable (Az-UV-biotin), azobenzene (AZO) linker or the dialkoxy-diphenylsilane (DADPS) linker, have also been used in different experimental setups [45, 99, 100].

Although these methods provide a powerful tool to monitor cellular thiol redox state in site-specific and proteome-wide manners, they miss the information on the exact type of oxidative PTMs (e.g., -SOH, -S-S, and -S-SNO). However, chemical probes like dimedone and its derivatives (DAz and DYn) can specifically target and label sulfenylated cysteines (-SOH) [90, 101, 102]. The DiaAlk probe has been used to label  $\text{SO}_2\text{H}$ , providing a means to identify sulfenylated proteins as well [91]. Collectively, the next generation of cysteine-reactive probes to

distinguish and quantify different OxiPTMs in cysteine redox proteomics will greatly aid in the discovery of the mechanisms underlying redox signaling.



## Redox-sensitive transcription factors

Redox homeostasis is of great importance for healthy physiology in all organisms [103]. At the molecular level, several transcription factors act as redox sensors and are essential for redox homeostasis maintenance by activating a number of target genes involved in antioxidant function and detoxification in response to redox stress. These transcription factors include p53, nuclear factor E2-related factor 2 (NRF2), hypoxia-inducible factors (HIFs), the Forkhead box O proteins (FOXOs), etc. (Fig. 3). Below we provide a brief introduction of these transcription factors with respect to their roles in redox homeostasis.

### p53

As described before, p53 is activated upon exposure to ROS but has remained unclear by which exact mechanisms (the DDR, redox signaling, or both). Upregulated p53 in response to ROS induces antioxidant genes, including *GPX1* and *GRX3* that are important for ROS clearance and cell survival [21, 22]. p53 also triggers the expression of pro-oxidant genes including *PIG3* and *PIG6* that contribute to ROS-dependent cell death [23]. It has been shown that p53 activates pro- or antioxidant genes seemingly dependent on the protein level of p53 or the specific oxidizing conditions [104]. Furthermore, p53-dependent genes implicated in metabolism regulation also aid in maintaining redox homeostasis [105].

### NRF2

At physiological conditions, NRF2 interacts with Kelch-like ECH-associated protein 1 (KEAP1), a component of Cullin 3 (CUL3)-based E3 ubiquitin ligase complex, which mediates NRF2 ubiquitylation and subsequent proteasomal degradation. Oxidation of specific cysteines in KEAP1 leads to the formation of a homodimer [106] which prevents its inhibitory effects on NRF2, resulting in NRF2 stabilization and translocation to the nucleus. Activated NRF2 functions as a transcription factor that binds to the specific antioxidant response element (ARE) and activates several antioxidant genes, including heme oxygenase-1 (*HMOX1*), glutamate-cysteine ligase modifier subunit (*GCLM*), and thioredoxin reductase 1 (*TXNRD*) [107]. NRF2 also activates genes involved in DNA damage repair, protein assembly, and the anti-inflammatory response and many others. Inactivation of NRF2 signaling is correlated with age-related pathological hallmarks and chronic diseases, such as loss of proteostasis, genomic instability, neurodegeneration, and cancer [108]. Since its roles in cellular detoxification, NRF2 has been found to be upregulated in several tumors.

### HIF

Hypoxia-inducible factors (e.g., HIF-1 $\alpha$ ) are key transcriptional regulators of the cellular response to oxygen deficiency (i.e., hypoxia), [109, 110]. Paradoxically, hypoxia is also associated with an elevated level of H<sub>2</sub>O<sub>2</sub> through, for instance, dysregulation of the mitochondrial electron transport chain (ETC) [111]. Mitochondrial ROS production has actually been shown to be crucial for HIF activation in response to hypoxia [112]. Like p53 and NRF2, PTMs downstream of ROS lead to loss of the continuous proteasomal degradation, which in the

case of HIF-1 $\alpha$  is under control of the Von Hippel Lindau tumor suppressor (pVHL), a substrate recognition component of an E3 ubiquitin ligase [113]. Under normal conditions, pVHL targets hydroxylated HIF-1 $\alpha$  for ubiquitination and proteasome degradation. Inactivation of pVHL by loss of gene expression or mutations leads to HIF-1 $\alpha$  stabilization and activation. Stabilized HIF-1 $\alpha$  translocates to the nucleus and in turn activates several target genes by binding to the specific hypoxia-response element (HRE). HIF-driven genes have been implicated in diverse processes, including angiogenesis, cell proliferation, metabolic reprogramming and apoptosis. These transcriptional responses are not only important to combat hypoxia and collateral oxidative stress in healthy [114, 115] but also tumor cells. In particular, HIF-1 $\alpha$ -dependent lymphangiogenesis in response to hypoxia is important to sustain the oxygen and metabolite supply in growing solid tumors and facilitate metastasis [116].

### **FOXOs**

FOXOs are a family of transcription factors that are downstream of and negatively regulated by the phosphoinositide-3-kinase–protein kinase B/Akt (PI3K-PKB/Akt) pathway by trapping FOXOs in the cytoplasm upon phosphorylation. FOXOs are being activated upon exposure to various cellular stresses including ROS (e.g., H<sub>2</sub>O<sub>2</sub>) [117]. The activation of FOXOs by H<sub>2</sub>O<sub>2</sub> involves two distinct mechanisms. One depends on redox signaling-activated JNK (upstream of FOXOs) which induces phosphorylation of FOXOs, on sites distinct from those phosphorylated by PKB/Akt, resulting in nuclear localization [118]. The other mechanism relies on cysteine oxidation on FOXOs which results in disulfide formation between FOXOs and nuclear transporters like Transportin 1 (TNPO1 for FOXO4) or Importin 7 and 8 (IPO7 and 8 for FOXO3) [119, 120], facilitating FOXOs nuclear translocation and transcriptional activation. ROS-activated FOXOs induce several antioxidant genes like Superoxide dismutase2 (*SOD2*), *GPX1*, Catalase, and Peroxiredoxin 3 and 5 (*PRDX3/5*) [121], all of which are involved in scavenging excess O<sub>2</sub><sup>•-</sup> or H<sub>2</sub>O<sub>2</sub> in cells.

As mentioned above because of the importance of NRF2, HIF and FOXOs in supporting redox homeostasis and cell survival, it is maybe not surprising that they are still active in cancer cells. Indeed, it has been shown that their activity is actually essential for outgrowth, progression and metastasis of certain tumors [116, 122, 123]. One could propose that once the oncogenic barrier has been crossed, the function in the maintenance of (redox) homeostasis of these transcription factors no longer protects from oncogenic transformation but becomes supportive of the tumor cells. A similar observation has been made for some of the roles of p53 [6], but given its frequent loss in cancer it is from the viewpoint of tumor evolution apparently often more beneficial to lose its tumor suppressive functions in cell cycle arrest and apoptosis than to rely on its role in homeostasis. Taken together, studying the activity of these TFs in the context of cancer is important to understand the underlying mechanisms in cancer development, and to develop and monitor cancer treatments by targeting these TFs or their upstream and downstream redox signaling pathways.

## Outline of this thesis

This thesis covers two major aspects: A review and two mechanistic studies on the redox regulation of p53 (**Chapters 2, 3 and 4**) and technological innovations to study redox biology (**Chapters 5 and 6**). Both will aid in unraveling the molecular mechanisms that underlay homeostasis control, disease onset and therapy response.

In **Chapter 2**, we give an overview of the literature on the regulation of p53 by the DNA damage response and by redox signaling. Oftentimes these pathways are considered to always fire simultaneously. We provide a perspective on how these pathways could be acting as separate ways to regulate the activity of p53 in terms of upstream kinase activation, PTMs and downstream transcriptional response.

In **Chapter 3**, we put the model proposed in **Chapter 2** to the test and show that we can indeed dissect oxidative signaling and DNA damage signaling by applying different chemical compounds (diamide vs. Neocarzinostatin). We demonstrate that p53 is activated by oxidative and DNA damage signaling through differential mechanisms. Oxidative signaling activates p53 mainly through the p38MAPK pathway, independent of the ATM-dependent DNA damage response. Our results provide a theoretical basis for the idea that induction of oxidizing conditions (probably by inhibition of reductive capacity) could be a strategy to reactivate p53 as a treatment for cancers expressing wild-type but reduced levels of p53. A benefit as compared to using classical chemotherapeutics to induce DNA damage as a trigger to reactivate p53 is that redox-dependent activation not necessarily causes collateral DNA damage. This limits mutation accumulation in both healthy and tumor tissues and potentially prevents the induction of novel oncogenic lesions or tumor progression and therapy resistance.

Besides the regulation of p53 by upstream redox signaling, cysteines in p53 itself have long been known to be sensitive to oxidation [21, 63, 64]. However, the protocols used to detect reversible oxidation in general preclude the identification of the type of oxidative modification. In **Chapter 4**, we describe the observation that p53 forms disulfide-dependent interactions with several proteins in live cells, including with well-known functional regulators like 53BP1 and 14-3-3 $\theta$ , depending on Cys277. The precise functional consequence of these redox-dependent interactions remains largely unclear, but it is the first time that p53 is shown to form covalent, disulfide-linked protein-protein interactions. The implications of these findings are discussed.

In recent years, researchers have been able to quantitatively monitor cysteine reactivity or identify the bulk or organ-specific cysteine oxidation profiles in a proteome-wide and site-specific manner in both physiological and challenged conditions using advanced thiol-reactive chemical probes and Mass spectrometry (MS)-based techniques [98, 100, 124]. These technological advances gave an in-depth overview of proteome-wide cysteine oxidation profiling in physiology and disease and greatly aid in better understanding the mechanisms of redox regulation of specific proteins at specific cysteines. In **Chapter 5** we evaluate and

optimize two thiol-labeling approaches: BIAM and IAAyne-DADPS, aiming to set up an effective MS-based protocol to identify redox-regulated cysteines in our laboratory. By connecting this method to the protocol we use for the identification of intermolecular disulfide-dependent complexes, we will enable to monitor how the 'thiolome' alters in response to several conditions at multiple levels. Two methods show reasonable labeling results both in vitro and in cell lysates, whereas more optimization (e.g., to further increase the labeling efficiency) is required to get a more comprehensive and robust result.

Besides p53, other transcription factors (TFs) like NRF2 [125, 126], the Forkhead box O proteins (FOXOs) [121, 127] and Hypoxia-inducible factor (HIF) [128] are also activated by cellular stresses including oxidative stress/redox signaling. However, little is known about the simultaneous and dynamic regulation regarding each TF in response to oxidants and in fundamental biological processes including proliferation, development, and response to (chemo)therapeutics. In **Chapter 6**, we establish two fluorescence-based transcriptional reporters (p53/Myc/FOXO<sup>NLS</sup> and TCF/HIF/NRF2<sup>NES</sup>) that will enable us to simultaneously monitor these TF activities together with two oncogenic TFs (TCF and c-Myc), both in live cells and in various in vivo models. It will be interesting to learn how these TFs differentially respond when cells are challenged with compounds that perturb the (localized) cellular redox state (e.g., reducing agents, chemotherapeutics, inhibitors of the Trx/TrxR system or H<sub>2</sub>O<sub>2</sub> production by localized DAAO [129] and others).



## References

1. Hanahan D., Weinberg R.A. Hallmarks of cancer: the next generation. *Cell*, 2011. 144(5): 646-674.
2. Bishop J.M. Cellular oncogenes and retroviruses. *Annu. Rev. Biochem.*, 1983. 52: 301-354.
3. Levine A.J., Momand J., Finlay C.A. The p53 tumour suppressor gene. *Nature*, 1991. 351(6326): 453-456.
4. Eliyahu D., Michalovitz D., Eliyahu S., et al. Wild-type p53 can inhibit oncogene-mediated focus formation. *Proc. Natl. Acad. Sci. U. S. A.*, 1989. 86(22): 8763-8767.
5. Finlay C.A., Hinds P.W., Levine A.J. The p53 proto-oncogene can act as a suppressor of transformation. *Cell*, 1989. 57(7): 1083-1093.
6. Maddocks O.D., Berkers C.R., Mason S.M., et al. Serine starvation induces stress and p53-dependent metabolic remodelling in cancer cells. *Nature*, 2013. 493(7433): 542-546.
7. Kruiswijk F., Labuschagne C.F., Vousden K.H. p53 in survival, death and metabolic health: a lifeguard with a licence to kill. *Nat. Rev. Mol. Cell Biol.*, 2015. 16(7): 393-405.
8. Duffy M.J., Synnott N.C., O'Grady S., et al. Targeting p53 for the treatment of cancer. *Semin. Cancer Biol.*, 2020.
9. Haupt Y., Maya R., Kazaz A., et al. Mdm2 promotes the rapid degradation of p53. *Nature*, 1997. 387(6630): 296-299.
10. Brooks C.L., Gu W. p53 regulation by ubiquitin. *FEBS Lett.*, 2011. 585(18): 2803-2809.
11. Meek D.W., Anderson C.W. Posttranslational modification of p53: cooperative integrators of function. *Cold Spring Harb. Perspect. Biol.*, 2009. 1(6): a000950.
12. Mordes D.A., Cortez D. Activation of ATR and related PIKKs. *Cell Cycle*, 2008. 7(18): 2809-2812.
13. Bulavin D.V., Saito S., Hollander M.C., et al. Phosphorylation of human p53 by p38 kinase coordinates N-terminal phosphorylation and apoptosis in response to UV radiation. *EMBO J.*, 1999. 18(23): 6845-6854.
14. Milne D.M., Campbell L.E., Campbell D.G., et al. p53 is phosphorylated in vitro and in vivo by an ultraviolet radiation-induced protein kinase characteristic of the c-Jun kinase, JNK1. *J. Biol. Chem.*, 1995. 270(10): 5511-5518.
15. Jones R.G., Plas D.R., Kubek S., et al. AMP-Activated Protein Kinase Induces a p53-Dependent Metabolic Checkpoint. *Mol. Cell*, 2005. 18(3): 283-293.
16. El-Deiry W.S., Tokino T., Velculescu V.E., et al. WAF1, a potential mediator of p53 tumor suppression. 1993. 75(4): 817-825.
17. Bunz F., Dutriaux A., Lengauer C., et al. Requirement for p53 and p21 to sustain G2 arrest after DNA damage. 1998. 282(5393): 1497-1501.
18. te Poele R.H., Okorokov A.L., Jardine L., et al. DNA damage is able to induce senescence in tumor cells in vitro and in vivo. *Cancer Res.*, 2002. 62(6): 1876-1883.
19. Nakano K., Vousden K.H. PUMA, a novel proapoptotic gene, is induced by p53. *Mol. Cell*, 2001. 7(3): 683-694.
20. Oda E., Ohki R., Murasawa H., et al. Noxa, a BH3-only member of the Bcl-2 family and candidate mediator of p53-induced apoptosis. *Science*, 2000. 288(5468): 1053-1058.
21. Tan M., Li S., Swaroop M., et al. Transcriptional activation of the human glutathione peroxidase promoter by p53. *J. Biol. Chem.*, 1999. 274(17): 12061-12066.

22. Brynczka C., Labhart P., Merrick B.A. NGF-mediated transcriptional targets of p53 in PC12 neuronal differentiation. *BMC Genomics*, 2007. 8: 139.
23. Ostrakhovitch E.A., Cherian M.G. Role of p53 and reactive oxygen species in apoptotic response to copper and zinc in epithelial breast cancer cells. *Apoptosis*, 2005. 10(1): 111-121.
24. Polyak K., Xia Y., Zweier J.L., et al. A model for p53-induced apoptosis. *Nature*, 1997. 389(6648): 300-305.
25. Murphy M.P. How mitochondria produce reactive oxygen species. *Biochem. J.*, 2009. 417(1): 1-13.
26. Bae Y.S., Kang S.W., Seo M.S., et al. Epidermal Growth Factor (EGF)-induced Generation of Hydrogen Peroxide: ROLE IN EGF RECEPTOR-MEDIATED TYROSINE PHOSPHORYLATION\*. *J. Biol. Chem.*, 1997. 272(1): 217-221.
27. Chen K., Kirber M.T., Xiao H., et al. Regulation of ROS signal transduction by NADPH oxidase 4 localization. *J. Cell Biol.*, 2008. 181(7): 1129-1139.
28. Kuroda J., Nakagawa K., Yamasaki T., et al. The superoxide-producing NAD(P)H oxidase Nox4 in the nucleus of human vascular endothelial cells. *Genes Cells*, 2005. 10(12): 1139-1151.
29. Holmstrom K.M., Finkel T. Cellular mechanisms and physiological consequences of redox-dependent signalling. *Nat. Rev. Mol. Cell Biol.*, 2014. 15(6): 411-421.
30. Lismont C., Revenco I., Franssen M. Peroxisomal Hydrogen Peroxide Metabolism and Signaling in Health and Disease. *Int. J. Mol. Sci.*, 2019. 20(15).
31. Sies H., Jones D.P. Reactive oxygen species (ROS) as pleiotropic physiological signalling agents. *Nature Reviews Molecular Cell Biology*, 2020. 21(7): 363-383.
32. Pak V.V., Ezeriņa D., Lyublinskaya O.G., et al. Ultrasensitive Genetically Encoded Indicator for Hydrogen Peroxide Identifies Roles for the Oxidant in Cell Migration and Mitochondrial Function. *Cell Metab.*, 2020. 31(3): 642-653.e646.
33. Winterbourn C.C. The biological chemistry of hydrogen peroxide. *Methods Enzymol.*, 2013. 528: 3-25.
34. Mishina N.M., Bogdanova Y.A., Ermakova Y.G., et al. Which Antioxidant System Shapes Intracellular H<sub>2</sub>O<sub>2</sub> Gradients? *Antioxid Redox Signal*, 2019. 31(9): 664-670.
35. De Henau S., Pagès-Gallego M., Pannekoek W.J., et al. Mitochondria-Derived H<sub>2</sub>O<sub>2</sub> Promotes Symmetry Breaking of the *C. elegans* Zygote. *Dev. Cell*, 2020. 53(3): 263-271.e266.
36. Stocker S., Van Laer K., Mijuskovic A., et al. The Conundrum of Hydrogen Peroxide Signaling and the Emerging Role of Peroxiredoxins as Redox Relay Hubs. *Antioxid Redox Signal*, 2018. 28(7): 558-573.
37. Stocker S., Maurer M., Ruppert T., et al. A role for 2-Cys peroxiredoxins in facilitating cytosolic protein thiol oxidation. *Nat. Chem. Biol.*, 2018. 14(2): 148-155.
38. Sobotta M.C., Liou W., Stöcker S., et al. Peroxiredoxin-2 and STAT3 form a redox relay for H<sub>2</sub>O<sub>2</sub> signaling. *Nat. Chem. Biol.*, 2015. 11(1): 64-70.
39. van Dam L., Pagès-Gallego M., Polderman P.E., et al. The Human 2-Cys Peroxiredoxins form Widespread, Cysteine-Dependent- and Isoform-Specific Protein-Protein Interactions. *Antioxidants*, 2021. 10(4): 627.
40. Bertolotti M., Bestetti S., García-Manteiga J.M., et al. Tyrosine kinase signal modulation: a matter of H<sub>2</sub>O<sub>2</sub> membrane permeability? *Antioxid Redox Signal*, 2013. 19(13): 1447-1451.
41. Lee S.-R., Kwon K.-S., Kim S.-R., et al. Reversible Inactivation of Protein-tyrosine Phosphatase 1B in A431 Cells Stimulated with Epidermal Growth Factor\*. *J. Biol. Chem.*, 1998. 273(25): 15366-15372.

42. Lennicke C., Cochemé H.M. Redox regulation of the insulin signalling pathway. *Redox Biology*, 2021. 42: 101964.
43. Truong T.H., Ung P.M., Palde P.B., et al. Molecular Basis for Redox Activation of Epidermal Growth Factor Receptor Kinase. *Cell Chem Biol*, 2016. 23(7): 837-848.
44. Rampon C., Volovitch M., Joliot A., et al. Hydrogen Peroxide and Redox Regulation of Developments. *Antioxidants (Basel, Switzerland)*, 2018. 7(11): 159.
45. Petrova B., Liu K., Tian C., et al. Dynamic redox balance directs the oocyte-to-embryo transition via developmentally controlled reactive cysteine changes. *Proc. Natl. Acad. Sci. U. S. A.*, 2018. 115(34): E7978-e7986.
46. Owusu-Ansah E., Banerjee U. Reactive oxygen species prime *Drosophila* haematopoietic progenitors for differentiation. *Nature*, 2009. 461(7263): 537-541.
47. Su B., Mitra S., Gregg H., et al. Redox regulation of vascular smooth muscle cell differentiation. *Circ. Res.*, 2001. 89(1): 39-46.
48. Jang Y.-Y., Sharkis S.J. A low level of reactive oxygen species selects for primitive hematopoietic stem cells that may reside in the low-oxygenic niche. *Blood*, 2007. 110(8): 3056-3063.
49. Rodríguez-Colman M.J., Schewe M., Meerlo M., et al. Interplay between metabolic identities in the intestinal crypt supports stem cell function. *Nature*, 2017. 543(7645): 424-427.
50. Brinkmann V., Reichard U., Goosmann C., et al. Neutrophil extracellular traps kill bacteria. *Science*, 2004. 303(5663): 1532-1535.
51. Cano Sanchez M., Lancel S., Boulanger E., et al. Targeting Oxidative Stress and Mitochondrial Dysfunction in the Treatment of Impaired Wound Healing: A Systematic Review. *Antioxidants (Basel)*, 2018. 7(8).
52. Harman D. Aging: a theory based on free radical and radiation chemistry. *J. Gerontol.*, 1956. 11(3): 298-300.
53. López-Otín C., Blasco M.A., Partridge L., et al. The hallmarks of aging. *Cell*, 2013. 153(6): 1194-1217.
54. Van Remmen H., Ikeno Y., Hamilton M., et al. Life-long reduction in MnSOD activity results in increased DNA damage and higher incidence of cancer but does not accelerate aging. *Physiol. Genomics*, 2003. 16(1): 29-37.
55. Yang W., Li J., Hekimi S. A Measurable increase in oxidative damage due to reduction in superoxide detoxification fails to shorten the life span of long-lived mitochondrial mutants of *Caenorhabditis elegans*. *Genetics*, 2007. 177(4): 2063-2074.
56. Van Raamsdonk J.M., Hekimi S. Superoxide dismutase is dispensable for normal animal lifespan. *Proc. Natl. Acad. Sci. U. S. A.*, 2012. 109(15): 5785-5790.
57. Kalyanaraman B., Cheng G., Hardy M., et al. Teaching the basics of reactive oxygen species and their relevance to cancer biology: Mitochondrial reactive oxygen species detection, redox signaling, and targeted therapies. *Redox Biol*, 2018. 15: 347-362.
58. Aggarwal V., Tuli H.S., Varol A., et al. Role of Reactive Oxygen Species in Cancer Progression: Molecular Mechanisms and Recent Advancements. *Biomolecules*, 2019. 9(11): 735.
59. Hornsveld M., Dansen T.B. The Hallmarks of Cancer from a Redox Perspective. *Antioxid Redox Signal*, 2016. 25(6): 300-325.
60. Wu S., Lu H., Bai Y. Nrf2 in cancers: A double-edged sword. *Cancer Med*, 2019. 8(5): 2252-2267.
61. Hosios A.M., Vander Heiden M.G. The redox requirements of proliferating mammalian cells. *J. Biol.*

Chem., 2018. 293(20): 7490-7498.

62. Glasauer A., Chandel N.S. Targeting antioxidants for cancer therapy. *Biochem. Pharmacol.*, 2014. 92(1): 90-101.

63. Hainaut P., Milner J. Redox modulation of p53 conformation and sequence-specific DNA binding in vitro. *Cancer Res.*, 1993. 53(19): 4469-4473.

64. Held J.M., Danielson S.R., Behring J.B., et al. Targeted quantitation of site-specific cysteine oxidation in endogenous proteins using a differential alkylation and multiple reaction monitoring mass spectrometry approach. *Mol. Cell. Proteomics*, 2010. 9(7): 1400-1410.

65. Buzek J., Latonen L., Kurki S., et al. Redox state of tumor suppressor p53 regulates its sequence-specific DNA binding in DNA-damaged cells by cysteine 277. *Nucleic Acids Res.*, 2002. 30(11): 2340-2348.

66. Augustyn K.E., Merino E.J., Barton J.K. A role for DNA-mediated charge transport in regulating p53: Oxidation of the DNA-bound protein from a distance. *Proc. Natl. Acad. Sci. U. S. A.*, 2007. 104(48): 18907-18912.

67. Wu G.S. The functional interactions between the p53 and MAPK signaling pathways. *Cancer Biol. Ther.*, 2004. 3(2): 156-161.

68. Son Y., Cheong Y.-K., Kim N.-H., et al. Mitogen-Activated Protein Kinases and Reactive Oxygen Species: How Can ROS Activate MAPK Pathways? *Journal of Signal Transduction*, 2011. 2011: 792639.

69. Matsuzawa A., Ichijo H. Redox control of cell fate by MAP kinase: physiological roles of ASK1-MAP kinase pathway in stress signaling. *Biochim. Biophys. Acta*, 2008. 1780(11): 1325-1336.

70. Nadeau P.J., Charette S.J., Landry J. REDOX reaction at ASK1-Cys250 is essential for activation of JNK and induction of apoptosis. *Mol. Biol. Cell*, 2009. 20(16): 3628-3637.

71. Templeton D.J., Aye M.S., Rady J., et al. Purification of reversibly oxidized proteins (PROP) reveals a redox switch controlling p38 MAP kinase activity. *PLoS One*, 2010. 5(11): e15012.

72. Nelson K.J., Bolduc J.A., Wu H., et al. H<sub>2</sub>O<sub>2</sub> oxidation of cysteine residues in c-Jun N-terminal kinase 2 (JNK2) contributes to redox regulation in human articular chondrocytes. *J. Biol. Chem.*, 2018. 293(42): 16376-16389.

73. Achanta G., Huang P. Role of p53 in Sensing Oxidative DNA Damage in Response to Reactive Oxygen Species-Generating Agents. *Cancer Res.*, 2004. 64(17): 6233-6239.

74. Chen K., Albano A., Ho A., et al. Activation of p53 by oxidative stress involves platelet-derived growth factor-beta receptor-mediated ataxia telangiectasia mutated (ATM) kinase activation. *J. Biol. Chem.*, 2003. 278(41): 39527-39533.

75. Driessens N., Versteyhe S., Ghaddab C., et al. Hydrogen peroxide induces DNA single- and double-strand breaks in thyroid cells and is therefore a potential mutagen for this organ. *Endocr. Relat. Cancer*, 2009. 16(3): 845-856.

76. Nadeau P.J., Charette S.J., Toledano M.B., et al. Disulfide Bond-mediated multimerization of Ask1 and its reduction by thioredoxin-1 regulate H<sub>2</sub>O<sub>2</sub>-induced c-Jun NH<sub>2</sub>-terminal kinase activation and apoptosis. *Mol. Biol. Cell*, 2007. 18(10): 3903-3913.

77. Sanchez-Prieto R., Rojas J.M., Taya Y., et al. A role for the p38 mitogen-activated protein kinase pathway in the transcriptional activation of p53 on genotoxic stress by chemotherapeutic agents. *Cancer Res.*, 2000. 60(9): 2464-2472.

78. Kurz E.U., Douglas P., Lees-Miller S.P. Doxorubicin activates ATM-dependent phosphorylation of multiple downstream targets in part through the generation of reactive oxygen species. *J. Biol. Chem.*,

2004. 279(51): 53272-53281.

79. Morgan B., Van Laer K., Owusu T.N., et al. Real-time monitoring of basal H<sub>2</sub>O<sub>2</sub> levels with peroxiredoxin-based probes. *Nat. Chem. Biol.*, 2016. 12(6): 437-443.

80. Chen X., Zhong Z., Xu Z., et al. 2',7'-Dichlorodihydrofluorescein as a fluorescent probe for reactive oxygen species measurement: Forty years of application and controversy. *Free Radic. Res.*, 2010. 44(6): 587-604.

81. Gutscher M., Sobotta M.C., Wabnitz G.H., et al. Proximity-based protein thiol oxidation by H<sub>2</sub>O<sub>2</sub>-scavenging peroxidases. *J. Biol. Chem.*, 2009. 284(46): 31532-31540.

82. Albrecht S.C., Barata A.G., Grosshans J., et al. In vivo mapping of hydrogen peroxide and oxidized glutathione reveals chemical and regional specificity of redox homeostasis. *Cell Metab.*, 2011. 14(6): 819-829.

83. Barata A.G., Dick T.P. In vivo imaging of H<sub>2</sub>O<sub>2</sub> production in *Drosophila*. *Methods Enzymol.*, 2013. 526: 61-82.

84. Belousov V.V., Fradkov A.F., Lukyanov K.A., et al. Genetically encoded fluorescent indicator for intracellular hydrogen peroxide. *Nat Methods*, 2006. 3(4): 281-286.

85. Bilan D.S., Pase L., Joosen L., et al. HyPer-3: a genetically encoded H(2)O(2) probe with improved performance for ratiometric and fluorescence lifetime imaging. *ACS Chem. Biol.*, 2013. 8(3): 535-542.

86. Markvicheva K.N., Bilan D.S., Mishina N.M., et al. A genetically encoded sensor for H<sub>2</sub>O<sub>2</sub> with expanded dynamic range. *Bioorg. Med. Chem.*, 2011. 19(3): 1079-1084.

87. Knoefler D., Thamsen M., Koniczek M., et al. Quantitative in vivo redox sensors uncover oxidative stress as an early event in life. *Mol. Cell*, 2012. 47(5): 767-776.

88. Niethammer P., Grabher C., Look A.T., et al. A tissue-scale gradient of hydrogen peroxide mediates rapid wound detection in zebrafish. *Nature*, 2009. 459(7249): 996-999.

89. Kritsiligkou P., Shen T.K., Dick T.P. A comparison of Prx- and OxyR-based H(2)O(2) probes expressed in *S. cerevisiae*. *J. Biol. Chem.*, 2021. 297(1): 100866.

90. Reddie K.G., Seo Y.H., Muse Iii W.B., et al. A chemical approach for detecting sulfenic acid-modified proteins in living cells. *Mol. Biosyst.*, 2008. 4(6): 521-531.

91. Akter S., Fu L., Jung Y., et al. Chemical proteomics reveals new targets of cysteine sulfenic acid reductase. *Nat. Chem. Biol.*, 2018. 14(11): 995-1004.

92. Leichert L.I., Gehrke F., Gudiseva H.V., et al. Quantifying changes in the thiol redox proteome upon oxidative stress in vivo. *Proc. Natl. Acad. Sci. U. S. A.*, 2008. 105(24): 8197-8202.

93. Sethuraman M., McComb M.E., Heibeck T., et al. Isotope-coded Affinity Tag Approach to Identify and Quantify Oxidant-sensitive Protein Thiols\*. *Mol. Cell. Proteomics*, 2004. 3(3): 273-278.

94. Fu C., Hu J., Liu T., et al. Quantitative analysis of redox-sensitive proteome with DIGE and ICAT. *J. Proteome Res.*, 2008. 7(9): 3789-3802.

95. Topf U., Suppanz I., Samluk L., et al. Quantitative proteomics identifies redox switches for global translation modulation by mitochondrially produced reactive oxygen species. *Nature Communications*, 2018. 9(1): 324.

96. Lowe O., Rezende F., Heidler J., et al. BIAM switch assay coupled to mass spectrometry identifies novel redox targets of NADPH oxidase 4. *Redox Biol*, 2019. 21: 101125.

97. Fuhrmann D.C., Wittig I., Brüne B. TMEM126B deficiency reduces mitochondrial SDH oxidation by LPS, attenuating HIF-1 $\alpha$  stabilization and IL-1 $\beta$  expression. *Redox Biol*, 2019. 20: 204-216.

98. Weerapana E., Wang C., Simon G.M., et al. Quantitative reactivity profiling predicts functional cysteines in proteomes. *Nature*, 2010. 468(7325): 790-795.
99. Rabalski A.J., Bogdan A.R., Baranczak A. Evaluation of Chemically-Cleavable Linkers for Quantitative Mapping of Small Molecule-Cysteine Reactivity. *ACS Chem. Biol.*, 2019. 14(9): 1940-1950.
100. Fu L., Li Z., Liu K., et al. A quantitative thiol reactivity profiling platform to analyze redox and electrophile reactive cysteine proteomes. *Nat. Protoc.*, 2020. 15(9): 2891-2919.
101. Poole L.B., Zeng B.B., Knaggs S.A., et al. Synthesis of chemical probes to map sulfenic acid modifications on proteins. *Bioconjug. Chem.*, 2005. 16(6): 1624-1628.
102. Paulsen C.E., Truong T.H., Garcia F.J., et al. Peroxide-dependent sulfenylation of the EGFR catalytic site enhances kinase activity. *Nat. Chem. Biol.*, 2011. 8(1): 57-64.
103. Ursini F., Maiorino M., Forman H.J. Redox homeostasis: The Golden Mean of healthy living. *Redox Biol*, 2016. 8: 205-215.
104. Sablina A.A., Budanov A.V., Ilyinskaya G.V., et al. The antioxidant function of the p53 tumor suppressor. *Nat. Med.*, 2005. 11(12): 1306-1313.
105. Itahana Y., Itahana K. Emerging Roles of p53 Family Members in Glucose Metabolism. *Int. J. Mol. Sci.*, 2018. 19(3).
106. Fourquet S., Guerois R., Biard D., et al. Activation of NRF2 by nitrosative agents and H<sub>2</sub>O<sub>2</sub> involves KEAP1 disulfide formation. *J. Biol. Chem.*, 2010. 285(11): 8463-8471.
107. Brigelius-Flohé R., Flohé L. Basic principles and emerging concepts in the redox control of transcription factors. *Antioxid Redox Signal*, 2011. 15(8): 2335-2381.
108. Schmidlin C.J., Dodson M.B., Madhavan L., et al. Redox regulation by NRF2 in aging and disease. *Free Radic. Biol. Med.*, 2019. 134: 702-707.
109. Kaelin W.G., Jr., Ratcliffe P.J. Oxygen sensing by metazoans: the central role of the HIF hydroxylase pathway. *Mol. Cell*, 2008. 30(4): 393-402.
110. Jiang B.H., Rue E., Wang G.L., et al. Dimerization, DNA binding, and transactivation properties of hypoxia-inducible factor 1. *J. Biol. Chem.*, 1996. 271(30): 17771-17778.
111. Hernansanz-Agustín P., Ramos E., Navarro E., et al. Mitochondrial complex I deactivation is related to superoxide production in acute hypoxia. *Redox Biol*, 2017. 12: 1040-1051.
112. Hamanaka R.B., Chandel N.S. Mitochondrial reactive oxygen species regulate hypoxic signaling. *Curr. Opin. Cell Biol.*, 2009. 21(6): 894-899.
113. Haase V.H. The VHL tumor suppressor: master regulator of HIF. *Curr. Pharm. Des.*, 2009. 15(33): 3895-3903.
114. Chan S.Y., Zhang Y.Y., Hemann C., et al. MicroRNA-210 controls mitochondrial metabolism during hypoxia by repressing the iron-sulfur cluster assembly proteins ISCU1/2. *Cell Metab.*, 2009. 10(4): 273-284.
115. Semenza G.L. HIF-1: upstream and downstream of cancer metabolism. *Curr. Opin. Genet. Dev.*, 2010. 20(1): 51-56.
116. Balamurugan K. HIF-1 at the crossroads of hypoxia, inflammation, and cancer. *Int. J. Cancer*, 2016. 138(5): 1058-1066.
117. Dansen T.B. Forkhead Box O transcription factors: key players in redox signaling. *Antioxid Redox Signal*, 2011. 14(4): 559-561.
118. Essers M.A., Weijzen S., de Vries-Smits A.M., et al. FOXO transcription factor activation by oxidati-

- ve stress mediated by the small GTPase Ral and JNK. *EMBO J.*, 2004. 23(24): 4802-4812.
119. Putker M., Madl T., Vos H.R., et al. Redox-dependent control of FOXO/DAF-16 by transportin-1. *Mol. Cell*, 2013. 49(4): 730-742.
120. Putker M., Vos H.R., van Dorenmalen K., et al. Evolutionary acquisition of cysteines determines FOXO paralog-specific redox signaling. *Antioxid Redox Signal*, 2015. 22(1): 15-28.
121. Klotz L.O., Sánchez-Ramos C., Prieto-Arroyo I., et al. Redox regulation of FoxO transcription factors. *Redox Biol*, 2015. 6: 51-72.
122. Kerr E.M., Gaude E., Turrell F.K., et al. Mutant Kras copy number defines metabolic reprogramming and therapeutic susceptibilities. *Nature*, 2016. 531(7592): 110-113.
123. Hornsveld M., Smits L.M.M., Meerlo M., et al. FOXO Transcription Factors Both Suppress and Support Breast Cancer Progression. *Cancer Res.*, 2018. 78(9): 2356-2369.
124. Xiao H., Jedrychowski M.P., Schweppe D.K., et al. A Quantitative Tissue-Specific Landscape of Protein Redox Regulation during Aging. *Cell*, 2020. 180(5): 968-983.e924.
125. Ishii T., Itoh K., Takahashi S., et al. Transcription factor Nrf2 coordinately regulates a group of oxidative stress-inducible genes in macrophages. *J. Biol. Chem.*, 2000. 275(21): 16023-16029.
126. Itoh K., Chiba T., Takahashi S., et al. An Nrf2/small Maf heterodimer mediates the induction of phase II detoxifying enzyme genes through antioxidant response elements. *Biochem. Biophys. Res. Commun.*, 1997. 236(2): 313-322.
127. de Keizer P.L., Burgering B.M., Dansen T.B. Forkhead box o as a sensor, mediator, and regulator of redox signaling. *Antioxid Redox Signal*, 2011. 14(6): 1093-1106.
128. Chandel N.S., Maltepe E., Goldwasser E., et al. Mitochondrial reactive oxygen species trigger hypoxia-induced transcription. *Proceedings of the National Academy of Sciences*, 1998. 95(20): 11715-11720.
129. Bogdanova Y.A., Schultz C., Belousov V.V. Local Generation and Imaging of Hydrogen Peroxide in Living Cells. *Curr. Protoc. Chem. Biol.*, 2017. 9(2): 117-127.





# *Chapter 2*

## **ROS induced p53 activation: DNA damage, redox signaling or both?**

Tao Shi and Tobias B. Dansen

Center for Molecular Medicine, Molecular Cancer Research, University Medical Center Utrecht, Universiteitsweg 100, 3584 CG Utrecht, The Netherlands.

Antioxidants & Redox Signaling

Volume 33, Number 12, 2020

DOI: 10.1089/ars.2020.8074

## Abstract

**Significance:** The p53 tumor suppressor has been dubbed the “guardian of genome” because of its various roles in the response to DNA damage such as DNA damage repair, cell cycle arrest, senescence and apoptosis, all of which are in place to prevent mutations from being passed on down the lineage. **Recent Advances:** Reactive oxygen species (ROS), for instance H<sub>2</sub>O<sub>2</sub> derived from mitochondrial respiration, have long been regarded mainly as a major source of cellular damage to DNA and other macro molecules. **Critical Issues:** More recently, ROS have been shown to also play important physiological roles as second messengers in so-called redox signaling. It is, therefore, not clear whether the observed activation of p53 by ROS is mediated through the DNA damage response, redox signaling or both. In this review, we will discuss the similarities and differences between p53 activation in response to DNA damage and redox signaling in terms of upstream signaling and downstream transcriptional program activation. **Future Directions:** Understanding whether and how DNA damage and redox signaling-dependent p53 activation can be dissected could be useful to develop anti-cancer therapeutic p53-reactivation strategies that do not depend on the induction of DNA damage and the resulting additional mutational load.

**Keywords:** p53; redox signaling; cancer therapeutics; cysteine oxidation; DNA damage

## Introduction

p53 activation in response to DNA damage induces various biological responses, including cell cycle arrest (which buys cells time for DNA damage repair), senescence and apoptosis when DNA damage cannot be repaired. Collectively these responses ensure that potentially oncogenic mutations are not passed on down the lineage and hence prevent the onset and development of tumors. It is therefore not surprising that a large fraction of cancers lack p53 expression altogether or carry p53 mutations that render the protein inactive. But tumors can also develop in the context of wild-type p53 or mutant p53 that does not have a complete loss of function (82), and triggering the endogenous response of p53 to DNA damage plays an important role in the molecular basis for several anti-cancer therapies. For example, DNA damage-inducing therapies like radiotherapy and chemotherapeutic agents can activate p53 and restore p53-dependent apoptosis in cancer cells (102,103). Note that not all benefits of radiotherapy and chemotherapy are elicited through p53, but in this review we will focus on the p53-dependent response. However, irradiation and chemotherapy also elicit adverse effects, such as causing damage to healthy tissue surrounding the tumor as well as the generation of additional mutations. This could eventually result in selection for cells with inactive p53 function that become resistant to the treatment, or the development of new tumors in previously healthy tissue. It would therefore be important to explore strategies that activate p53 in tumor cells with a minimum of collateral DNA damage and toxicity.

p53 has long been known to be activated in response to elevated reactive oxygen species (ROS) (56,101,111), and oxidative post-translational modification of its cysteines was

suggested to be implicated from early on (27,29,56,71,128). Endogenous ROS are formed for instance as a by-product of mitochondrial respiration and are, at physiological levels, the second messengers in so-called redox signaling: a form of signal transduction that revolves around oxidized cysteines as a PTM that regulate protein function (64,65).

Redox signaling is reversible: when the (local) cellular redox homeostasis has been restored the oxidized cysteines are reduced again mainly by the thioredoxin (TRX) and glutaredoxin (GRX) systems, both of which both depend on the availability of a reduced form of NADP+(NADPH) that is generated in, for instance, the Pentose Phosphate Pathway (PPP) and by Isocitrate Dehydrogenases in the cytosol and the mitochondria. The production of ROS by mitochondrial respiration and reduction of oxidized thiols by NADPH-dependent systems illustrates the tight link between ROS, redox signaling and cellular metabolism. Prolonged elevated production of ROS can lead to oxidative stress and cellular damage. Indeed, the most important ROS in redox signaling, hydrogen peroxide ( $H_2O_2$ ), has been shown to be capable of triggering the canonical DNA damage response pathways involved in both single and double stand breaks (44), and subsequent p53 activation and apoptosis (162). However, there is also evidence that redox signaling can activate p53 through upstream stress kinases such as c-Jun N terminal kinase (JNK) and this has also been implicated in p53 reactivation in some cancer therapies (142). p53 itself is also directly regulated by redox signaling as some of its cysteines are prone to oxidation. The sensitivity of p53 to cysteine oxidation has been the basis for the development of p53-specific, cysteine-directed alkylation agents aimed to stabilize mutant p53 (24). This would mean that p53 dependent cellular functions, including tumor suppression, might be re-activated in cells that are irresponsive to DNA damage signaling by engaging redox stress signaling to p53.

Most studies on p53 activation by ROS or redox signaling deploy  $H_2O_2$  treatment as a stimulus. But since  $H_2O_2$  also triggers DNA damage signaling, it is therefore often difficult to pinpoint whether the ensuing p53 activation can be attributed to the DNA damage response, to redox signaling dependent activation or both (**Fig.1**). In this review, we will summarize the evidence for differential regulation of p53 by DNA damage and redox signaling. Further, we will discuss how this knowledge could aid in the development of novel anti-cancer therapies that are aimed at reactivating p53 and eventually contributing to treatment efficacy and prevention of drug resistance.

## **p53 basics**

### *The p53 protein and regulation of its activity*

The human p53 protein is encoded by the TP53 gene on chromosome 17p13.1 and consists of six major domains: two intrinsically disordered N-terminal transactivation domains (TADs), a proline-rich domain (PRD), a central DNA-binding domain(DBD), and a tetramerization domain(TD) followed by an intrinsically disordered C-terminal regulatory domain (CTD) (83). Under basal conditions, p53 levels are kept low through the action of MDM2, an E3 ubiquitin

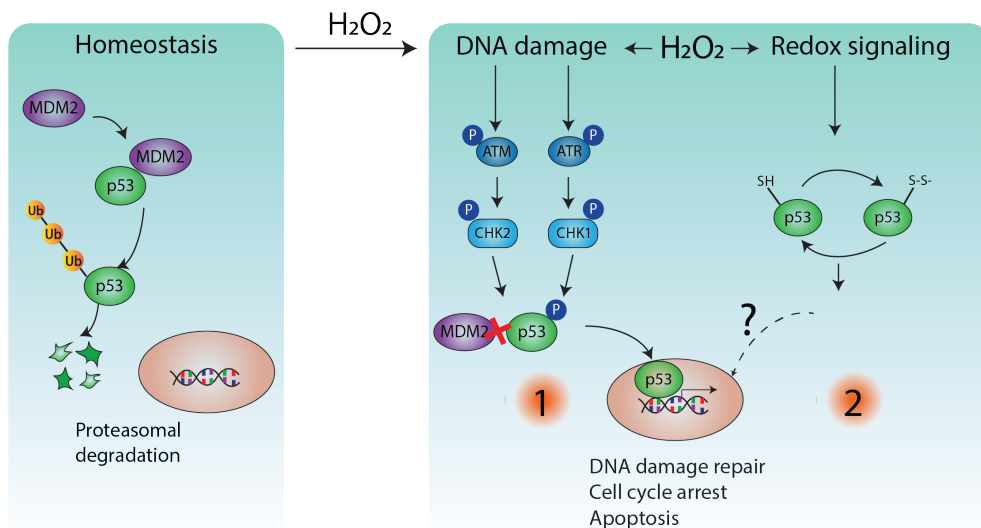


**Figure 1. Potential Mechanisms of p53 activation by H<sub>2</sub>O<sub>2</sub>**

Under basal conditions, p53 is rapidly degraded by the proteasome after polyubiquitination by MDM2 (Ub in yellow). Upon high levels of H<sub>2</sub>O<sub>2</sub>, p53 gets stabilized and activated, which could be mediated by H<sub>2</sub>O<sub>2</sub>-induced DNA damage (1), H<sub>2</sub>O<sub>2</sub>-mediated redox signaling (2), or both signaling pathways. Upon DNA damage, ATM and ATR kinases become active (for details see Figure 2), and in turn phosphorylate p53 directly or indirectly (mediated by CHK2 and CHK1), which stabilizes p53 by disrupting its binding to MDM2 (1). In redox signaling, oxidation of cysteines in signaling pathways upstream of p53 or in p53 itself lead to stabilization and activation of p53(2). Stabilized p53 accumulates in the nucleus and activates target genes which are involved in DNA damage repair, cell cycle arrest or apoptosis. ATM, Ataxia-Telangiectasia Mutated protein; ATR, Ataxia Telangiectasia and Rad3-related protein; CHK1, checkpoint kinase 1; CHK2, checkpoint kinase 2.

ligase that binds to the N-terminus of p53 and targets it for proteasomal degradation upon poly-ubiquitinylation (14,19,60). When cells encounter stress, p53 undergoes post-translational modification (PTMs) on certain residues, for example, phosphorylation on S15, 20 and 37 after DNA damage, that interrupt the interaction with MDM2, thereby facilitating p53 stabilization (143,187). Besides phosphorylation, other PTMs including acetylation, methylation, SUMOylation and NEDDylation have been shown to be involved in the regulation of p53 stability and function (14,100). For example, Lysine-acetylation of p53 inhibits MDM2-dependent ubiquitination and thus prevents p53 degradation (75,76). Acetylation on K120, located in the DNA binding domain, steers the p53 transcriptional program more towards apoptosis (155). In addition, methylation on K370, K372 and K382 can augment (69) or inhibit p53 (141) function depending on the site modified.

#### *Transcriptional targets of p53*

p53 transactivates its target genes by binding to a specific responsive element (RE) within the promoter or other regulatory regions. Generally, the responsive element is composed

of two copies of the palindromic consensus sequence PuPuPuC(A/T)(A/T)GPyPyPy, separated by 0-13 bp (46). p53 transcriptionally regulates a large amount of target genes that are implicated in various biological processes that contribute to its function as a tumor suppressor, including DNA damage repair, cell cycle arrest, senescence and apoptosis (131). But tumor suppression is likely not the original function of p53, since homologs can be found in organisms that do not get cancer like the roundworm *C. elegans*, and the unicellular choanoflagellae (10). Indeed, p53 is also involved in processes like cellular metabolism and in some cases p53 actually contributes to the survival of cells, including tumor cells (4). Of relevance for the topic of this review, p53 has a number of transcriptional targets that are directly or indirectly involved with redox homeostasis (see Feedback between p53-dependent transcription and redox and oxidative damage signaling section). What downstream targets are transcribed upon p53 activation depends on the cell type, but may also vary depending on the type of cellular stress (7). This suggests that transcriptional target regulation could also depend on specific cofactors or chromatin status.

### *p53 status in cancer*

Altered p53 function, be it enhanced or decreased, has been implicated in several diseases including for instance the age-related Huntington's (8), Parkinson's (18) and Alzheimer's (39) diseases. For this review we will focus on the role of p53 in cancer, but we do not exclude that the described molecular mechanisms of p53 regulation may be of relevance in other diseases or in healthy tissue.

Because of its involvement in multiple tumor suppressive mechanisms, loss of p53 wild-type function is widespread in cancer. Inactivation of p53 helps to evade growth arrest, blocks apoptosis and allows DNA mutations to accumulate that could benefit further tumor development: all of which are Hallmarks of Cancer as outlined by Hanahan & Weinberg (58). p53 inactivation may occur through three general mechanisms: loss of p53 expression altogether, inactivating mutations in the p53 gene itself or the impairment of signaling pathways regulating p53 activity. Approximately 95% of the mutations that hamper p53 function found in cancer are located in the core DNA-binding domain (55), 75% of which are missense mutations that result in loss of p53 wild-type function (125). These mutations can be classified into two categories: contact and structural mutations. Contact mutations disturb the p53 DNA binding affinity but have little effects on p53 structure and folding. Structural mutations grossly affect p53 folding and function and/or lead to destabilization of the entire protein (116). In addition to loss of tumor suppressive function, so called p53 gain-of-function (GOF) variants are found in cancer, which confer the protein with oncogenic features that contribute to enhanced proliferation or that promote metastasis (98,120). It may however be difficult to distinguish whether these features are the direct result of the p53 mutation or the consequence of another underlying oncogenic mutation that becomes apparent in the absence of normal p53 function. The inactivation of wild-type p53 is often caused by the overexpression of MDM2 (113) and MDM4 (95) or loss of the activity of its inhibitor

ARF (140). A large fraction of cancers carries p53 mutations or display loss of p53 response despite the presence of wild type p53. Reactivation of p53 or restoration of the wild-type activity in p53 mutants could therefore be promising treatments in those tumors (20).

## **DNA damage response (DDR) signaling to p53**

### *DNA damage occurrence and repair*

DNA damage occurs thousands of times every day in each cell, and oxidative damage is a major contributor (153). Mitochondrial respiration is often cited as an endogenous source of oxidative DNA damage (57,107). It is however unlikely that highly reactive molecules make their way from the mitochondria into the nucleus without reacting with biomolecules en route. Indeed, experimental evidence suggests that mitochondria-derived ROS does not lead to oxidation of proteins in the cytoplasm (47,115), suggesting that ROS production and clearance is compartmentalized within the cell as reviewed by for instance (53,85,159). It would therefore may be more likely that mitochondrial ROS leads to oxidation of free nucleotides in the cytoplasm that are then later incorporated in RNA and DNA. Oxidative DNA-damage may also derive from ROS producing enzymes that reside within the nucleus, like for instance NOX4 (91) and the chromatin remodeler LSD1 (124). Exogenous sources of DNA damage include UV and ionizing radiation and environmental mutagens (**Fig.2**). In the case of cancer, treatment with radiotherapy or chemotherapy is also an important source of DNA damage. Various damage types can be induced by these insults, including 8-OHdG (8-hydroxy-2'-deoxyguanosine) from oxidative damage, abasic sites (also known as AP sites), single strand breaks (SSBs), double strand breaks (DSBs), and DNA adducts. Among those, DSBs are particularly detrimental as this may lead to loss of genetic material or aberrant fusion of broken chromosomes that can result in oncogenic translocations. To deal with DNA damage and maintain genomic integrity, an elaborate network consisting of a plethora of protein kinases and other regulators is in place that detects the damage and signals to downstream transcription factors, including p53, to ensure an appropriate response. This network is referred to as the DNA damage response (DDR). Activation of the DDR induces cell cycle arrest and activates repair systems to repair damaged DNA (67). Generally, six repair pathways counteract against different types of DNA damage: base excision repair (BER), mismatch repair (MMR), nucleotide excision repair (NER), translesion DNA synthesis (TLS), nonhomologous end joining (NHEJ), and homologous recombination (HR) (156). The DDR also initiates apoptosis to eliminate damaged cells in case the damage is not repaired in time (67). If DNA damage cannot be successfully repaired, mutations can persist in the genome and passed on down the lineage when cells are proliferating, increasing the risk of mutation accumulation in genes like oncogenes and tumor suppressors that could lead to tumor onset and progression. For a more extensive description of DNA damage signaling and repair we would like to refer to the several excellent reviews that have been written on this topic (156). A brief overview touching upon some key aspects in the context of p53 is given below.

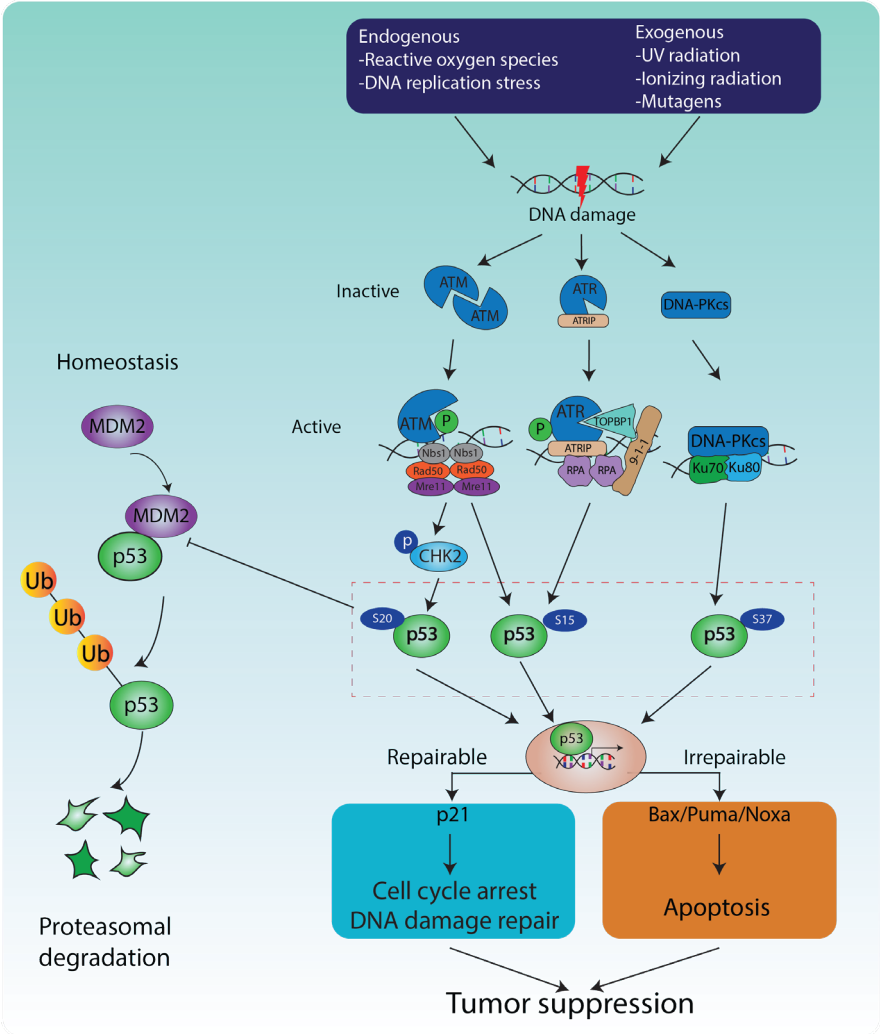


**Figure 2. p53 activation by DNA damage**

DNA damage can be induced by either endogenous or exogenous sources (indicated in dark blue box). DNA damage-induced p53 activation is dependent on three members of phosphatidylinositol 3-kinase-like kinase (PIKK) family: ATM, ATR and the DNA-PK complex. The inactive ATM dimer rapidly monomerizes and becomes active upon DNA double strand breaks, by binding to the MRN complex and DNA. ATM undergoes autophosphorylation on Ser1981 which further activates it, leading to phosphorylation of p53 on Ser15 and indirectly on Ser20 which is mediated by CHK2. ATR and its cofactor ATRIP become active by DNA single strand breaks bound by the TOPBP1, RPA and 9-1-1 complex. ATR also undergoes autophosphorylation on Thr1989 and phosphorylates p53 on Ser15. DNA-PKcs is activated by DNA double strand breaks and the Ku70/80 heterodimer. Active DNA-PKcs phosphorylates p53 on Ser37. All of these phosphorylations blocks MDM2 binding to p53 and thereby facilitate p53 stabilization and activation. p53 could transactivates multiple target genes that are involved in cell cycle arrest, DNA damage repair and apoptosis. DNA-PKcs, DNA-dependent protein kinase catalytic subunit; RPA, replication protein A; ATRIP, ATR-interacting protein; TOPBP1, topoisomerase II-binding protein 1.

### *Oxidative DNA damage and repair*

Oxidative DNA damage results from direct modification by ROS and other oxidizing agents, including hydroxyl radicals, one-electron oxidants and singlet oxygen (25). 8-oxo-2'-deoxyguanine (8-oxo-dG, also named 8-OHdG) is the most common oxidation-derived DNA lesion. Incorporation of 8-oxo-dG leads to pairing with adenine rather than with cytosine, resulting in mutations after DNA replication. Generally, 8-oxo-dG is repaired by the base excision repair (BER) pathway, after the enzyme Oxoguanine glycosylase 1 (OGG1) has removed 8-oxo-dG from the DNA (Reviewed in (138)). MutT homolog 1 (MTH1) and mutY homolog (MYH) are involved in removal of 8-oxo-dG from the nucleotide pool, preventing its incorporation in DNA (3). Higher levels of 8-oxo-dG have been observed in various cancers and inhibitors of OGG1 (43,77) and MTH1 (50,70,173) are being developed with the idea to use increased oxidative DNA damage and ensuing cell death as anti-cancer therapy. Indeed, targeting BER combined with DNA damaging-agents has shown synthetic lethality in cancer cells (168).

### *p53 activation by DNA damage*

DDR signaling downstream of the different types of DNA damage depends largely on two kinase networks, that both signal to eventually stabilize p53 (**Fig. 2**). Ataxia-Telangiectasia Mutated protein (ATM) occurs as a noncovalent homodimer in an inactive state under basal conditions. Upon DNA DSBs, the ATM dimer will rapidly monomerize and become active, which is promoted by the MRN complex (Mre11, Rad50, and Nbs1 (Nibrin) and DNA. Activation induces autophosphorylation on Ser1981 in the FAT domain. The activated monomer can directly phosphorylate p53 on Ser15, but will also activate CHK2, which in turn phosphorylates p53 at Ser20 (108) (**Fig. 2**). ATR and its cofactor ATRIP become activated by single stranded DNA and SSBs bound by TOPBP1, RPA and the 9-1-1 complex (114). Like ATM, ATR undergoes autophosphorylation on a threonine residue in the FAT domain (T1989) and subsequently becomes active and phosphorylates its substrates, including p53 Ser15 (**Fig. 2**). Phosphorylation of p53 on Ser15 leads to p53 stabilization by disrupting the interaction with MDM2 and thereby blocks p53 ubiquitination and proteasomal degradation. Both p53 phosphorylation on Ser15 and protein stabilization occurs rapidly upon DNA damage, and can be detected within minutes by Western blotting or immunofluorescence staining (15,87,174). Additionally, the DNA-dependent protein kinase (DNA-PK) complex, which consists of DNA-PKcs and the Ku70/80 heterodimer, phosphorylates p53 on Ser37 upon DNA strand breaks (114,176). The latter also facilitates p53 activation upon DNA damage through hindering the inhibitory effect of MDM2(143). Besides serine phosphorylation as a means to facilitate p53 activation upon DNA damage, lysine acetylation also positively regulates p53 activation by destabilizing the MDM2-p53 interaction and enhancing p53 transcriptional response upon DNA damage (76,134). Generally, DNA damage-activated p53 accumulates in the nucleus (104,187) and induces the transcription of many target genes involved in the DNA damage response (e.g. *GADD45a*), cell cycle arrest



or senescence (e.g. p21), and apoptosis (e.g. Bax, Noxa and Puma). The main players in DDR signaling are outlined in **Fig. 2**.

The tumor suppressive function of p53 has been attributed to combinations of these responses (cell cycle arrest, DNA repair, senescence and apoptosis). However, this concept is challenged by studies showing that p53-dependent apoptosis in response to DNA damage is dispensable for its tumor suppressive function (35,63). Both studies showed that p53 status during radiation treatment had no effect on the responsiveness of a lymphoma model. Instead, p53-activity was needed to combat tumor outgrowth long after the DDR was inactivated again. In line with this, mice that lack of p21, Puma or Noxa do not phenocopy p53 knockout mice in the development of thymic lymphoma, supporting the view that cell cycle arrest and apoptosis might not be the only p53-dependent tumor suppressive functions (161). Mechanisms underlying p53 in tumor suppression could also be context dependent. For example, it has been observed that Puma and Noxa deficiency enhanced tumorigenesis in Myc-induced lymphomagenesis (110). Meanwhile, this study also demonstrated that tumor progression induced by loss of both genes was not as dramatic as that caused by loss of one allele of p53, suggesting that indeed non-apoptotic functions of p53, for instance its role in metabolism (78), could be involved in its tumor suppressive role (110). Collectively, the role of p53 in tumor suppression might not be mediated only by the DNA damage response, but probably depends on specific target genes and programs in different cellular contexts.

## Redox signaling and p53

### *Endogenous ROS generation and scavenging*

Reactive oxygen species (ROS), such as superoxide anions ( $O_2^{\cdot-}$ ), hydroxyl radicals ( $\cdot OH$ ) and hydrogen peroxide ( $H_2O_2$ ) are highly reactive substances that can be generated by endogenous processes in the cell, including mitochondrial respiration (117) and NADPH oxidases like NOX2 and NOX4 that generate  $O_2^{\cdot-}$  by catalyzing electron transfer from NADPH to molecular oxygen upon for instance growth factor receptor activation (reviewed in (146)). The radical superoxide ( $O_2^{\cdot-}$ ) is rapidly dismutated to the more stable  $H_2O_2$  by superoxide dismutases (SOD). Hydrogen peroxide is subsequently cleared by the action of peroxiredoxins (PRDXs) and glutathione peroxidases (GPXs) in the cytosol and other cellular compartments and catalase in peroxisomes. Several excellent reviews on the sources and clearance of ROS are available, see for instance (146). Hydrogen peroxide can form hydroxyl radicals in the presence of iron ( $Fe^{2+}$ ) in the Fenton reaction. Hydroxyl radicals are extremely reactive and short-lived and induce lipid peroxidation and subsequent ferroptosis, which can be prevented by the action of the selenoprotein GPX4 (73).

Two robust reduction systems are in place to maintain cellular redox homeostasis: the TRX and the glutathione (GSH) systems. TRX catalyzes the reduction of disulfides that form between cysteine thiols in proteins upon oxidation. An intramolecular disulfide is formed in this process linking the cysteines in the TRX CXXC motif. Oxidized TRX, in turn,

is recycled by the selenoprotein thioredoxin reductase (TRXR) at the expense of NADPH. The glutathione system uses a set of enzymes that use the highly abundant, thiol-containing atypical tripeptide GSH to quench oxidation and to reduce non-structural disulfides, thereby forming oxidized GSH (GSSG). The glutathione system. Like the TRX system, also depends eventually on the oxidation NADPH to NADP<sup>+</sup> for its recycling. It has been proposed that the high glucose uptake of tumor cells even when ample oxygen is present (known as the Warburg effect) might not be related to a high demand in ATP production, but rather to the need for keeping the redox state in check through production of NADPH in the Pentose Phosphate Pathway (96).

### *Redox signaling*

The thiols in protein cysteine side chains can be oxidized to form a range of post-translational modifications, that can either activate, modify or inactivate protein function (64). For the purpose of this review we focus on redox signaling initiated by ROS, but would like to point out that redox signaling is also controlled by modification of cysteines by reactive nitrogen species (1) and reactive sulfur species (51). Reversible, rather than irreversible, thiol oxidation is likely the most important for signaling purposes because it is important to be able to switch a cascade on and off. Direct oxidation of thiols by hydrogen peroxide results in formation of Cysteine sulfenic acid (-SOH), which is regarded highly instable, although chemical modification with dimesone-based probes are being used for its detection (62,182). Sulfenic acid rapidly reacts with nearby thiols to condense to a disulfide, which can then be reversed by the action of TRX or GRX. When sulfenic acid reacts further with H<sub>2</sub>O<sub>2</sub> it can form sulfinic acid (-SO<sub>2</sub>H) and sulfonic acid (-SO<sub>3</sub>H). Whereas sulfinic acid can be reduced by Sulfiredoxin1 (SRX1) (13,28) at the expense of ATP, sulfonic acid can no longer be reduced in vivo. It was long thought that only peroxiredoxins would form sulfinic acids (see also below), but a recent study using a novel chemical approach detected many more sulfinic acid modified proteins, the biological relevance of which can now be started to be elucidated (2). Several protein kinases like JNK and p38MAPK are regulated upstream by redox modifications, meaning that redox signaling and 'classical' signal transduction by phosphorylation are intertwined.

### *Oxidative stress versus redox signaling*

ROS were long considered to be only harmful by-products of mitochondrial respiration and detrimental to cells. In fact, the free radical theory of aging (59) put ROS as the central cause of aging; a theory that is now outdated but still popular by the general public. Indeed, ROS can cause damage to biomolecules, including DNA, but at physiological levels ROS are also involved in redox signaling as explained above. Redox signaling has been shown to play vital roles in the regulation of various fundamental biological processes, including stem cell self-renewal, cell cycle progression and tissue regeneration (64). However, the boundary between oxidative stress and redox signaling is not very clear, and unfortunately in the literature terms like ROS, oxidative stress, free radicals, redox stress and so on are

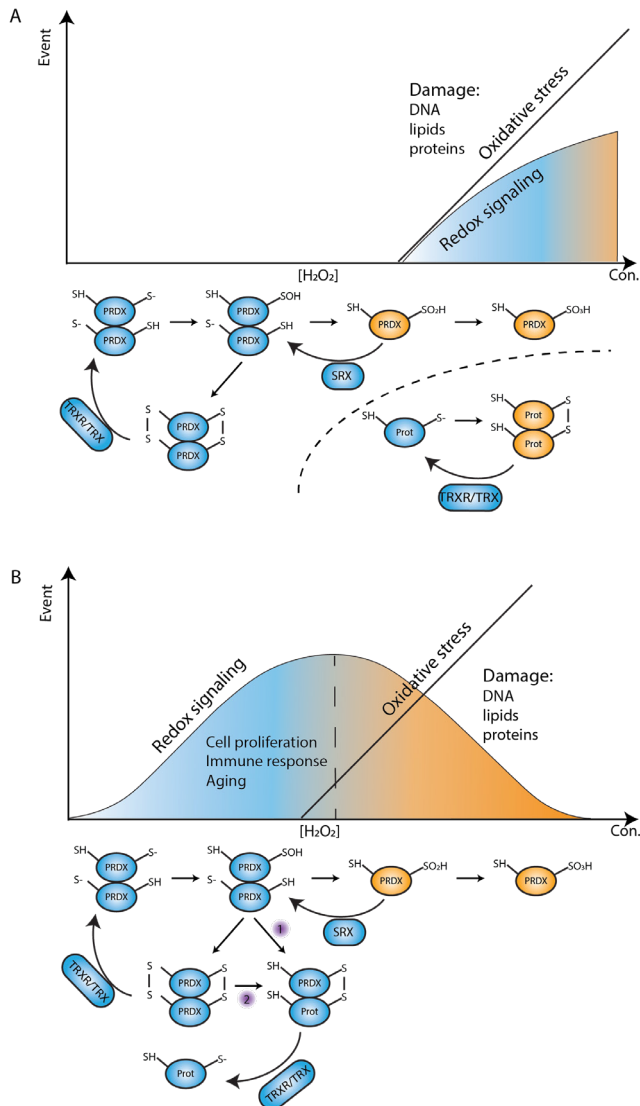


**Figure 3. Two Peroxiredoxin-dependent models for defining oxidative stress versus redox signaling.**

**(A)** The Flood-gate model. At very low [H<sub>2</sub>O<sub>2</sub>], Peroxiredoxins (PRDX) scavenge all H<sub>2</sub>O<sub>2</sub> and no damage or redox signaling occurs. With the increase of [H<sub>2</sub>O<sub>2</sub>], PRDX undergoes hyperoxidation to the sulfinic acid form, which is less easily slowly recycled by SRX, thereby leading to a local build-up of H<sub>2</sub>O<sub>2</sub> that oxidizes biomolecules to initiate redox signaling and oxidative stress more or less at the same time

**(B)** The PRDX Relay model. At very low [H<sub>2</sub>O<sub>2</sub>], PRDX is oxidized but transfers the oxidation to target proteins by two possible mechanisms (1 and 2). When H<sub>2</sub>O<sub>2</sub> levels are so high, or the TRX system is insufficient to reduce PRDX, PRDX becomes overoxidized to the sulfinic acid and sulfonic acid form. This results in shut down of redox signaling, H<sub>2</sub>O<sub>2</sub> levels can begin to rise leading to oxidative stress and damage. PRDXs, peroxiredoxins; TRX, thioredoxin; TRXR, Thioredoxin Reductase; NADPH, Nicotinamide adenine dinucleotide phosphate; SRX, Sulphiredoxin.

frequently being used seemingly at random. What further complicates matters, is that many statements regarding ROS levels are based on experiments in tissue culture systems, using methods that are not very sensitive. Only since a couple of years tools are available that are capable of detecting endogenous, steady state levels of  $H_2O_2$  (112,115). On top of that, treatment with ROS modulating agents at levels that are overtly toxic in one cell type might be harmless in another, and it may be difficult, if not impossible, to attribute observed effects to redox signaling or to oxidative stress. It is therefore good to keep in mind that when this review mentions low or high levels of ROS, this is meant as a comparison within one and the same model system, where 'low' represents (near) endogenous, unperturbed levels, and 'high' levels are associated with for instance exposure to exogenous oxidants or depletion of the antioxidant system, for instance in response to treatment with compounds, genetic approaches or withdrawal of metabolites. A definition of what levels of  $H_2O_2$  can be considered oxidative stress and what redox signaling has been proposed by Sies et al. (146). The field is also not on one line about whether ROS induced redox signaling and oxidative damage are part of the same continuum or whether these phenomena occur in a biphasic fashion, as explained below.

$H_2O_2$  in the form of  $H_2O_2$  is considered the most important species for intracellular signaling (165), because superoxide anions and hydroxyl radicals are considered too reactive and short lived to be able to confer specificity and  $H_2O_2$  is the ultimate product of superoxide anions. In the subsequent discussion, we will mainly focus on  $H_2O_2$ -mediated redox signaling and oxidative stress.

The high abundance and reactivity of the PRDXs make these proteins likely to react first when  $H_2O_2$  is present in the cell. This means that peroxide levels probably remain low in cells as long as the NADPH-dependent TRX system is able to recycle peroxiredoxins fast enough. PRDXs can also become hyperoxidized to the sulfinic acid ( $-SO_2H$ ) form, which requires SRX for recycling, but this process is relatively slow, and might confer local build-up of  $H_2O_2$ . It has been proposed that it is this build-up of  $H_2O_2$  upon overoxidation of PRDX what starts redox signaling in the so-called flood-gate model (**Fig. 3A**) (129,178). Such a model would mean that at low  $[H_2O_2]$  there is no signaling, until there is overoxidation of PRDX, and that from  $[H_2O_2]$  higher than that signaling and damage would roughly occur at the same time, because the intrinsic reactivity of most cysteine thiols is not much higher than that of other biomolecules like DNA and unsaturated fatty acids. More recently, however, it has been shown that oxidized PRDX can facilitate the oxidation of client proteins in a redox relay (**Fig. 3B**), where it transfers the oxidation to client proteins (41,130,148,150,151,166). This is an attractive explanation for how intrinsically unreactive protein thiols can become oxidized in response to low  $[H_2O_2]$ , as is observed in numerous proteomics studies. In this model redox signaling starts at very low  $[H_2O_2]$ : sufficient to oxidize PRDX. Redox signaling would then gradually change to (DNA) damage signaling when more PRDX molecules become overoxidized and  $H_2O_2$  is able to escape their scavenging function (**Fig. 3B**). Such a model is in agreement with observations in a complete SOD knockout *C. elegans* worm,

that showed that a redox signal conveyed by low  $[H_2O_2]$  levels is required for lifespan extension, but that higher levels are detrimental (163). The aforementioned concentration-dependent effects of  $H_2O_2$  and the two models for how these would affect redox signaling versus oxidative damage are of relevance for the topic of this review. In the 'floodgate' model, low levels of  $H_2O_2$  would not activate p53 through redox signaling nor DNA damage, whereas higher levels would activate p53 simultaneously through redox signaling and the DNA damage response. In the (PRDX) relay model redox signaling dependent activation of p53 would already start at low levels of  $H_2O_2$  and DNA damage dependent activation would happen only at higher levels of  $H_2O_2$ . We would like to argue that in the relay model there would be more opportunity to regulate a differential response to more oxidizing conditions versus DNA damage.

Because of the concentration-dependent effects of  $H_2O_2$  triggering redox signaling, DNA damage signaling, or both simultaneously, it is not always clear how to dissect which effect can be attributed to what signaling mode. Furthermore, the concept of redox signaling is relatively unexplored in the field of cancer biology and in some studies might not have been considered as an explanation for the observed p53-dependent effects in response to  $H_2O_2$ . We propose that an approach that makes use of compounds that lower the reductive capacity rather than directly induce oxidation would be more informative to dissect how redox signaling activates p53. Potential candidates for such compounds are for instance inhibitors of the thioredoxin reductase like Auranofin, but also inhibitors of metabolic pathways that interfere with NADPH recycling. Treatment with these compounds would keep redox signaling to p53 initiated by endogenous  $H_2O_2$  longer in an 'on' state without exposure to excessive amounts of exogenous oxidants. As mentioned earlier, careful manipulation and assessment of the cellular redox state is not trivial. Therefore, careful controls are needed to check ROS levels and which signaling cascades (redox signaling and DNA damage signaling) are activated to what extent upon treatment with these compounds. Below we have outlined evidence that cysteine-oxidation dependent redox signaling controls p53 activity independent of the DNA damage response.

#### *Redox signaling upstream of p53*

Several studies have shown that signaling cascades upstream of p53 can be initiated or modulated by redox signaling (i.e. by reversible cysteine oxidation of key regulators in these signaling cascades). With the rapid developments in the field it is probably possible to find redox-regulated proteins in every signaling pathway in the cell in the literature, but here we will focus on redox signaling through ATM and the stress-activated protein kinases JNK and Mitogen-activated kinase (p38MAPK) pathways.

*Redox regulation of ATM.* As mentioned earlier, ATM is a kinase upstream of p53 that is activated when DNA double strand breaks (DSBs) occur. Activation of ATM upon exposure to oxidizing agents has been observed a long time ago (92). Although it is unquestionable that high levels of  $H_2O_2$  will lead to DSBs, it is not entirely clear whether levels of endogenously

generated  $H_2O_2$  are actually sufficient to do so (36,44). Furthermore, the high reactivity and abundance of Peroxiredoxins as described earlier begs the question as to how endogenous levels of  $H_2O_2$  would be able to travel from the site of production (e.g. mitochondria, ER or NOX at the plasma membrane) through the cytoplasm into the nucleus to directly oxidize the DNA. It might be that induction of DSBs by  $H_2O_2$  is often inferred from the assessment of ATM activity as evidenced by detection of its auto-phosphorylation or phosphorylation of its substrates like Chk2. However, Guo et al. (54) showed that ATM can be activated by  $H_2O_2$  in vitro in the absence of the MRN complex or DNA, suggesting that ATM activation by  $H_2O_2$  can occur independent of the DNA damage pathway.

Whereas DNA damage results in dissociation of the inactive, (non-covalent) dimer to the active monomeric form,  $H_2O_2$ -induced ATM activation results in the formation of active, disulfide-bond dependent dimers involving Cys2991(**Fig. 4**). Mutation of this cysteine results in loss of  $H_2O_2$ -induced ATM activity while retaining kinase activity in the presence of the MRN complex and DNA. In vivo, Guo et al. (54) also observed ATM autophosphorylation and phosphorylation of CHK2 and p53 upon a low level of  $H_2O_2$ , whereas  $\gamma$ H2AX and phospho-Kap1, markers that are widely used as markers of DNA damage, were not induced. Furthermore,  $H_2O_2$ -induced phosphorylation of p53 by ATM was blocked by antioxidant treatment, but not when ATM was activated in the presence of the MRN complex and DNA. These observations suggest that  $H_2O_2$  and DNA damage activate ATM through distinct mechanisms and with distinct outcomes and that an active ATM signaling cascade does not necessarily mean that DSBs are present. From the perspective of this review, it means that in principle redox signaling can activate ATM and p53 in the absence of DNA damage and hence without the risk of introducing novel mutations that could lead to cancer initiation or progression.

*Redox regulation of the JNK/p38MAPK pathways to p53.* The stress activated protein kinases JNK and p38MAPK play several roles in the context of tumor biology and treatment including the regulation of inflammation, survival, migration and differentiation (170). These functions may be both positively or negatively regulated, depending on the cell type and stimulus. Furthermore, there is cross talk between these pathways, making it sometimes difficult to pinpoint a certain response to JNK or p38MAPK, or both. Both kinases are regulated through their own set of scaffold proteins that assemble a cascade of mitogen-activated protein kinase kinase kinase (MAPKKK) (such as ASK1, MEKK1 and MEKK2/3), and mitogen-activated protein kinase kinases (MAPKK). JNK is activated by phosphorylation through MKK4 and MKK7 whereas MKK3 and MKK6 signal to p38MAPK (170). Activated JNK and p38MAPK phosphorylate several transcription factors, including p53, on [ST]P sites to mediate a cellular stress response. Depending on the study, phosphorylation by p38MAPK and/or JNK was found to occur in a stimulus-dependent manner on p53Ser15, Ser20, Ser33, Thr81 and Ser392 (121). Because the evidence for these phosphorylation events come from various independent studies and in light of the above described challenges in the interpretation of what amounts of ROS induce redox signaling versus oxidative damage, it

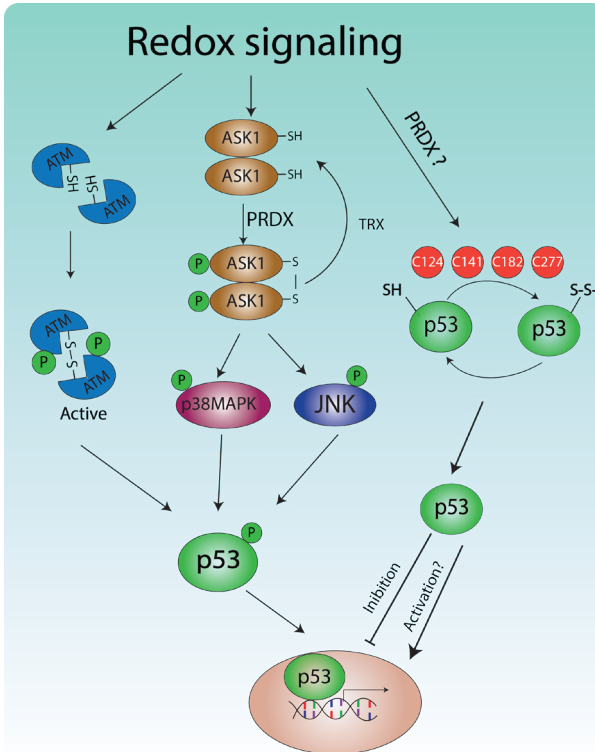


**Figure 4. Redox signaling to p53.** Several signaling pathways upstream of p53 or controlled by redox signaling. ATM forms active, disulfide-dependent dimers upon cysteine oxidation and phosphorylate p53 on Ser15. ASK-1 is oxidized in a PRDX-relay dependent fashion and the active, disulfide dependent dimer signals to JNK and p38MAPK, which in turn phosphorylate and thereby stabilize p53. Furthermore, cysteines in p53 itself have also been shown to be prone to oxidation, including C124, C141, C182 and C277. It is not fully understood how these redox modifications regulate p53 protein stability and activities, and whether or not a PRDX-relays play a role in mediating p53 oxidation. ASK-1: Apoptosis Signaling Kinase-1.

is not always clear how exclusive these modifications are for either p38MAPK or JNK and for either DNA damage or Oxidative challenges. Both the JNK and p38MAPK pathway are under the upstream control of the MAPKKK ASK-1, which is one of the first kinases in human cells that was shown to be regulated by the cellular redox state through thioredoxin activity (133). ASK-1 is an inactive dimer under normal conditions, but forms an active intermolecular disulfide-dependent homodimer upon oxidation of Cys250 (118). This intermolecular disulfide-dependent dimer is continuously being turned over by TRX (**Fig. 4**). More recently, Jarvis et al (79) showed that ASK-1 is also the first example of a PRDX-relay regulated protein in human cells. Oxidized PRDX1 forms a transient, disulfide dependent heterodimer with ASK-1 which was required for subsequent disulfide-dependent homodimerization of ASK-1 and p38MAPK and JNK activation. Another example of redox regulation of kinase signaling upstream of p53 is the S-glutathionylation of Cys238 of MEKK1, which inactivates its activity by hampering ATP binding, thereby preventing downstream activation of MKK4/7 and JNK (38).

#### *Redox-dependent modification of cysteines in p53*

Even though the intrinsic reactivity of the cysteines in p53 is much lower as compared to that of for instance cysteines in the catalytic centers of proteins like PRDX and TRX, several studies found that p53 itself is redox sensitive both in vitro and in vivo, as outlined

below (see also **Fig. 4**). Human p53 has ten cysteines (Cys124, 135, 141, 176, 182, 229, 238, 242, 275 and 277), all of which reside within its DNA binding domain (145). Three of these (Cys176, 238 and 242) coordinate a zinc atom together with His179 and hence are important to maintain the p53 structure (34). Mutation of any of these three cysteines results in a conformational change and loss of p53 DNA binding abilities (109,128). In vitro, p53 has been shown to be able to form intramolecular disulfide bonds between Cys182 and any of the three zinc-coordinating cysteines (Cys176, 238 and 242) accompanied by the loss of Zinc (137) and collapse of its normal structure. Since Cys176, Cys182, 229, 242 and 277 are predicted to be exposed on the surface of p53 based on its 3D structure (i.e. PDB ID 4HJE (32) or 2ADY (89)), these are likely more prone to oxidation as compared to buried cysteines. Indeed, by using a highly sensitive and reproducible oxidation analysis approach that makes use of multiple reaction monitoring mass spectrometry, Held et al. (61) quantified the site-specific cysteine oxidation sensitivity of endogenous p53 and found that Cys182 was particularly susceptible to oxidation upon treatment of cells with diamide (a thiol-directed oxidizing agent), whereas in vitro both Cys182 and Cys277 were potential targets of diamide. Cys182 is located within the H1 helix region that is involved in the tetramerization of p53. Cys182 has also been suggested to be S-glutathionylated, leading to tetramer dissociation (152). Another study showed that S-glutathionylation could also happen on Cys124 and Cys141 both upon DNA damage and oxidant exposure, leading to decreased p53 transcriptional activity, which can be restored by antioxidant treatment (167). This finding is somewhat surprising, since these two cysteines are not exposed on the surface of the protein, suggesting that S-glutathionylation of these residues occurs when the protein is (partly) unfolded.

#### *p53-dependent transcription in response to redox signaling*

As noted above, in vitro and in vivo experiments showed that oxidative modification of cysteines in p53 decreases its DNA-bind affinity and inhibits transcriptional activity by several mechanisms including loss of Zn-binding, conformational change, steric hindrance or impaired p53 tetramerization (49,56,123,152,167). Loss of zinc and the ensuing conformational change could be due to direct oxidation of p53 on the zinc coordinating cysteines (C176, C238 and C242) when relatively high amounts of oxidants are being used. However, other studies showed that reversible oxidation of Cys277 aids in the recognition of specific p53 response elements and thus in the activation of a different set of target genes in response to redox regulation (6,23,136). Cys277 is positioned in the major DNA groove and is, according to the crystal structure PDB ID 2ADY (89), located closest to the pyrimidine base that is paired with the first purine preceding the C in the 5'-PuPuPuC(A/T)(A/T)GPyPyPy-3' p53 binding motif (see **Fig. 5A,B**). That first purine preceding the C, which is a bit further away from Cys277, has been shown to be important in the differential regulation of p53 transcriptional targets under oxidizing conditions. For instance, binding of p53 to the *CDKN1A* promoter (encoding p21), which has an A at that position, is not affected by oxidizing conditions. Conversely, the *GADD45a* promoter has a G in that position (see



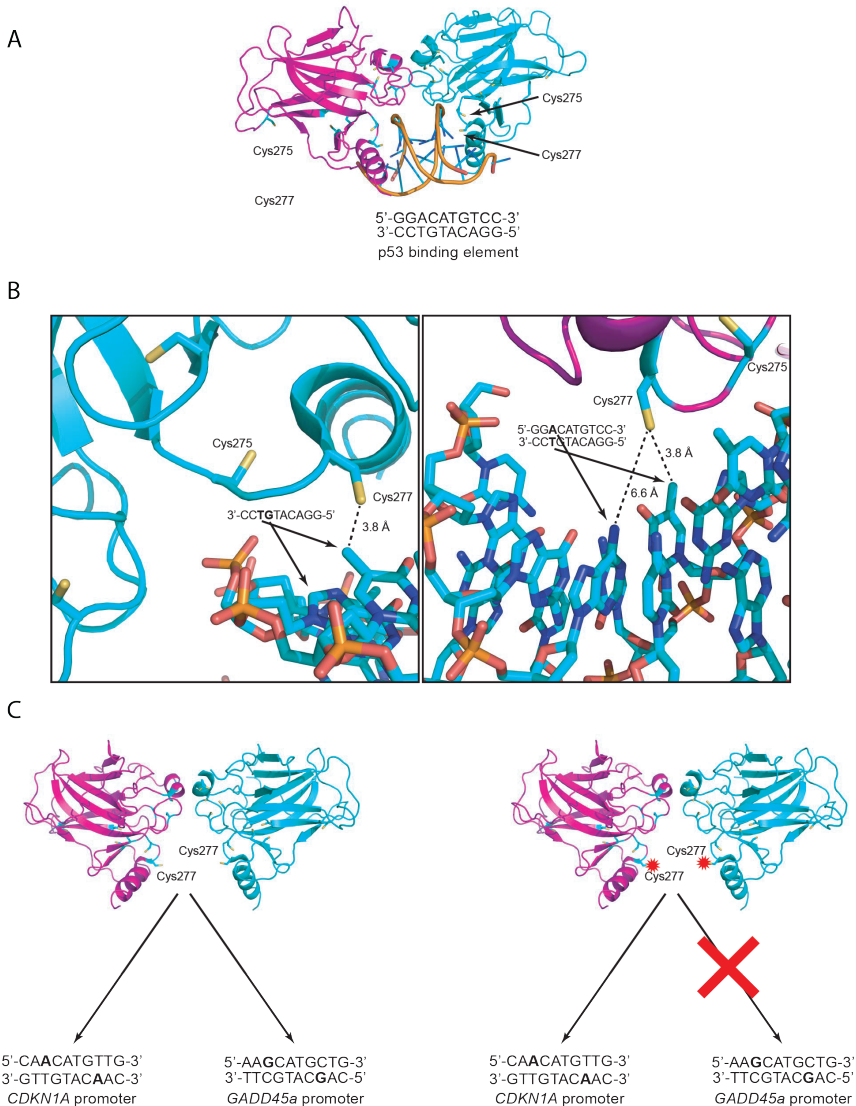


**Figure 5. Differential regulation of p53 targets in response to oxidizing conditions.**

(A) The crystal structure of a p53 homodimer bound to a consensus DNA sequence, based on PDB ID 2ADY (89), rendered by the authors using PyMol software. One monomer is indicated in green, the other in magenta. The positions of Cys275 and Cys277 close to the DNA are indicated. (B) Zoom in on the region near Cys275 and Cys277 and the p53-binding motif on the DNA. The two panels show the structure from a different angle. Note that Cys277 is closest to the DNA, and that the base-pair preceding the CATG motif (here A-T) is in closest proximity. (C) Oxidation of Cys277 has been shown to interfere with binding to p53 targets that have a G-C pair at the position preceding the CATG motif in their promoter (like GADD45a), but not with targets that have an A-T pair (like p21). The nature of the oxidative modification is currently not known, but it is unlikely that a large modification like glutathione would not affect the p21 promoter binding sequence as well.

**Fig. 5C**) and binding of p53 is inhibited upon oxidant treatment. Although different studies (23) using completely different techniques find the same differential regulation of *CDKN1A* and *GADD45a* promoter binding by p53, it is not entirely clear what the mechanism for this differential regulation is. Buzek et al. (23) performed pull-down assays using synthetic oligonucleotides and found less binding of p53 to the synthetic *GADD45a* binding element in lysates from cells treated with UV up to 24 hours prior to lysis, whereas binding to the *CDKN1A* binding element was not affected. This result suggests that the effect is mediated through modification of p53, and not oxidation of the p53 binding element, since the synthetic oligonucleotides were not present at the time of UV irradiation. Work from the Barton group (6,136) has suggested that cysteines in p53 are oxidized through so called DNA charge transfer, and that this is mediated by oxidation of the G in the *GADD45a* promoter p53 binding element, which is an A in the *CDKN1A* promoter. It is not entirely clear whether or to what extent DNA charge transfer occurs within cells, and whether this would be an effective strategy for differential regulation of p53 transcriptional targets through oxidation of a specific G. The p53 structure bound to the DNA in (**Fig. 5B**) might give some hints on the nature of the oxidative modification on p53 that could be at the basis of the differential target regulation. There is not much space between Cys277 and the DNA, making smaller modifications like for instance sulfenic acid more likely than large ones like Glutathionylation, which would probably also interfere with *CDKN1A* promoter binding. Disulfide formation with Cys275 would likely have a similar effect, although it is not clear how this would change the conformation of p53 precisely. Schaefer et al. (136) concluded that disulfide formation between Cys275 and Cys277 determines the differential regulation of p53 transcriptional targets upon oxidation, but the assay used does not discriminate disulfides from other forms of reversible Cysteine oxidation. Held et al. (61) determined reversible cysteine oxidation of p53 extracted from cells treated with the thiol specific oxidant diamide and found that Cys277 was much more sensitive to oxidation than Cys275, excluding extensive disulfide formation between these residues. Collectively, all these studies show differential regulation of p53 transcriptional targets, which depends both on oxidation of Cys277 in p53 and a G in the p53 binding element.

Another way redox signaling could influence the choice of transcriptional targets of p53 can be through redox-dependent interactions with for instance transcriptional co-activators or chromatin remodelers like has been shown for FOXO transcription factors (40). This has however not been explored so far for p53.

*Differential transcriptional output in response to type of stress?* It has been suggested that p53 transactivates different target genes in response to DNA damage versus in response to redox signaling (139). However, many studies describing p53 target genes have only applied one type of stress in one cell line, often with little consensus between studies (48). Furthermore, differential gene regulation in response to redox signaling and/or DNA damage may not be black and white but rather a continuum. The latter might also be due to the fact that it can be difficult to expose cells to DNA damage in the absence of

redox signaling and vice versa, depending on the compounds used. It has been suggested that many DNA damage-based chemotherapeutic drugs, including doxorubicin, cisplatin, mitomycin, fluorouracil and bleomycin are associated with the induction of 'oxidative stress' and hence redox signaling (31,105,183). The mechanisms by which most anti-cancer drugs generate oxidizing conditions have not been fully understood, however, most of them do so both in cancer cells and healthy cells, and has been linked to drug toxicity and resistance (97,126,144,158). Some studies suggest that redox signaling induced p38MAPK activity towards p53 is required for the tumor suppressive effects of some DNA damaging compounds like cisplatin (17). The latter could suggest that activation of this pathway by redox signaling in the absence of DNA damage could be a strategy to activate p53 without the increasing the mutational load.

#### *Feedback between p53 dependent transcription and redox and oxidative damage signaling*

p53 transactivates several genes that encode for enzymes involved in both the production and clearance of ROS, although it is not always clear whether these are truly induced in response to only DNA damage or only in response to redox signaling. Furthermore, p53 transcriptional targets play several roles in cellular metabolism, and thereby influence redox signaling through for instance the regulation of ROS production in mitochondrial respiration, as well as NADPH recycling in the Pentose Phosphate Pathway. The regulation of Iron and GSH homeostasis by p53 contribute to the susceptibility to undergo ferroptosis. Many of the described effects of p53 on ROS production and scavenging, redox homeostasis and metabolism are cell-type-specific and may even seem to work in opposite directions, which makes it difficult to draw a clear, unambiguous picture. The main purpose of this review is to point out the differences and commonalities between redox signaling and DNA damage dependent upstream of p53 activation, but p53 target gene transcription may contribute to the regulation of the transition point from redox signaling to oxidative damage. We will therefore give a brief overview of some of the roles of p53 target genes in redox homeostasis, metabolism and oxidative (DNA) damage below.

*p53 transcriptionally regulates both pro- and antioxidant enzymes.* p53 drives the expression of several antioxidant enzymes including Glutathione Peroxidase (GPX1) (154), MnSOD (72) and Glutaredoxins (GRX3) (21), supporting ROS clearance and cell survival. Additionally, p53 increases GSH level by transcriptionally activating glutaminase 2 (GLS2) that catalyzes the conversion of glutamine to glutamate, which can be used for GSH biosynthesis (68). May be counterintuitively, p53 also transactivates pro-oxidant genes like p53-Induced Genes 3 and 6 (PIG3 and PIG6) that have been suggested to contribute to ROS-dependent cell death (122,127). Pro-apoptotic BAX and PUMA are involved in mitochondrial pore opening and the subsequent release of ROS contributes to apoptosis (122). The extent of induction of anti- and pro-oxidants seems dependent on the level of p53 activation (132), although it is not fully clear what the molecular mechanism behind this differential regulation may be.

*Metabolic regulation of redox homeostasis by p53.* Several excellent reviews on metabolic regulation by p53 (see for instance (93,94)). Contrary to its role as a tumor suppressor, it has been suggested that in some cases the role of p53 in metabolism actually may support cancer cells to adapt the harsh environments and thereby support tumor growth (reviewed in (169)). From the perspective of redox homeostasis, metabolic processes that play a role in the production and scavenging of ROS are of interest. In general, p53 seems to steer metabolism towards OXPHOS and away from glycolysis, and, in line with this, loss of p53 leads to a more glycolytic phenotype in cancer cells, which may underlie the so called “Warburg effect” (164). p53 lowers glycolysis through transcriptional downregulation of glucose transporters (GLUT1 and GLUT4) and thus inhibits glucose uptake (186). In addition, p53-induced TP53-induced glycolysis and apoptosis regulator (TIGAR) inhibits the activity of phosphofructokinase 1(PFK1), the enzyme that catalyzes the rate-limiting step in glycolysis and thereby shuttles glucose into the Pentose Phosphate Pathway (PPP) (11,12). Suppression of PFKFB3 by p53 has a similar effect. Conversely, p53 also has the ability to inhibit the PPP by directly inactivating its rate-limiting enzyme glucose-6-phosphate dehydrogenase (G6PDH) (81). NADPH, the key regenerator of both PRDX, TRX and GSH dependent redox homeostasis and ROS scavenging is recycled in the PPP, thereby directly linking transcriptional output downstream of p53 with its upstream activation by ROS, be it by redox signaling or (oxidative) DNA damage.

OXPHOS is an important source of endogenous ROS production, although the amounts produced depend greatly on mitochondrial health. p53 maintains mitochondrial health and promotes OXPHOS through the transcription of subunit1 cytochrome c oxidase (COX1) (119), Synthesis of Cytochrome c Oxidase 2 (SCO2) (106) and induction of AIF, a mitochondrial protein that facilitates the proper assembly and function of respiratory complex I (149,160) but that also doubles as an inducer of apoptosis when released from mitochondria (26). Moreover, p53 transcriptionally activates RRM2B to prevent mitochondrial DNA depletion syndrome, and mutations in RRM2B are a frequent cause of mitochondrial dysfunction (16).

Next to the above described effects on glycolytic pathways, p53 also plays a role in lipid metabolism, thereby providing an alternative source for the TCA cycle, to regenerate FADH<sub>2</sub> and NADH required for the Electron Transport Chain and OXPHOS dependent ATP production and thus supporting cell survival for instance under metabolic stress (172). p53 facilitates the transport of fatty acid to mitochondria through the induction of carnitine O-octanoyltransferase (CROT) expression (84), and promotes fatty acid oxidation (FAO) by inducing LPIN1 gene expression under nutrient limitation in a ROS dependent manner (5). Consistent with the role of p53 in enhancing lipid breakdown, p53 was shown to repress lipogenesis by inhibiting G6PD activity (81) and repression of SREBP1c, which otherwise transcribes several lipogenic enzymes (180).

*p53 and ferroptosis.* In the presence of iron, H<sub>2</sub>O<sub>2</sub> can form lipid peroxides in the Fenton reaction. This may switch ROS from a redox signal to a damage signal, because damage

by lipid peroxides is rapid and widespread. Iron-dependent lipid peroxidation plays a key role in ferroptosis, a programmed form of non-apoptotic cell death that proceeds through and depends on iron (hence the name). Ferroptosis is accompanied by DNA damage and ATM has been suggested to be involved in its regulation (30). There are two main pathways that inhibit ferroptosis: one involves GPX4 and hence depends on GSH (181), whereas the other, recently discovered pathway depends on Ferroptosis Suppressor Protein 1 (FSP1) and ubiquinone (42). p53 activity seems to have dual roles in the regulation of ferroptosis. We have already mentioned above that p53 regulates NADPH levels needed for GSSG reduction as well as GSH biosynthesis. But p53 also limits ferroptosis through the inhibition of the dipeptidyl- peptidase-4 (DPP4) in a transcription independent manner (179). Conversely, p53 downregulates of SLC7A11, a cystine/glutamate antiporter also known as xCT that also ensures the maintenance of sufficient GSH levels to keep GPX4 active, thereby promoting ferroptosis (80). For a more detailed description of the role of p53 in the regulation of ferroptosis see for instance (86). What is important for this review is that p53 can change ROS from a redox signal to a damage signal through the activation or inhibition of ferroptosis. This illustrates again that ROS levels, and whether these are merely involved in signaling or in damage are highly context dependent.

## **Exploiting redox-signaling-based p53 reactivation in cancer therapies?**

As mentioned in the introduction of this review, the p53-dependent DNA damage response is the molecular basis underlying many conventional cancer treatments including irradiation and chemotherapeutics. More than 20 years ago, p53-dependent apoptosis was found to be a determinant for tumor cell death upon DNA damage induction upon Adriamycin treatment (102). The therapeutic effects of other widely-used chemotherapeutics such as Cisplatin, doxorubicin and 5-FU have also been attributed to generation of DNA breaks and subsequent p53-dependent apoptosis (22,33,135,171,177)(Fig.6A).

### *Reactivation of p53 by MDM2 inhibition*

A downside of genotoxic treatments is that these may increase the mutational load of both the tumor and the surrounding tissue. The tumor might acquire mutations that enable therapy resistance and progression to a more aggressive cancer phenotype, whereas mutations in surrounding tissue could be the start of novel lesions (**Fig.6A**). With this in mind, efforts have been made to find compounds that would stabilize p53 without inducing genotoxic stress, for instance by disruption of the p53-MDM2 interaction. The most famous example of such a compound are the Nutlins, but others have been developed as well (88). Several clinical trials using MDM2 antagonists as combination therapy have been performed but none has gained FDA approval for cancer treatment so far (157,185). Although a number of those small molecules showed anti-tumor activity both in vitro and in vivo without major toxicity in normal tissue, several drawbacks have been predicted including selection for loss of wildtype p53, which could hamper also other therapeutic options and worsen the tumor phenotype (147). Another small molecule referred to as RITA (Reactivation of p53 and induction of

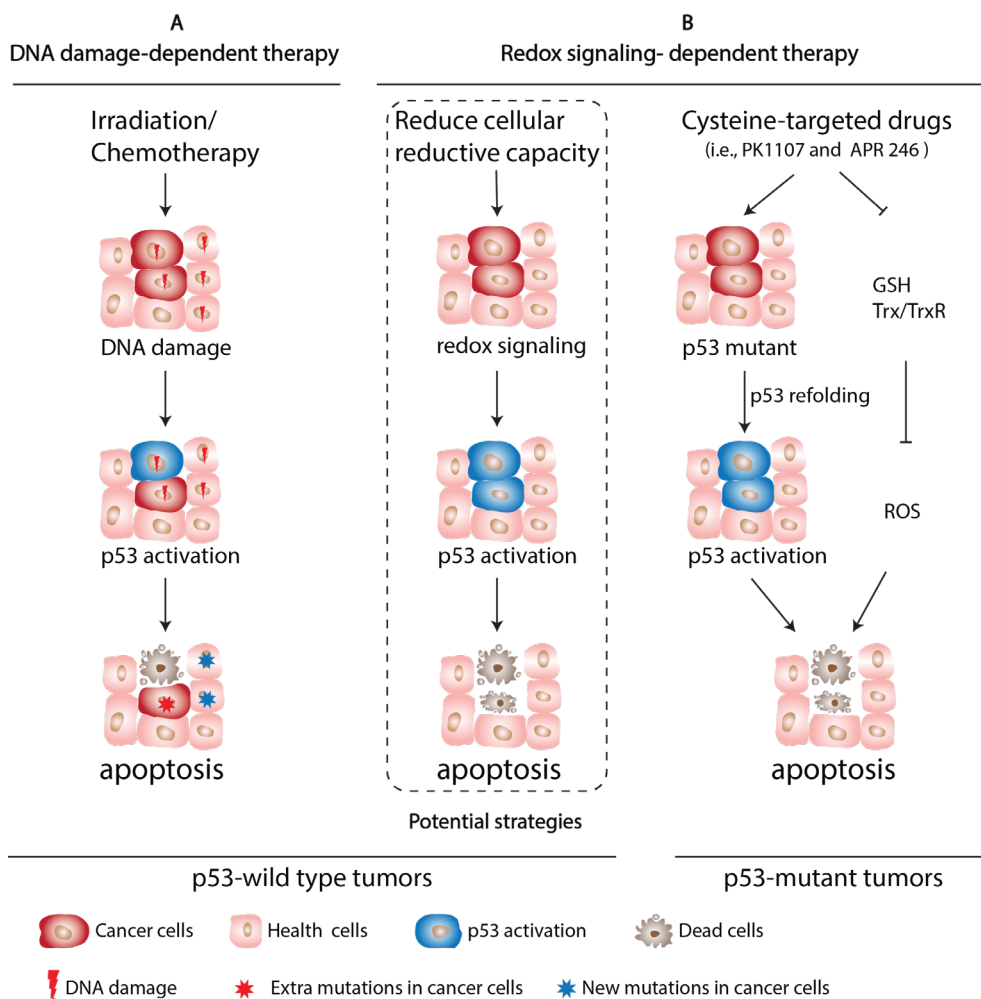


**Figure 6. Differential regulation of p53 targets in response to oxidizing conditions.**

(A) The crystal structure of a p53 homodimer bound to a consensus DNA sequence, based on PDB ID 2ADY (89), rendered by the authors using PyMol software. One monomer is indicated in green, the other in magenta. The positions of Cys275 and Cys277 close to the DNA are indicated. (B) Zoom in on the region near Cys275 and Cys277 and the p53-binding motif on the DNA. The two panels show the structure from a different angle. Note that Cys277 is closest to the DNA, and that the base-pair preceding the CATG motif (here A-T) is in closest proximity. (C) Oxidation of Cys277 has been shown to interfere with binding to p53 targets that have a G-C pair at the position preceding the CATG motif in their promoter (like GADD45a), but not with targets that have an A-T pair (like p21). The nature of the oxidative modification is currently not known, but it is unlikely that a large modification like glutathione would not affect the p21 promoter binding sequence as well.

tumor cell apoptosis), was developed originally in an attempt to bind p53 and inhibit MDM2-mediated degradation (74). However, the mechanism by which RITA increases p53 activity is still not fully understood, and it also induces cell death, be it to a lesser extent, in p53 mutant

and p53-null cells. Of relevance for this review, RITA was also shown to induce ROS, JNK/p38MAPK signaling and the DDR, which contribute to its p53-independent killing of (tumor) cells (142,175).

#### *Reactivation of mutant p53: a role for cysteines?*

Strategies like inhibition of MDM2 or interference with upstream redox signaling pathways to stabilize p53 would not be sensible in tumors that express mutant p53, which is the case in a large proportion of cancers. Compound library screens designed to selectively kill tumor cells expressing mutant p53 have yielded candidate drugs that seemed to be able to refold and transcriptionally reactivate several otherwise inactive mutant forms of p53 (**Fig. 6B**) (reviewed in (45,90)). The first of these compounds, PRIMA-1 and its successor APR-26 (PRIMA-1MET) turned out to be converted to an active methylene quinuclidinone (MQ) that in turn forms covalent adducts with cysteines in the p53 DNA binding domain in vitro and displayed p53-dependent tumor suppressive effects in cultured cells. Several other compounds aimed at reactivation of p53, were reported to directly modify p53 cysteines (24). The sulfonyl pyrimidine PK11007 is a mild thiol-binding compound and has been shown to preferentially alkylate Cys182 and Cys277 in both wild type and mutant p53 (9). This study showed that alkylation of Cys182 and Cys277 by PK11007 increased the protein stability of the p53 Y220C mutant without compromising its DNA-binding activity. Of note, PK11007 increased levels of p53 target genes, including p21, MDM2 and PUMA, in a dose-dependent manner and induced tumor cell death (9). However, and may be not unexpected given the low intrinsic reactivity of p53 cysteines, in vivo these compounds turn out to have many other targets including TRXR and GSH, and the mechanism of action is therefore far from clear but seems to at least synergize with the expression of mutant p53 (**Fig. 6C**). Indeed, several of these compounds originally developed with the idea to selectively kill cells with mutant p53 later turned out to also display cytotoxicity in p53 wildtype and p53 null cells. May be coincidentally, the p53-independent cytotoxic effects of several of these compounds turned out to derive from elevated ROS levels (9,24,184).

#### *Reactivation of wildtype p53 by redox signaling?*

Tumor cells in general encounter more oxidants from for instance the immune response, but also due to altered metabolism, continuous NOX activation and ER stress due to the unfolded protein response. But tumor cells do thrive which means they must have upregulated their antioxidant defense system to cope with this oxidative burden (52,99). The generation of NADPH in the PPP as a reducing equivalent for the TRX and GSH system is indeed essential for tumor cells (66), and so are sufficient amounts of cysteine imported through the cystine/glutamate transporter SLC7A11/xCT (37), or alternatively de novo synthesized though Transsulfuration pathway (188). It has been suggested that due to the high simultaneous production and scavenging of ROS in tumor cells, the redox balance would be more easily flipped (52). Treatment with inhibitors of for instance TRXR, or metabolic intervention to prevent NADPH production or boost ROS from the electron

transport chain, could then push tumor cells, but not healthy cells, over the edge (Fig.6B). The classical view is that this would be due to accumulation of endogenous ROS leading to DNA damage and subsequent apoptosis. But as extensively discussed earlier in this review, it is unclear whether endogenous ROS is actually capable of directly oxidizing DNA. We would like to argue that it might be plausible that in the context of tumor cell metabolism redox signaling is triggered more rapidly and for prolonged amounts of time, thereby providing a handle to activate several pathways downstream of for instance JNK/p38MAPK, ATM and p53 as outlined above.

## Concluding remarks

Treatment of cells with high amounts of hydrogen peroxide or other ROS-inducing agents have long been known to trigger both p53 stabilization and the cellular DNA damage response, and since DNA damage is known to lead to p53 activation it has been largely assumed that ROS-induced DNA damage was responsible for subsequent ATM/ATR activation and downstream signaling to stabilize p53. But with the upcoming field of redox signaling it has become clear that ROS, in the form of H<sub>2</sub>O<sub>2</sub>, also acts as a signaling molecule that triggers cascades like JNK/p38MAPK that can activate p53 independent of the DNA damage response. As outlined in this review, it may therefore be difficult to dissect whether the roles of p53 in response to oxidizing conditions described in older literature are due to DNA damage or redox signaling, or both. Part of the answer may lie in the concentration and nature of the oxidants used. Besides, as we outlined, it is currently not yet clear whether endogenous H<sub>2</sub>O<sub>2</sub>, derived from respiration would surpass levels that would directly damage the nuclear DNA. Furthermore, sensitivity to ROS varies greatly between cell types, and careful controls are therefore needed to be able to pinpoint which signaling cascades (redox signaling, stress kinase signaling and the DNA damage response) are activated to what extent upon treatment with compounds that modulate the cellular redox state, although, admittedly this is not trivial, especially in in vivo settings. Understanding redox signaling dependent p53 stabilization could open up avenues to explore compounds that reactivate endogenous p53 without inducing extra mutations that could otherwise contribute to tumor resistance or progression.

## References

1. Adams L, Franco MC, Estevez AG. Reactive nitrogen species in cellular signaling. *Exp Biol Med* (Maywood) 240: 711-7, 2015.
2. Akter S, Fu L, Jung Y, et al. Chemical proteomics reveals new targets of cysteine sulfinic acid reductase. *Nat Chem Biol* 14: 995-1004, 2018.
3. Al-Tassan N, Chmiel NH, Maynard J, et al. Inherited variants of MYH associated with somatic G:C-->T:A mutations in colorectal tumors. *Nat Genet* 30: 227-32, 2002.
4. Amaravadi RK, Yu D, Lum JJ, et al. Autophagy inhibition enhances therapy-induced apoptosis in a Myc-induced model of lymphoma. *J Clin Invest* 117: 326-36, 2007.
5. Assaily W, Rubinger DA, Wheaton K, et al. ROS-mediated p53 induction of Lpin1 regulates fatty acid



- oxidation in response to nutritional stress. *Mol Cell* 44: 491-501, 2011.
6. Augustyn KE, Merino EJ, Barton JK. A role for DNA-mediated charge transport in regulating p53: Oxidation of the DNA-bound protein from a distance. *Proc Natl Acad Sci U S A* 104: 18907-12, 2007.
  7. Aylon Y, Oren M. The Paradox of p53: What, How, and Why? *Cold Spring Harb Perspect Med* 6, 2016.
  8. Bae BI, Xu H, Igarashi S, et al. p53 mediates cellular dysfunction and behavioral abnormalities in Huntington's disease. *Neuron* 47: 29-41, 2005.
  9. Bauer MR, Joerger AC, Fersht AR. 2-Sulfonylpyrimidines: Mild alkylating agents with anticancer activity toward p53-compromised cells. *Proc Natl Acad Sci U S A* 113: E5271-80, 2016.
  10. Belyi VA, Ak P, Markert E, et al. The origins and evolution of the p53 family of genes. *Cold Spring Harb Perspect Biol* 2: a001198, 2010.
  11. Bensaad K, Cheung EC, Vousden KH. Modulation of intracellular ROS levels by TIGAR controls autophagy. *Embo j* 28: 3015-26, 2009.
  12. Bensaad K, Tsuruta A, Selak MA, et al. A p53-inducible regulator of glycolysis and apoptosis. *Cell* 126: 107-20, 2006.
  13. Biteau B, Labarre J, Toledano MB. ATP-dependent reduction of cysteine-sulphinic acid by *S. cerevisiae* sulphiredoxin. *Nature* 425: 980-4, 2003.
  14. Bode AM, Dong Z. Post-translational modification of p53 in tumorigenesis. *Nat Rev Cancer* 4: 793-805, 2004.
  15. Borodkina A, Shatrova A, Abushik P, et al. Interaction between ROS dependent DNA damage, mitochondria and p38 MAPK underlies senescence of human adult stem cells. *Aging (Albany NY)* 6: 481-95, 2014.
  16. Bourdon A, Minai L, Serre V, et al. Mutation of RRM2B, encoding p53-controlled ribonucleotide reductase (p53R2), causes severe mitochondrial DNA depletion. *Nat Genet* 39: 776-80, 2007.
  17. Bragado P, Armesilla A, Silva A, et al. Apoptosis by cisplatin requires p53 mediated p38alpha MAPK activation through ROS generation. *Apoptosis* 12: 1733-42, 2007.
  18. Bretau S, Allen C, Ingham PW, et al. p53-dependent neuronal cell death in a DJ-1-deficient zebrafish model of Parkinson's disease. *J Neurochem* 100: 1626-35, 2007.
  19. Brooks CL, Gu W. p53 regulation by ubiquitin. *FEBS Lett* 585: 2803-9, 2011.
  20. Brown CJ, Lain S, Verma CS, et al. Awakening guardian angels: drugging the p53 pathway. *Nat Rev Cancer* 9: 862-73, 2009.
  21. Brynczka C, Labhart P, Merrick BA. NGF-mediated transcriptional targets of p53 in PC12 neuronal differentiation. *BMC Genomics* 8: 139, 2007.
  22. Burns ER, Beland SS. Induction by 5-fluorouracil of a major phase difference in the circadian profiles of DNA synthesis between the Ehrlich ascites carcinoma and five normal organs. *Cancer Lett* 20: 235-9, 1983.
  23. Buzek J, Latonen L, Kurki S, et al. Redox state of tumor suppressor p53 regulates its sequence-specific DNA binding in DNA-damaged cells by cysteine 277. *Nucleic Acids Res* 30: 2340-8, 2002.
  24. Bykov VJN, Eriksson SE, Bianchi J, et al. Targeting mutant p53 for efficient cancer therapy. *Nat Rev Cancer* 18: 89-102, 2018.
  25. Cadet J, Davies KJA, Medeiros MH, et al. Formation and repair of oxidatively generated damage in cellular DNA. *Free Radic Biol Med* 107: 13-34, 2017.

26. Cande C, Cecconi F, Dessen P, et al. Apoptosis-inducing factor (AIF): key to the conserved caspase-independent pathways of cell death? *J Cell Sci* 115: 4727-34, 2002.
27. Cardaci S, Filomeni G, Rotilio G, et al. Reactive oxygen species mediate p53 activation and apoptosis induced by sodium nitroprusside in SH-SY5Y cells. *Mol Pharmacol* 74: 1234-45, 2008.
28. Chang TS, Jeong W, Woo HA, et al. Characterization of mammalian sulfiredoxin and its reactivation of hyperoxidized peroxiredoxin through reduction of cysteine sulfinic acid in the active site to cysteine. *J Biol Chem* 279: 50994-1001, 2004.
29. Chen K, Albano A, Ho A, et al. Activation of p53 by oxidative stress involves platelet-derived growth factor-beta receptor-mediated ataxia telangiectasia mutated (ATM) kinase activation. *J Biol Chem* 278: 39527-33, 2003.
30. Chen PH, Wu J, Ding CC, et al. Kinome screen of ferroptosis reveals a novel role of ATM in regulating iron metabolism. *Cell Death Differ*, 2019.
31. Chen Y, Jungsuwadee P, Vore M, et al. Collateral damage in cancer chemotherapy: oxidative stress in nontargeted tissues. *Mol Interv* 7: 147-56, 2007.
32. Chen Y, Zhang X, Dantas Machado AC, et al. Structure of p53 binding to the BAX response element reveals DNA unwinding and compression to accommodate base-pair insertion. *Nucleic Acids Res* 41: 8368-76, 2013.
33. Cheng M, He B, Wan T, et al. 5-Fluorouracil nanoparticles inhibit hepatocellular carcinoma via activation of the p53 pathway in the orthotopic transplant mouse model. *PLoS One* 7: e47115, 2012.
34. Cho Y, Gorina S, Jeffrey PD, et al. Crystal structure of a p53 tumor suppressor-DNA complex: understanding tumorigenic mutations. *Science* 265: 346-55, 1994.
35. Christophorou MA, Ringshausen I, Finch AJ, et al. The pathological response to DNA damage does not contribute to p53-mediated tumour suppression. *Nature* 443: 214-7, 2006.
36. Cleaver JE, Brennan-Minnella AM, Swanson RA, et al. Mitochondrial reactive oxygen species are scavenged by Cockayne syndrome B protein in human fibroblasts without nuclear DNA damage. *Proc Natl Acad Sci U S A* 111: 13487-92, 2014.
37. Combs JA, DeNicola GM. The Non-Essential Amino Acid Cysteine Becomes Essential for Tumor Proliferation and Survival. *Cancers (Basel)* 11, 2019.
38. Cross JV, Templeton DJ. Oxidative stress inhibits MEK1 by site-specific glutathionylation in the ATP-binding domain. *Biochem J* 381: 675-83, 2004.
39. Culmsee C, Landshamer S. Molecular insights into mechanisms of the cell death program: role in the progression of neurodegenerative disorders. *Curr Alzheimer Res* 3: 269-83, 2006.
40. Dansen TB, Smits LM, van Triest MH, et al. Redox-sensitive cysteines bridge p300/CBP-mediated acetylation and FoxO4 activity. *Nat Chem Biol* 5: 664-72, 2009.
41. Delaunay A, Pflieger D, Barrault MB, et al. A thiol peroxidase is an H<sub>2</sub>O<sub>2</sub> receptor and redox-transducer in gene activation. *Cell* 111: 471-81, 2002.
42. Doll S, Freitas FP, Shah R, et al. FSP1 is a glutathione-independent ferroptosis suppressor. *Nature* 575: 693-698, 2019.
43. Donley N, Jaruga P, Coskun E, et al. Small Molecule Inhibitors of 8-Oxoguanine DNA Glycosylase-1 (OGG1). *ACS Chem Biol* 10: 2334-43, 2015.
44. Driessens N, Versteyhe S, Ghaddhab C, et al. Hydrogen peroxide induces DNA single- and double-strand breaks in thyroid cells and is therefore a potential mutagen for this organ. *Endocr Relat Cancer* 16: 845-56, 2009.

45. Duffy MJ, Synnott NC, Crown J. Mutant p53 as a target for cancer treatment. *Eur J Cancer* 83: 258-265, 2017.
46. el-Deiry WS, Kern SE, Pietenpol JA, et al. Definition of a consensus binding site for p53. *Nat Genet* 1: 45-9, 1992.
47. Ermakova YG, Bilan DS, Matlashov ME, et al. Red fluorescent genetically encoded indicator for intracellular hydrogen peroxide. *Nat Commun* 5: 5222, 2014.
48. Fischer M. Census and evaluation of p53 target genes. *Oncogene* 36: 3943-3956, 2017.
49. Fojta M, Kubicarova T, Vojtesek B, et al. Effect of p53 protein redox states on binding to supercoiled and linear DNA. *J Biol Chem* 274: 25749-55, 1999.
50. Gad H, Koolmeister T, Jemth AS, et al. MTH1 inhibition eradicates cancer by preventing sanitation of the dNTP pool. *Nature* 508: 215-21, 2014.
51. Giles GI, Nasim MJ, Ali W, et al. The Reactive Sulfur Species Concept: 15 Years On. *Antioxidants (Basel)* 6, 2017.
52. Glasauer A, Chandel NS. Targeting antioxidants for cancer therapy. *Biochem Pharmacol* 92: 90-101, 2014.
53. Go YM, Jones DP. Redox compartmentalization in eukaryotic cells. *Biochim Biophys Acta* 1780: 1273-90, 2008.
54. Guo Z, Kozlov S, Lavin MF, et al. ATM activation by oxidative stress. *Science* 330: 517-21, 2010.
55. Hainaut P, Hollstein M. p53 and human cancer: the first ten thousand mutations. *Adv Cancer Res* 77: 81-137, 2000.
56. Hainaut P, Milner J. Redox modulation of p53 conformation and sequence-specific DNA binding in vitro. *Cancer Res* 53: 4469-73, 1993.
57. Halliwell B. Effect of diet on cancer development: is oxidative DNA damage a biomarker? *Free Radic Biol Med* 32: 968-74, 2002.
58. Hanahan D, Weinberg RA. Hallmarks of cancer: the next generation. *Cell* 144: 646-74, 2011.
59. Harman D. Aging: a theory based on free radical and radiation chemistry. *J Gerontol* 11: 298-300, 1956.
60. Haupt Y, Maya R, Kazaz A, et al. Mdm2 promotes the rapid degradation of p53. *Nature* 387: 296-9, 1997.
61. Held JM, Danielson SR, Behring JB, et al. Targeted quantitation of site-specific cysteine oxidation in endogenous proteins using a differential alkylation and multiple reaction monitoring mass spectrometry approach. *Mol Cell Proteomics* 9: 1400-10, 2010.
62. Heppner DE, Dustin CM, Liao C, et al. Direct cysteine sulfonylation drives activation of the Src kinase. *Nat Commun* 9: 4522, 2018.
63. Hinkal G, Parikh N, Donehower LA. Timed somatic deletion of p53 in mice reveals age-associated differences in tumor progression. *PLoS One* 4: e6654, 2009.
64. Holmstrom KM, Finkel T. Cellular mechanisms and physiological consequences of redox-dependent signalling. *Nat Rev Mol Cell Biol* 15: 411-21, 2014.
65. Hornsveld M, Dansen TB. The Hallmarks of Cancer from a Redox Perspective. *Antioxid Redox Signal* 25: 300-25, 2016.
66. Hosios AM, Vander Heiden MG. The redox requirements of proliferating mammalian cells. *J Biol Chem* 293: 7490-7498, 2018.

67. Hosoya N, Miyagawa K. Targeting DNA damage response in cancer therapy. *Cancer Sci* 105: 370-88, 2014.
68. Hu W, Zhang C, Wu R, et al. Glutaminase 2, a novel p53 target gene regulating energy metabolism and antioxidant function. *Proc Natl Acad Sci U S A* 107: 7455-60, 2010.
69. Huang J, Sengupta R, Espejo AB, et al. p53 is regulated by the lysine demethylase LSD1. *Nature* 449: 105-8, 2007.
70. Huber KV, Salah E, Radic B, et al. Stereospecific targeting of MTH1 by (S)-crizotinib as an anticancer strategy. *Nature* 508: 222-7, 2014.
71. Hupp TR, Meek DW, Midgley CA, et al. Activation of the cryptic DNA binding function of mutant forms of p53. *Nucleic Acids Res* 21: 3167-74, 1993.
72. Hussain SP, Amstad P, He P, et al. p53-induced up-regulation of MnSOD and GPx but not catalase increases oxidative stress and apoptosis. *Cancer Res* 64: 2350-6, 2004.
73. Ingold I, Berndt C, Schmitt S, et al. Selenium Utilization by GPX4 Is Required to Prevent Hydroperoxide-Induced Ferroptosis. *Cell* 172: 409-422.e21, 2018.
74. Issaeva N, Bozko P, Enge M, et al. Small molecule RITA binds to p53, blocks p53-HDM-2 interaction and activates p53 function in tumors. *Nat Med* 10: 1321-8, 2004.
75. Ito A, Kawaguchi Y, Lai CH, et al. MDM2-HDAC1-mediated deacetylation of p53 is required for its degradation. *Embo j* 21: 6236-45, 2002.
76. Ito A, Lai CH, Zhao X, et al. p300/CBP-mediated p53 acetylation is commonly induced by p53-activating agents and inhibited by MDM2. *Embo j* 20: 1331-40, 2001.
77. Jacobs AC, Calkins MJ, Jadhav A, et al. Inhibition of DNA glycosylases via small molecule purine analogs. *PLoS One* 8: e81667, 2013.
78. Jain AK, Barton MC. p53: emerging roles in stem cells, development and beyond. *Development* 145, 2018.
79. Jarvis RM, Hughes SM, Ledgerwood EC. Peroxiredoxin 1 functions as a signal peroxidase to receive, transduce, and transmit peroxide signals in mammalian cells. *Free Radic Biol Med* 53: 1522-30, 2012.
80. Jiang L, Kon N, Li T, Wang SJ, et al. Ferroptosis as a p53-mediated activity during tumour suppression. *Nature* 520: 57-62, 2015.
81. Jiang P, Du W, Wang X, et al. p53 regulates biosynthesis through direct inactivation of glucose-6-phosphate dehydrogenase. *Nat Cell Biol* 13: 310-6, 2011.
82. Jochemsen AG. Reactivation of p53 as therapeutic intervention for malignant melanoma. *Curr Opin Oncol* 26: 114-9, 2014.
83. Joerger AC, Fersht AR. Structural biology of the tumor suppressor p53. *Annu Rev Biochem* 77: 557-82, 2008.
84. Jogl G, Hsiao YS, Tong L. Structure and function of carnitine acyltransferases. *Ann N Y Acad Sci* 1033: 17-29, 2004.
85. Kaludercic N, Deshwal S, Di Lisa F. Reactive oxygen species and redox compartmentalization. *Front Physiol* 5: 285, 2014.
86. Kang R, Kroemer G, Tang D. The tumor suppressor protein p53 and the ferroptosis network. *Free Radic Biol Med* 133: 162-168, 2019.
87. Kastan MB, Onyekwere O, Sidransky D, et al. Participation of p53 protein in the cellular response to

DNA damage. *Cancer Res* 51: 6304-11, 1991.

88. Khoury K, Domling A. P53 mdm2 inhibitors. *Curr Pharm Des* 18: 4668-78, 2012.

89. Kitayner M, Rozenberg H, Kessler N, et al. Structural basis of DNA recognition by p53 tetramers. *Mol Cell* 22: 741-53, 2006.

90. Kogan S, Carpizo D. Pharmacological targeting of mutant p53. *Transl Cancer Res* 5: 698-706, 2016.

91. Kuroda J, Nakagawa K, Yamasaki T, et al. The superoxide-producing NAD(P)H oxidase Nox4 in the nucleus of human vascular endothelial cells. *Genes Cells* 10: 1139-51, 2005.

92. Kurz EU, Douglas P, Lees-Miller SP. Doxorubicin activates ATM-dependent phosphorylation of multiple downstream targets in part through the generation of reactive oxygen species. *J Biol Chem* 279: 53272-81, 2004.

93. Labuschagne CF, Zani F, Vousden KH. Control of metabolism by p53 - Cancer and beyond. *Biochim Biophys Acta Rev Cancer* 1870: 32-42, 2018.

94. Lacroix M, Riscal R, Arena G, et al. Metabolic functions of the tumor suppressor p53: Implications in normal physiology, metabolic disorders, and cancer. *Mol Metab*, 2019.

95. Laurie NA, Donovan SL, Shih CS, et al. Inactivation of the p53 pathway in retinoblastoma. *Nature* 444: 61-6, 2006.

96. Liberti MV, Locasale JW. The Warburg Effect: How Does it Benefit Cancer Cells? *Trends Biochem Sci* 41: 211-218, 2016.

97. Lin ST, Lo YW, Chang SJ, et al. Redox-proteomic analysis of doxorubicin resistance-induced altered thiol activity in uterine carcinoma. *J Pharm Biomed Anal* 78-79: 1-8, 2013.

98. Liu DP, Song H, Xu Y. A common gain of function of p53 cancer mutants in inducing genetic instability. *Oncogene* 29: 949-56, 2010.

99. Liu Y, Li Q, Zhou L, et al. Cancer drug resistance: redox resetting renders a way. *Oncotarget* 7: 42740-42761, 2016.

100. Liu Y, Tavana O, Gu W. p53 modifications: exquisite decorations of the powerful guardian. *J Mol Cell Biol*, 2019.

101. Lotem J, Peled-Kamar M, Groner Y, et al. Cellular oxidative stress and the control of apoptosis by wild-type p53, cytotoxic compounds, and cytokines. *Proc Natl Acad Sci U S A* 93: 9166-71, 1996.

102. Lowe SW, Bodis S, McClatchey A, et al. p53 status and the efficacy of cancer therapy in vivo. *Science* 266: 807-10, 1994.

103. Mandinova A, Lee SW. The p53 pathway as a target in cancer therapeutics: obstacles and promise. *Sci Transl Med* 3: 64rv1, 2011.

104. Marchenko ND, Hanel W, Li D, et al. Stress-mediated nuclear stabilization of p53 is regulated by ubiquitination and importin-alpha3 binding. *Cell Death Differ* 17: 255-67, 2010.

105. Marcillat O, Zhang Y, Davies KJ. Oxidative and non-oxidative mechanisms in the inactivation of cardiac mitochondrial electron transport chain components by doxorubicin. *Biochem J* 259: 181-9, 1989.

106. Matoba S, Kang JG, Patino WD, et al. p53 regulates mitochondrial respiration. *Science* 312: 1650-3, 2006.

107. Maynard S, Schurman SH, Harboe C, et al. Base excision repair of oxidative DNA damage and association with cancer and aging. *Carcinogenesis* 30: 2-10, 2009.

108. Meek DW, Anderson CW. Posttranslational modification of p53: cooperative integrators of function. *Cold Spring Harb Perspect Biol* 1: a000950, 2009.

109. Meplan C, Richard MJ, Hainaut P. Redox signalling and transition metals in the control of the p53 pathway. *Biochem Pharmacol* 59: 25-33, 2000.
110. Michalak EM, Jansen ES, Happo L, et al. Puma and to a lesser extent Noxa are suppressors of Myc-induced lymphomagenesis. *Cell Death Differ* 16: 684-96, 2009.
111. Milne DM, Campbell LE, Campbell DG, et al. p53 is phosphorylated in vitro and in vivo by an ultraviolet radiation-induced protein kinase characteristic of the c-Jun kinase, JNK1. *J Biol Chem* 270: 5511-8, 1995.
112. Mishina NM, Bogdanova YA, Ermakova YG, et al. Which Antioxidant System Shapes Intracellular H<sub>2</sub>O<sub>2</sub> Gradients? *Antioxid Redox Signal* 31: 664-670, 2019.
113. Momand J, Zambetti GP, Olson DC, et al. The mdm-2 oncogene product forms a complex with the p53 protein and inhibits p53-mediated transactivation. *Cell* 69: 1237-45, 1992.
114. Mordes DA, Cortez D. Activation of ATR and related PIKKs. *Cell Cycle* 7: 2809-12, 2008.
115. Morgan B, Van Laer K, Owusu TN, et al. Real-time monitoring of basal H<sub>2</sub>O<sub>2</sub> levels with peroxiredoxin-based probes. *Nat Chem Biol* 12: 437-43, 2016.
116. Muller PA, Vousden KH. p53 mutations in cancer. *Nat Cell Biol* 15: 2-8, 2013.
117. Murphy MP. How mitochondria produce reactive oxygen species. *Biochem J* 417: 1-13, 2009.
118. Nadeau PJ, Charette SJ, Toledano MB, et al. Disulfide Bond-mediated multimerization of Ask1 and its reduction by thioredoxin-1 regulate H<sub>2</sub>O<sub>2</sub>-induced c-Jun NH<sub>2</sub>-terminal kinase activation and apoptosis. *Mol Biol Cell* 18: 3903-13, 2007.
119. Okamura S, Ng CC, Koyama K, et al. Identification of seven genes regulated by wild-type p53 in a colon cancer cell line carrying a well-controlled wild-type p53 expression system. *Oncol Res* 11: 281-5, 1999.
120. Olive KP, Tuveson DA, Ruhe ZC, et al. Mutant p53 gain of function in two mouse models of Li-Fraumeni syndrome. *Cell* 119: 847-60, 2004.
121. Olsson A, Manzl C, Strasser A, et al. How important are post-translational modifications in p53 for selectivity in target-gene transcription and tumour suppression? *Cell Death Differ* 14: 1561-75, 2007.
122. Ostrakhovitch EA, Cherian MG. Role of p53 and reactive oxygen species in apoptotic response to copper and zinc in epithelial breast cancer cells. *Apoptosis* 10: 111-21, 2005.
123. Parks D, Bolinger R, Mann K. Redox state regulates binding of p53 to sequence-specific DNA, but not to non-specific or mismatched DNA. *Nucleic Acids Res* 25: 1289-95, 1997.
124. Perillo B, Ombra MN, Bertoni A, et al. DNA oxidation as triggered by H3K9me2 demethylation drives estrogen-induced gene expression. *Science* 319: 202-6, 2008.
125. Petitjean A, Mathe E, Kato S, et al. Impact of mutant p53 functional properties on TP53 mutation patterns and tumor phenotype: lessons from recent developments in the IARC TP53 database. *Hum Mutat* 28: 622-9, 2007.
126. Pham NA, Hedley DW. Respiratory chain-generated oxidative stress following treatment of leukemic blasts with DNA-damaging agents. *Exp Cell Res* 264: 345-52, 2001.
127. Polyak K, Xia Y, Zweier JL, et al. A model for p53-induced apoptosis. *Nature* 389: 300-5, 1997.
128. Rainwater R, Parks D, Anderson ME, et al. Role of cysteine residues in regulation of p53 function. *Mol Cell Biol* 15: 3892-903, 1995.
129. Rhee SG, Woo HA. Multiple functions of peroxiredoxins: peroxidases, sensors and regulators of the intracellular messenger H<sub>2</sub>O<sub>2</sub>, and protein chaperones. *Antioxid Redox Signal* 15: 781-94, 2011.

130. Rhee SG, Woo HA, Kil IS, et al. Peroxiredoxin functions as a peroxidase and a regulator and sensor of local peroxides. *J Biol Chem* 287: 4403-10, 2012.
131. Riley T, Sontag E, Chen P, et al. Transcriptional control of human p53-regulated genes. *Nat Rev Mol Cell Biol* 9: 402-12, 2008.
132. Sablina AA, Budanov AV, Ilyinskaya GV, et al. The antioxidant function of the p53 tumor suppressor. *Nat Med* 11: 1306-13, 2005.
133. Saitoh M, Nishitoh H, Fujii M, et al. Mammalian thioredoxin is a direct inhibitor of apoptosis signal-regulating kinase (ASK) 1. *Embo j* 17: 2596-606, 1998.
134. Sakaguchi K, Herrera JE, Saito S, et al. DNA damage activates p53 through a phosphorylation-acetylation cascade. *Genes Dev* 12: 2831-41, 1998.
135. Sanchez-Prieto R, Rojas JM, Taya Y, et al. A role for the p38 mitogen-activated protein kinase pathway in the transcriptional activation of p53 on genotoxic stress by chemotherapeutic agents. *Cancer Res* 60: 2464-72, 2000.
136. Schaefer KN, Geil WM, Sweredoski MJ, et al. Oxidation of p53 through DNA charge transport involves a network of disulfides within the DNA-binding domain. *Biochemistry* 54: 932-41, 2015.
137. Scotcher J, Clarke DJ, Mackay CL, et al. Redox regulation of tumour suppressor protein p53: identification of the sites of hydrogen peroxide oxidation and glutathionylation. *4: 1257-1269*, 2013.
138. Scott TL, Rangaswamy S, Wicker CA, et al. Repair of oxidative DNA damage and cancer: recent progress in DNA base excision repair. *Antioxid Redox Signal* 20: 708-26, 2014.
139. Seemann S, Hainaut P. Roles of thioredoxin reductase 1 and APE/Ref-1 in the control of basal p53 stability and activity. *Oncogene* 24: 3853-63, 2005.
140. Sherr CJ, Weber JD. The ARF/p53 pathway. *Curr Opin Genet Dev* 10: 94-9, 2000.
141. Shi X, Kachirskaja I, Yamaguchi H, et al. Modulation of p53 function by SET8-mediated methylation at lysine 382. *Mol Cell* 27: 636-46, 2007.
142. Shi Y, Nikulenkov F, Zawacka-Pankau J, et al. ROS-dependent activation of JNK converts p53 into an efficient inhibitor of oncogenes leading to robust apoptosis. *Cell Death Differ* 21: 612-23, 2014.
143. Shieh SY, Ikeda M, Taya Y, et al. DNA damage-induced phosphorylation of p53 alleviates inhibition by MDM2. *Cell* 91: 325-34, 1997.
144. Shin HJ, Kwon HK, Lee JH, et al. Etoposide induced cytotoxicity mediated by ROS and ERK in human kidney proximal tubule cells. *Sci Rep* 6: 34064, 2016.
145. Shlomai J. Redox control of protein-DNA interactions: from molecular mechanisms to significance in signal transduction, gene expression, and DNA replication. *Antioxid Redox Signal* 13: 1429-76, 2010.
146. Sies H, Berndt C, Jones DP. Oxidative Stress. *Annu Rev Biochem* 86: 715-748, 2017.
147. Skalniak L, Kocik J, Polak J, et al. Prolonged Idasanutlin (RG7388) Treatment Leads to the Generation of p53-Mutated Cells. *Cancers (Basel)* 10, 2018.
148. Sobotta MC, Liou W, Stocker S, et al. Peroxiredoxin-2 and STAT3 form a redox relay for H<sub>2</sub>O<sub>2</sub> signaling. *Nat Chem Biol* 11: 64-70, 2015.
149. Stambolsky P, Weisz L, Shats I, et al. Regulation of AIF expression by p53. *Cell Death Differ* 13: 2140-9, 2006.
150. Stocker S, Maurer M, Ruppert T, et al. A role for 2-Cys peroxiredoxins in facilitating cytosolic protein thiol oxidation. *Nat Chem Biol* 14: 148-155, 2018.
151. Stocker S, Van Laer K, Mijuskovic A, et al. The Conundrum of Hydrogen Peroxide Signaling and

- the Emerging Role of Peroxiredoxins as Redox Relay Hubs. *Antioxid Redox Signal* 28: 558-573, 2018.
152. Sun XZ, Vinci C, Makmura L, et al. Formation of disulfide bond in p53 correlates with inhibition of DNA binding and tetramerization. *Antioxid Redox Signal* 5: 655-65, 2003.
153. Swenberg JA, Lu K, Moeller BC, et al. Endogenous versus exogenous DNA adducts: their role in carcinogenesis, epidemiology, and risk assessment. *Toxicol Sci* 120 Suppl 1: S130-45, 2011.
154. Tan M, Li S, Swaroop M, et al. Transcriptional activation of the human glutathione peroxidase promoter by p53. *J Biol Chem* 274: 12061-6, 1999.
155. Tang Y, Luo J, Zhang W, et al. Tip60-dependent acetylation of p53 modulates the decision between cell-cycle arrest and apoptosis. *Mol Cell* 24: 827-39, 2006.
156. Tian H, Gao Z, Li H, et al. DNA damage response--a double-edged sword in cancer prevention and cancer therapy. *Cancer Lett* 358: 8-16, 2015.
157. Tisato V, Voltan R, Gonelli A, et al. MDM2/X inhibitors under clinical evaluation: perspectives for the management of hematological malignancies and pediatric cancer. *J Hematol Oncol* 10: 133, 2017.
158. Tokarska-Schlattner M, Wallimann T, Schlattner U. Multiple interference of anthracyclines with mitochondrial creatine kinases: preferential damage of the cardiac isoenzyme and its implications for drug cardiotoxicity. *Mol Pharmacol* 61: 516-23, 2002.
159. Ushio-Fukai M. Compartmentalization of redox signaling through NADPH oxidase-derived ROS. *Antioxid Redox Signal* 11: 1289-99, 2009.
160. Vahsen N, Cande C, Briere JJ, et al. AIF deficiency compromises oxidative phosphorylation. *Embo j* 23: 4679-89, 2004.
161. Valente LJ, Gray DH, Michalak EM, et al. p53 efficiently suppresses tumor development in the complete absence of its cell-cycle inhibitory and proapoptotic effectors p21, Puma, and Noxa. *Cell Rep* 3: 1339-45, 2013.
162. Valverde M, Lozano-Salgado J, Fortini P, et al. Hydrogen Peroxide-Induced DNA Damage and Repair through the Differentiation of Human Adipose-Derived Mesenchymal Stem Cells. *Stem Cells Int* 2018: 1615497, 2018.
163. Van Raamsdonk JM, Hekimi S. Superoxide dismutase is dispensable for normal animal lifespan. *Proc Natl Acad Sci U S A* 109: 5785-90, 2012.
164. Vander Heiden MG, Cantley LC, et al. Understanding the Warburg effect: the metabolic requirements of cell proliferation. *Science* 324: 1029-33, 2009.
165. Veal EA, Day AM, Morgan BA. Hydrogen peroxide sensing and signaling. *Mol Cell* 26: 1-14, 2007.
166. Veal EA, Findlay VJ, Day AM, et al. A 2-Cys peroxiredoxin regulates peroxide-induced oxidation and activation of a stress-activated MAP kinase. *Mol Cell* 15: 129-39, 2004.
167. Velu CS, Niture SK, Doneanu CE, et al. Human p53 is inhibited by glutathionylation of cysteines present in the proximal DNA-binding domain during oxidative stress. *Biochemistry* 46: 7765-80, 2007.
168. Visnes T, Grube M, Hanna BMF, et al. Targeting BER enzymes in cancer therapy. *DNA Repair (Amst)* 71: 118-126, 2018.
169. Vousden KH, Ryan KM. p53 and metabolism. *Nat Rev Cancer* 9: 691-700, 2009.
170. Wagner EF, Nebreda AR. Signal integration by JNK and p38 MAPK pathways in cancer development. *Nat Rev Cancer* 9: 537-49, 2009.
171. Wang S, Konorev EA, Kotamraju S, et al. Doxorubicin induces apoptosis in normal and tumor cells via distinctly different mechanisms. Intermediacy of H<sub>2</sub>O<sub>2</sub>- and p53-dependent pathways. *J Biol*



Chem 279: 25535-43, 2004.

172. Wang SJ, Yu G, Jiang L, et al. p53-Dependent regulation of metabolic function through transcriptional activation of pantothenate kinase-1 gene. *Cell Cycle* 12: 753-61, 2013.

173. Warpman Berglund U, Sanjiv K, et al. Validation and development of MTH1 inhibitors for treatment of cancer. *Ann Oncol* 27: 2275-2283, 2016.

174. Wartlick F, Bopp A, Henninger C, et al. DNA damage response (DDR) induced by topoisomerase II poisons requires nuclear function of the small GTPase Rac. *Biochim Biophys Acta* 1833: 3093-3103, 2013.

175. Weillbacher A, Gutekunst M, Oren M, et al. RITA can induce cell death in p53-defective cells independently of p53 function via activation of JNK/SAPK and p38. *Cell Death Dis* 5: e1318, 2014.

176. Williams GJ, Hammel M, Radhakrishnan SK, et al. Structural insights into NHEJ: building up an integrated picture of the dynamic DSB repair super complex, one component and interaction at a time. *DNA Repair (Amst)* 17: 110-20, 2014.

177. Wood WC, Budman DR, Korzun AH, et al. Dose and dose intensity of adjuvant chemotherapy for stage II, node-positive breast carcinoma. *N Engl J Med* 330: 1253-9, 1994.

178. Wood ZA, Poole LB, Karplus PA. Peroxiredoxin evolution and the regulation of hydrogen peroxide signaling. *Science* 300: 650-3, 2003.

179. Xie Y, Zhu S, Song X, et al. The Tumor Suppressor p53 Limits Ferroptosis by Blocking DPP4 Activity. *Cell Rep* 20: 1692-1704, 2017.

180. Yahagi N, Shimano H, Matsuzaka T, et al. p53 Activation in adipocytes of obese mice. *J Biol Chem* 278: 25395-400, 2003.

181. Yang WS, SriRamaratnam R, Welsch ME, et al. Regulation of ferroptotic cancer cell death by GPX4. *Cell* 156: 317-331, 2014.

182. Yin Q, Huang C, Zhang C, et al. In situ visualization and detection of protein sulfenylation responses in living cells through a dimedone-based fluorescent probe. *Org Biomol Chem* 11: 7566-73, 2013.

183. Yokoyama C, Sueyoshi Y, Ema M, et al. Induction of oxidative stress by anticancer drugs in the presence and absence of cells. *Oncol Lett* 14: 6066-6070, 2017.

184. Yu X, Vazquez A, Levine AJ, et al. Allele-specific p53 mutant reactivation. *Cancer Cell* 21: 614-25, 2012.

185. Zawacka-Pankau J, Selivanova G. Pharmacological reactivation of p53 as a strategy to treat cancer. *J Intern Med* 277: 248-259, 2015.

186. Zhang C, Liu J, Liang Y, et al. Tumour-associated mutant p53 drives the Warburg effect. *Nat Commun* 4: 2935, 2013.

187. Zhang Y, Xiong Y. A p53 amino-terminal nuclear export signal inhibited by DNA damage-induced phosphorylation. *Science* 292: 1910-5, 2001.

188. Zhu J, Berisa M, Schworer S, et al. Transsulfuration Activity Can Support Cell Growth upon Extracellular Cysteine Limitation. *Cell Metab* 30: 865-876.e5, 2019.

## Abbreviation

5-FU: 5-fluorouracil

8-OH-dG: 8-hydroxy-2'-deoxyguanosine

a-KG: a-ketoglutarate

AMPK: AMP-activated protein kinase  
ASK-1: Apoptosis Signaling Kinase-1  
ATM: Ataxia-Telangiectasia Mutated protein  
ATR: Ataxia Telangiectasia and Rad3-related protein  
ATRIP: ATR-interacting protein  
BER: Base excision repair  
Chk1: Checkpoint kinase  
Chk2: checkpoint kinase  
COX1: Subunit1 cytochrome c oxidase  
CROT: O-octanoyltransferase  
CTD: C-terminal regulatory domain  
CuZnSOD: Cu,Zn superoxide dismutase  
Cys: Cysteine  
DDR: DNA damage response  
DSBs: Double strand breaks  
DNA: Deoxyribonucleic acid  
DNA-PKcs: DNA-dependent protein kinase catalytic subunit  
FADH2: Flavin adenine dinucleotide  
FAO: Fatty acid oxidation  
FDXR: Ferredoxin reductase  
Fe<sup>2+</sup>: Irons  
FOXO: Forkhead box O transcription factor  
G6PDH: Glucose-6-phosphate dehydrogenase  
GLUTs: Glucose transporters  
Gpx: Glutathione Peroxidase  
GR: Glutathione reductase  
Grx: Glutaredoxins  
GSH: Glutathione  
GSSG: GSH dimer  
H<sub>2</sub>O<sub>2</sub>: Hydrogen Peroxide  
HR: Homologous recombination  
ISCU: Iron-sulfur cluster assembly enzyme  
JNK: Protein kinases C-Jun N terminal kinase  
MAPKKK: Mitogen-activated protein kinase kinase kinase  
MAPKK: Mitogen-activated protein kinase kinases  
MDM2: Mouse double minute 2 homolog MDM2, E3 ubiquitin protein ligase  
MMR: Mismatch repair  
MnSOD: Manganese superoxide dismutase  
MQ: Methylene quinuclidinone  
MRN: Mre11, Rad50, and Nbs1 complex  
MTH1: MutT homolog 1  
MYH: MutY homolog  
NADH: Nicotinamide adenine dinucleotide  
NADPH: Nicotinamide Adenine Dinucleotide Phosphate  
NER: Nucleotide excision repair  
NHEJ: Nonhomologous end joining  
NOX: NADPH oxidase

$O_2^{\cdot-}$ : Superoxide anions  
OH $\cdot$ : Hydroxyl radicals  
OGG1: Oxoguanine glycosylate 1  
OXPHOS: Oxidative phosphorylation  
p21: Cyclin-dependent kinase inhibitor 1A  
p38MAPK: Mitogen-activated kinase  
P53: Tumor protein 53  
PARK2: Parkin  
PDH: Pyruvate dehydrogenase  
PDHK2: PDH kinase2  
PFK1: Phosphofructokinase 1  
PIGs: p53-induced genes  
PGM: Phosphoglycerate mutase  
PPP: Pentose Phosphate Pathway  
PRD: Proline-rich domain  
PRDX: Peroxiredoxin  
PTMs: Post-translational modification  
RE: Responsive element  
RITA: Reactivation of p53 and induction of tumor cell apoptosis  
RNA: Ribonucleic acid  
ROS: Reactive Oxygen Species  
RPA: Replication protein A  
SAT1: Spermidine/spermine N1-acetyltransferase 1  
SCO2: Synthesis of Cytochrome c Oxidase 2  
SOD: Superoxide dismutase  
SOH: Sulfenic acid  
SO<sub>2</sub>H: Sulfinic acid  
SO<sub>3</sub>H: Sulfonic acid  
Srx: Sulphiredoxin  
SSBs: Single strand breaks  
TADs: Transactivation domain  
TCA: Tricarboxylic acid  
TD: Tetramerization domain  
Tigar: TP53-induced glycolysis and apoptosis regulator  
TLS: Translesion DNA synthesis  
TopBP1: Topoisomerase II-binding protein 1  
Trx: Thioredoxin  
TrxR: Thioredoxin reductase  
xCT: Cystine/glutamate transporter



# *Chapter 3*

## **DNA damage and oxidant stress activate p53 through differential upstream signaling pathways**

Tao Shi<sup>1</sup>, Daan M. K. van Soest<sup>1</sup>, Paulien E. Polderman<sup>1</sup>, Boudewijn M.T. Burgering<sup>1,2</sup> and Tobias B. Dansen<sup>1,3</sup>

<sup>1</sup>Center for Molecular Medicine, Molecular Cancer Research and <sup>2</sup>Oncode Institute, University Medical Center Utrecht, Universiteitsweg 100 3584 CG Utrecht, The Netherlands.

<sup>3</sup>Correspondence to: [t.b.dansen@umcutrecht.nl](mailto:t.b.dansen@umcutrecht.nl).

Free Radical Biology and Medicine 172 (2021) 298–311

DOI: [10.1016/j.freeradbiomed.2021.06.013](https://doi.org/10.1016/j.freeradbiomed.2021.06.013)

## Abstract

Stabilization and activation of the p53 tumor suppressor are triggered in response to various cellular stresses, including DNA damaging agents and elevated Reactive Oxygen Species (ROS) like H<sub>2</sub>O<sub>2</sub>. When cells are exposed to exogenously added H<sub>2</sub>O<sub>2</sub>, ATR/CHK1 and ATM/CHK2 dependent DNA damage signaling is switched on, suggesting that H<sub>2</sub>O<sub>2</sub> induces both single and double strand breaks. These collective observations have resulted in the widely accepted model that oxidizing conditions lead to DNA damage that subsequently mediates a p53-dependent response like cell cycle arrest and apoptosis. However, H<sub>2</sub>O<sub>2</sub> also induces signaling through stress-activated kinases (SAPK, e.g., JNK and p38MAPK) that can activate p53. Here we dissect to what extent these pathways contribute to functional activation of p53 in response to oxidizing conditions. Collectively, our data suggest that p53 can be activated both by SAPK signaling and the DDR independently of each other, and which of these pathways is activated depends on the type of oxidant used. This implies that it could in principle be possible to modulate oxidative signaling to stimulate p53 without inducing collateral DNA damage, thereby limiting mutation accumulation in both healthy and tumor tissues.

**Keywords:** Oxidative signaling, DNA damage response, p53 activation, p38MAPK, differential pathways

## Introduction

p53 transcriptional activity induces a wide range of cellular processes including cell cycle arrest, DNA damage repair, senescence, apoptosis and metabolism. Collectively these programs ensure genome integrity, lower the chance to pass on DNA mutations down the lineage and hence provide tumor suppressive function. Nevertheless, p53-dependent programs such as transient cell cycle arrest and the regulation of metabolism can also function to support cell survival, for instance upon nutrient depletion, by providing means to maintain cellular energy levels and control redox balance [1]

Under basal, unstressed conditions p53 activity is low as a result of the continuous turnover of the p53 protein, which is under control of MDM2 dependent poly-ubiquitylation and subsequent proteasomal degradation. Stabilization of p53 is the outcome of several cellular stress signaling pathways. Upon DNA double strand breaks, ATM undergoes activating autophosphorylation and phosphorylates p53 on Ser15, but also activates CHK2 which in turn phosphorylates p53 on Ser20 [2, 3]. These two phosphorylation events facilitate p53 stabilization by preventing MDM2-mediated p53 ubiquitylation and subsequent proteasomal degradation [4]. In addition to ATM kinase, two members of the stress-activated protein kinase (SAPK) family: c-Jun N-terminal kinase (JNK) and p38MAPK have also been shown to mediate p53 activation in response to UV irradiation, some chemotherapeutic agents but also upon exposure to Reactive Oxygen Species like H<sub>2</sub>O<sub>2</sub>, all of which also have been shown to induce DNA damage [5-7]. JNK phosphorylates p53 on Ser 20 and Thr 81[8,

9], whereas p38MAPK has been implicated in phosphorylation on Ser15, 33, 37 and 46 [5, 7]. Because JNK and p38MAPK are both proline-directed Ser/Thr protein kinases, it may be difficult to distinguish whether and which of these kinases specifically target a certain site. In any case, these PTMs also induce p53 stabilization and transcriptional activity.

As mentioned, many treatments that engage the cellular DNA damage response also activate SAPK signaling and vice versa. It is therefore often difficult to pinpoint which of these pathways is the predominant activator of p53 [10, 11]. For Reactive Oxygen Species (ROS), such as superoxide anions ( $O_2^{\cdot-}$ ), hydroxyl radicals ( $HO^{\cdot}$ ) and hydrogen peroxide ( $H_2O_2$ ), the classical view is that these indeed contribute to damage to proteins, lipids and DNA [12, 13]. Exogenously added  $H_2O_2$  indeed induces both the DNA damage response pathways associated with single and double DNA breaks [14-16]. Based on these observations it has been suggested that  $H_2O_2$  that is generated endogenously as a consequence of for instance mitochondrial respiration can directly contribute to mutations in genomic DNA, and therefore could be a driver of aging and tumor initiation and progression [17, 18].

In the literature various terms (e.g. oxidative stress, redox signaling) for signaling in response to elevated ROS are being used. For a clear definition we would like to refer to the review by Sies and Jones [12], in which the authors discriminate between oxidative eustress and oxidative distress, depending on the levels of  $H_2O_2$ . The term Redox signaling is mostly associated with physiological  $H_2O_2$  levels and specific signaling that is regulated through reversible cysteine oxidation, whereas oxidative distress may result from random oxidative damage to cellular constituents including the DNA, leading to induction of the DNA damage response (DDR) through activation of ATM and ATR. However, it is not always clear where the border between eustress and distress lies. In this study we compared and dissected effects that are triggered in response to treatment with oxidants and DNA-damaging agents, to model and dissect what happens during therapeutic activation of p53. Because in most cases the concentration of oxidants used is well above what would be considered to occur endogenously, we have opted to use the term 'oxidative signaling' for the observed responses downstream of exposure to oxidants that trigger signaling as measured by i.e. SAPK activation, to distinguish it from the oxidant-induced DDR as well as from redox signaling under physiological levels of ROS.

ROS induced SAPK activation indeed occurs independent of DNA damage as a result of oxidative signaling through the reversible oxidation of protein cysteine-thiols [12].  $H_2O_2$  leads for instance to disulfide-dependent dimerization and activation of ASK-1, which activates JNK and p38MAPK followed by p53 stabilization [19, 20]. To complicate things further, ATM has also been reported to be activated by cysteine oxidation independent of DNA DSBs [21]. Taken together, and as we recently outlined in detail [22], it remains unclear which upstream signaling pathways (ATM, JNK and p38MAPK) are responsible for oxidant-induced p53 activation in response to which signaling pathways (DNA damage or oxidative signaling, or both) and to what extent.

In the present study, we aim to dissect signaling cascades upstream of p53 in response to DNA damage signaling and oxidative signaling. We show that p53 activation in response to DNA damage is mainly mediated by the ATM kinase, whereas oxidative signaling-mediated p53 activation depends mostly on p38MAPK and is independent of the ATM-dependent DNA damage response. ATM, JNK and p38MAPK are all activated by H<sub>2</sub>O<sub>2</sub>, but only ATM and JNK are required for H<sub>2</sub>O<sub>2</sub>-induced p53 activation. The thiol oxidant diamide activates both JNK and p38MAPK but not ATM, and p53 activation by diamide depends on p38MAPK. Collectively, we show that functional p53 activation by oxidative signaling and DNA damage is mediated by distinct signaling pathways. Our observations imply that for therapeutic strategies p53 can in principle be reactivated by oxidative signaling without collateral DNA damage, lowering the chance of inducing mutations that drive tumor progression or initiate new malignancies in healthy neighboring tissue.

## Materials and methods

### Reagents and antibodies

5-Fluorouracil (5-FU), Etoposide, Diamide, H<sub>2</sub>O<sub>2</sub>, Neocarzinostatin (NCS), Auranofin (AFN) and ATM inhibitor (KU55933) were from Sigma. Oxaliplatin, Doxorubicin, Mitomycin C, JNK inhibitor (SP600126) and p38MAPK inhibitor (PH797804) were from Bio-Connect Life Sciences. Nutlin-3a was from Sanbio.

Antibodies were used as follows: CHK2 (A-11), CHK1 (G-4), p53 (DO-1), p21 (M-19), JNK (D-2) and c-Jun (SC-1694) were from Santa Cruz Biotechnology. ATM (D2E2), pp53 (Ser15) (CS9286), pCHK2 (Thr68) (CS2661), pCHK1 (S345) (CS2348), p-C-Jun (Ser63) (CS9261), pJNK (Thr183/Tyr185)(CS9251), p38MAPK(CS9212), pp38MAPK (Thr180/Tyr182) (CS4511), pATF-2 (Thr71) (CS24329) and pERK1/2 (T202/Y204) (CS4370) were from Cell Signaling Technology. Phospho-Histone H2AX (Ser139) and GAPDH (MAB374) were from EMD Millipore. pATM (Ser1981) (ab81292) from abcam. HRP or fluorescently labeled secondary antibodies were used for detection on Western blot.

### Cell culture

Non-small-cell-lung cancer cells (NCI-H1299, ATCC® CRL-5803™) [23] cells were cultured in DMEM high-glucose (4,5g/L) supplemented with 10 % FBS, 2 mM L-glutamine and 100 Units Penicillin-Streptomycin (All from Sigma Aldrich). RPE<sup>Tert</sup> and RPE<sup>Tert</sup> p53-KO cells (a gift from dr. René Medema [24]) were cultured in DMEM/F-12 high-glucose supplemented with 10 % FBS and 100 U Penicillin-Streptomycin (Sigma Aldrich). All cell types were cultured at 37 °C under a 6 % CO<sub>2</sub> atmosphere. Cell transfection was carried out using PEI (Sigma Aldrich).

### Plasmids and lentiviral transduction

Plasmids containing the sequences for HyPer7-NLS and HyPer7-NES were a kind gift from Dr. Vsevolod Belousov [25]. The HyPer7-NLS and -NES sequences were cloned into



a modified form of the lentiviral backbone pLV-H2B-mNeon-ires-Puro, where the puromycin resistance cassette was replaced by a blasticidin resistance gene [26, 27] by infusion cloning using primers designed in SnapGene software (See **Table S1**). The PCR products were isolated from a 1% agarose gel using a gel extraction kit (Qiagen). The PCR products were ligated into the linearized backbone (digested with BstBI and NheI, New England Biolabs) using the In-Fusion HD cloning kit (Takara), according to manufacturer's protocol. Lentiviral HyPer7-NLS and HyPer7-NES constructs were transfected into HEK293T cells together with third-generation packaging vectors. Virus was purified from filtered media (0.45  $\mu\text{m}$ ) by ultracentrifugation and RPE<sup>Tert</sup> cells were infected and selected with Blasticidin (20  $\mu\text{g}/\text{ml}$ , Bio connect). The correct localization of the HyPer7-NLS and -NES proteins was confirmed by fluorescence microscopy (see **Fig. 1A & C**).

pDONR223-p53-WT plasmid was a gift from Jesse Boehm & William Hahn & David Root (Addgene plasmid # 81754, [28]). The p53 cysteine mutant (C182S, C229S, C277S) was generated by site-directed mutagenesis PCR using pDONR223-p53-WT as a template using the primers indicated in Table S1. Plasmids (pcDNA3) expressing Flag-His-p53-WT and -cysteine mutant were obtained through Gateway cloning (Life Technologies) following the standard procedure.

Stable, doxycycline-inducible p53 expressing cells were generated by transduction with lentiviral pInducer20-Flag-p53 in the p53-KO RPE<sup>Tert</sup> or H1299 background, followed by the selection with 400  $\mu\text{g}/\text{ml}$  (for RPE<sup>Tert</sup> cells) and 600  $\mu\text{g}/\text{ml}$  (for H1299 cells) Neomycin for 2 weeks. pInducer20 plasmid was a gift from Stephen Elledge (Addgene plasmid # 44012) [29]. pInducer20-Flag-p53 was made through Gateway cloning following standard procedures [30]. The inducible expression of p53 was confirmed by Western blotting and polyclonal cells were used for subsequent experiments.

### Western Blotting

RPE<sup>Tert</sup> or H1299 cells were seeded in 6-well dishes and growing to be around 80 % confluency, followed by treatments with different compounds for the indicated time. Cells were then directly scraped in 1X sample buffer (2 % SDS, 5 % 2-mercaptoethanol, 10 % glycerol, Tris-HCl pH 6.8, 0.002 % bromophenol blue). Samples were run on SDS-PAGE gels (Biorad system), followed by a standard Western blotting precure. Briefly, samples were transferred to polyvinylidene difluoride (PVDF) or nitrocellulose membranes. Membranes were then blocked with 2 % BSA TBS-Tween (TBST, 1 % v/v) solution for 1h at 4 °C, followed by incubation with primary antibodies overnight at 4 °C. After washing the membrane with TBST solution, secondary antibody staining was performed using HRP or fluorescence-conjugated antibodies for 1h at 4 °C. After washed three times with TBST, membranes were analyzed by Image Quant LAS or Typhoon-Biomolecular Imager.

### Ubiquitylation assay

HEK293T cells were transiently transfected with Flag-His-p53 and His-ubiquitin expression

constructs. After 48 h, cells were treated with or diamide (15 min) followed by lysis in buffer containing 100 mM  $\text{NaH}_2\text{PO}_4/\text{Na}_2\text{HPO}_4$ , 10 mM Tris pH 8, 8 M Urea, 10 mM Imidazole and 0.2 % Triton X-100 and sonication. Cell lysates were then centrifuged at 10,000 rpm for 10 min, and 50  $\mu\text{l}$  of supernatant was taken as input sample and ubiquitinated proteins were enriched by incubation with Ni-NTA beads for 2 h at room temperature. The Ni-NTA beads were washed twice with the above indicated lysis buffer, followed by a wash with elution buffer (100 mM NaCl, 20 % glycerol, 20 mM Tris pH 8.0, 1 mM DTT and 10 mM Imidazole). In the end, ubiquitinated proteins were resuspended in 1X sample buffer (2 % SDS, 5 % 2-mercaptoethanol, 10 % glycerol, Tris-HCl pH 6.8, 0.002 % bromophenol blue), boiled at 95 °C for 8 mins, and further analyzed by standard Western blotting.

### **Immunofluorescence microscopy**

RPE<sup>Tert</sup> cells were grown on glass coverslips in 6-well dishes for three days and then treated with PBS, diamide, or NCS for 1 h. Cells were washed twice with cold PBS and fixed (3.7 % Formaldehyde solution) for 15 min at room temperature. Fixed cells were permeabilized using 0.1 % Triton for 5 min followed by blocking with 2 % BSA (w/v) plus purified goat IgG in 1:10,000 in PBS for 30-60 min at room temperature. After that, cells were incubated with primary antibodies (1:500 dilution for Anti-p53 and pH2AX (Ser139)) overnight, followed by 1 h incubation with secondary antibodies labeled with Alexa fluor 568 (ThermoFisher) and Hoechst 33342 (Life Technologies) after washing twice with PBS. All antibody incubations were performed at 4°C and in the dark. Coverslips were mounted with a drop of mounting medium, sealed with nail polish to prevent drying, and saved in the dark at 4 °C until analysis. Imaging was performed on a Zeiss Axio Imager Z1 and images were processed using ImageJ software.

HyPer7-NLS and NES RPE<sup>Tert</sup> were grown in 35 x 10 mm cellview cell culture dishes (627860, Greiner). Live cells were stained with Hoechst 33342 (Life Technologies) for 15 min at room temperature and imaged on a ZEISS confocal laser scanning microscope (LSM880).

### **RNA isolation and qPCR**

Total RNA was isolated from Doxycycline-inducible p53 expressing RPE<sup>Tert</sup> p53 KO cells (treated with or without doxycycline) using the RNeasy kit (QIAGEN). 500 ng RNA was used for cDNA synthesis using the iScript cDNA Synthesis Kit (BIO-RAD) according to the manufacturer's instructions. qPCR experiments were carried out using SYBR Green FastStart Master Mix [31] on a CFX Connect Real-time PCR detection system (Bio-RAD). qPCR cycle settings were as follows: pre-denaturation at 95 °C for 10 min, followed by 39 cycles of denaturation at 95 °C for 10 s, annealing at 58 °C for 10 s, and extension at 72 °C for 30 s. Relative gene expression was calculated using  $2^{-\Delta\Delta\text{CT}}$  method by taking GAPDH as a reference gene. All the primers used for qPCRs are shown in Table S1.

### **Cell viability assay**

Cell viability was evaluated using a dual Calcein-AM/Sytox-Blue assay, where Calcein-AM

is used to stain live cells and Sytox blue to identify dead cells.  $1 \times 10^4$  RPE<sup>Tert</sup> and RPE<sup>Tert</sup> p53 KO cells were seeded in 96-well plates. The next day, cells were treated with diamide, H<sub>2</sub>O<sub>2</sub> or NCS at the indicated concentrations for 72 h, followed by addition of a mix of Calcein-AM/Sytox Blue at a final concentration of 1  $\mu$ M for both dyes. The plates were mixed gently and incubated at 37°C for 30 min, and then evaluated on a Spectra Max Fluorometer: Ex. 485 nm / Em. 535 nm for Calcein and Ex. 444 nm / Em. 460 nm for Sytox-Blue. The ratio of Calcein/Sytox-Blue was calculated and relative cell viability was determined by normalizing to untreated cells (considered as 100% cell viability).

### Flow cytometry

To assess the effect of the various treatments on the DNA damage response and H<sub>2</sub>O<sub>2</sub>-dependent redox state (measured as the ratio of oxidation and reduction of the H<sub>2</sub>O<sub>2</sub>-specific sensor HyPer7), RPE<sup>Tert</sup> cells stably expressing HyPer7-NLS and NES were treated with diamide, or NCS for the indicated times. To prevent post-harvest HyPer7 oxidation or reduction, cells were washed with PBS containing 100 mM NEM prior to trypsinization. Cells were then fixed with 4 % Formaldehyde solution for 10 min at room temperature, followed by incubation with ice-cold 70 % Ethanol overnight at 4 °C. Cells were resuspended in PBS and washed with PBS buffer twice, and stained with anti-Phospho-Histone H2AX (Ser139) PE-conjugated antibody (0.25  $\mu$ g/sample) for 30 min at room temperature. After that, cells were resuspended in PBS buffer with 1 % BSA and 0.05 % Tween and analyzed on a FACSCelesta Flow Cytometer (BD Bioscience). HyPer7 fluorescence was detected using Ex405/Em525/50 (reduced) and Ex488/Em30/30 (oxidized) lasers and filter sets.

For cell cycle profile assessment, dox-inducible p53 expressing RPE<sup>Tert</sup> p53 KO cells with or without Dox addition were treated with H<sub>2</sub>O<sub>2</sub>, diamide or NCS. After 24 h, cells were washed with PBS, trypsinized, and fixed with 70% ethanol overnight at 4 °C. Cells were washed twice with and resuspended in staining buffer (PBS with 0.1% BSA and 0.05% Tween and DAPI) for 30 min in the dark on ice. Cells were then analyzed on a FACSCelesta Flow Cytometer (BD Bioscience).

Cell death was assessed using Propidium Iodide (PI) (sigma-Aldrich) exclusion and Annexin V-FITC (IQ Products) staining. RPE<sup>Tert</sup> p53 KO cells and H1299 cells with or without doxycycline were treated with diamide, H<sub>2</sub>O<sub>2</sub> or NCS for 24 h. Culture media, PBS buffer used to wash cells and trypsinized cells were collected in the same tube. Samples were washed once with PBS and resuspended in 1X Annexin V Binding Buffer (10 mM pH 7.4 HEPES, 140 mM NaCl and 2.5 mM CaCl<sub>2</sub>) containing PI and Annexin V-FITC and incubated for 30 min in the dark on ice. Cells were then analyzed on a FACSCelesta Flow Cytometer (BD Bioscience).

### Timelapse Video fluorescence microscopy

Monoclonal RPE<sup>Tert</sup> cells expressing either HyPer7-NLS or HyPer7-NES were plated in 8-well chamber slides (ibidi) and imaged using a Cell Observer microscope (Zeiss) with

a 10 x Objective. The HyPer7 fluorescent protein was excited at 385 nm and 475 nm consecutively and the subsequent emission was measured using a BP514/44 filter. The different treatments were added after measuring the first timepoint, upon which imaging was continued.

Image processing was performed using FIJI imaging software. A background signal was obtained by imaging cells not expressing HyPer7, and this was subtracted from the HyPer7 images. The images were then thresholded to show only fluorescence inside cells and the images obtained with 495 nm excitation were divided by the images obtained by 385 nm excitation; This ratio describes the average degree of HyPer7 oxidation of all the cells in view (about 250 cells). Finally, the average ratio per timepoint was calculated per treatment and normalized to the first timepoint.

### Statistical Analysis

All statistical analysis was performed in GraphPad Prism 8 software. One-way ANOVA method followed by Dunnett's multiple comparisons, was used to evaluate the statistical significance of qPCR data, and an adjusted p value < 0.05 was considered to be statistically significant. A Student's t-test was used to evaluate the difference of cell death in p53-off and p53-on cells upon each treatment, and a p-value < 0.05 was considered to be statistically significant.

## Results

### Differential activation of oxidative signaling and the DNA damage response

H<sub>2</sub>O<sub>2</sub> is known to induce signaling, part of which is mediated through the activation of stress-activated kinases (SAPK, e.g., JNK and p38MAPK). But H<sub>2</sub>O<sub>2</sub> also activates key kinases involved in the DNA damage response (e.g., ATM and ATR) (**Fig. S1A**). Likewise, several genotoxic agents that are being used as chemotherapeutics have been suggested to act, at least in part, through the production of ROS and hence could start or modulate oxidative signaling and trigger stress-activated kinases (**Fig. S1B-D**).

To be able to dissect the DDR and oxidative signaling-based responses, we investigated whether it is possible to activate these pathways independently. To this end we stably expressed the H<sub>2</sub>O<sub>2</sub>-specific HyPer7 probe in non-transformed, human Telomerase immortalized Retinal Pigment Epithelial (RPE<sup>Tert</sup>) cells using lentiviral transduction. RPE<sup>Tert</sup> cells have been shown to have a wildtype p53 protein and response [32]. Some of the benefits of the HyPer7 probe as compared to earlier versions are its insensitivity to pH changes and enhanced sensitivity. The probe reports on the ratio of the H<sub>2</sub>O<sub>2</sub> dependent oxidation ( $\lambda$ Ex488 nm /  $\lambda$ Em 530/30 nm) and reduction ( $\lambda$ Ex405 nm /  $\lambda$ Em 525/50 nm) by the thioredoxin system [25]. HyPer7 oxidation was assessed along with positivity for the DNA damage response marker H2AX-pSer139 (aka  $\gamma$ H2AX) by flow cytometry upon treatment with diamide, H<sub>2</sub>O<sub>2</sub> or Neocarzinostatin (NCS). In order to assess H<sub>2</sub>O<sub>2</sub>-dependent redox perturbations in the vicinity of the DNA, nuclear localized HyPer7 (HyPer7-NLS) was used

(**Fig. 1A**). We found that it is indeed possible to induce the DDR and oxidizing conditions separately for prolonged time periods. The thiol-specific oxidant diamide, which is thought to act largely through oxidation of the GSH pool, rapidly but transiently induced HyPer7 oxidation, without affecting  $\gamma$ H2AX levels for up to 6 hrs after treatment (**Fig. 1B-1D, S2B-C**). As mentioned, alterations in the ratio of the HyPer7 probe are a measure of the combined rate of oxidation (by  $H_2O_2$ ) and reduction (by the thioredoxin system) [33], which makes it difficult to distinguish whether the diamide-induced increase in HyPer7 ratio stems from an increase of  $H_2O_2$  from endogenous sources or from a loss of reductive power or both. In any case, the ratio of the  $H_2O_2$ -specific HyPer7 probe correlates with that of PRDX oxidation/reduction and hence is a good read-out for the induction of  $H_2O_2$ -dependent signaling. The DNA damaging agent NCS induced a buildup of  $\gamma$ H2AX signal that peaked 1 h after treatment, without evidence of changes in the HyPer7 ratio. Treatment with  $H_2O_2$  resulted in both HyPer7 oxidation and phosphorylation of H2AX, in line with the idea that this compound indeed induces both oxidative signaling and the DDR [34] (**Fig. 1B-1D, S2**). Note that the kinetics of H2AX phosphorylation by  $H_2O_2$  follow those of NCS. The oxidation of HyPer7 by diamide happens slightly slower as compared to  $H_2O_2$ . We next asked whether NCS could induce oxidative signaling in the cytoplasm, which has been proposed in a previous study [35]. To this end, we evaluated the HyPer7 ratio in RPE<sup>Tert</sup> cells stably expressing cytoplasmic localized HyPer7 (HyPer7-NES) (**Fig. 1E**) as well as  $\gamma$ H2AX positivity in parallel. Under the conditions used, NCS did not generate  $H_2O_2$  in the cytoplasm either but again induced a substantial nuclear DNA damage response (**Fig. 1F-1H**). Not surprisingly, both diamide and  $H_2O_2$  treatment rapidly induced HyPer7 oxidation in the cytoplasm similar to what was observed for the nucleus (**Fig. 1F&1G**). The induction of DNA damage by  $H_2O_2$  and NCS but not by diamide in RPE<sup>Tert</sup> cells was further corroborated by immunofluorescence microscopy (**Fig. 1I**), and over a broad range of concentrations by video timelapse fluorescence microscopy and Western blot (**Fig. S2**).  $H_2O_2$  could be measured by the HyPer7 probe starting at a concentration of 5  $\mu$ M bolus addition, and the signal was saturated above  $\sim$ 100  $\mu$ M. DNA damage signaling was detected from concentrations as low as 25  $\mu$ M (**Fig. S1A, S2A, S2C**). The induction of HyPer7 oxidation without evidence of DNA damage signaling by diamide was observed up until concentrations of  $\sim$ 250  $\mu$ M. Above 500  $\mu$ M, diamide did induce minor phosphorylation of CHK2 and H2AX (**Fig. S2B-C**) but also invariably led to complete loss of cell viability within 24 hrs irrespective of p53 status (see also **Fig. S4**). The dynamics of HyPer7 oxidation and reduction were slightly slower in case of diamide as compared to  $H_2O_2$  (**Fig. S2A&2B**). Taken together, diamide and NCS can serve as model compounds in this study to dissect to what extent the effects of  $H_2O_2$  treatment are mediated through oxidative signaling, the DDR or both. Furthermore, these data already indicate that oxidizing conditions do not necessarily lead to a DDR.

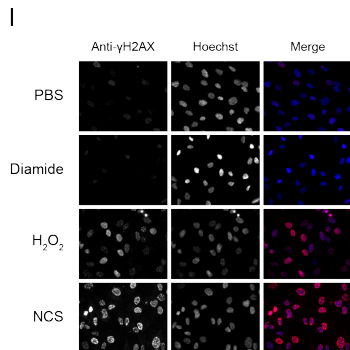
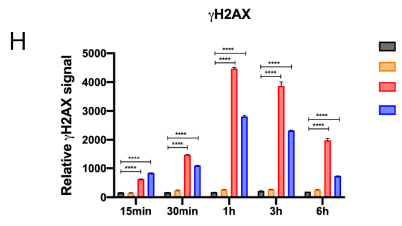
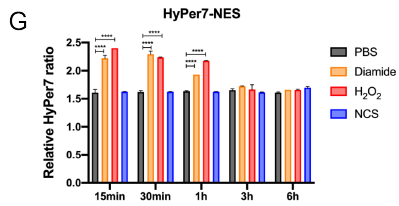
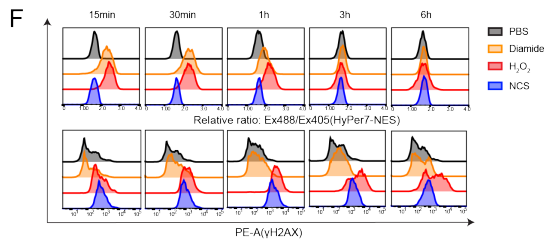
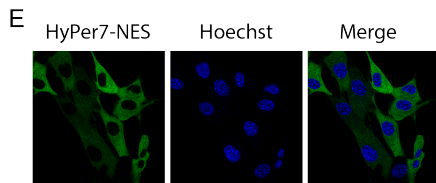
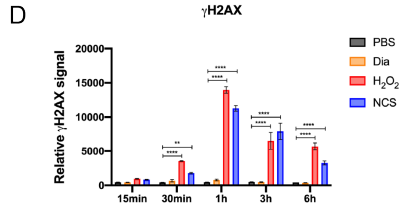
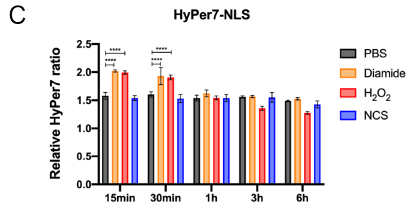
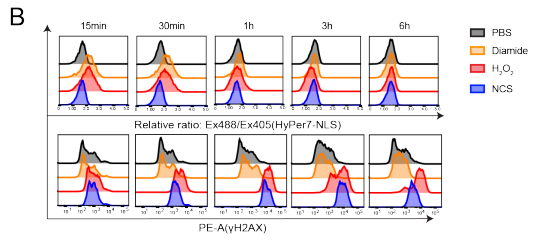
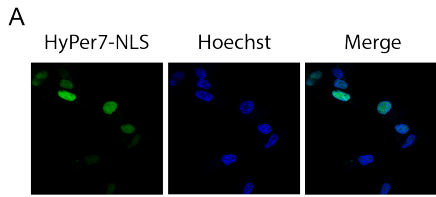


### Figure 1. Oxidative signaling and DNA damage signaling can be induced independent of each other.

(A) Microscopy staining nuclear localized HyPer7(HyPer7- NLS) in RPE<sup>Tert</sup> cells. Nuclei were stained with Hoechst. (B) RPE<sup>Tert</sup> cells stably expressing HyPer7- NLS were treated with PBS, diamide (200  $\mu$ M), H<sub>2</sub>O<sub>2</sub> (200  $\mu$ M) or Neocarzinostatin (NCS) (250 ng/ml) for the indicated times. The ratio of oxidized (Ex 488 nm / Em 530/30 nm) over reduced (Ex405 nm / Em 525/50 nm) HyPer7 and the level of  $\gamma$ H2AX (H2AX-pSer139) were evaluated by Flow Cytometry. (C) Quantification of geometric mean of the HyPer7- NLS ratio from three independent experiments. The error bars stand for the standard division (SD) of the geometric means. The statistical analysis was performed by using One-way ANOVA followed by Multiple comparisons test (Dunnett) under each time point. \*, p value < 0.05; \*\*, p value < 0.005, \*\*\*, p value < 0.0005, \*\*\*\*, p value < 0.0001. (D) Quantification of geometric mean of  $\gamma$ H2AX from three independent experiments. The error bars stand for the standard division (SD) of the geometric means. The statistical analysis was performed by using One-way ANOVA followed by Multiple comparisons test (Dunnett) under each time point. \*, p value < 0.05; \*\*, p value < 0.005; \*\*\*, p value < 0.0005; \*\*\*\*, p value < 0.0001. (E) Microscopy staining cytoplasmic localized HyPer7(HyPer7-NES) in RPE<sup>Tert</sup> cells. Nuclei were stained with Hoechst. (F) RPE<sup>Tert</sup> cells stably expressing HyPer7- NLS were treated with PBS, diamide (200  $\mu$ M), H<sub>2</sub>O<sub>2</sub> (200  $\mu$ M) or Neocarzinostatin (NCS) (250 ng/ml) for the indicated times. The ratio of oxidized (Ex 488 nm / Em 530/30 nm) over reduced (Ex405 nm / Em 525/50 nm) HyPer7 and the level of  $\gamma$ H2AX (H2AX-pSer139) were evaluated by Flow Cytometry. (G) Quantification of geometric mean of the HyPer7-NLS ratio from three independent experiments. The error bars stand for the standard division (SD) of the geometric means. The statistical analysis was performed by using One-way ANOVA followed by Multiple comparisons test (Dunnett) under each time point. \*, p value < 0.05; \*\*, p value < 0.005, \*\*\*, p value < 0.0005, \*\*\*\*, p value < 0.0001. (H) Quantification of geometric mean of  $\gamma$ H2AX from three independent experiments. The error bars stand for the standard division (SD) of the geometric means. The statistical analysis was performed by using One-way ANOVA followed by Multiple comparisons test (Dunnett) under each time point. \*, p value < 0.05; \*\*, p value < 0.005; \*\*\*, p value < 0.0005; \*\*\*\*, p value < 0.0001. (I) Epifluorescence microscopy staining for  $\gamma$ H2AX in RPE<sup>Tert</sup> cells upon 1h treatment of diamide (200  $\mu$ M), H<sub>2</sub>O<sub>2</sub> (200  $\mu$ M) or NCS (250 ng/ml). Nuclei were stained with Hoechst and  $\gamma$ H2AX were stained with an anti- $\gamma$ H2AX primary antibody and Alexa Fluor 568 as the secondary antibody.

### Oxidative signaling activates p53 independent of the DDR

Now that we had found means to selectively induce oxidizing conditions without triggering the DDR, we set out to explore whether and how this contributes to p53 stabilization and activation upon exposure to H<sub>2</sub>O<sub>2</sub>. To this end, RPE<sup>Tert</sup> cells were exposed to diamide or H<sub>2</sub>O<sub>2</sub> for various timepoints (Fig. 2A). NCS was used as a positive control for DDR activation in the absence of oxidative signaling (as shown in Fig. 1B). In line with the absence of  $\gamma$ H2AX induction in the previous experiment, diamide also did not trigger the DDR pathway, as evidenced by the absence of ATM-pS1981, CHK2-pThr68, CHK1-pSer345 and p53-pSer15 induction. Nevertheless, prolonged (6 h) treatment with diamide surmounted in p53 stabilization to comparable levels as those induced by NCS (1 h) or H<sub>2</sub>O<sub>2</sub> (6 h), and this was accompanied by accumulation of the p53 transcriptional target gene product p21 (Fig. 2A). Indeed, p21 was not induced in CRISPR/CAS9-derived RPE<sup>Tert</sup> p53 KO cells (Fig. 2B). Both oxidizing compounds (but not NCS) trigger JNK (T183/Y185) phosphorylation, albeit more

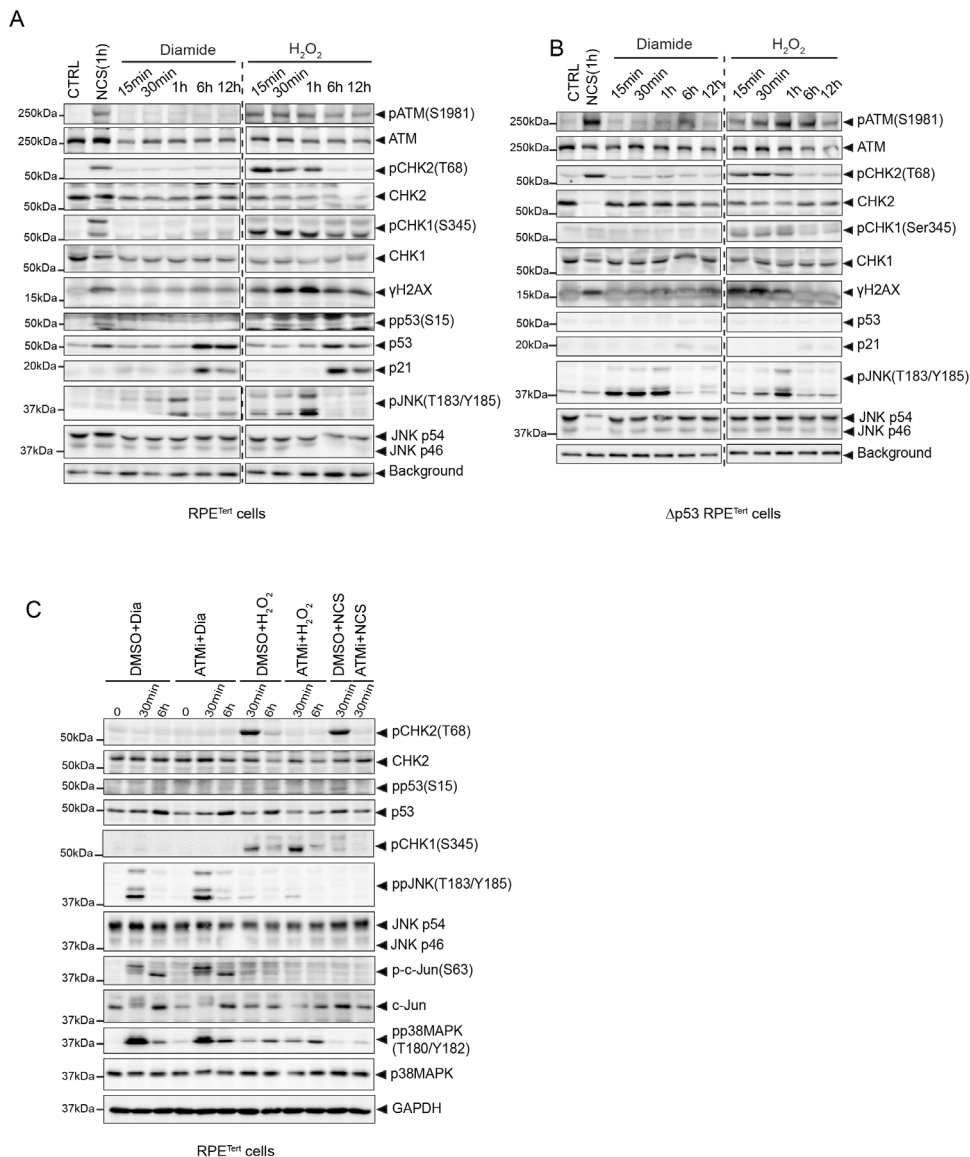


**Figure 2. Oxidative signaling activates p53 independent of the ATM-dependent DNA damage response.**

(A) RPE<sup>Tert</sup> cells were treated with NCS (250 ng/ml), diamide (200  $\mu$ M) and H<sub>2</sub>O<sub>2</sub> (200  $\mu$ M) for the indicated time. Phosphorylation states of ATM (S1981), CHK2 (T68), CHK1 (S345), H2AX (S139), p53 (S15), JNK (T183/Y185), endogenous p53 and p21 levels, and the total protein level of ATM, CHK2, CHK1 and JNK were evaluated by immunoblotting. (B) Same treatment as in (A), but using RPE<sup>Tert</sup> p53 KO cells. (C) RPE<sup>Tert</sup> cells were pretreated with DMSO or ATM inhibitor (ATMi) KU5933 (10  $\mu$ M) for 1h, followed by treatment with diamide (200  $\mu$ M), H<sub>2</sub>O<sub>2</sub> (200  $\mu$ M) or NCS (250 ng/ml) for the indicated time. p53 level, phosphorylation state of CHK2 (T68), CHK1 (S345), p53 (S15), JNK (T183/Y185), p38MAPK (T180/Y182) and p-c-Jun (S63), and the total protein level of CHK2, JNK, c-Jun, p38MAPK and GAPDH as a loading control were evaluated by immunoblotting.



pronounced by diamide, indicating that the SAPK pathway acts downstream of oxidative signaling and independent of the DDR. Note that the stabilization of p53 by H<sub>2</sub>O<sub>2</sub> and diamide was observed long after JNK or CHK2 phosphorylation had ceased.

To further elucidate signaling downstream of oxidative signaling and the DDR, we assessed whether ATM activity was required for the observed stabilization of p53 by oxidizing (diamide/H<sub>2</sub>O<sub>2</sub>) versus DNA damaging (H<sub>2</sub>O<sub>2</sub>/NCS) conditions using the ATM inhibitor KU55933 (ATMi). Inhibition of ATM abolished p53 phosphorylation on Ser15 and stabilization induced by H<sub>2</sub>O<sub>2</sub> and NCS, whereas it had no effect on diamide-induced p53 stabilization (**Fig. 2C**). This suggests that whereas the DDR downstream of H<sub>2</sub>O<sub>2</sub> proceeds through ATM, oxidative signaling does not. Phosphorylation of CHK2, but not CHK1, in response to H<sub>2</sub>O<sub>2</sub> was indeed largely abolished upon treatment with ATMi, suggesting that ATM and not ATR signaling plays a dominant role in p53 activation upon H<sub>2</sub>O<sub>2</sub>-induced DNA damage (**Fig. 2C**). Diamide induced the activation of JNK and p38MAPK to a larger extent as compared to H<sub>2</sub>O<sub>2</sub>, and this was also not affected by treatment with ATMi. If oxidative signaling-induced p53 stabilization depends on SAPK activation, this observation could be an explanation as to why oxidative signaling downstream of H<sub>2</sub>O<sub>2</sub> fails to stabilize p53 in the presence of ATMi; something we will explore later in this study.

p53 has been reported to undergo cysteine oxidation upon oxidizing conditions (e.g., diamide treatment) both in vitro and in live cells [36]. To test whether cysteine oxidation plays a potential role in diamide and H<sub>2</sub>O<sub>2</sub>-mediated p53 stabilization, we devised a Flag-tagged p53 (C182SC229SC277S) mutant, which was expressed from a doxycycline-inducible promoter in RPE<sup>Tert</sup> p53 KO cells. The other cysteines in p53 are either not surface-exposed or are part of the Zn-finger and crucial for p53 structure (**Fig. S3A**) [37, 38]. C182 and C277 were shown to be most sensitive to oxidation [36, 39]. This triple cysteine mutant was still stabilized upon treatment with diamide or H<sub>2</sub>O<sub>2</sub> (**Fig. S3B**), suggesting that redox modifications on these cysteines do not significantly contribute to p53 protein stabilization in response to oxidative signaling.

Collectively, our results indicate that oxidative signaling and the ATM-dependent DNA damage signaling responses as observed upon H<sub>2</sub>O<sub>2</sub> exposure can be induced independent of each other, and that both pathways can lead to p53 stabilization and activation.

### **Diamide and H<sub>2</sub>O<sub>2</sub> stabilize p53 through inhibition of its ubiquitin-dependent degradation**

Several cellular stresses, including DNA damage, have been shown to induce stabilization of p53 through interference with MDM2-dependent ubiquitinylation and subsequent proteasomal degradation [40, 41]. To explore whether diamide and H<sub>2</sub>O<sub>2</sub>-induced p53 stabilization also depend on inhibition of protein breakdown, p53 protein decay dynamics were assessed in the presence of these compounds in combination with the protein synthesis inhibitor cycloheximide (CHX). p53 levels rapidly declined under control conditions

and persisted upon treatment with the positive control Nutlin-3a (an MDM2 inhibitor). Treatment with diamide, and to a lesser extent  $H_2O_2$ , resulted in attenuated p53 decay, suggesting that these oxidants interfere with MDM2-dependent degradation (**Fig. 3A & 3B**). In accordance, ubiquitinylation of p53 was inhibited upon diamide and  $H_2O_2$  treatment (**Fig. 3C**). Several enzymes involved in the (de)ubiquitinylation reaction depend on catalytic

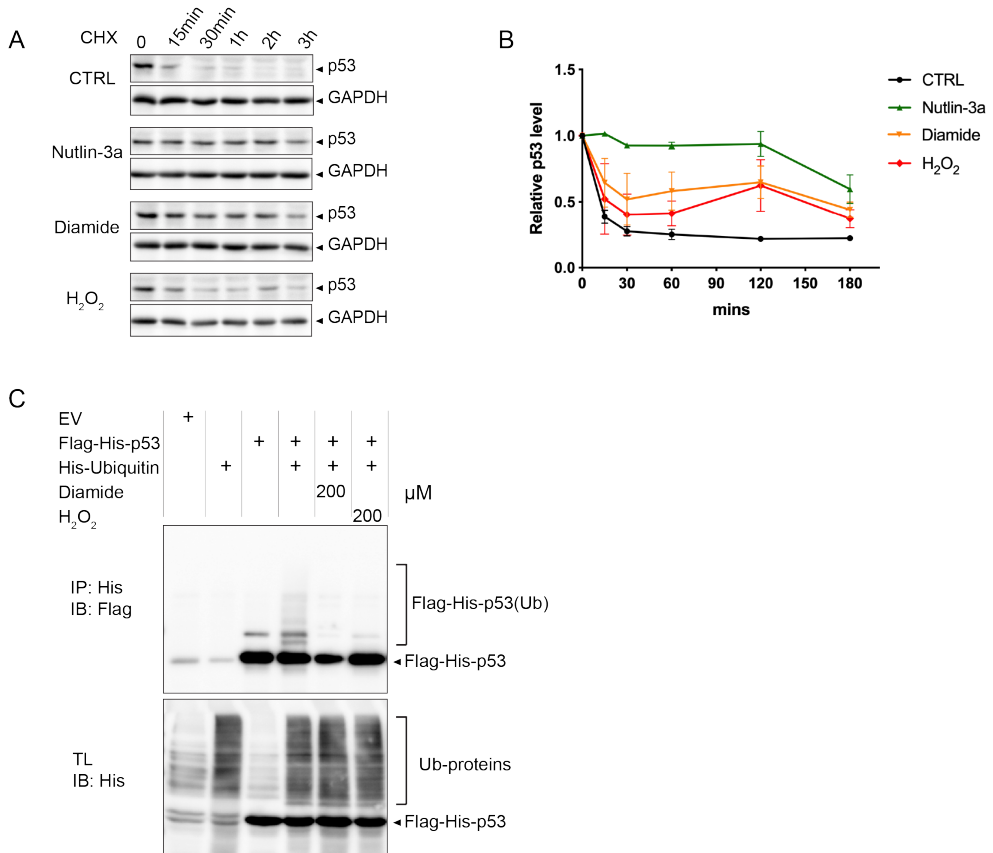


**Figure 3. Diamide and  $H_2O_2$  stabilize p53 by inhibition of protein degradation and ubiquitination.** (A) RPE<sup>Tert</sup> cells were treated with Cycloheximide (CHX, 10  $\mu$ g/ml) to block protein synthesis and at the same time exposed to Nutlin-3a (10  $\mu$ M), diamide (200  $\mu$ M) or  $H_2O_2$  (200  $\mu$ M) for the indicated time. Total cell lysates were loaded for evaluating the levels of endogenous p53 and GAPDH (as a loading control). (B) Quantification of p53 protein intensity relative to GAPDH shown in (A) from two independent experiments. (C) HEK293T cells expressing Flag-His-p53 alone or in combination with His-ubiquitin were treated with diamide (200  $\mu$ M) or  $H_2O_2$  (200  $\mu$ M) for 15 min. p53 ubiquitination was evaluated by His-pulldown using Ni-NTA beads and immunoblotting with anti-Flag antibody. The presented data are representative for three independent experiments.

cysteines and thus may be negatively regulated through oxidation. However, total protein ubiquitinylation appeared unaffected suggesting a specific effect of oxidants on ubiquitin-dependent p53 degradation (**Fig. 3C**).

### **Diamide and H<sub>2</sub>O<sub>2</sub> dependent p53 activation are mediated by different Stress Activated Protein Kinases (SAPKs)**

To further investigate how p53 was stabilized and activated by redox-dependent signaling, we made use of inhibitors of JNK and p38MAPK kinases (**Fig. 4A**): two SAPKs that have previously been shown to be activated by oxidative signaling and that have both been implicated in p53 activation [5, 6, 42]. Also in our experiments these pathways were activated by both diamide and H<sub>2</sub>O<sub>2</sub>, although diamide generally resulted in a slightly stronger activation (see also earlier in **Fig. 2**). Pre-treatment with the JNK inhibitor SP600125 almost completely abolished H<sub>2</sub>O<sub>2</sub> induced p53 stabilization and activation, evidenced by loss of p21 induction, whereas diamide-dependent signaling towards p53 remained unaffected. Conversely, inhibition of p38MAPK by pre-treatment with PH797804 largely blocked diamide-induced p53 stabilization and p21 induction, but did not inhibit H<sub>2</sub>O<sub>2</sub> induced p53 stabilization. Note that the effect of PH797804 on p53 was evident despite some p38MAPK activity remained as judged by the phosphorylation status of its target ATF2-pT71 (**Fig. 4B**). Pre-treatment with both inhibitors indeed blocked the induction of p53 and p21 induced by either oxidative signaling stimulus (**Fig. 4C**). These observations strongly indicate that even though diamide and H<sub>2</sub>O<sub>2</sub> both activate p38MAPK and JNK, diamide-dependent p53 activation is mediated by p38MAPK, whereas H<sub>2</sub>O<sub>2</sub> mediated p53 activation is mediated by JNK. We showed earlier (**Fig. 2**) that H<sub>2</sub>O<sub>2</sub> also requires ATM signaling, whereas p38MAPK does not. The experiments using the JNK inhibitor suggest that under these conditions, ATM signaling is still active (induction of CHK2-pT68, **Fig. 4B**), but not sufficient for p53 activation. Apparently both JNK and ATM activity are needed for full activation of p53 by H<sub>2</sub>O<sub>2</sub> treatment.

The specificity of kinase inhibitors depends on the type of inhibitor and the used concentration. IC50 values are often determined *in vitro* and do not necessarily reflect concentrations needed in tissue culture systems. We examined whether the used concentrations cross-reacted with other signaling pathways downstream of H<sub>2</sub>O<sub>2</sub>. As is clear from **Fig. 4A**, SP600125 inhibited diamide and H<sub>2</sub>O<sub>2</sub>-induced JNK activation (pJNK and p-c-Jun), but did not greatly affect the phosphorylation of CHK1, CHK2, ERK and P38MAPK. Likewise, the p38MAPK inhibitor PH797804 did not affect JNK, CHK1, CHK2 or ERK phosphorylation, and combined SP600125 and PH797804 inhibition did not affect CHK1, CHK2 or ERK phosphorylation (**Fig. 4C&4D**). Although it is difficult to exclude any off-target effects altogether, these results indicate that at least the pathways under study are selectively inhibited by the used treatments.

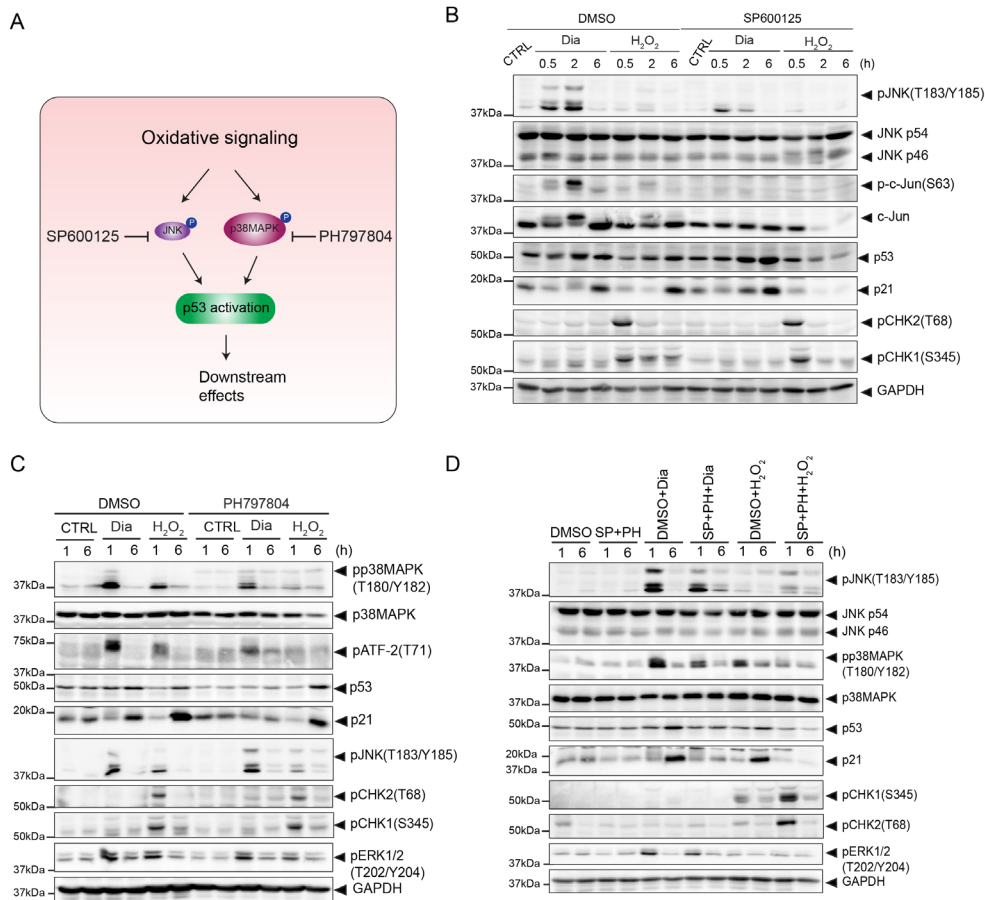


**Figure 4. p38MAPK, not JNK, is required for oxidative signaling-mediated p53 activation.**

**(A)** Overview of p53 activation through p38MAPK and JNK under oxidative signaling. p38MAPK and JNK are activated in response to oxidative signaling, which leads to p53 activation. SP600125 and PH797804 are inhibitors for JNK and p38MAPK, respectively. **(B)** JNK is dispensable for diamide-mediated p53 activation, but is essential for H<sub>2</sub>O<sub>2</sub>-induced p53 activation. RPE<sup>Tert</sup> cells were pre-treated with DMSO or SP600125 (20 μM) for 2h, followed by treatment with diamide (200 μM) or H<sub>2</sub>O<sub>2</sub> (200 μM) for the indicated time. The total protein levels of JNK (p54 and p46), c-Jun, p53, p21 and GAPDH, and phosphorylation states of JNK(T183/Y185), c-Jun(S63), CHK2(T68), CHK1(S345), ERK1/2(T202/Y204) and p38MAPK(T180/Y182) were detected by immunoblotting. **(C)** p38MAPK is indispensable for diamide-induced, but not for H<sub>2</sub>O<sub>2</sub>-induced p53 activation. RPE<sup>Tert</sup> cells were pre-treated with DMSO or PH797804 (10 μM) for 2h, followed by treatment with diamide (200 μM) or H<sub>2</sub>O<sub>2</sub> (200 μM) for the indicated time. The total protein levels of p38MAPK, p53, p21 and GAPDH, and phosphorylation states of p38MAPK (T180/Y182), ATF-2 (T71), JNK (T183/Y185), CHK2 (T68), CHK1 (S345) and ERK1/2 (T202/Y204) were evaluated by immunoblotting. **(D)** RPE<sup>Tert</sup> cells were pre-treated with DMSO or SP600125 (20 μM) and PH797804 (10 μM) together for 2 h, followed by treatment with diamide (200 μM) or H<sub>2</sub>O<sub>2</sub> (200 μM) for the indicated time. The total protein levels of JNK (p54 and p46), p38MAPK, p53, p21 and GAPDH, and phosphorylation states of JNK(T183/Y185), p38MAPK(T180/Y182), CHK2 (T68), CHK1 (S345) and ERK1/2 (T202/Y204) were evaluated by immunoblotting analysis.

## Oxidative signaling activates p53-dependent transcriptional activity

The above presented data (see e.g. Fig. 2 and 4) already show that activation of oxidative signaling either by diamide or H<sub>2</sub>O<sub>2</sub> treatment induces p21 expression in a p53 dependent manner. The notion that DDR and oxidative signaling dependent p53 activation proceeds through different upstream kinase signaling cascades could in principle lead to an induction

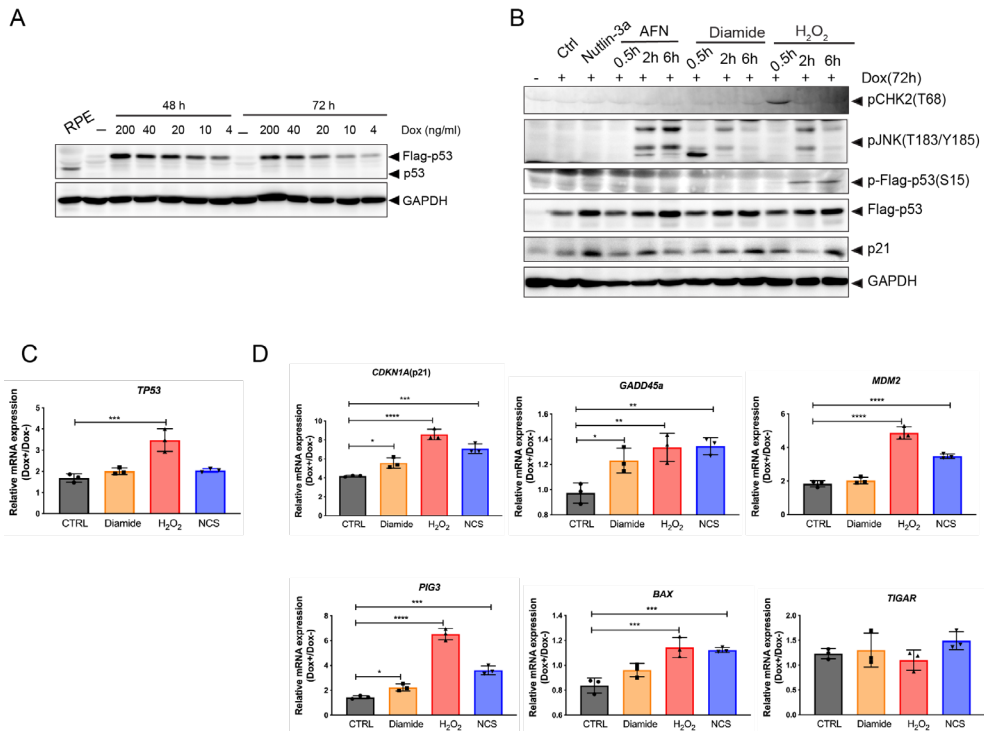


**Figure 5. Oxidative signaling induces p53-dependent transcriptional activation.**

(A) Immunoblotting analysis of RPE<sup>Tert</sup> p53 KO cells expressing Dox-inducible p53, treated with a range of doxycycline (dox, 4-200 ng/ml). Wildtype p53 in RPE<sup>Tert</sup> cells is used as a reference for endogenous levels. (B) p53 expression was induced with 4 ng/ml Dox for 72h to mimic near-endogenous levels, followed by treatment with Nutlin-3a (10 μM), Auranofin (AFN) (10 μM), diamide (200 μM) or H<sub>2</sub>O<sub>2</sub> (200 μM) for the indicated time. Total cell lysates were analyzed for the levels of Flag-p53, p21 and GAPDH, and phosphorylation states of CHK2(T68), JNK(T183/Y182) and Flag-p53(S15) by immunoblotting. (C) p53 expression was induced with 4 ng/ml Dox for 48h, followed by treatment with diamide (200 μM), H<sub>2</sub>O<sub>2</sub> (200 μM) or NCS (500 ng/ml) for 24 h. (D) The expression of p53 target genes was measured in both Dox- (p53-off) and Dox+ (p53-on) cells by qPCR. The ratio of the gene expression (relative to GAPDH) in p53-on cells over that in p53-off cells was calculated to assess p53-dependent transcriptional target activation. The data is presented as the mean and standard deviation (SD) from three independent experiments. Statistical analysis was performed by using One-way ANOVA followed by Multiple comparisons test (Dunnett). \*, p value < 0.05; \*\*, p value < 0.005; \*\*\*, p value < 0.0005; \*\*\*\* p value < 0.0001.

of different p53 transcriptional targets due to alternative PTM or cofactor binding. In order to evaluate p53-dependent gene transcription we established doxycycline-inducible Flag-p53 expressing RPE<sup>Tert</sup> p53 KO cells. Doxycycline (dox) treatment was optimized to induce Flag-p53 levels similar to endogenous p53 in the parental RPE<sup>Tert</sup> cell line under basal conditions (4 ng/ml dox treatment for 48 h or 72 h, **Fig. 5A**). Ectopically expressed Flag-p53 in these cells mimicked the response to diamide and H<sub>2</sub>O<sub>2</sub> observed in wildtype RPE<sup>Tert</sup> cells (**Fig. 5B**). Next, we evaluated the expression of TP53 itself and some of its target genes associated with cell cycle arrest (CDKN1A and GADD45a), apoptosis (BAX and PIG3), p53 turnover (MDM2) and metabolism (TIGAR) upon oxidative signaling and DNA damage. We found that TP53 mRNA levels were increased by almost 2-fold upon addition of doxycycline, and this was significantly increased by H<sub>2</sub>O<sub>2</sub> treatment, suggesting that H<sub>2</sub>O<sub>2</sub> regulates p53 levels not only at the level of stabilization (**Fig. 5C** and **Fig. 4A&4B**). p53 transcriptional targets CDKN1A (p21), GADD45a and PIG3 were further activated both by oxidative signaling and DDR signaling to p53 to some extent, whereas MDM2 and BAX were significantly induced only by DNA damage signaling to p53 (H<sub>2</sub>O<sub>2</sub> and NCS). No obvious change in the induction of TIGAR was observed upon either treatment. Collectively, these observations suggest that both oxidative signaling and the DDR can activate p53, and that there seems to be some target selectivity depending on which upstream pathway activates p53.

### **Oxidative signaling and DNA damage trigger p53-dependent cell cycle arrest and cell death**

To further examine the biological consequences of p53 activation by oxidative signaling and DNA damage, we evaluated cell viability in RPE Tert and RPE Tert p53 KO cells in response to addition of diamide, H<sub>2</sub>O<sub>2</sub> and NCS (**Fig. S4**). Especially diamide and H<sub>2</sub>O<sub>2</sub> treatment resulted in a higher loss of cell viability in a p53-dependent manner. To better understand the cause of the reduced cell viability when p53 was present, we assessed cell cycle profiles in RPE<sup>Tert</sup> p53 KO cells expressing doxycycline inducible p53 upon diamide, H<sub>2</sub>O<sub>2</sub> and NCS treatment for 24 hrs. We observed that both oxidative signaling and DNA damage triggers a mild p53-dependent cell cycle arrest with cells ending up with 4N DNA (**Fig. 6A&6B**), meaning that they are likely arrested in G2 or M phase or arrest in G1 upon mitotic bypass after replication [43]. Furthermore, we observed that both diamide and H<sub>2</sub>O<sub>2</sub> treatment induced significantly more cell death following p53 expression, indicating that oxidative signaling can trigger p53-dependent cell death (**Fig. 6C&6D**). Note that NCS did not induce pronounced cell death in RPE cells when p53 was inducibly expressed, whereas it did induce cell death in H1299 cells (**Fig. S5A&S5B**), which could be in line with the general notion that cancer cells are more vulnerable to chemotherapeutic drugs than untransformed cells [44]. Both diamide and H<sub>2</sub>O<sub>2</sub> also induced p53-dependent cell death in H1299 cells (**Fig. S5A& S5B**). Collectively, our data reveal that oxidative signaling can activate p53 to induce cell death in the absence of the DDR both in untransformed and human cancer cells.

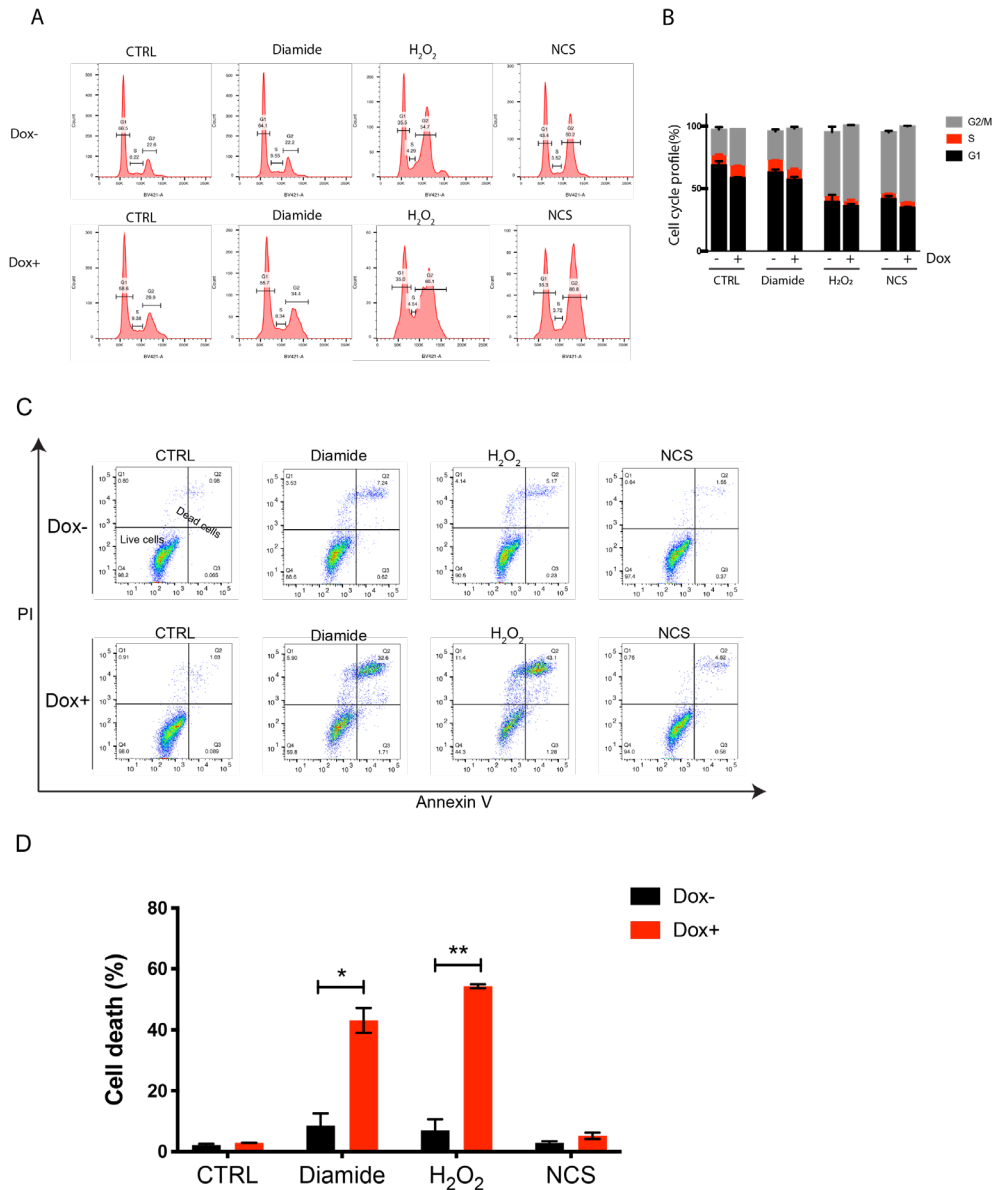


**Figure 6. Oxidative signaling and DNA damage induce p53-dependent cell cycle arrest and cell death.**

(A) Histogram plots showing cell cycle profile in Dox inducible expressing p53 RPE<sup>Tert</sup> cells upon induction of oxidative and DNA damage signaling as measured by Flow Cytometry (DAPI staining). Dox-inducible expressing p53 RPE<sup>Tert</sup> cells were cultured with or without Dox for 48 h, followed by the addition of diamide (200  $\mu$ M), H<sub>2</sub>O<sub>2</sub> (200  $\mu$ M) and NCS (500 ng/ml) for 24 h. Cell cycle profile was then measured by Flow Cytometry using DAPI staining. The plots show representative samples from three independent experiments. (B) Quantification of cell cycle profile from three independent experiments. (C) Dot plots showing cell death in Dox inducible expressing p53 RPE<sup>Tert</sup> cells upon induction of oxidative and DNA

damage signaling as measured by Flow Cytometry (PI-exclusion assay). Dox-inducible expressing p53 RPE<sup>Tert</sup> cells were cultured with or without Dox for 48 h, followed by the addition of diamide (250  $\mu$ M), H<sub>2</sub>O<sub>2</sub> (300  $\mu$ M) and NCS (500 ng/ml) for 24 h. Cell death was then measured by Flow Cytometry using Propidium iodide (PI) and Annexin V-FITC staining. The plots show representative samples from three independent experiments. **(D)** Quantification of cell death from three independent experiments. A student's t-test was used to analyse statistical difference in cell death between Dox- and Dox+ RPE<sup>Tert</sup> cells upon each treatment. \*, p value < 0.05. \*\*, p value < 0.005.

## Discussion

The observations that exposure to ROS (H<sub>2</sub>O<sub>2</sub>, O<sub>2</sub><sup>•-</sup>, HO<sup>•</sup>) either from endogenous or exogenous sources can activate the DDR as well as p53 [4, 14, 45] has given credence to the idea that ROS activates p53 downstream of signaling in response to oxidative DNA damage. In line with this notion, (enhanced) mitochondrial respiration and the ensuing O<sub>2</sub><sup>•-</sup> / H<sub>2</sub>O<sub>2</sub> production is frequently cited as a source of oxidative DNA damage and mutation in genomic DNA in tumors [17, 18]. But H<sub>2</sub>O<sub>2</sub> also acts as a second messenger in redox signaling, which plays an essential role in regulating protein functions and biological processes [12], including several phosphorylation cascades upstream of p53 [19, 20]. In this paper we have used the term 'oxidative signaling' to discriminate DNA damage signaling and other signaling downstream of oxidants, because the term 'redox signaling' usually refers to endogenous oxidant levels rather than challenges with oxidants as a model for therapeutic treatments. The engagement of multiple signaling cascades downstream of oxidants has made it difficult to attribute p53 activation in response to elevated H<sub>2</sub>O<sub>2</sub> levels to activation of the DDR, oxidative signaling or both [22]. What further complexes understanding ROS-induced p53 activation is the observation that ATM can also be activated by oxidative signaling in the absence of DNA damage [46]. Furthermore, treatment with several DNA damaging chemotherapeutic drugs, such as doxorubicin, cisplatin and 5-fluorouracil, can lead to enhanced ROS production (**Fig. S1**) [47, 48]. In this work, we set out to dissect DNA damage signaling and oxidative signaling upstream of p53, by applying treatments that we titrated and validated to either induce only the DDR (as judged by gamma-H2AX, pCHK2 and CHK1), only oxidative signaling (as judged by oxidation of the H<sub>2</sub>O<sub>2</sub> specific HyPer7 probe and SAPK activation) or both. NCS induced a DNA damage response, without evidence of elevated H<sub>2</sub>O<sub>2</sub> within 6 h. Diamide only led to oxidative signaling without activation of the DDR, whereas H<sub>2</sub>O<sub>2</sub> indeed induced both DDR and oxidative signaling, each with similar kinetics as observed for NCS and diamide respectively.

Other studies did find that treatment with NCS resulted in the elevated oxidation of 2,7-dichlorodihydrofluorescein (H2DCF-DA) in U2OS cells [35]. The different cell lines used, specificity of the used detection method or drug concentrations applied may underlie this apparent discrepancy. Besides the lack of HyPer7 oxidation induced by NCS, we also found no evidence of NCS-induced oxidative signaling as judged by p38MAPK or JNK activation in H1299 and HEK293T cells (not shown) at the concentration range used in this study, which we think further validates the approach. As mentioned, it has been shown that ATM can also



be activated in the absence of DNA damage through disulfide-dependent homodimerization in response to oxidant treatment [21]. In contrast to our findings, that study found that both H<sub>2</sub>O<sub>2</sub> and diamide were capable of disulfide-dependent activating ATM and subsequent p53-Ser15 phosphorylation, whereas we found no evidence that diamide could activate ATM as judged by p53-pSer15, CHK2-Thr68 or γ-H2AX in all cell lines we tested. On the other hand, the same study found induction of pCHK2 but not γ-H2AX in response to H<sub>2</sub>O<sub>2</sub>, whereas in our study H<sub>2</sub>O<sub>2</sub> did induce both pCHK2 and γ-H2AX as well as activation of p38MAPK and JNK, suggesting that H<sub>2</sub>O<sub>2</sub> triggers both the canonical DDR along with oxidative signaling. Again, differences in the precise protocol for treatment and cell lines used might underlie these contrasting observations.

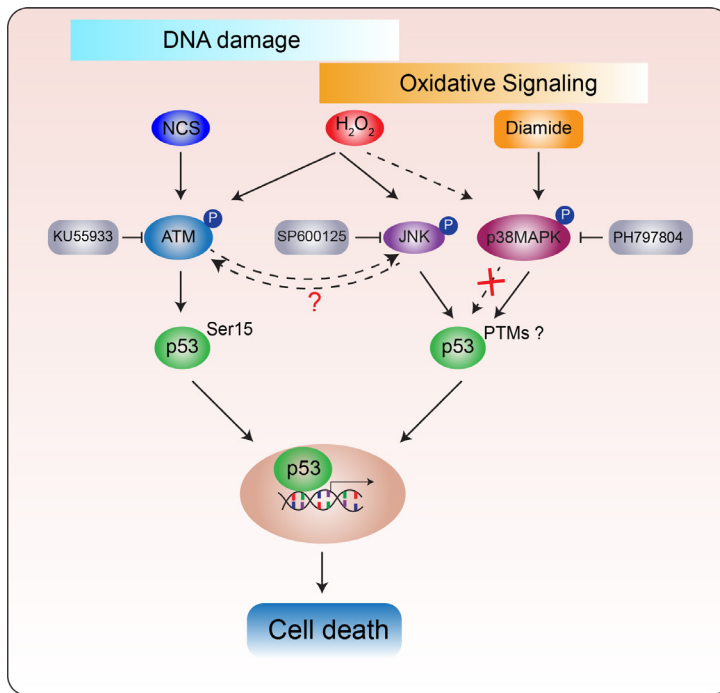


**Figure 7. Distinct upstream kinase-dependent signaling pathways activate p53 in response to DNA damage and oxidative signaling.**

NCS and H<sub>2</sub>O<sub>2</sub> both trigger the ATM-dependent DNA damage response and downstream p53 activation. Inhibition of ATM indeed abolishes NCS and H<sub>2</sub>O<sub>2</sub>-induced p53 activation. H<sub>2</sub>O<sub>2</sub> also activates JNK, and this was also required for H<sub>2</sub>O<sub>2</sub>-induced p53 activation, whereas inhibition of JNK abrogated p53 activation by H<sub>2</sub>O<sub>2</sub>, no effects on the ATM pathway were observed, suggesting that JNK and ATM somehow mediate p53 activation through synergistic pathways, but the details remains to be unraveled. p38MAPK is also activated by H<sub>2</sub>O<sub>2</sub>, but it was required for H<sub>2</sub>O<sub>2</sub>-induced p53 activation (dashed line). In contrast, diamide-induced oxidative signaling activates p53 through p38MAPK, independent of ATM and JNK. p53 induces transcriptional target genes and cell death in response to both the DDR and oxidative signaling. Our data indicate that p53 can be activated by oxidative signaling without inducing collateral DNA damage, thereby lowering the risk for the acquisition of new mutations driving tumor progression and initiation.

With the described selection of treatments that trigger only the DDR, only oxidative signaling or both we were able to dissect how p53 is activated upstream by these pathways. We observed that p53 was activated by DNA damage and oxidative signaling through distinct upstream kinases, that both seem to converge on the inhibition of MDM2-dependent p53 degradation (**Fig. 7**). It is not clear as yet whether this is due to lower MDM2 levels or activity in response to oxidant treatment or loss of the p53-MDM2 interaction. In any case, protein (de)ubiquitinylation in general seemed unaffected by oxidant treatment (**Fig. 3**). ATM was required for p53 activation in response to NCS and H<sub>2</sub>O<sub>2</sub>-induced DNA damage, but dispensable for p53 activation induced by diamide-mediated oxidative signaling. p38MAPK activity on the other hand was required for p53 stabilization and activation upon diamide-induced oxidative signaling, but not for NCS and H<sub>2</sub>O<sub>2</sub>-induced p53 activation. Our results furthermore showed that JNK was required for p53 activation by H<sub>2</sub>O<sub>2</sub>, although inhibition of ATM also completely blocked H<sub>2</sub>O<sub>2</sub>-induced p53 activation. This could suggest that ATM activation also somehow requires JNK activity in case of H<sub>2</sub>O<sub>2</sub> dependent activation, although this remains to be further explored. H<sub>2</sub>O<sub>2</sub> activates both JNK and p38MAPK, which suggests that H<sub>2</sub>O<sub>2</sub> treatment would still result in p53 stabilization in the presence of JNK inhibitor through the p38MAPK pathway, but we did not find clear evidence for this. This could be because the extent of p38MAPK activation by H<sub>2</sub>O<sub>2</sub> is much lower as compared to diamide dependent activation, or there might be other undiscovered pathways induced by diamide but not H<sub>2</sub>O<sub>2</sub> that act in concert with p38MAPK.

ATM, p38MAPK, JNK and p53 have all been shown to be subject to oxidative modification on cysteines [21, 36, 49, 50]. Our data suggests that at least modification of surface-exposed, non-Zn-finger cysteines in p53 does not underlie p53 stabilization in response to oxidant treatment (**Fig. S3**). It will be interesting to explore whether differential cysteine oxidation of ATM, p38MAPK and JNK in response to diamide versus H<sub>2</sub>O<sub>2</sub> could explain the observed differential responses to these compounds.

We found that activation of p53 by both oxidative signaling and the DDR resulted in transcriptional activation of p53 targets, and there seemed to be some differential effects dependent on which pathways were activated. It has been proposed that different stresses, including oxidative signaling and DNA damage would lead to distinct transcriptional programs of p53 [51]. Differential regulation in response to specific stressors could stem from alternative co-factor binding, specific PTMs or the simultaneous engagement of parallel signaling pathways, and it has also been suggested that oxidant-induced p53 target gene promoters bear distinct p53 consensus motifs [52]. However, in our study we did not observe a black and white effect of p53-dependent gene expression in response to differential stresses. We found that p21, GADD45a and PIG3 were induced by both oxidative signaling and DNA damage, whereas MDM2 and BAX were more induced by DNA damage signaling upstream of p53 (H<sub>2</sub>O<sub>2</sub> and NCS) than oxidative signaling (diamide). Since most previous studies did not carefully compare the induction of target genes in response to compounds that only induce the DDR or oxidative signaling, it is difficult to compare our observations to

these studies. Furthermore, our selection of p53 target genes is rather limited and mostly aimed at showing that both DDR and oxidative signaling induced p53 stabilization also activates its transcriptional activity.

Arguably the prime p53-dependent tumor suppressive response is the induction of apoptosis, which is the goal of many anti-cancer therapies that are aimed at the reactivation or restoration of wild-type p53 function. Primary cancer-therapies including several chemotherapeutics and irradiation elicit DNA damage and trigger the DDR and downstream p53-dependent apoptosis in multiple tumor types [53, 54]. Some chemotherapeutics used in the clinic, like Cisplatin and Doxorubicin have been shown to activate both JNK and p38MAPK along with the DDR [7, 55], but it is not entirely clear which of these pathways represents the dominant mechanism behind their efficacy. But the induction of DNA damage comes with the risk of generating new mutations. These may induce novel oncogenic events in surrounding tissue, but also drive tumor progression and therapy resistance through tumor evolution by mutation and selection. The data presented here suggest that p53 can be activated to trigger an apoptotic response independent of the DDR through oxidative signaling without risking the induction of collateral DNA damage and the ensuing tumor cell evolution. Several compounds have been developed with the aim to directly restore a p53 tumor suppressive response. Nutlin-3a and analogs for instance act by inhibition of MDM-2 dependent ubiquitinylation of p53 and clinical trials using these compounds are underway [56] Another p53-directed compound, APR-246, that aims to refold mutant p53 was shown to bind directly to cysteines on p53, but also to other cellular thiols and thereby affect the cellular redox state, and it has been suggested that its effect could be due to a combination of these two [57], which could be in line with the findings described in this study.

Tumor cells, as compared to healthy cells, in general have higher ROS levels, for instance through altered metabolism, and as a result need to augment their antioxidant capacity in order to survive and thrive. It has been suggested that due to the simultaneously elevated production and scavenging of ROS in tumor cells, the redox state would be more easily tilted to more oxidizing [58]. With that in mind, further enhancing ROS levels using pro-oxidant approaches have been suggested as a strategy to induce tumor cell death [59]. But inhibition of the cellular reductive capacity, like we do here by using diamide, could in principle trigger a p53 response without the risk of collateral DNA damage as explained above. Such therapies may for instance be aimed at inhibition of the TrxR/Trx system (using e.g. Auranofin) [60, 61] or depletion of NADPH [62] but it remains to be explored whether such approaches would indeed be feasible. Importantly, it will need to be established whether the here described p38MAPK-dependent response to oxidants is functional in various wild-type p53 expressing cancer cell lines and tumor model systems. If so, the observation that oxidative signaling and the DDR activate p53-apoptosis through distinct upstream signaling cascades may contribute to new ideas for developing therapeutic strategies.

## Author contributions

T.S. and T.B.D. designed the study and wrote the manuscript. B.M.T.B. reviewed and commented on the manuscript. T.S. performed most of the experiments. P.E.P established the doxycycline-inducible Flag-p53 expressing system in cells and assisted with experiments and laboratory management. D.M.K.v.S. cloned and produced HyPer7 lentivirus and performed video timelapse microscopy experiments.

## Declaration of interests

The authors declare there is no conflict of interest.

## Acknowledgments

We are grateful for suggestions and input from our colleagues at the department of Molecular Cancer Research, University Medical Center Utrecht. We thank Jeroen van den Berg and René Medema for sharing their RPE<sup>Tert</sup> p53 KO cell line, and Vsevolod Belousov for sharing the HyPer7 construct. The work was made possible with grants from the China Scholarship Council (CSC no. 201606300046) to T.S. and from the Dutch Cancer Society (KWF UU 2014-6902) to T.B.D. B.M.T.B is part of the Oncode Institute, which is partly financed by the Dutch Cancer Society (KWF Kankerbestrijding) and was funded by the gravitation program CancerGenomiCs.nl from the Netherlands Organization for Scientific Research (NWO).

## References

1. F. Kruiswijk, C.F. Labuschagne, K.H. Vousden, p53 in survival, death and metabolic health: a lifeguard with a licence to kill, *Nat. Rev. Mol. Cell Biol.* 16 (7) (2015) 393-405.
2. A. Hirao, et al., DNA damage-induced activation of p53 by the checkpoint kinase Chk2, *Science* 287 (5459) (2000) 1824-1827.
3. C.E. Canman, et al., Activation of the ATM kinase by ionizing radiation and phosphorylation of p53, *Science* 281 (5383) (1998) 1677-1679.
4. N.H. Chehab, et al., Phosphorylation of Ser-20 mediates stabilization of human p53 in response to DNA damage, *Proc. Natl. Acad. Sci. U. S. A.* 96 (24) (1999) 13777-13782.
5. D.V. Bulavin, et al., Phosphorylation of human p53 by p38 kinase coordinates Nterminal phosphorylation and apoptosis in response to UV radiation, *EMBO J.* 18 (23) (1999) 6845-6854.
6. D.M. Milne, et al., p53 is phosphorylated in vitro and in vivo by an ultraviolet radiation-induced protein kinase characteristic of the c-Jun kinase, JNK1, *J. Biol. Chem.* 270 (10) (1995) 5511-5518.
7. R. Sanchez-Prieto, et al., A role for the p38 mitogen-activated protein kinase pathway in the transcriptional activation of p53 on genotoxic stress by chemotherapeutic agents, *Canc. Res.* 60 (9) (2000) 2464-2472.
8. Q.B. She, W.Y. Ma, Z. Dong, Role of MAP kinases in UVB-induced phosphorylation of p53 at serine 20, *Oncogene* 21 (10) (2002) 1580-1589.
9. T. Buschmann, et al., Jun NH2-terminal kinase phosphorylation of p53 on Thr-81 is important for p53 stabilization and transcriptional activities in response to stress, *Mol. Cell Biol.* 21 (8) (2001) 2743-2754.

10. T. Shi, T.B. Dansen, Reactive oxygen species induced p53 activation: DNA damage, redox signaling, or both? *Antioxidants Redox Signal.* 33 (12) (2020) 839-859.
11. G.S. Wu, The functional interactions between the p53 and MAPK signaling pathways, *Canc. Biol. Ther.* 3 (2) (2004) 156-161.
12. H. Sies, D.P. Jones, Reactive oxygen species (ROS) as pleiotropic physiological signalling agents, *Nat. Rev. Mol. Cell Biol.* 21 (7) (2020) 363-383.
13. K.M. Holmstrom, T. Finkel, Cellular mechanisms and physiological consequences of redox-dependent signalling, *Nat. Rev. Mol. Cell Biol.* 15 (6) (2014) 411-421.
14. L. Benitez-Bribiesca, P. Sanchez-Suarez, Oxidative damage, bleomycin, and gamma radiation induce different types of DNA strand breaks in normal lymphocytes and thymocytes. A comet assay study, *Ann. N. Y. Acad. Sci.* 887 (1999) 133-149.
15. N. Driessens, et al., Hydrogen peroxide induces DNA single- and double-strand breaks in thyroid cells and is therefore a potential mutagen for this organ, *Endocr. Relat. Canc.* 16 (3) (2009) 845-856.
16. M. Valverde, et al., Hydrogen peroxide-induced DNA damage and repair through the differentiation of human adipose-derived mesenchymal stem cells, *Stem Cell. Int.* 2018 (2018) 1615497.
17. S.P. Jackson, J. Bartek, The DNA-damage response in human biology and disease, *Nature* 461 (7267) (2009) 1071-1078.
18. M. Valko, et al., Free radicals, metals and antioxidants in oxidative stress-induced cancer, *Chem. Biol. Interact.* 160 (1) (2006) 1-40.
19. A. Matsuzawa, H. Ichijo, Redox control of cell fate by MAP kinase: physiological roles of ASK1-MAP kinase pathway in stress signaling, *Biochim. Biophys. Acta* 1780 (11) (2008) 1325-1336.
20. P.J. Nadeau, et al., Disulfide Bond-mediated multimerization of Ask1 and its reduction by thioredoxin-1 regulate H<sub>2</sub>O<sub>2</sub>-induced c-Jun NH<sub>2</sub>-terminal kinase activation and apoptosis, *Mol. Biol. Cell* 18 (10) (2007) 3903-3913.
21. Z. Guo, et al., ATM activation by oxidative stress, *Science* 330 (6003) (2010) 517-521.
22. G. Giaccone, et al., Neuromedin B is present in lung cancer cell lines, *Canc. Res.* 52 (9 Suppl) (1992) 2732s-2736s.
23. J. van den Berg, et al., A limited number of double-strand DNA breaks is sufficient to delay cell cycle progression, *Nucleic Acids Res.* 46 (19) (2018) 10132-10144.
24. V.V. Pak, et al., Ultrasensitive genetically encoded indicator for hydrogen peroxide identifies roles for the oxidant in cell migration and mitochondrial function, *Cell Metabol.* 31 (3) (2020) 642-653, e6.
25. J. Drost, et al., Sequential cancer mutations in cultured human intestinal stem cells, *Nature* 521 (7550) (2015) 43-47.
26. A.C.F. Bolhaqueiro, et al., Ongoing chromosomal instability and karyotype evolution in human colorectal cancer organoids, *Nat. Genet.* 51 (5) (2019) 824-834.
27. E. Kim, et al., Systematic functional interrogation of rare cancer variants identifies oncogenic alleles, *Canc. Discov.* 6 (7) (2016) 714-726.
28. K.L. Meerbrey, et al., The pINDUCER lentiviral toolkit for inducible RNA interference in vitro and in vivo, *Proc. Natl. Acad. Sci. U. S. A.* 108 (9) (2011) 3665-3670.
29. J.L. Hartley, G.F. Temple, M.A. Brasch, DNA cloning using in vitro site-specific recombination, *Genome Res.* 10 (11) (2000) 1788-1795.
30. N. Vahsen, et al., AIF deficiency compromises oxidative phosphorylation, *EMBO J.* 23 (23) (2004)

4679-4689.

31. X.R. Jiang, et al., Telomerase expression in human somatic cells does not induce changes associated with a transformed phenotype, *Nat. Genet.* 21 (1) (1999) 111-114.
32. N.M. Mishina, et al., Which antioxidant system shapes intracellular H<sub>2</sub>O<sub>2</sub> gradients? *Antioxidants Redox Signal.* 31 (9) (2019) 664-670.
33. H. Sies, D.P. Jones, Reactive oxygen species (ROS) as pleiotropic physiological signalling agents, *Nat. Rev. Mol. Cell Biol.* 21 (7) (2020) 363-383.
34. M.A. Kang, et al., DNA damage induces reactive oxygen species generation through the H2AX-Nox1/Rac1 pathway, *Cell Death Dis.* 3 (2012) e249.
35. J.M. Held, et al., Targeted quantitation of site-specific cysteine oxidation in endogenous proteins using a differential alkylation and multiple reaction monitoring mass spectrometry approach, *Mol. Cell. Proteomics* 9 (7) (2010) 1400-1410.
36. Y. Cho, et al., Crystal structure of a p53 tumor suppressor-DNA complex: understanding tumorigenic mutations, *Science* 265 (5170) (1994) 346-355.
37. M. Kitayner, et al., Structural basis of DNA recognition by p53 tetramers, *Mol. Cell.* 22 (6) (2006) 741-753.
38. R. Rainwater, et al., Role of cysteine residues in regulation of p53 function, *Mol. Cell Biol.* 15 (7) (1995) 3892-3903.
39. S.Y. Fuchs, et al., Mdm2 association with p53 targets its ubiquitination, *Oncogene* 17 (19) (1998) 2543-2547.
40. Y. Haupt, et al., Mdm2 promotes the rapid degradation of p53, *Nature* 387 (6630) (1997) 296-299.
41. K.Z. Guyton, et al., Activation of mitogen-activated protein kinase by H<sub>2</sub>O<sub>2</sub>. Role in cell survival following oxidant injury, *J. Biol. Chem.* 271 (8) (1996) 4138-4142.
42. M. Hornsveld, et al., A FOXO-dependent replication checkpoint restricts proliferation of damaged cells, *Cell Rep.* 34 (4) (2021) 108675.
43. E. Dickens, S. Ahmed, Principles of cancer treatment by chemotherapy, *Surgery* 36 (3) (2018) 134-138.
44. S. Xie, et al., Reactive oxygen species-induced phosphorylation of p53 on serine 20 is mediated in part by polo-like kinase-3, *J. Biol. Chem.* 276 (39) (2001) 36194-36199.
45. T.T. Paull, Mechanisms of ATM activation, *Annu. Rev. Biochem.* 84 (2015) 711-738.
46. Y. Chen, et al., Collateral damage in cancer chemotherapy: oxidative stress in nontargeted tissues, *Mol. Interv.* 7 (3) (2007) 147-156.
47. C. Yokoyama, et al., Induction of oxidative stress by anticancer drugs in the presence and absence of cells, *Oncol Lett* 14 (5) (2017) 6066-6070.
48. D.J. Templeton, et al., Purification of reversibly oxidized proteins (PROP) reveals a redox switch controlling p38 MAP kinase activity, *PLoS One* 5 (11) (2010), e15012.
49. K.J. Nelson, et al., H<sub>2</sub>O<sub>2</sub> oxidation of cysteine residues in c-Jun N-terminal kinase 2 (JNK2) contributes to redox regulation in human articular chondrocytes, *J. Biol. Chem.* 293 (42) (2018) 16376-16389.
50. S. Seemann, P. Hainaut, Roles of thioredoxin reductase 1 and APE/Ref-1 in the control of basal p53 stability and activity, *Oncogene* 24 (24) (2005) 3853-3863.
51. J. Buzek, et al., Redox state of tumor suppressor p53 regulates its sequence-specific DNA binding in

DNA-damaged cells by cysteine 277, *Nucleic Acids Res.* 30 (11) (2002) 2340-2348.

52. S.W. Lowe, et al., p53 status and the efficacy of cancer therapy in vivo, *Science* 266 (5186) (1994) 807-810.

53. A. Mandinova, S.W. Lee, The p53 pathway as a target in cancer therapeutics: obstacles and promise, *Sci. Transl. Med.* 3 (64) (2011) 64rv1.

54. D. Yan, G. An, M.T. Kuo, C-Jun, N-terminal kinase signalling pathway in response to cisplatin, *J. Cell Mol. Med.* 20 (11) (2016) 2013-2019.

55. A. Burgess, et al., Clinical Overview of MDM2/X-targeted therapies, *Front Oncol* 6 (2016) 7.

56. S.E. Eriksson, et al., p53 as a hub in cellular redox regulation and therapeutic target in cancer, *J. Mol. Cell Biol.* 11 (4) (2019) 330-341.

57. A. Glasauer, N.S. Chandel, Targeting antioxidants for cancer therapy, *Biochem. Pharmacol.* 92 (1) (2014) 90-101.

58. Z. Zou, et al., Induction of reactive oxygen species: an emerging approach for cancer therapy, *Apoptosis* 22 (11) (2017) 1321-1335.

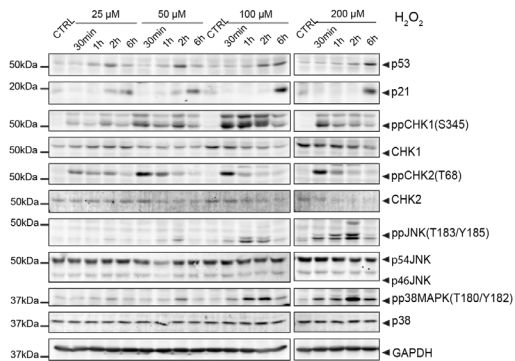
59. C. Marzano, et al., Inhibition of thioredoxin reductase by auranofin induces apoptosis in cisplatin-resistant human ovarian cancer cells, *Free Radic. Biol. Med.* 42 (6) (2007) 872-881.

60. A. Sobhakumari, et al., Susceptibility of human head and neck cancer cells to combined inhibition of glutathione and thioredoxin metabolism, *PloS One* 7 (10) (2012), e48175.

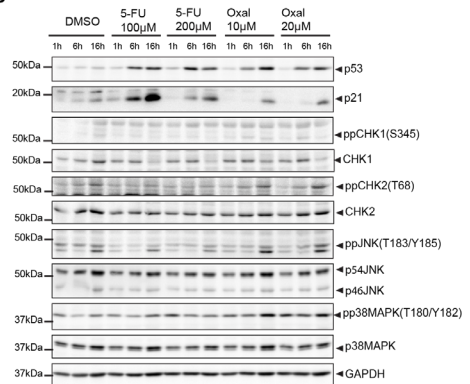
61. M. Polimeni, et al., Modulation of doxorubicin resistance by the glucose-6-phosphate dehydrogenase activity, *Biochem. J.* 439 (1) (2011) 141-149.

## Supplementary Figures

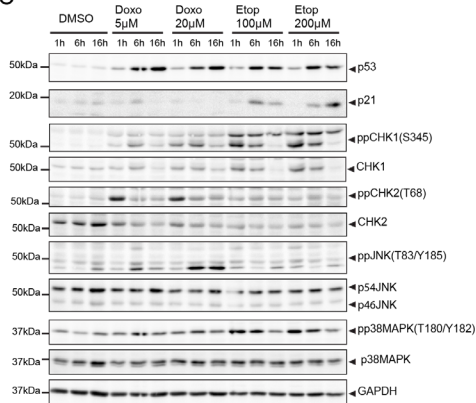
A



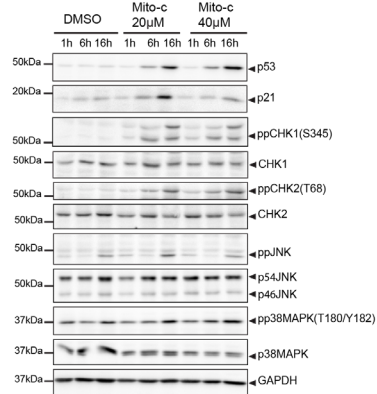
B



C



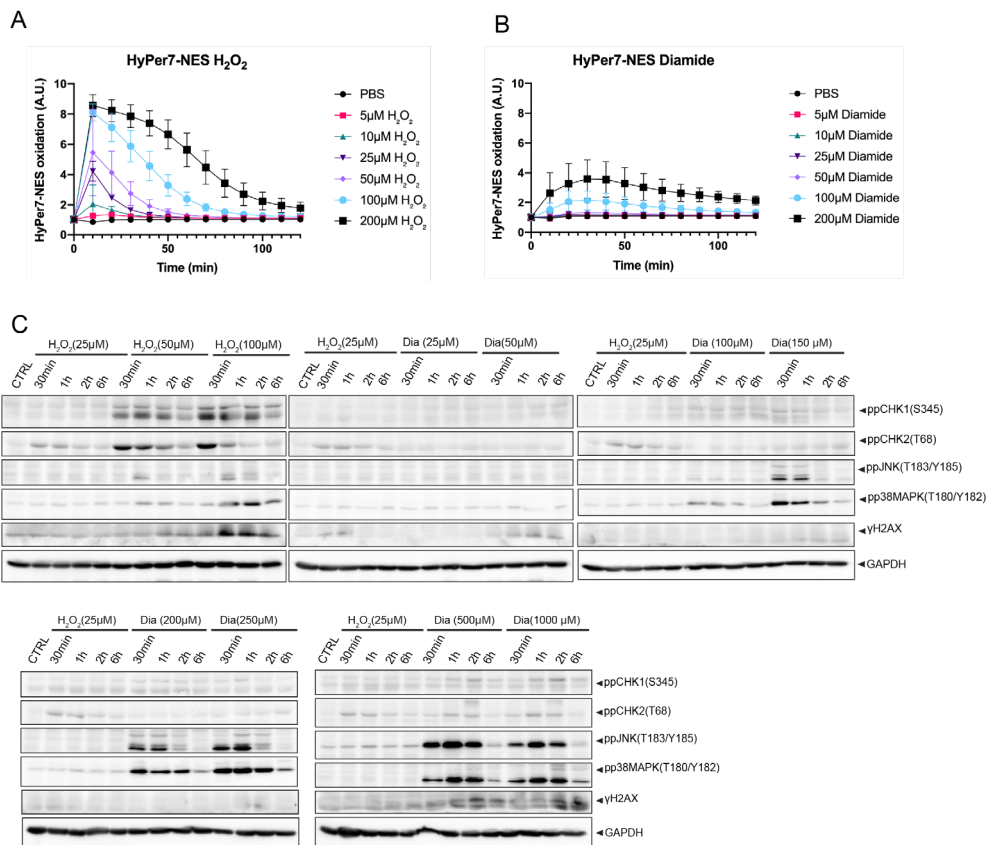
D



### Supplementary Figure 1. Both activation of DNA damage response (DDR) and stress-activated kinases (SAPK) upon H<sub>2</sub>O<sub>2</sub> and chemotherapeutic drugs.

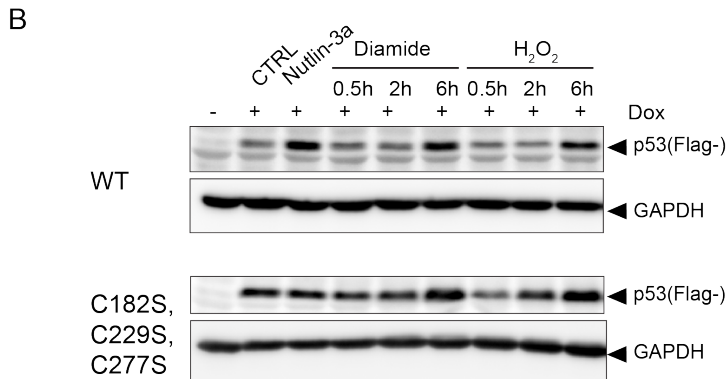
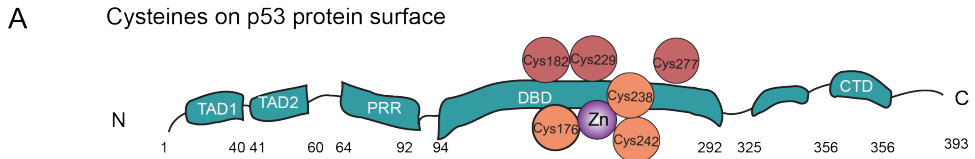
(A) RPE<sup>Ter</sup> were treated with H<sub>2</sub>O<sub>2</sub> in different concentrations for the indicated time. Phosphorylation states of CHK1 (S345), CHK2 (T68), JNK (T183/Y185) and p38MAPK (T180/Y182), endogenous p53, p21, CHK1, CHK2, JNK, p38MAPK and GAPDH (as a loading control) protein levels were evaluated by immunoblotting. (B) RPE<sup>Ter</sup> were treated with DMSO (CTRL), 5-FU (100 μM and 200 μM) and Oxaliplatin (Oxal, 10 μM and 20 μM) for the indicated time. Phosphorylation states of CHK1(S345), CHK2(T68), JNK (T183/Y185) and p38MAPK (T180/Y182), endogenous p53, p21, CHK1, CHK2, JNK, p38MAPK and GAPDH (as a loading control) protein levels were evaluated by immunoblotting. (C) RPE<sup>Ter</sup> were treated with DMSO (CTRL), Doxorubicin (Doxo, 5 μM and 20 μM) and Etoposide (Etop, 100 μM and 200 μM) for the indicated time. Phosphorylation states of CHK1(S345), CHK2(T68), JNK (T183/Y185) and p38MAPK(T180/Y182), endogenous p53, p21, CHK1, CHK2, JNK, p38MAPK and GAPDH (as a loading control) protein levels were evaluated by immunoblotting. (D) RPE<sup>Ter</sup> were treated with DMSO (CTRL) and Mitomycin C (Mito-c, 20 μM and 40 μM) for the indicated time. Phosphorylation states of CHK1 (S345), CHK2 (T68), JNK (T183/Y185) and p38MAPK (T180/Y182), endogenous p53, p21, CHK1, CHK2, JNK, p38MAPK and GAPDH (as a loading control) protein levels were evaluated by immunoblotting.





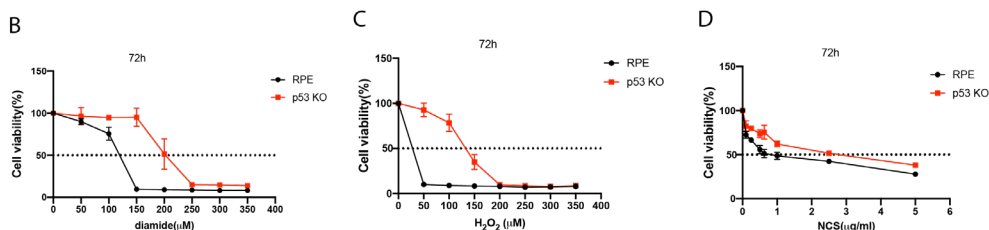
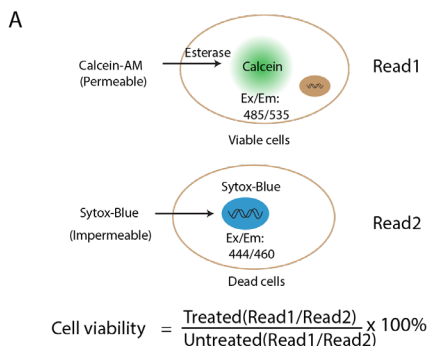
**Supplementary Figure 2. HyPer7(NES) oxidation, DNA damage response (DDR) and stress-activated kinases (SAPK) activation upon  $H_2O_2$  and diamide titration.**

HyPer7-NES oxidation upon the titration of  $H_2O_2$  (**A**) and diamide (**B**). RPE<sup>Tert</sup> cells stably expressing HyPer7-NES were treated with PBS and a titration of  $H_2O_2$  or diamide as indicated. HyPer7 signal of oxidized (Ex 488 nm / Em 530/30 nm) and reduced state (Ex405 nm / Em 525/50 nm) was monitored in live cells using time-lapse microscopy. HyPer7 oxidation is indicated by the ratio of oxidized over reduced version. (**C**) DDR and SAPK activation upon  $H_2O_2$  and diamide titration. RPE<sup>Tert</sup> cells were challenged by different concentrations of  $H_2O_2$  or diamide for different time courses. Total cell lysate was collected to evaluate the state of DDR and SAPK-related proteins.



**Supplementary Figure 3. p53 triple cysteines mutant is stabilized by oxidant signaling.**

**(A)** Scheme of cysteines on p53 protein surface. Cys176, Cys182, Cys229, Cys248, Cys242 and Cys277 are predicted to be exposed on the surface of p53 protein, which are suggested to be more oxidation-prone. Cys176, Cys238 and Cys242 (in light brown) are coordinating with a Zinc and essential for p53 structure. The p53 protein domains are referencing to the database on The TP53 WEB SITE (<http://p53.fr/>). TAD, Transactivation Domain; PRR, Proline-Rich Domain; DBD, DNA-binding Domain; TD, Tetramerization Domain; CTD, C-terminal regulatory Domain. **(B)** RPE<sup>Tert</sup> p53 KO cells expressing Dox-inducible (Flag-) p53 triple cysteine mutant (C182, C229 and C277) were treated with Nutlin-3a (10 μM), diamide (200 μM) and H<sub>2</sub>O<sub>2</sub> (200μM) for the indicated time. Flag-p53 and GAPDH levels were evaluated by immunoblotting.



**Supplementary Figure 4. RPE<sup>Tert</sup> cells are more sensitive to oxidative signaling and DNA damaging than p53 KO RPE<sup>Tert</sup> cells.**

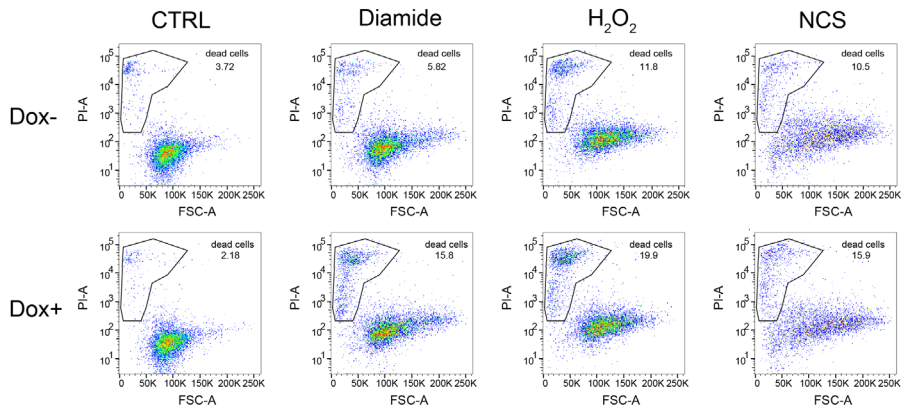
(A) A dual Calcein-AM/Sytox-Blue assay was applied to determine cell viability. Calcein-AM is cell membrane permeable that can be taken up by live cells and cleaved by Esterase in cells, resulting in a green fluorescent protein which is detected upon the excitation at 486 nm and emission at 535 nm. Sytox-Blue is cell membrane impermeable, which can only stain nucleic acids in dead cells. The fluorescence was detected when excited at 444 nm and filtered at 460 nm. Two fluorescent signals were captured on a Spectra Max fluorometer. The ratio of Calcein-AM/Sytox-Blue was evaluated and cell viability was determined by normalizing to untreated cases (considered as 100% cell viability).

(B) Cell viability of RPE<sup>Tert</sup> cells and p53KO RPE<sup>Tert</sup> cells upon treatment of diamide for 72h.

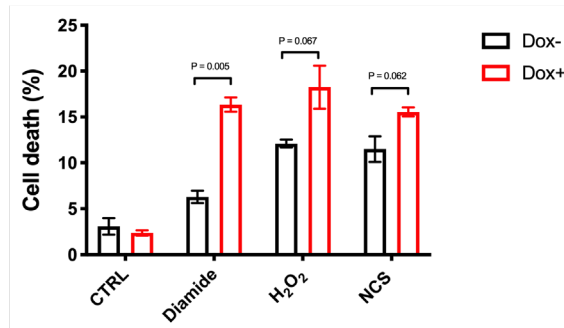
(C) Cell viability of RPE<sup>Tert</sup> cells and p53KO RPE<sup>Tert</sup> cells upon treatment of H<sub>2</sub>O<sub>2</sub> for 72h.

(D) Cell viability of RPE<sup>Tert</sup> cells and p53KO RPE<sup>Tert</sup> cells upon treatment of NCS for 72h.

A



B



H1299 cells

**Supplementary Figure 5. Oxidative signaling and DDR induced, p53-dependent cell death in H1299 cells,**

(A) Dox-inducible p53 expressing H1299 cells were cultured with or without Dox for 48 h, followed by treatment with diamide (200  $\mu$ M), H<sub>2</sub>O<sub>2</sub> (500  $\mu$ M) and NCS (500 ng/ml) for 24 h. Cell death was then measured by Flow Cytometry using Propidium iodide (PI) staining. The data is from a representative sample from two independent experiments. (B) Quantification of cell death from two independent experiments. Bars show mean and SD of two independent experiments, A student's t-test was used to analyse statistical difference of cell death between Dox- and Dox+ H1299 cells upon each treatment. p value < 0.05 is considered to be statistically significant.





# Chapter 4

## **p53 forms redox-dependent protein-protein interactions through cysteine 277**

Tao Shi<sup>1</sup>, Paulien E. Polderman<sup>1</sup>, Marc Pagès-Gallego<sup>1</sup>, Robert M. van Es<sup>1</sup>, Harmjan R. Vos<sup>1</sup>, Boudewijn M.T. Burgering<sup>1,2</sup> and Tobias B. Dansen<sup>1,3</sup>

<sup>1</sup>Center for Molecular Medicine, Molecular Cancer Research

<sup>2</sup>Onco Institute, University Medical Center Utrecht, Universiteitsweg 100  
3584 CG Utrecht, The Netherlands.

<sup>3</sup>Correspondence to: [t.b.dansen@umcutrecht.nl](mailto:t.b.dansen@umcutrecht.nl).

Accepted by *Antioxidants* after peer review

## Abstract

Reversible cysteine oxidation plays an essential role in redox signaling by reversibly altering protein structure and function. Cysteine oxidation may lead to intra- and intermolecular disulfide formation, and the latter can drastically stabilize protein-protein interactions in a more oxidizing milieu. The activity of the tumor suppressor p53 is regulated at multiple levels, including various post-translational modification (PTM) and protein-protein interactions. In the past decades, p53 has been shown to be a redox sensitive protein, and undergoes reversible cysteine oxidation both *in vitro* and *in vivo*. It is not clear however, whether p53 also forms intermolecular disulfides with interacting proteins and whether these redox-dependent interactions contribute to the regulation of p53. In the present study, by combining (co-)immunoprecipitation, quantitative Mass spectrometry and Western blot we found that p53 forms disulfide-dependent interactions with several proteins under oxidizing conditions. Cysteine 277 is required for most of the disulfide-dependent interactions of p53, including those with 14-3-3 $\theta$  and 53BP1. These interaction partners may play a role in fine-tuning p53 activity under oxidizing conditions.

## Introduction

The transcription factor p53 is a key player in the cellular stresses response and is activated by DNA damage, and by oncogenic, oxidative and metabolic stress [1]. p53 activation triggers cell cycle arrest and apoptosis, but is also involved in cellular survival programs through the induction of DNA damage repair and metabolic regulation. Collectively, these programs contribute to the maintenance of genome integrity and protect the organism from over-proliferation of cells that carry oncogenic mutations. p53 stabilization and function is controlled by post-translational modifications (PTMs) like phosphorylation, acetylation, ubiquitination and methylation that may vary dependent on the type of stress [2].

Reactive oxygen species (ROS), mainly in the form of hydrogen peroxide ( $H_2O_2$ ), act as a second messenger in so-called redox signaling which involves oxidative modification of cysteine thiol side chains to regulate the function of target proteins [3, 4]. Oxidation of thiols to form sulfenic acid (S-OH) or disulfide (S-S-) is reversible by the cellular antioxidant system, enabling to switch the redox signal on and off. The extent of cysteine oxidation in the cellular proteome therefore depends on the rates of production and clearance of ROS and the rates of oxidation and reduction of thiols. A particular attractive mode of redox modification is the formation of intermolecular disulfides, because it can stabilize otherwise weak protein-protein interactions. In this way protein function can be modified to an extent that correlates with the local redox environment. Intermolecular disulfide formation has been shown to play roles in signaling in species from yeast to human [5].

p53 has also been found to be oxidized on multiple cysteines upon oxidant treatment, both *in vitro* and *in live cells*. *In vitro*, C182 and C277 were identified to be reactive to the alkylating agent N-ethylmaleimide [6]. C182 can also form an intramolecular disulfide bond



with one of the three Zinc-binding cysteines (C176, 238 and 242), resulting in the loss of Zinc and protein unfolding [7]. Consistently, Held et al. quantified the extent of site-specific reversible cysteine oxidation in endogenous p53 and found that both C182 and C277 were sensitive to the thiol oxidant diamide [8], but the exact type of reversible cysteine oxidation remained unknown. Here we set out to study whether p53 forms disulfide-dependent intermolecular interactions upon oxidation. To this end we combined immunoprecipitation and quantitative Mass spectrometry on wild type and p53 cysteine mutants expressed in HEK293T cells to identify redox-dependent interaction partners of p53. Intriguingly, in line with the observations by Held et al., diamide but not H<sub>2</sub>O<sub>2</sub> induced oxidative stress, stimulated the formation of disulfide-dependent complexes with p53. Some well-known p53 regulators were among the identified disulfide-dependent binders, including 14-3-3 $\theta$  and 53BP1 and these depended on the presence of C277. Nevertheless, the p53 277S mutant was still activated by Nutlin-3 treatment, oxidative signaling and DNA damage, suggesting that the identified disulfide dependent interactors are not critical for p53 function per se. We propose that the observed covalent interactions with p53 could be involved in fine tuning the spatiotemporal p53 response by stabilization otherwise weak protein-protein interactions under oxidizing conditions.

## Materials and methods

### Constructs, reagents and antibodies

The pDONR223-p53 WT plasmid was a gift from Jesse Boehm, William Hahn and David Root (Addgene plasmid # 81754 [9]). pDON223-p53 Cysteine mutants (Cys to Ser or Ala) were generated by site-directed mutagenesis PCR using pDONR223-p53 WT as the template. The primers used for mutagenesis PCR are shown in Table S1. N-terminally tagged Flag- and HA-p53 expression as well as doxycycline inducible Flag-p53 WT and -C277S constructs were obtained by a Gateway cloning with pcDNA3 or pInducer20 backbones (pInducer20 was a gift from Stephen Elledge (Addgene plasmid # 44012) [10]).

Diamide (D3648), Hydrogen peroxide solution 30% (7722-84-1), Neocarzinostatin (NCS) (N9162), Auranofin (AFN) (A6733) and N-Ethylmaleimide (NEM)(E3876) were from Sigma. Nutlin-3 (10004372) was from Sanbio. 14-3-3 $\theta$  siRNA (sc-29586) was from Santa Cruz Biotechnology.

Anti-Flag<sup>®</sup>M2 affinity gel (A220), anti-HA agarose (A2095), Anti-FLAG<sup>®</sup> (rabbit)(F7425) and anti-FlagM2 antibody (F1804) were from Sigma. Antibodies against p53(DO-1), p21(M-19), 53BP1(H-300) and 14-3-3 $\theta$  (5J20) were from Santa Cruz Technology. Anti-pCHK2(Thr68) (CS2661) antibody was from Cell Signaling Technology. Anti-GAPDH (MAB374) antibody was from EMD Millipore. Anti-HA (12CA5) antibody was prepared in house from hybridoma cell lines. Goat anti-mouse IgG-HRP (170-6516) and Goat anti-rabbit IgG-HRP (170-6515) were from Bio-Rad. Fluorescence-conjugated secondary antibodies: IRDye 680RD goat anti-mouse IgG (925-68070), IRDye 800CW goat anti-mouse IgG (926-32210), IRDye 680 goat

anti-rabbit IgG (926-32221) and IRDye 800CW goat anti-rabbit IgG (926-32211) from Li-Cor.

### **Cell culture**

HEK293T, non-small-cell-lung cancer cells (NCI-H1299) (p53-deficient) cells were cultured in DMEM high-glucose (4,5 g/L) containing 10% FBS, 2 mM L-glutamine and 100 Units Penicillin-Streptomycin (All from Sigma Aldrich), under a 6% CO<sub>2</sub> atmosphere and at 37 °C. Transient transfections were performed using the polyethyleneimine (PEI) transfection reagent (Sigma Aldrich). p53 KO RPE<sup>Tert</sup> cells were a gift from René Medema [11], and cultured in DMEM/F-12 high-glucose supplemented with 10 % FBS and 100 U Penicillin-Streptomycin (Sigma Aldrich) under a 6% CO<sub>2</sub> atmosphere and at 37 °C. Doxycycline-inducible expressing Flag-p53 WT and C277S cells were generated by transduction with lentiviral constructs pInducer20-Flag-p53 WT and C277S in the p53-KO RPE<sup>Tert</sup> cells, followed by the selection by Neomycin (400 µg/ml) for 2 weeks. The dox-inducible expression of Flag-p53 was confirmed by Western blot detection and polyclonal cells were used for subsequent experiments.

### **Cell lysis, Immunoprecipitation and Western blot**

For total lysates, cells seeded in 6-well dishes were directly scraped in loading sample buffer (Tris-HCl pH 6.8, 2% SDS, 5% 2-mercaptoethanol, 10% glycerol, 0.002% bromophenol blue). For immunoprecipitation experiments, HEK293T or H1299 cells were seeded in 10 cm-dishes and transiently transfected with the indicated constructs. 48hrs after transfection, cells were treated with diamide or H<sub>2</sub>O<sub>2</sub> for the indicated time, followed by incubation with 100 mM N-ethylmaleimide (NEM) in PBS at 37°C for 5 min to prevent post-lysis oxidation and to inactivate disulfide-reducing enzymes. Cells were scraped in the same NEM buffer and collected by centrifugation at 1500 rpm for 5 min. Cell pellets were resuspended in 1ml of lysis buffer containing 50 mM Tris pH 7.5, 1% Triton, 1,5 mM MgCl<sub>2</sub>, 1 mM EDTA, 100 mM NaCl supplemented with Aprotinin, Leupeptin, NaF and 100 mM Iodoacetamide to further prevent post-lysis oxidation.

Cell lysates were subsequently centrifuged at 14,000 rpm for 10 min. 50 µl of supernatants were taken as a control ('input') and the rest was used for immunoprecipitation and incubated with 15 µl of anti-FlagM2 or HA Affinity beads. After 2 hours of incubation at 4 °C, beads were washed with wash buffer (50 mM Tris pH 7.5, 1% Triton, 1,5 mM MgCl<sub>2</sub>, 1 mM EDTA, 1M NaCl supplemented with Aprotinin, Leupeptin and NaF) three times to minimize non-specific binding and enrich for disulfide-dependent interactions. After washing, samples were firstly resuspended in 1x non-reducing sample buffer (without β-mercaptoethanol) and boiled at 95 °C for 10 mins. Half of the samples were loaded for non-reducing sample detection and the rest half was added 5x reducing buffer (with β-mercaptoethanol), boiled again at 95 °C for 5 mins, and loaded for reducing sample detection.

For SDS-PAGE followed by Western blot, samples were run on 7.5 % or 10 % SDS-PAGE gels depending on the molecular weight of the proteins of interest. After that, proteins were transferred to a PVDF (polyvinylidene difluoride), nitrocellulose or immobilon-FL membrane

(Millipore) through a traditional wet transfer method. Membranes were blocked with 2% BSA in TBST for 1h at 4°C and then incubated with primary antibodies overnight at 4°C, followed by washing with TBST solution before secondary antibody staining. Secondary antibody staining was performed using HRP or fluorescence-conjugated secondary antibodies for 1h at 4°C. For imaging, membranes were washed again with TBST and subsequently analyzed on an Image Quant LAS (for HRP) or Typhoon-Biomolecular Imager (for fluorescence).

### **Sample preparation for Mass spectrometry**

HEK293T cells were seeded in 15 cm-dishes (4 replicates per condition) and transfected with 20 µg of Flag-p53, Flag-C182SC277S or Flag-C182S DNA constructs. After 48 h, cells were treated with diamide for 15 min, followed by incubation with 100 mM NEM in PBS at 37°C for 5 min to alkylate free thiols and prevent post-lysis oxidation. Cells were scraped in NEM buffer and all replicates were collected in the same 15 ml tube followed by centrifugation at 1500 rpm for 5 min. Cell pellets were lysed in 8 ml of lysis buffer as describe in 2.3 and 1% of supernatant was taken as input. 80 µl of FlagM2 agarose beads were taken for immunoprecipitation against Flag following the procedure as described above (2.3). After final cleaning of the beads, 1% beads solution was taken for Western blotting detection pre-MS and the rest was used for MS experiment. Proteins on beads were incubated with reduction and alkylation buffer (1 M Ammonium bicarbonate, 50 mM Acetonitrile, 10 mM TCEP, 40 mM CAA and 8M urea) at room temperature for 30 min, and then digested with 250 ng of trypsin overnight at 37 °C on a shaker. Peptides were then loaded on C18 stagetips and washed twice with 0.1% formic acid solution (diluted in water). Peptides on C18 stagetips are stable and can be stored at 4°C up to one month.

### **Mass Spectrometry**

Mass Spectrometry was performed as previously described [12]. Briefly, peptides were separated on a 30-cm pico-tip column (75 µm ID, New Objective) and were packed in-house with 3 µm aquapur gold C-18 material (Dr. Maisch) using a 140-min gradient (7–80% ACN 0.1% FA), delivered by an easy-nLC 1000 (LC 120, Waltham, MA, USA, Thermo Scientific), and electro-sprayed directly into an Orbitrap Fusion Tribrid Mass Spectrometer (LC 120, Waltham, MA, USA, Thermo Scientific) and ran in data-dependent mode with the resolution of the full scan set at 240000, after which the top N peaks were selected for HCD fragmentation (30% collision energy) using the top speed option with a cycle time of 1 second. with a target intensity of 1E4. The Mass Spectrometry proteomics data was submitted to ProteomeXchange via the PRIDE database with identifier PXD026893 [13]. These can be accessed by the reviewers using the following credentials Username: reviewer\_pxd026893@ebi.ac.uk Password: 9MvIBO03

### **Mass spectrometry data analysis**

The raw Mass spectrometry files were processed using Maxquant software (version 1.5.2.8). The human protein database of UniProt was searched with both proteins and

peptides (false discovery rate set to 1%). Data analysis regarding the identified proteins was further analysed in R (version 3.6.1). Proteins were filtered for reverse hits and standard contaminants. Proteins with less than 2 peptides were also removed. Label-Free-Quantification (LFQ) values were log<sub>2</sub>-transformed and the proDA (inference of protein differential abundance by probabilistic dropout analysis) model was used to impute missing values for following data analysis [14] Significant hits between conditions (e.g., CTRL vs Diamide) were judged by at least 2-fold change in protein abundance with an adjusted p-value (Benjamini-Hochberg) smaller than 0.01. The ggplot2 package was required to plot the data. The R scripts, raw and processed data are deposited in <https://github.com/Taoshi2021/p53-oxidation>.

### **Immunofluorescence microscopy**

RPE<sup>Tert</sup> p53 KO cells expressing Doxycycline-inducible Flag-p53 WT and C277S were grown on glass coverslips in 6-well dishes and treated with Dox for 48 h. The cells were then fixed with 3.7% Formaldehyde solution at room temperature for 15 min, followed by permeabilization using 0.1% Triton for 5 min and subsequent blocking with 2% BSA (w/v) and purified goat IgG in 1:10,000 in PBS for 45 min at room temperature. The cells were then incubated with the primary antibody DO-1 against p53 at a final 1:500 dilution overnight, followed by 1 h incubation with a secondary antibody conjugated with Alexa fluor 488 (ThermoFisher) and Hoechst 33,342 (Life Technologies) after washing twice with PBS. All antibody staining was performed at 4°C and in the dark. Finally, the coverslips were mounted in a drop of mounting medium and saved at 4°C in the dark for further analysis. Imaging was performed on a Zeiss confocal microscope LSM880 and images were processed in Fiji (ImageJ) software.

### **Ubiquitination assay**

HEK293T cells in 10-cm dishes were transiently transfected with the in the text indicated DNA constructs. After 48 h, cells were treated with H<sub>2</sub>O<sub>2</sub> or diamide for 15 min, and then scraped in lysis buffer (100 mM NaH<sub>2</sub>PO<sub>4</sub>/Na<sub>2</sub>HPO<sub>4</sub>, 10 mM Tris, 8 M Urea, 10 mM NEM, 10 mM Imidazole and 0.2% Triton X-100, pH 8.0). Cell lysates were sonicated and then centrifuged at 10,000 rpm for 10 min. 50 µl of supernatant were taken as a control for input and the remainder was subjected to pulldown using Ni-NTA beads to enrich for His-Ubiquitin-tagged proteins. After 2 h of incubation at room temperature, beads were washed twice with wash buffer (100 mM NaH<sub>2</sub>PO<sub>4</sub>/Na<sub>2</sub>HPO<sub>4</sub>, 10 mM Tris, 8 M Urea, 10 mM Imidazole and 0.2% Triton X-100, pH 6.3), followed by one-time wash with elution buffer (100 mM NaCl, 20% glycerol, 20 mM Tris, 1 mM DTT and 10 mM Imidazole, pH 8.0). Ultimately, samples were resuspended in 1x reducing sample buffer for subsequent analysis.

### **RNA isolation and qPCR**

p53 target gene expression was analysed by qPCR on RNA extracted from Dox-inducible expressing p53 WT and C277S in p53 KO RPE<sup>Tert</sup> cells. Total RNA was isolated using a

RNeasy kit (QUIAGEN). 500 ng of RNA was used for cDNA synthesis according to the manufacturer's instructions using the an iScript cDNA Synthesis Kit (BIO-RAD). qPCR was performed with SYBR Green FastStart Master Mix in the CFX Connect Real-time PCR detection system (Bio-RAD). The procedures were as follows: pre-denaturing at 95 °C for 10 min, followed by denaturing at 95°C for 10 seconds, annealing at 58°C for 10 seconds and extending at 72 °C for 30 seconds for 39 cycles. All the primers used for the qPCRs are shown in Table S1.

### Sequence alignment

The p53 protein sequence of vertebrate species and its paralogs (p63 and p73) were downloaded from ENSEMBL database [15]. Sequence alignment was performed in Jalview (version 15.0) software and was colored by the extent of conservation (threshold 15) [16].

### Gene Ontology enrichment analysis

Gene Ontology (GO) enrichment analysis was performed using the online PANTHER Classification System (<http://pantherdb.org/>). 162 proteins that were identified to significantly bind to wild-type p53 upon diamide treatment were selected for GO analysis with the annotation sets of 'biological process', 'molecular function', and 'cellular component'. All genes (Homo sapiens) in the database were used as the reference list. p value was evaluated by the classic Fisher test, and the value lower 0.001 was a cutoff of significance.

## Results

### p53 forms intermolecular disulfide-dependent complexes upon oxidation

p53 has long been known to be prone to reversible oxidation on cysteines both in vitro and in vivo [8, 17, 18] (also reviewed in [19]), but the chemical identity of the reversible oxidation is generally lost during sample preparation. Reversible cysteine oxidation can result in intermolecular disulfide formation and the latter has been shown to play important roles in tuning protein function and signal transduction [5]. Intermolecular disulfide-dependent complexes can be detected based on migrational behavior with large mass-shifts on SDS-PAGE under non-reducing conditions followed by Western blot. Reduction of the same sample by beta-mercaptoethanol dissociates the complex and p53 migrates at its monomeric mass. Flag-p53 wildtype (WT) expressed in HEK293T cells indeed formed multiple redox-sensitive protein complexes upon treatment with the thiol-specific oxidant diamide (**Fig. 1A**). Complex formation was dose-dependent and dissolved over time by the cellular anti-oxidant system (**Fig. 1A, B** and **Fig. S1A**). A number of distinct bands was observed, suggesting that p53 forms complexes with a specific set of proteins rather than crosslink with proteins randomly. The extent of p53-containing disulfide-dependent protein complexes peaked 15 min after diamide treatment and was largely resolved 1h after of diamide-addition, regardless of whether diamide was washed out (**Fig. 1B** and **Fig. S1A**). Surprisingly, H<sub>2</sub>O<sub>2</sub> did not induce clear p53 redox-dependent complexes even at concentrations well above those

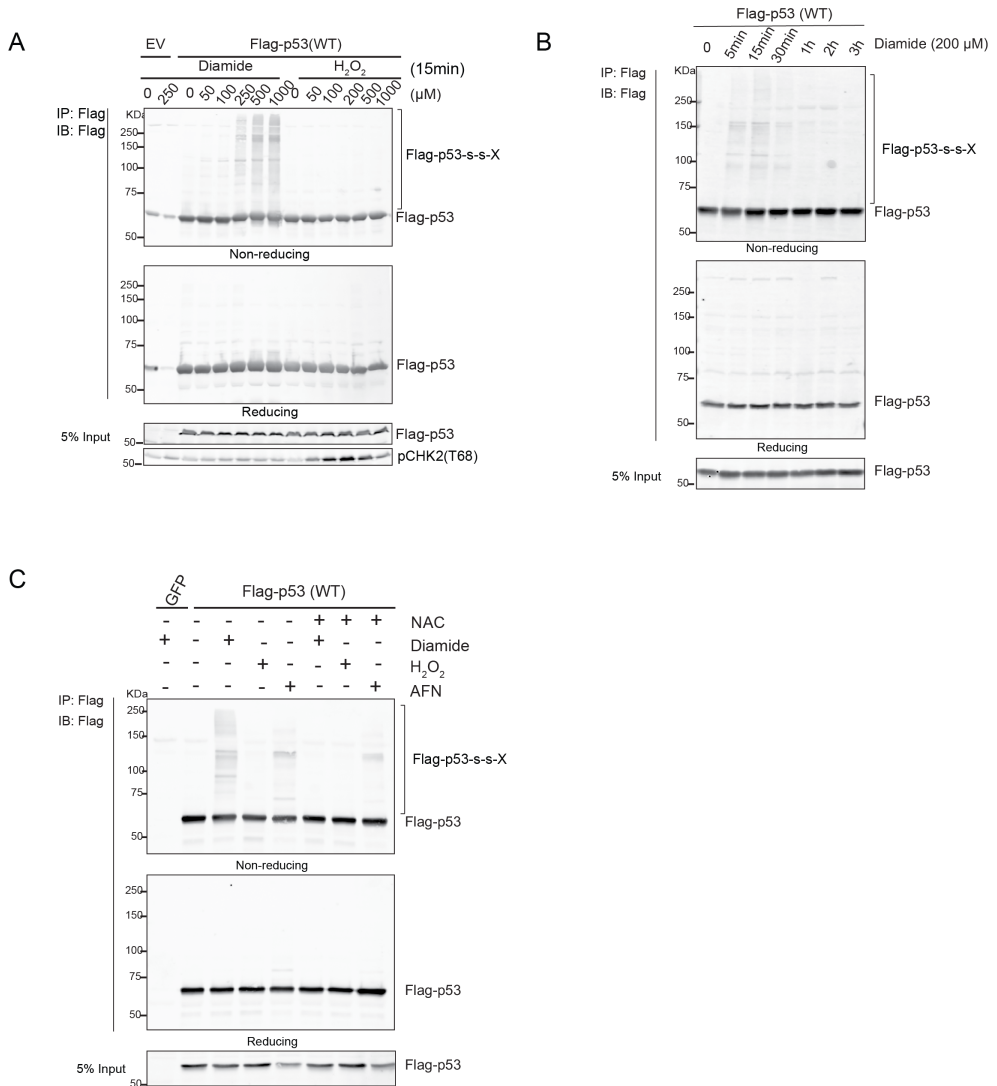


**Figure 1. p53 forms redox-sensitive protein-protein interactions upon oxidant treatment.**

(A) Diamide, but not H<sub>2</sub>O<sub>2</sub>, induces redox-dependent interactions between p53 and other proteins in a dose-dependent manner. Flag-p53 immunoprecipitated from diamide-treated HEK293T cells migrates in several high-molecular weight bands under non-reducing conditions. pCHK2 levels indicate that H<sub>2</sub>O<sub>2</sub>, but not diamide, induces an ATM-dependent DNA damage response. (B) Diamide-induced p53 complexes are reversible and resolved over time by the cellular antioxidant system. (C) AFN treatment also induces the formation of p53 complexes, be it with a pattern distinct from diamide. NAC pre-treatment prevents most diamide-induced complex formation.

that induce a DNA damage response or upon prolonged treatment (Fig. 1A and Fig. S1B, C). This is consistent with the previous finding that endogenous p53 is more susceptible to diamide-dependent oxidation as compared to H<sub>2</sub>O<sub>2</sub>-dependent oxidation [8].

Diamide is a thiol-specific oxidizing agent, that most probably induces redox signaling by lowering of the cellular reductive capacity, for instance through oxidation of glutathione [20]. We tested whether inhibition of the cellular Thioredoxin (Trx) system, using the Thioredoxin Reductase (TrxR) inhibitor Auranofin (AFN) [21, 22]. Indeed, AFN treatment also led to redox-dependent complex formation of p53 (**Fig. 1C**). However, diamide and AFN did not result in identical patterns of disulfide-dependent interactions with p53 as judged by the protein shifts on the blot. There could be several molecular mechanisms that underlie these differences.

### **p53 forms disulfide-dependent protein complexes through C277**

Next, we questioned which cysteine(s) in p53 is(are) involved in the observed intermolecular disulfide-dependent complexes. The p53 protein has ten cysteines that are all located in the DNA-binding domain (**Fig. 2A**). Three of these (C176, C238 and C242) coordinate a zinc atom and are indispensable for maintaining p53 structure and function [18] (**Fig. 2C**). Site-directed mutagenesis (Cys to Ser (**Fig. 2B, C**) or Cys to Ala (**Fig. S2A**)) was therefore carried out for non-zinc finger cysteines. To test whether these p53 cysteine mutants were still functional, C>S and C>A mutants were expressed in p53-deficient H1299 cells and examined for their capability to induce p21 expression. p53 C277 mutants (either to Ser or Ala) induced similar levels of p21 as WT p53 did, but lost the majority of redox-dependent high-molecular weight complexes on non-reducing SDS-PAGE in both H1299 cells and HEK293T cells (**Fig. 2B, C** and **Fig. S2A**), suggesting that C277 partakes in redox-dependent intermolecular disulfides. Other cysteine mutants like C134S and C141S resulted in the loss of p53 transcriptional activity (**Fig. 2B**), whereas C135A and C141A did not (**Fig. S2A**), possibly because Alanine is a better substitute in terms of hydrophobicity for these cysteines. The observed smear on SDS-PAGE under non-reducing conditions for the C134S and C141S mutants is similar to that of the Zn-finger mutant C176S (**Fig. 2B** and **Fig. S2B**), and could indeed be an indication for unfolding and random intermolecular disulfide formation. Consistently, the C134A and C141A mutant displayed a pattern of redox-dependent binding partners that was more similar to WT p53 (**Fig. S2A**). C275S and C275A had both impaired transcriptional activity but did not show signs of altered folding like the C176S mutant (**Fig. 2B** and **Fig. S2A**). This suggests that the C275 residue is essential for p53 transcriptional activity without grossly affecting its structure. Taken together, p53 forms reversible intermolecular disulfides involving C277 under oxidizing conditions (**Fig. 2B** and **Fig. S2A, B**). The observation that p21 expression is still triggered by the C277 mutant could suggest that oxidation of this cysteine does not represent an on/off switch but rather a way to fine tune p53 activity or transcriptional target selection.

### **Identification of p53 disulfide-dependent binding partners by MS**

We set out to identify the disulfide-dependent interaction partners of p53. Using co-IP experiments with differentially tagged p53 constructs we first excluded the formation of disulfide-dependent p53 dimers or oligomers (**Fig. S3**).

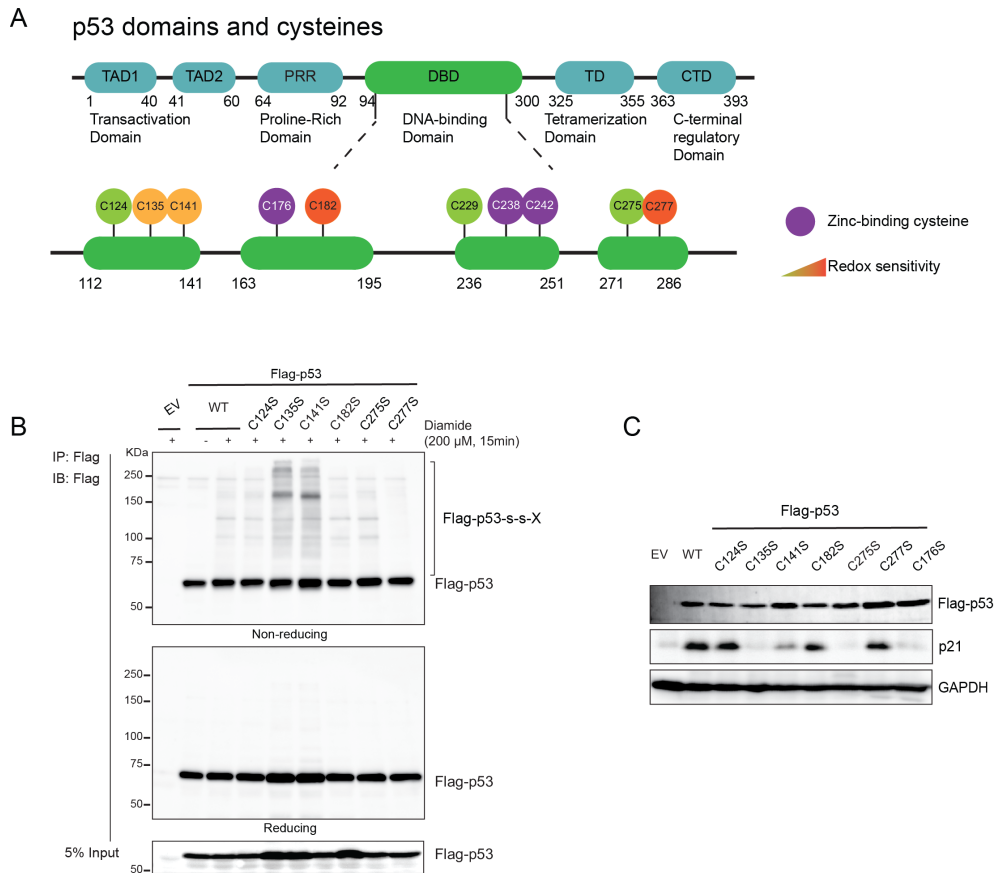


**Figure 2. p53 forms disulfide-dependent protein-protein interactions through cysteine 277.**

**(A)** Scheme of domains and cysteines of p53 protein. The p53 protein contains two Transactivation Domains (TAD1 and TAD2), Proline-Rich Domain (PRR), DNA-binding Domain (DBD), Tetramerization Domain (TD) and C-terminal regulatory Domain (CTD). All of ten cysteines of p53 are located within its DBD, among which C176, C238 and C242 (in purple) are Zinc-coordinating cysteines and are essential for maintaining p53 structure. C176, C182, C229, C242 and C277 are surface-exposed cysteines. C135, C141, C182 and C277 have been shown to be prone to redox regulation (in yellow and orange). The p53 protein domains and regions are referenced to the TP53 WEB SITE (<http://p53.fr/>) database. **(B)** Cysteine-dependent p53 protein complexes. C277 is required for most of redox-dependent interactions of p53 protein. IP and WB against Flag were performed in NCI-H1299 cells (p53-deficient) that were transiently expressing p53 WT and cysteine mutants (to Serine). **(C)** The transcriptional activity of p53 cysteine mutants was evaluated by checking p21 level in H1299 cells.

We performed quantitative LC-MS/MS to identify candidate disulfide-dependent binding partners of p53 by comparing the interactome of WT p53 and two cysteine mutants (C182S and C182SC277S) (**Fig. 3A**). Sample quality assessment showed that the expression and pull-down of the Flag-p53 proteins, as well as the (absence of) induction of intermolecular disulfide-dependent complexes was highly reproducible over four biological replicates (**Fig.**



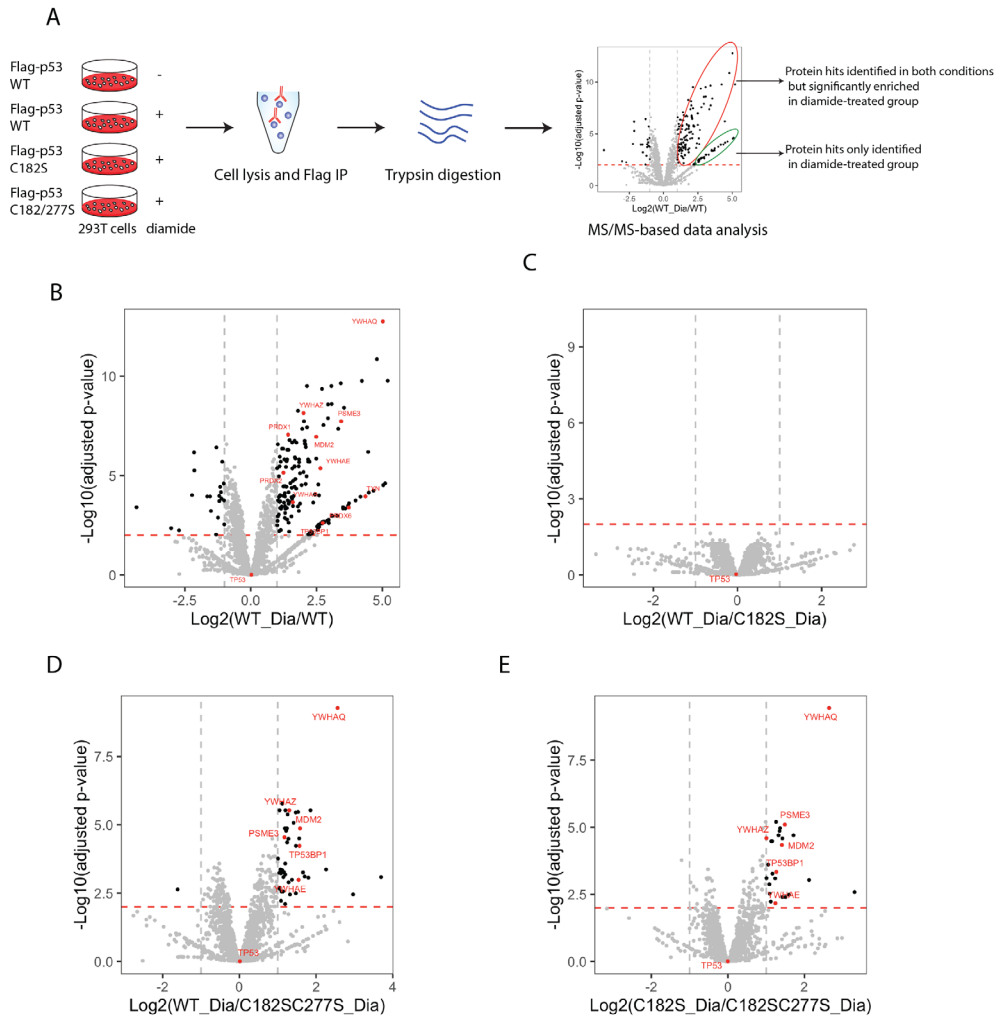


**Figure 3. Identification of disulfide-dependent p53 interactors by MS/MS analysis.**

(A) Scheme for the identification of p53 disulfide-dependent interactors by MS/MS. HEK293T cells were transfected with Flag-p53 WT, C182S, and C182SC277S. 48h after transfection, cells were treated with diamide, followed by immunoprecipitation and processing for MS/MS. MS data were further analyzed in R and plotted in a volcano plot. Protein hits with >2-fold enrichment and an adjusted p-value <0.01, are considered significant interactors (black dots). Hits circled in red are identified in both conditions, whereas the green circle indicates proteins identified in only one of the samples. Data analysis was based on 4 biological replicates for each condition. (B) Volcano plot showing interactors of Flag-p53 WT with and without diamide treatment. (C) Volcano plot showing interactors of Flag-p53 WT vs. C182S, both with diamide treatment. (D) Volcano plot showing interactors of Flag-p53 WT vs. C182SC277S, both with diamide treatment. (E) Volcano plot showing interactors of Flag-p53 C182S vs. C182SC277S, both with diamide treatment.

**S4A**). Overall raw MS data regarding the amount and intensity of identified proteins were also comparable between replicates (**Fig. S4B-D**). After filtering out the proteins with less than 2 peptides, 1889 proteins in total were identified (pulled down by the Flag beads). Out of which 162 proteins were identified to significantly bind to WT p53 upon diamide treatment (Log<sub>2</sub> fold change >1 and adjusted p-value < 0.01), including several proteins involved in redox signaling like Trx and PRDX family-members (**Fig. 3B**). Comparison of the proteins pulled down after diamide treatment with WT p53 versus C182S showed no significant changes in binding upon loss of C182 (**Fig. 3C**), consistent with our observations in the non-reducing SDS-PAGE and Western blot experiments (**Fig. 2B**). The C182SC277S double mutant on the other hand showed far less significant binders as compared to WT p53 or C182S, indicating that C277 is indeed required for many (but not all) of the intermolecular disulfide-dependent interactions of p53 (**Fig. 3D, E**). Precisely, out of the 162 diamide-induced interacting proteins, 19 proteins were dependent on C277, including several well-known p53-binding proteins (for a list see **Table S2**). Note that no proteins are significantly binding C182, whereas some proteins seem to require both C182 and C277 for binding (**Table S2**), which would be unexpected for intermolecular disulfide-dependent interactors. The explanation could be that binding of one protein to for instance C277 facilitates binding of another protein to C182, and other cysteines (e.g., C277) might compensate for the loss of single C182 to mediate the interaction with other proteins.

Gene Ontology (GO) analysis for 162 diamide-induced p53 interactors (**Fig. S5**) showed enrichment for several GO biological process terms related to the regulation of gene expression (**Fig. S5A**). From the perspective of GO molecular function, these binding partners were significantly associated with 'protein binding', but also with several terms related to disulfide oxidoreductase activity. May be not surprisingly, the GO molecular function terms 'p53 binding' and 'antioxidant activity' were also significantly enriched among the binding partners (**Fig. S5B**). The enriched GO cellular component terms points at a function in the nucleus, which can be expected for transcription factor binding partners (**Fig. S5C**).

### **C277-dependent interactions of p53 with 14-3-3 $\theta$ and 53BP1**

We were intrigued to find that the binding of a number of well-known p53 interactors and regulators was also affected by diamide treatment and depended on C277. These included (TP53BP1, MDM2, PSME3 and 14-3-3 family members (e.g., encoded by YWHAQ/E genes) [23-25] (**Fig. 3**). We therefore decided to focus initially on the further validation of these binding partners and exploration of how these could affect p53 function dependent on C277 oxidation.

14-3-3 $\theta$  (also known as 14-3-3 $\tau$ , shown in the volcano plot by its gene name YWHAQ), is the most significant hit identified to bind to p53 through C277 upon diamide in MS data (**Fig. 3**). The LFQ data of the individual biological replicates shows the reproducibility of this observation (**Fig. 4A**). Note that this protein indeed also is found to bind p53 without

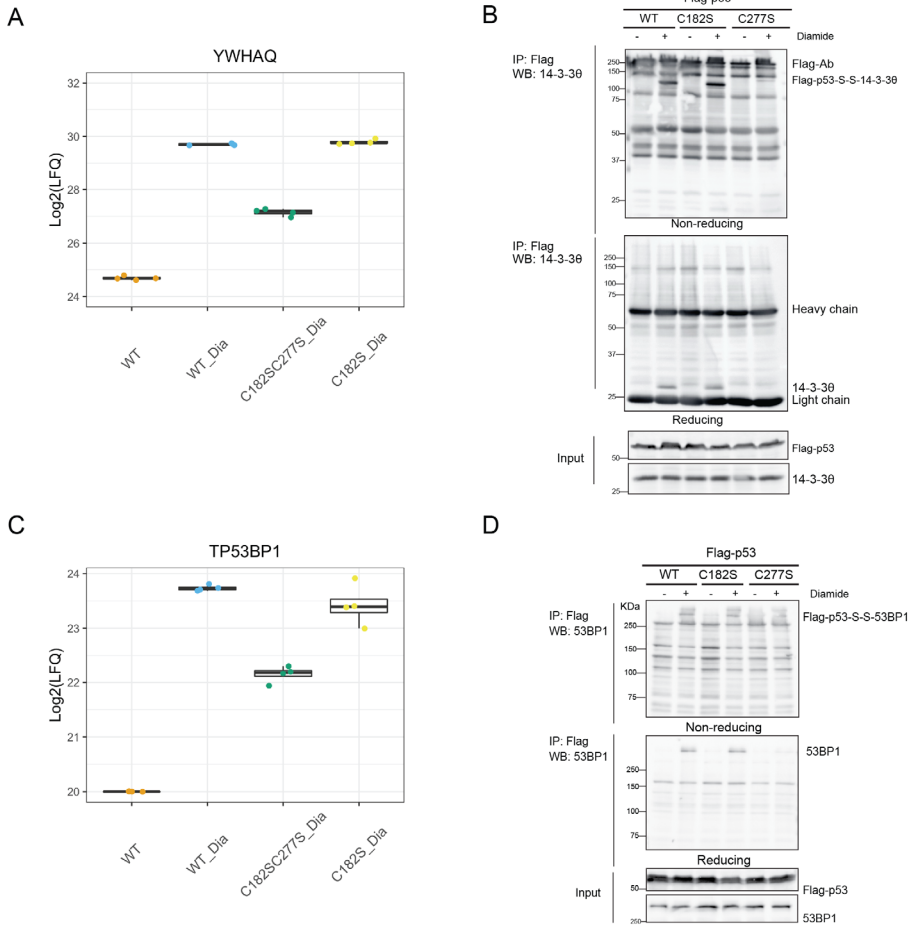


**Figure 4. Validation of disulfide-dependent binding partners of p53.**

(A) Comparison of the LFQ values of the YWHAQ gene product (encoding the 14-3-30 protein) in different conditions. (B) Validation of the disulfide-dependent interaction between p53 and 14-3-30 by IP followed by WB. (C) Comparison of the LFQ values of the TP53BP1 gene product (encoding the 53BP1 protein) in different conditions. Note that the TP53BP1 gene product was not found in any of the replicates of the untreated condition (WT) and a missing value (NA) was observed upon Log2 transformation. This was manually imputed by a value of 20(Log2) (near to the lowest value in the whole dataset) during data analysis. (D) Validation of disulfide-dependent interaction between p53 and 53BP1 by WB.

diamide treatment as previous described [26], but with far less intensity as compared to the binding upon diamide treatment. Immunoprecipitation followed by non-reducing and reducing SDS-PAGE and Western blotting confirmed that the diamide-induced p53/14-3-30 interaction was mediated by C277 (Fig. 4B). The redox-dependent interaction between Flag-p53 and 14-3-30 results in a molecular weight shift corresponding with over 100 kDa

in the non-reducing gel, which can be reduced and migrates as monomeric Flag-p53 (about 55 kDa) and 14-3-3 $\theta$  (28 kDa). This shows that the complex indeed is held together by an intermolecular disulfide involving p53 C277 (**Fig. 4B**). RNAi mediated-knockdown confirmed that the shifted band indeed contains 14-3-3 $\theta$  (**Fig. S6**). The pattern of other intermolecular disulfide-dependent complexes containing Flag-p53 seemed not to be affected by 14-3-3 $\theta$  knockdown, suggesting that this scaffold protein [27] does not mediate the other redox-dependent interactions of Flag-p53, for instance by forming complexes containing multiple disulfides (**Fig. S6**)

Diamide-induced and C277 dependent binding of 53BP1 was also validated. **Fig. 4C** shows the reproducibility of the LFQ data of the individual replicates for each condition. Note that without diamide treatment 53BP1 is not identified, and that the data for this condition represents identical imputed values (set to value 20 (Log2) which is near to the lowest value in the whole dataset). Both endogenous 53BP1 and overexpressed GFP-53BP1 can be co-immunoprecipitated by Flag or HA tagged p53. Paralleling reducing and non-reducing SDS-PAGE followed by Western blot shows that p53 and 53BP1 indeed form an intermolecular disulfide-dependent complex involving p53 C277 (**Fig. 4D** and **Fig. S7**). Without diamide treatment we observed very little 53BP1 binding to p53, although this protein-protein interaction has been extensively studied by others without the use of oxidizing conditions [28]. An explanation for this apparent discrepancy could lie in the sample preparation that we use for the identification of disulfide-dependent interactors. The immunoprecipitation protocol involves a high-salt wash (1 M NaCl) in order to lower the number of non-covalent binders. Indeed, milder washing conditions reveal 53BP1 binding also in the absence of diamide treatment, be it far less (**Fig. S7**). In the absence of diamide part of the bound GFP-53BP1 is visible as an intermolecular disulfide-dependent complex, suggesting that this disulfide can form under endogenous conditions. The GFP-53BP1 fraction that is pulled down with p53 that does not migrate as an intermolecular disulfide-dependent complex, and hence binds p53 only through non-covalent interactions [29] was most affected by the high salt wash (**Fig. S7**). Interestingly, both the disulfide-dependent and -independent interaction increase dramatically in WT cells upon diamide treatment, which could mean that part of the disulfide-stabilized p53 and GFP-53BP1 complex is reduced during sample preparation, while maintaining the interaction. Accordingly, far less disulfide-independent p53-53BP1 binding is pulled down by the p53 C277S mutant. A small amount of disulfide-dependent p53-S-S-53BP1 complex is observed upon washing with low-salt buffer, that disappears upon high-salt wash. This observation can be explained by the pull down of endogenous WT p53-S-S-GFP-53BP1 complexes with HA-p53 C277S in a non-covalent manner.

### **p53 C277 is dispensable for the response to Nutlin-3, oxidant treatment and DNA damage**

Disulfide-dependent binding of regulatory proteins could affect the transcriptional activity of p53 through for instance altered subcellular localization, (de)stabilization or differential target

promoter binding. To test this, we devised a doxycycline (Dox)-inducible system expressing WT or C277S in p53 KO RPE<sup>Tert</sup> cells (**Fig. 5A**). The localization of p53 WT and C277S was very similar and both were mainly present in the nucleus in these cells (**Fig. 5B**). After 48 h of Dox addition, we tracked p53 protein levels and activity upon Nutlin-3a treatment, diamide (**Fig. 5C-E**), and the DNA damaging agent NCS (**Fig. 5F-H**), and we found that both WT and C277S were stabilized and activated to a similar extent in response to these compounds. Diamide treatment also did not affect the response to Nutlin-3a (**Fig. 5C-E**). (Poly) ubiquitination of both WT and C277S was blocked to a similar extent in response to both diamide and H<sub>2</sub>O<sub>2</sub> (**Fig. 5I, J**). We previously showed that diamide-mediated oxidizing conditions induced p53 stabilization and activation, which was dependent on the upstream kinase p38MAPK [30]. p38MAPK-induced stabilization and activation of p53 was independent of surface-exposed p53 cysteines (including C277) [30], and could therefore obscure the effects of disulfide-dependent binding partners under the conditions tested. Furthermore, the majority of WT p53 is still reduced upon diamide treatment, and this could conceal potential regulatory effects of the disulfide-dependent interactions which have a relatively low stoichiometry.

### **p53 C277 is highly conserved throughout vertebrate evolution**

Cysteine is a highly conserved amino acid due to its function in catalytic centers and structural disulfides. On the other hand, the reactivity of the cysteine thiol group can also be detrimental to protein function when non-functional cysteines are acquired during evolution, especially on the surface of proteins, and these tend to be rapidly lost again. Paradoxically, cysteine has therefore been suggested to be both one of the most and one of the least conserved amino acids [31]. Although evolutionary conservation cannot unequivocally predict whether cysteines are functional or not, it is plausible that surface-exposed cysteines that are not conserved are dispensable for or even hamper protein function. We have previously shown that evolutionary acquisition and conservation of surface-exposed cysteines can be predictive of a functional role for a certain cysteine in redox signaling [32], and we thus analyzed the conservation of the cysteines in paralogs as well as vertebrate orthologs of human p53. In line with the strong conservation of functional cysteines, the Zn-coordinating cysteine homologous to human p53 C176, C238 and C242 are indeed present in all homologs of vertebrate species for which sequences were available, as well in the human p53 paralogs p63 and p73 (**Fig. 6A, B**). Mutation of these cysteines leads to loss of Zn-binding and inactivation of the protein (**Fig. 2C**). The non-Zn-binding cysteines at position 135, 141, 275 and 277 are also highly conserved in the human paralogs and vertebrate orthologs (C141 slightly less in Fish species), but have variable effects on p53 activity upon mutation (**Fig. 2C** and **Fig. S2A**). The activity of C135S and C141S is completely or largely impaired, whereas C135A and C141A induce p21 expression similar to p53 WT. These two cysteines are not surface exposed, and it could therefore be that mutation to Serine is a too hydrophilic substitution, that could lead to (partial) unfolding. This idea is supported by the strong, random disulfide formation observed for the C135S and C141S mutants,

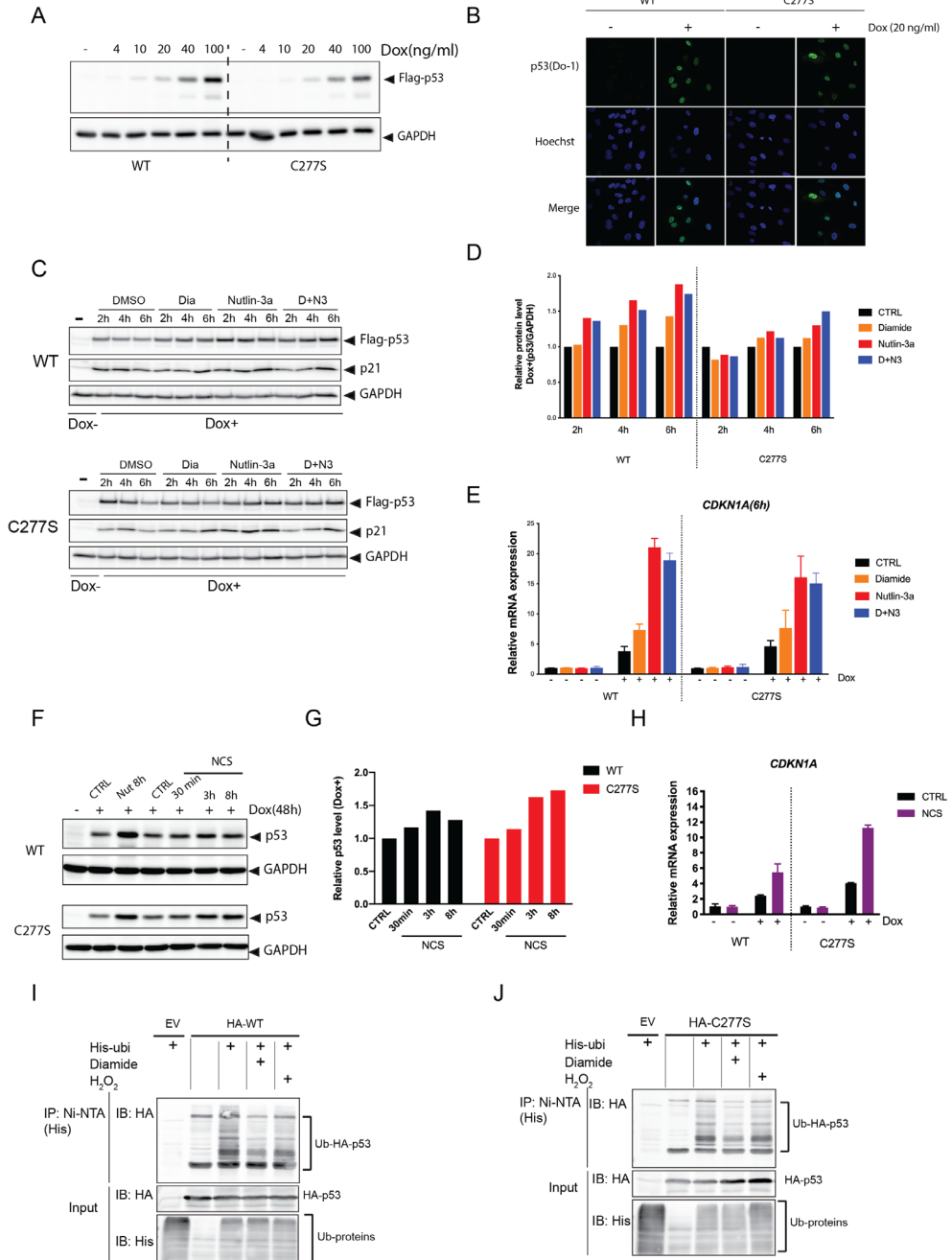


**Figure 5. p53C277S is stabilized and activated similar to p53 WT in response to Nutlin-3a, oxidant treatment and DNA damage.**

(A) Dox-inducible expression of Flag-p53 WT and C277S in p53 KO RPE<sup>Tert</sup> cells upon titration with doxycycline. (B) Immunofluorescence images showing the sub-cellular localization of Flag-p53 WT and C277S in dox-inducible p53 KO RPE<sup>Tert</sup> cells. Both are mainly localized in the nucleus. (C) Flag-p53 le-

vel in the dox-inducible expressing p53 WT and p53C277S RPE<sup>Tert</sup> cells upon different stimuli. Flag-p53 WT and C277S were induced by Dox (20 ng/ml, 48h) in p53 KO RPE<sup>Tert</sup> cells, followed by treatment with diamide (200  $\mu$ M), Nutlin-3a (10  $\mu$ M), or both (D+N3) for the indicated time. Total cell lysate was harvested and the levels of Flag-p53 WT, C277S, p21 and GAPDH (as a loading control) were evaluated. The blots are representative for the results of at least three independent experiments. **(D)** Quantification of Flag-p53 WT and C277S protein levels relative to GAPDH from (C). **(E)** CDKN1A (p21) mRNA expression in Dox-inducible expressing p53 WT and C277S RPE<sup>Tert</sup> cells upon different treatments as determined by qPCR. **(F)** Flag-p53 level in the Dox-inducible expressing p53 WT and C277S RPE<sup>Tert</sup> cells upon Neocarzinostatin (NCS) (250 ng/ml) or Nutlin-3 treatment. **(G)** Quantification of Flag-p53 WT and C277S protein levels relative to GAPDH from (F). **(H)** CDKN1A (p21) mRNA expression in Dox-inducible expressing p53 WT and C277S RPE Tert cells upon NCS treatment as determined by qPCR. Ubiquitination of p53 WT **(I)** and C277S **(J)** upon diamide or H<sub>2</sub>O<sub>2</sub> treatment. HEK293T cells transiently expressing HA-p53 (WT or C277S) and His-ubiquitin were treated with diamide (200  $\mu$ M) or H<sub>2</sub>O<sub>2</sub> (200  $\mu$ M) for 15 min. His-tag-Ubiquitinated proteins were precipitated using Ni-NTA agarose beads and analyzed by Western blot using His or HA antibodies.

reminiscent of the Zn-finger mutant C176S (**Fig. 2B**, and **Fig. S2B**). C275 is also highly conserved in all vertebrate p53 sequences analyzed, and the activity of C275S and C275A mutants is indeed lost. This may have to do with the fact that this cysteine is in close contact with the DNA, which leaves little room for side-chain substitution. The only non-Zn-binding, surface exposed cysteine in p53 that is conserved throughout evolution is C277, for which we show here that it is involved in intermolecular disulfide-dependent heterodimerization. However, mutation of this cysteine to either Ser or Ala does not grossly affect the ability of p53 to induce p21 when overexpressed. One could maybe argue that this means that redox regulation of C277 is not important in terms of fitness. On the other hand, we show here that C277 is redox sensitive and forms intermolecular disulfides with several regulatory proteins like MDM2 and 53BP1. It is tempting to speculate that if disulfide-dependent crosslinking of p53 would occur at random that this would partially impair p53 function or regulation, leading to negative selective pressure on C277, which seems not to be the case. Conversely, acquisition without fixation seems to be the case for the surface exposed C182 and C229, and to a lesser extent for C124. These three cysteines are not conserved in human p63 and p73, and variation in the amino acid in these homologous positions can be observed in p53 in many vertebrates including mammals. This could suggest that these cysteines are non-functional or even are associated with some loss in fitness. The apparent flexibility for having a cysteine at these positions or not is in agreement with the observation that mutants of these cysteines induce p21 similar to human wildtype p53 (**Fig. 2C** and **Fig. S2A**).

## Discussion

Oxidation of protein cysteine thiols leads to a suite of PTMs that can reversibly alter protein structure and function. In this way, cysteine oxidation-dependent redox signaling regulates a variety of biological processes including cell proliferation, differentiation, migration and regeneration [33-35]. The methods used to detect reversible protein oxidation





**Figure 6. p53 Cysteine conservation in vertebrate orthologs and human paralogs.**

(A) Alignment of human p53 protein sequences from 5 groups of vertebrate species including fish, amphibians, birds, reptiles and mammals. (B) The alignment of protein sequence among p53 and its paralogs p63 and p73 from Homo Sapiens. All protein sequences were downloaded from the Ensembl database and the sequence alignment was performed in Jalview (version 15.0) software. The alignments were colored based on the extent of conservation (Threshold 10). Cysteines were further colored in orange in Adobe Illustrator.

are in general based on differential alkylation of cysteines prior and post reduction, and hence the type of reversible oxidation (e.g., sulfenic acid, S-glutathionylation, sulfenamide, inter- or intramolecular disulfide) is lost in this process. Strategies using sequential reduction of specific oxidative PTMs have been used to discriminate for instance proteome-wide S-GSHylation and S-nitrosylation [36] by MS/MS. But no method exists to date to identify or distinguish intra- or intermolecular disulfides in a proteome-wide manner. The amount of theoretically possible tryptic digests containing peptides from two distinct proteins and an intact disulfide is virtually endless. Intermolecular disulfides can be identified for a protein of interest by first comparing the interactomes of the wildtype protein and a cysteine mutant and subsequently test whether the protein of interest and a cysteine-dependent interactor indeed migrate as a reduction-sensitive complex on SDS-PAGE under non-reducing conditions [5]. The tumor suppressor p53 had already been reported to undergo reversible cysteine oxidation in response to oxidizing agents both in vitro and at endogenous levels in live cells [8], but the nature of the reversible oxidation remained elusive in that study. In the present study, we provide evidence that cysteine oxidation of p53 leads to the formation of several intermolecular disulfide-dependent complexes, most of which depend on C277. This cysteine is also implicated in the binding to cysteine-directed covalent drugs aimed at refolding mutant p53 [37], which means that these compounds could also likely interfere with the intermolecular disulfide-dependent, p53-containing complexes described in this study.

A number of disulfide-dependent and validated hits from our MS screen are known interactors and regulators of p53, including MDM2, 53BP1 and 14-3-3. But the original studies describing the interactions of these proteins with p53 did not study redox or cysteine dependency [26, 28, 38]. We show that at least for 53BP1 the interaction with p53 is indeed not strictly dependent on the disulfide (**Fig. S7**). This experiment shows that the disulfide stabilizes the interaction in the co-immunoprecipitation assay and makes it resistant to a stringent high-salt wash. It remains to be seen to what extent this translates in the in vivo situation, and whether this means that in cells the strength or duration of the p53-53BP1 protein-protein interaction is also significantly enhanced as compared to a purely electrostatic interaction upon disulfide formation. The observation that the C277S mutant can still interact with 53BP1 suggests that the p53-53BP1 interaction occurs prior to oxidation, and that the disulfide forms between two cysteines that are already in close proximity. This could be a general concept for the formation of intermolecular disulfides, and potentially explains why p53 does not form random intermolecular disulfides with a wide range of

proteins. The disulfide could in this case either strengthen a functional protein-protein interaction or lead to a conformational change that alters the protein-protein interaction in such a way that it interferes with its function. If the latter were the case, one might predict that C277 would maybe not be conserved, similar to C182 and C229, whereas it displays strong evolutionary conservation. On the other hand, if the disulfide-dependent interaction would greatly enhance the regulatory function of an interaction partner we would expect to have observed differences in the transcriptional activity or stability in the C277S mutant, which we did not. The latter might be because multiple proteins with opposing regulatory functions for p53 seem to interact with C277. Since both the C277S and C277A mutants still have transcriptional activity, we can conclude that cysteine oxidation is not absolutely required for p53 function, but that it could maybe provide a means for fine-tuning target selection or the duration of a regulatory response. That we do not find an inhibitory effect of disulfide formation on p53 activity in the tested assays could also be due to the fact that the amount of non-covalently crosslinked p53 surpasses the amount of p53 partaking in intermolecular disulfide-dependent complexes.

Although the present study focuses on a potential functional role for redox regulation of p53, it might also be that the functional consequence lies 'at the other end' of the intermolecular disulfides. The disulfide mediated p53-53BP1 interaction may for instance alter the efficiency of 53BP1-dependent non-homologous end joining in DNA-damage repair. Likewise, locking p53 to MDM2 may interfere with the ubiquitination-dependent breakdown of MDM2 substrates other than p53. 14-3-3 proteins also have many more binding partners besides p53, and the intermolecular disulfide-dependent interaction may alter its adaptor function towards other proteins. We have previously shown that the FOXO transcription factors do not bind 14-3-3 proteins in a cysteine dependent manner [39], suggesting that not all 14-3-3 interactors bind in a redox-dependent manner. To what extent covalent binding of p53 to these proteins will affect their function depends of course on the stoichiometry of the interaction.

The intrinsic sensitivity for oxidation of cysteine thiols in proteins depends on a number of variables including their pKa, solvent accessibility and local protein folding. Reactivity to for instance  $H_2O_2$  can vary several orders of magnitude. It has therefore been proposed that within live cells oxidation of most cysteines by relatively low levels of  $H_2O_2$  probably occurs indirectly, for instance catalyzed by peroxiredoxins [12, 40]. In this study we observed that p53 forms intermolecular disulfides in response to diamide but not  $H_2O_2$  treatment. The work by Held et al. showed before that cysteines in endogenous p53 are oxidized by diamide and not by  $H_2O_2$ . Furthermore, the diamide-induced oxidation of p53 in live cells occurs at much lower concentrations as compared to in vitro on recombinant p53 [8]. These observations suggest that in live cells p53 cysteine oxidation also does not occur directly or requires an additional factor or catalyst. But since  $H_2O_2$  does not lead to p53 cysteine oxidation we propose that it is not mediated by a Peroxiredoxin dependent redox relay [12, 40]. Glutathione is due to its abundance the most likely direct target of the thiol oxidant diamide,

and it might be that p53 oxidation is mediated by oxidized glutathione, but future work is needed to explore this idea. Alternatively, diamide-induced inhibition of (GSH-dependent) disulfide reduction could expose the continuous turnover of intermolecular disulfides that form between p53 and interacting proteins. The differential pattern of proteome-wide cysteine oxidation in response to different oxidants is an example of specificity in redox signaling, and it is not unthinkable that a differential cellular response is required upon oxidizing conditions induced by more oxidants (i.e.  $H_2O_2$ ) or by lower reductive power (i.e. diamide or Auranofin).

Taken together, here we show that cysteine oxidation of p53 can come in the form of intermolecular disulfides involving a large but defined set of binding partners. Future studies are needed to understand their functional importance in the context of normal physiology and tumor biology.

## Acknowledgments

We thank our colleagues at the department of Molecular Cancer Research, University Medical Center Utrecht for suggestions and input. This work was supported by grants from the China Scholarship Council (CSC no. 201606300046) to T.S. and from the Dutch Cancer Society (KWF UU 2014-6902 and Alpe/Unique High Risk #11077) to T.B.D.. B.M.T.B is part of the Onco Institute, which is partly financed by the Dutch Cancer Society (KWF Kankerbestrijding) and was funded by the gravitation program CancerGenomiCs.nl from the Netherlands Organization for Scientific Research (NWO).

## Author contributions

T.S. and T.B.D. designed the study. T.S. drafted the manuscript. T.B.D. commented on and revised the manuscript. B.M.T.B. reviewed and commented on the manuscript. T.S. and P.E.P. performed most of the experiments. R.M.E. and H.R.V. conducted the Mass spectrometry experiment. M.P.G. assisted with the MS data analysis.

## Declaration of interests

No conflict of interest between the authors

## References

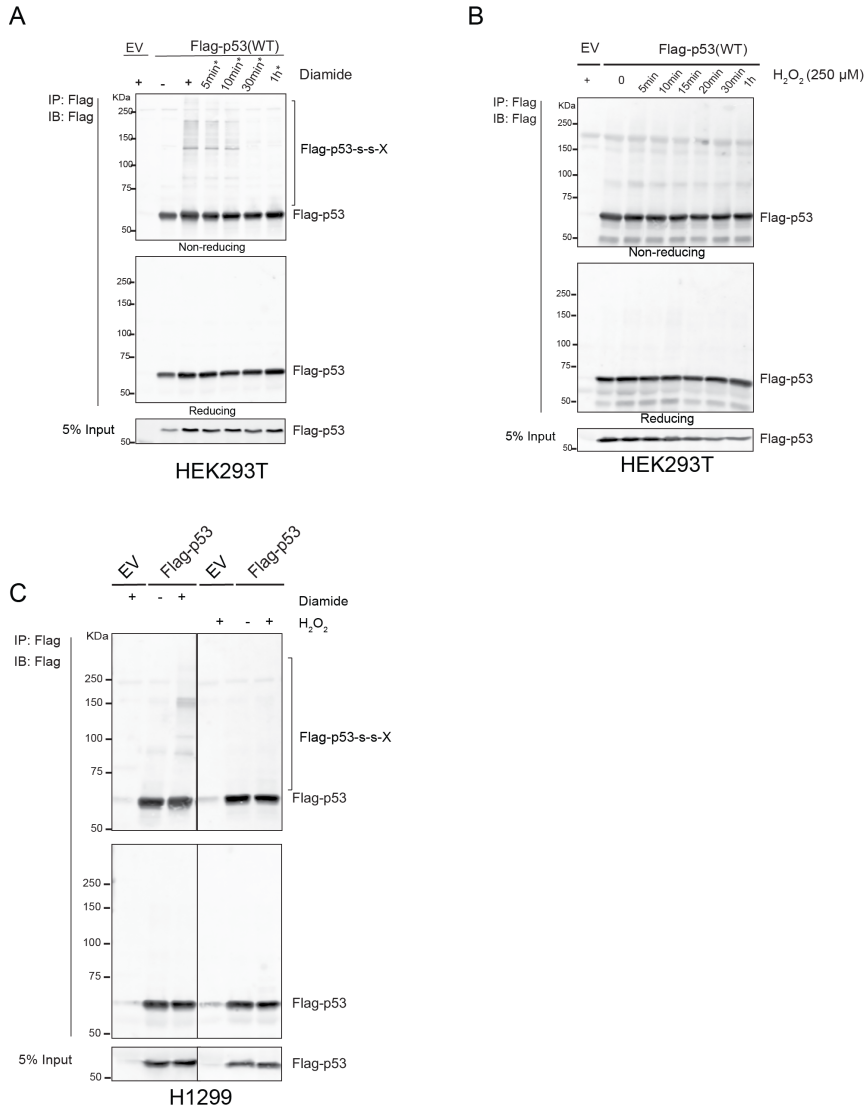
1. Kruiswijk F., Labuschagne C.F., Vousden K.H. p53 in survival, death and metabolic health: a lifeguard with a licence to kill. *Nat. Rev. Mol. Cell Biol.*, 2015. 16(7): 393-405.
2. Bode A.M., Dong Z. Post-translational modification of p53 in tumorigenesis. *Nature Reviews Cancer*, 2004. 4(10): 793-805.
3. Holmstrom K.M., Finkel T. Cellular mechanisms and physiological consequences of redox-dependent signalling. *Nat. Rev. Mol. Cell Biol.*, 2014. 15(6): 411-421.
4. Sies H., Jones D.P. Reactive oxygen species (ROS) as pleiotropic physiological signalling agents. *Nat. Rev. Mol. Cell Biol.*, 2020. 21(7): 363-383.
5. Putker M., Vos H.R., Dansen T.B. Intermolecular disulfide-dependent redox signalling. *Biochem. Soc. Trans.*, 2014. 42(4): 971-978.

6. Scotcher J., Clarke D.J., Weidt S.K., et al. Identification of Two Reactive Cysteine Residues in the Tumor Suppressor Protein p53 Using Top-Down FTICR Mass Spectrometry. *J. Am. Soc. Mass Spectrom.*, 2011. 22(5): 888-897.
7. Scotcher J., Clarke D.J., Mackay C.L., et al. Redox regulation of tumour suppressor protein p53: identification of the sites of hydrogen peroxide oxidation and glutathionylation. 2013. 4(3): 1257-1269.
8. Held J.M., Danielson S.R., Behring J.B., et al. Targeted quantitation of site-specific cysteine oxidation in endogenous proteins using a differential alkylation and multiple reaction monitoring mass spectrometry approach. *Mol. Cell. Proteomics*, 2010. 9(7): 1400-1410.
9. Kim E., Ilic N., Shrestha Y., et al. Systematic Functional Interrogation of Rare Cancer Variants Identifies Oncogenic Alleles. *Cancer Discov.*, 2016. 6(7): 714-726.
10. Meerbrey K.L., Hu G., Kessler J.D., et al. The pINDUCER lentiviral toolkit for inducible RNA interference in vitro and in vivo. *Proc. Natl. Acad. Sci. U. S. A.*, 2011. 108(9): 3665-3670.
11. van den Berg J., A G.M., Kielbassa K., et al. A limited number of double-strand DNA breaks is sufficient to delay cell cycle progression. *Nucleic Acids Res.*, 2018. 46(19): 10132-10144.
12. van Dam L., Pagès-Gallego M., Polderman P.E., et al. The Human 2-Cys Peroxiredoxins form Widespread, Cysteine-Dependent- and Isoform-Specific Protein-Protein Interactions. *Antioxidants*, 2021. 10(4): 627.
13. Perez-Riverol Y., Csordas A., Bai J., et al. The PRIDE database and related tools and resources in 2019: improving support for quantification data. *Nucleic Acids Res.*, 2019. 47(D1): D442-d450.
14. Ahlmann-Eltze C., Anders S. proDA: Probabilistic Dropout Analysis for Identifying Differentially Abundant Proteins in Label-Free Mass Spectrometry. *bioRxiv*, 2020: 661496.
15. Zerbino D.R., Achuthan P., Akanni W., et al. Ensembl 2018. *Nucleic Acids Res.*, 2018. 46(D1): D754-d761.
16. Waterhouse A.M., Procter J.B., Martin D.M., et al. Jalview Version 2--a multiple sequence alignment editor and analysis workbench. *Bioinformatics*, 2009. 25(9): 1189-1191.
17. Hainaut P., Milner J. Redox modulation of p53 conformation and sequence-specific DNA binding in vitro. *Cancer Res.*, 1993. 53(19): 4469-4473.
18. Rainwater R., Parks D., Anderson M.E., et al. Role of cysteine residues in regulation of p53 function. *Mol. Cell. Biol.*, 1995. 15(7): 3892-3903.
19. Shi T., Dansen T.B. Reactive Oxygen Species Induced p53 Activation: DNA Damage, Redox Signaling, or Both? *Antioxid Redox Signal*, 2020.
20. Pocsí I., Miskei M., Karanyi Z., et al. Comparison of gene expression signatures of diamide, H<sub>2</sub>O<sub>2</sub> and menadione exposed *Aspergillus nidulans* cultures--linking genome-wide transcriptional changes to cellular physiology. *BMC Genomics*, 2005. 6: 182.
21. Gromer S., Arscott L.D., Williams C.H., Jr., et al. Human placenta thioredoxin reductase. Isolation of the selenoenzyme, steady state kinetics, and inhibition by therapeutic gold compounds. *J. Biol. Chem.*, 1998. 273(32): 20096-20101.
22. Radenkovic F., Holland O., Vanderlelie J.J., et al. Selective inhibition of endogenous antioxidants with Auranofin causes mitochondrial oxidative stress which can be countered by selenium supplementation. *Biochem. Pharmacol.*, 2017. 146: 42-52.
23. Iwabuchi K., Bartel P.L., Li B., et al. Two cellular proteins that bind to wild-type but not mutant p53. *Proc. Natl. Acad. Sci. U. S. A.*, 1994. 91(13): 6098-6102.
24. Waterman M.J., Stavridi E.S., Waterman J.L., et al. ATM-dependent activation of p53 involves

dephosphorylation and association with 14-3-3 proteins. *Nat. Genet.*, 1998. 19(2): 175-178.

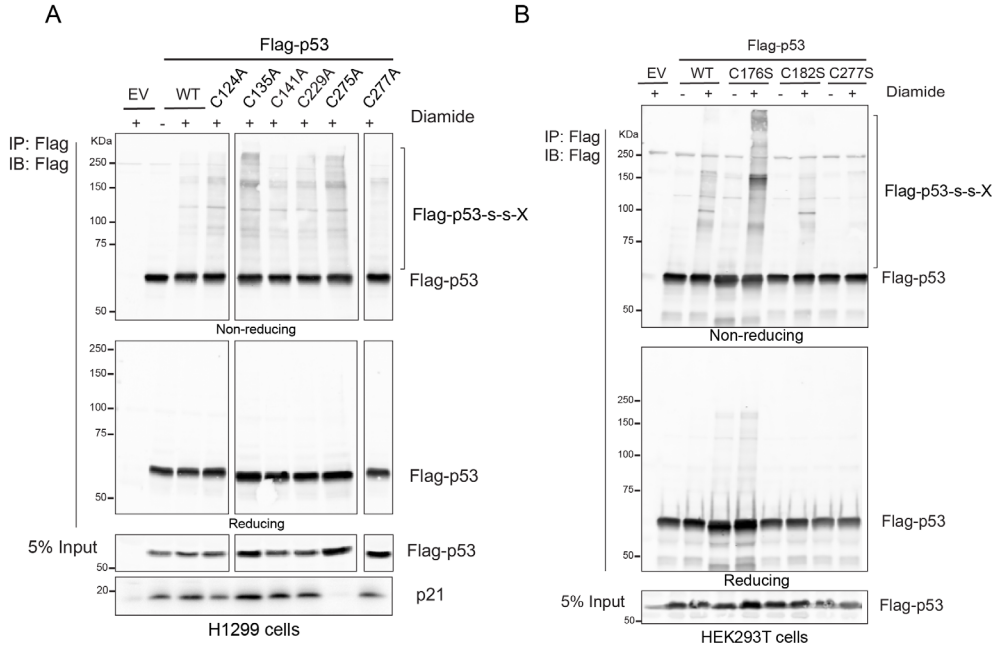
25. Zhang Z., Zhang R. Proteasome activator PA28 gamma regulates p53 by enhancing its MDM2-mediated degradation. *EMBO J.*, 2008. 27(6): 852-864.
26. Rajagopalan S., Sade R.S., Townsley F.M., et al. Mechanistic differences in the transcriptional activation of p53 by 14-3-3 isoforms. *Nucleic Acids Res.*, 2010. 38(3): 893-906.
27. Fu H., Subramanian R.R., Masters S.C. 14-3-3 proteins: structure, function, and regulation. *Annu. Rev. Pharmacol. Toxicol.*, 2000. 40: 617-647.
28. Cuella-Martin R., Oliveira C., Lockstone H.E., et al. 53BP1 Integrates DNA Repair and p53-Dependent Cell Fate Decisions via Distinct Mechanisms. *Mol. Cell*, 2016. 64(1): 51-64.
29. Derbyshire D.J., Basu B.P., Serpell L.C., et al. Crystal structure of human 53BP1 BRCT domains bound to p53 tumour suppressor. *EMBO J.*, 2002. 21(14): 3863-3872.
30. Shi T., van Soest D.M.K., Polderman P.E., et al. DNA damage and oxidant stress activate p53 through differential upstream signaling pathways. *Free Radic. Biol. Med.*, 2021. 172: 298-311.
31. Marino S.M., Gladyshev V.N. Cysteine function governs its conservation and degeneration and restricts its utilization on protein surfaces. *J. Mol. Biol.*, 2010. 404(5): 902-916.
32. Putker M., Vos H.R., van Dorenmalen K., et al. Evolutionary acquisition of cysteines determines FOXO paralog-specific redox signaling. *Antioxid Redox Signal*, 2015. 22(1): 15-28.
33. Hornsveld M., Dansen T.B. The Hallmarks of Cancer from a Redox Perspective. *Antioxid Redox Signal*, 2016. 25(6): 300-325.
34. Cameron Jenifer M., Gabrielsen M., Chim Ya H., et al. Polarized Cell Motility Induces Hydrogen Peroxide to Inhibit Cofilin via Cysteine Oxidation. *Curr. Biol.*, 2015. 25(11): 1520-1525.
35. Niethammer P., Grabher C., Look A.T., et al. A tissue-scale gradient of hydrogen peroxide mediates rapid wound detection in zebrafish. *Nature*, 2009. 459(7249): 996-999.
36. Yang J., Carroll K.S., Liebler D.C. The Expanding Landscape of the Thiol Redox Proteome. *Mol. Cell. Proteomics*, 2016. 15(1): 1-11.
37. Zhang Q., Bykov V.J.N., Wiman K.G., et al. APR-246 reactivates mutant p53 by targeting cysteines 124 and 277. *Cell Death Dis.*, 2018. 9(5): 439.
38. Fuchs S.Y., Adler V., Buschmann T., et al. Mdm2 association with p53 targets its ubiquitination. *Oncogene*, 1998. 17(19): 2543-2547.
39. Dansen T.B., Smits L.M., van Triest M.H., et al. Redox-sensitive cysteines bridge p300/CBP-mediated acetylation and FoxO4 activity. *Nat. Chem. Biol.*, 2009. 5(9): 664-672.
40. Stocker S., Maurer M., Ruppert T., et al. A role for 2-Cys peroxiredoxins in facilitating cytosolic protein thiol oxidation. *Nat. Chem. Biol.*, 2018. 14(2): 148-155.

## Supplementary Figures



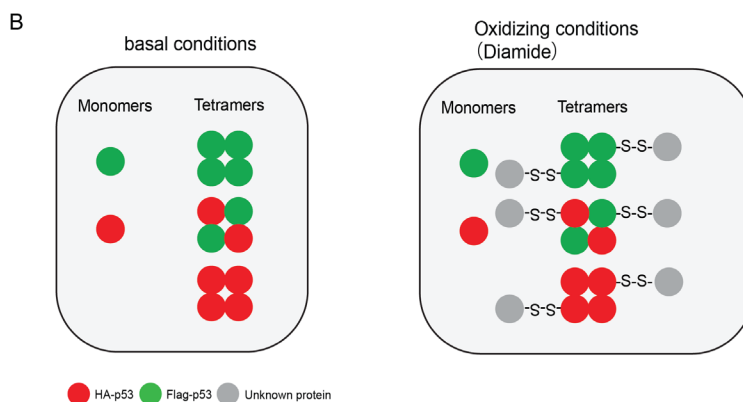
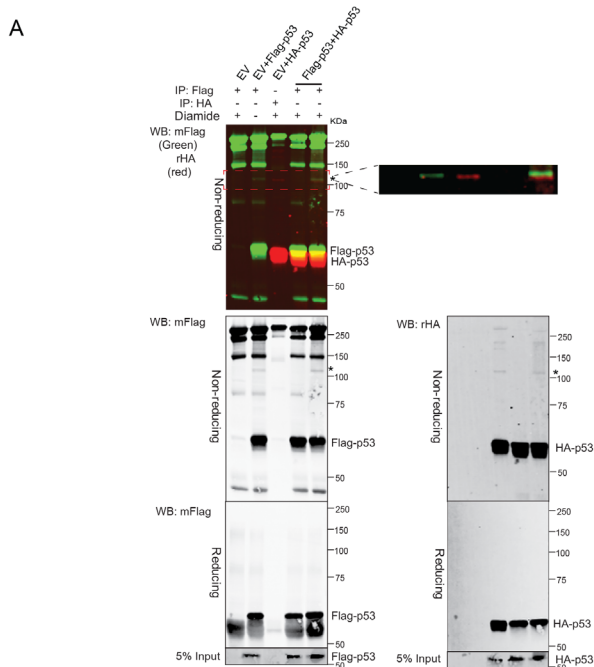
### Supplementary Figure 1. p53 forms reversible redox-dependent protein complexes upon diamide, not H<sub>2</sub>O<sub>2</sub>

(A) HEK293T cells transiently expressing Flag-p53 (WT) were treated with diamide for 15 min, followed by refreshing the medium. Protein samples were collected from the cells that were recovered with the indicated time (\*) after diamide removal. (B) No observation that p53 forms redox-dependent protein-protein interactions upon H<sub>2</sub>O<sub>2</sub> treatment in HEK293T cells. (C) No observation of p53 forming redox-dependent protein-protein interactions upon H<sub>2</sub>O<sub>2</sub> treatment in H1299 cells.



**Supplementary Figure 2. C277 is required for p53 disulfide-dependent protein interactions**

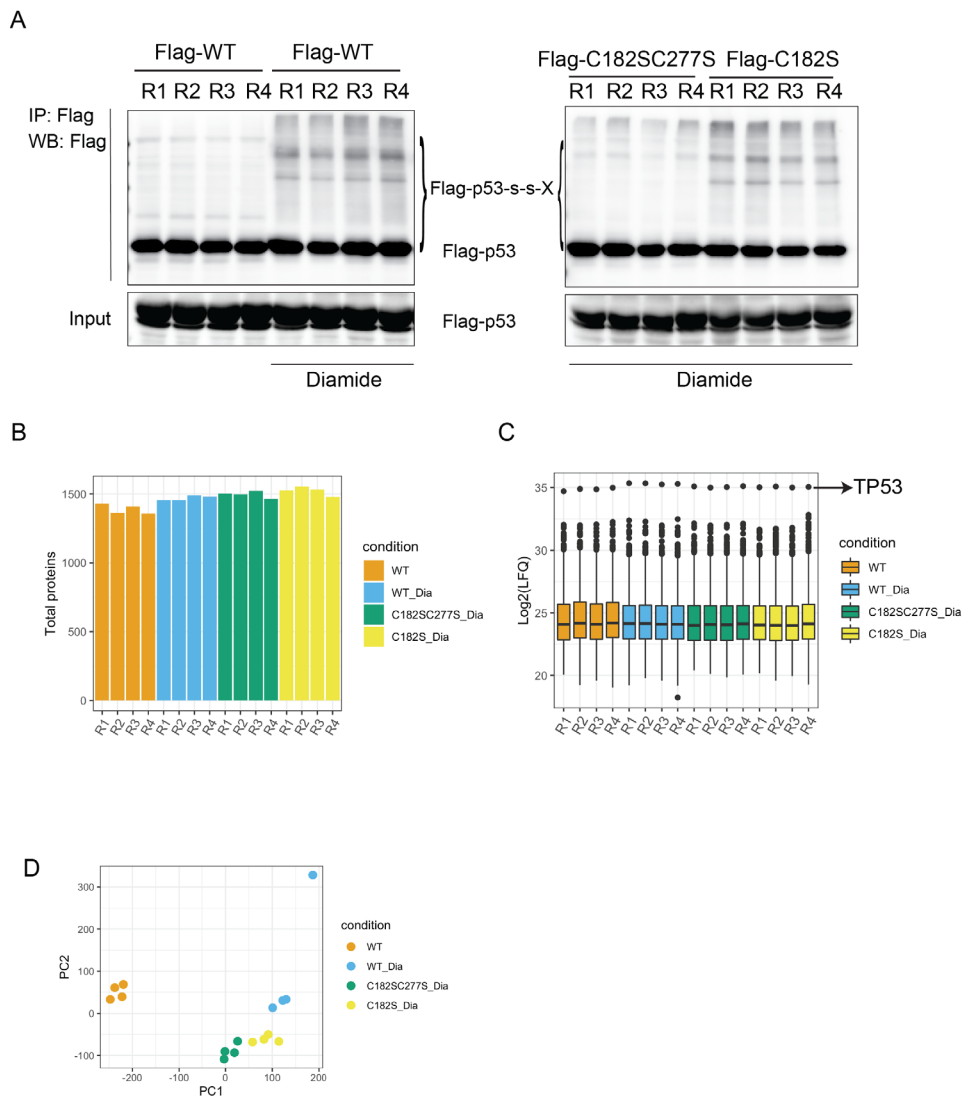
(A) Evaluation of disulfide-dependent protein complexes of p53 cysteine mutants (to Alanine) in H1299 cells. (B) Evaluation of disulfide-dependent protein complexes of p53 WT, C182S, C277S and C176S mutants in H293T cells.



**Supplementary Figure 3. p53 does not form disulfide-dependent homodimers upon diamide.**

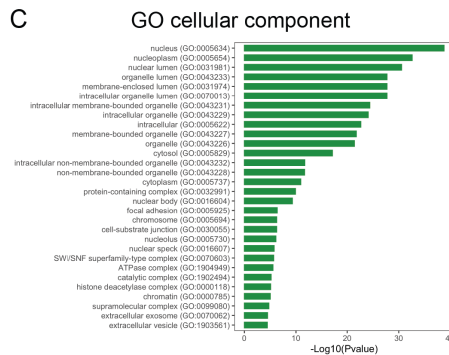
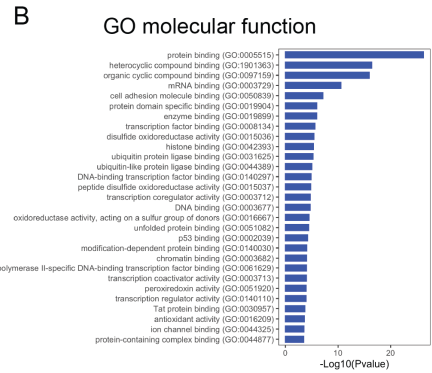
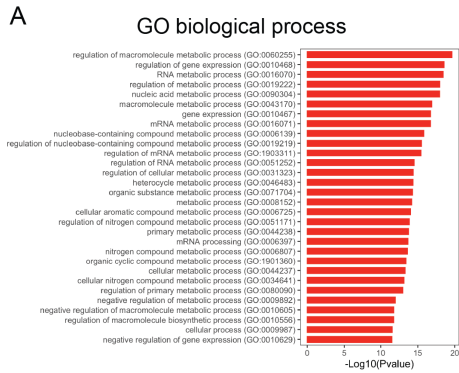
(A) Flag-p53 and HA-p53 were expressed in HEK293T cells either separately or co-expressed. Immunoprecipitation using anti-Flag or anti-HA was conducted after diamide treatment and Western blots were probed with different fluorescence-conjugated secondary antibodies against Flag (Green) or HA (Red). Flag-p53 (green) and HA-p53 (red) were both oxidized to form a complex (\*, around 100kDa) with another protein, but not as a homodimer or homo-oligomer as no overlapping signal of green and red was observed. p53 is known to function as a (non-disulfide dependent) tetramer, and Flag-p53 can indeed pull-down HA-p53. The high-molecular weight band containing HA-p53, which is independent of homodimerization of p53 as indicated in the model in (B). (B) HA-p53 and Flag-p53 form non-covalent tetramers of different composition (other combinations are possible). Diamide treatment induces the formation of disulfide-dependent complexes with an unknown protein. Although Flag-p53 binds HA-p53 non-covalently, HA-p53 can be found to migrate as a redox-sensitive complex in the Flag-directed IP.





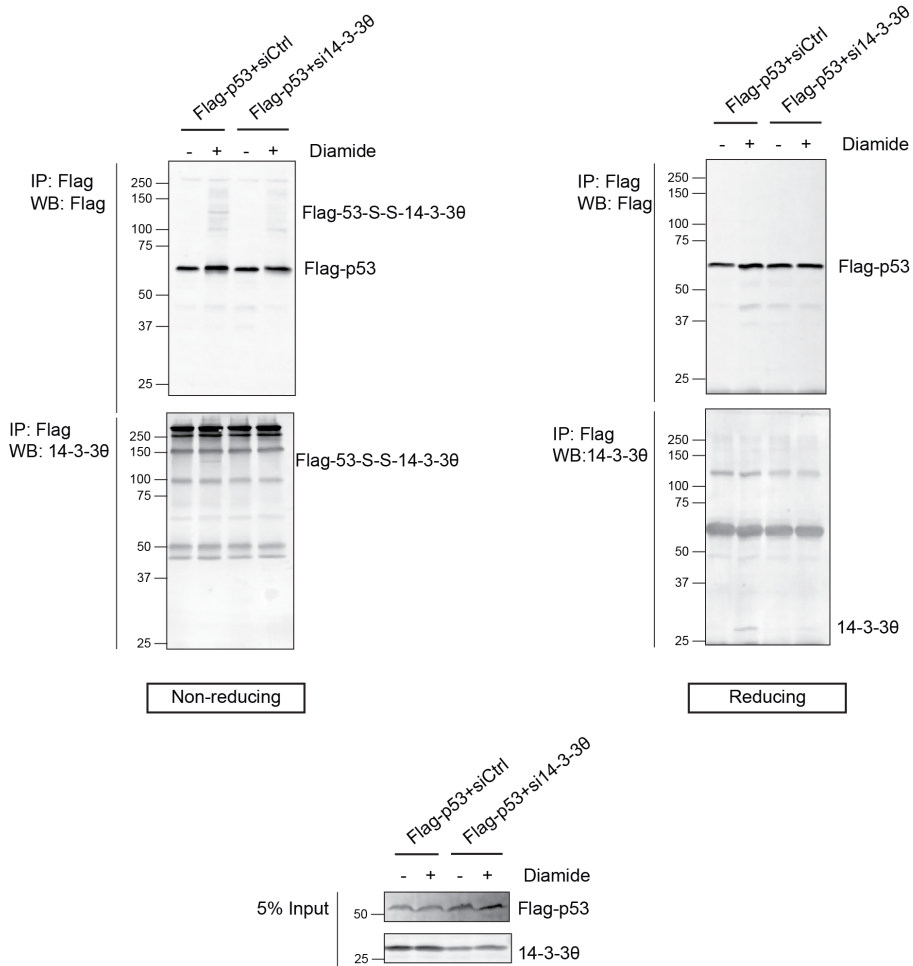
**Supplementary Figure 4. Reproducible results among 4 replicates in each condition**

(A) WB detection of p53 disulfide-dependent dimerization for the four replicates prepared for MS/MS analysis for each condition. (B) Bar graph showing the amounts of protein identified by MS in each replicate (R1, R2, R3, R4) and condition. (C) Box plot showing the distribution of Label-Free quantification (LFQ) intensity of proteins in each replicate and condition. Flag-p53 is displayed as the top outline with the highest and roughly equal LFQ value in all samples. (D) Principle component analysis (PCA) of LFQ value in all samples.



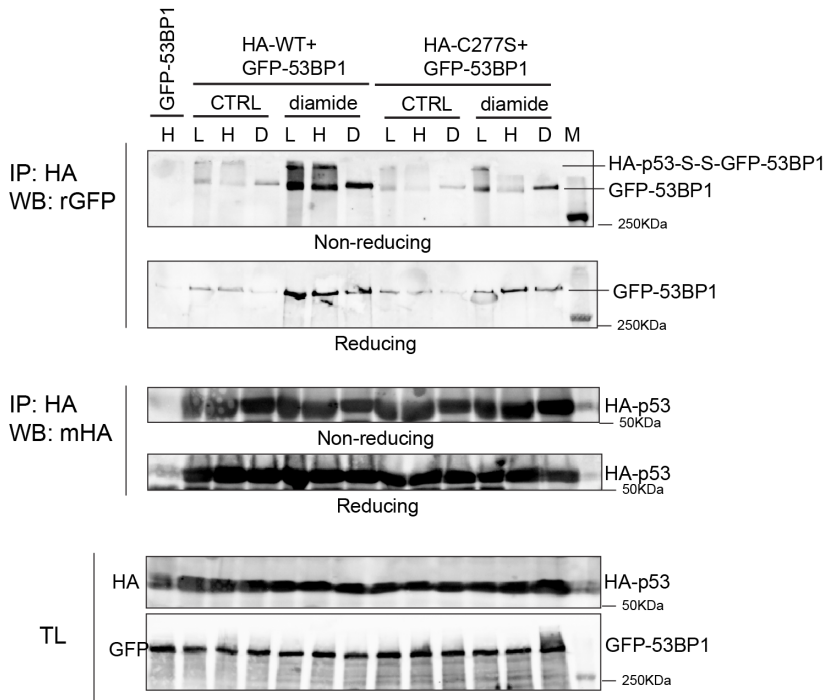
**Supplementary Figure 5. PANTHER Gene Ontology (GO) analysis of redox dependent-p53 binding partners.**

GO enrichment was performed in PANTHER Classification System online (<http://pantherdb.org/>) for 167 diamide-induced p53 interactors. Some of the top significant terms ( $p$ -value < 0.001) in biological process, molecular function and cellular component were presented in the bar plots. **(A)** GO analysis of biological process. **(B)** GO analysis of molecular function. **(C)** GO analysis of cellular component.



**Supplementary Figure 6. Validation of the disulfide-dependent interaction between p53 and 14-3-3θ**

HEK293T cells were transfected with Flag-p53 WT or along with siRNA for 14-3-3θ. After 48h of transfection, IP and WB against a Flag antibody were performed to examine the effects of si14-3-3θ on the p53-14-3-3θ interaction.



**Supplementary Figure 7. Further validation of the disulfide-dependent interaction between p53 and 53BP1**

HEK293T cells were transfected with HA-p53 WT or C277S alone or along with GFP-53BP1. 48 h after transfection and following 15-min diamide treatment, the p53-53BP1 complex was precipitated using HA-antibody coated beads. The beads were washed with a wash buffer containing low salt (L, 150 mM NaCl), high salt (H, 1 M NaCl) or high salt plus 10 mM DTT (D). The wash buffer was otherwise identical to the lysis buffer (see Methods section), minus the alkylating agent. The p53-53BP1 interaction was examined by WB using HA and GFP antibodies.

**Table S1 Primers for mutagenesis PCR**

Mutant	Primers (5'-3')
p53C124S	Forward: GGGACAGCCAAGTCTGTGACTAGCACGTA CTCCCCTGCCCTCA Reverse: TGAGGGCAGGGGAGTACGTGCTAGTCACAGACTTGGCTGTCCC
p53C124A	Forward: GGGACAGCCAAGTCTGTGACTGCCACGTA CTCCCCTGCCCTCA Reverse: TGAGGGCAGGGGAGTACGTGGCAGTCACAGACTTGGCTGTCCC
p53C135S	Forward: CCTGCCCTCAACAAGATGTTTAGCCA ACTGGCCAAGACCTGC Reverse: GCAGGTCTTGGCCAGTTGGCTAAACATCTTGTTGAGGGCAGG
p53C135A	Forward: CCTGCCCTCAACAAGATGTTTGCCCA ACTGGCCAAGACCTGC Reverse: GCAGGTCTTGGCCAGTTGGGCAAACATCTTGTTGAGGGCAGG
p53C141S	Forward: TGCCA ACTGGCCAAGACCAGCCCTGTGCAGCTGTGGGT Reverse: ACCCACAGCTGCACAGGGCTGGTCTTGGCCAGTTGGCA
p53C141A	Forward: TGCCA ACTGGCCAAGACCGCCCTGTGCAGCTGTGGGT Reverse: ACCCACAGCTGCACAGGGGCGGTCTTGGCCAGTTGGCA
p53C176S	Forward: ACGGAGGTTGTGAGGCGCAGCCCC ACCATGAGCGCTG Reverse: CAGCGCTCATGGTGGGGGCTGCGCCTCACAACCTCCGT
p53C182S	Forward: TGCCCC ACCATGAGCGCAGCTCAGATAGCGATGGTCT Reverse: AGACCATCGCTATCTGAGCTGCGCTCATGGTGGGGGCA
p53C229S	Forward: CCTGAGGTTGGCTCTGACAGTACCACCATCCA CTACA ACT Reverse: AGTTGTAGTGGATGGTGGTACTGT CAGAGCCAACCTCAGG
p53C229A	Forward: CCTGAGGTTGGCTCTGACGCTACCACCATCCA CTACA ACT Reverse: AGTTGTAGTGGATGGTGGTAGCGTCAGAGCCAACCTCAGG
p53C275S	Forward: ACAGCTTTGAGGTGCGTGTTAGTGCCTGTCCTGGGAGAGAC Reverse: GTCTCTCCAGGACAGGCACTAACACGCACCTCAAAGCTGT
p53C275A	Forward: ACAGCTTTGAGGTGCGTGTTGCTGCCTGTCCTGGGAGAGAC Reverse: GTCTCTCCAGGACAGGCAACACGCACCTCAAAGCTGT
p53C277S	Forward: GCCGGTCTCTCCAGGACTGGCACAAACACGCACCTCAA Reverse: GCCGGTCTCTCCAGGACTGGCACAAACACGCACCTCAA
p53C277A	Forward: TGAGGTGCGTGTTTGTGCCGCTCCTGGGAGAGACCGGCGCA Reverse: TGCGCCGGTCTCTCCAGGAGCGGCACAAACACGCACCTCA

**Table S2 Redox-dependent interactors of p53**

<b>Diamide-dependent binding partners</b>		
TLK2	YWHAB	TTC4
ARNT	ZFP36L2;ZFP36L1	SRSF3
C18orf25	SUPT4H1	PFDN2
PPP1R2;PPP1R2P3	BPTF	NUDC
UBXN7	SRSF5	SNW1
RANBP3	SAFB2	YARS
COPS2	CTTN	KHDRBS1
DCTPP1	ZXDC;ZXDA;ZXDB	TCOF1
TP53BP1	CIAPIN1	ARMC6
HDGFRP2	DUS1L	POGZ
PCYT1A	DNAJC9	USP48
YWHAE	PHAX	NUDCD2
SAFB	UBTF	HIRIP3
MDM2;MDM2 isoform KB9;mdm2	CD2BP2	MAP4
SLC4A1AP	HMGB1;HMGB1P1	EIF5A;EIF5A2;EIF5AL1
YWHAZ	MNAT1	MBD3
PSME3	FOXK2	RBM25
DFFA	RING1	IRF2BPL
YWHAQ	SRSF6	TPM3;DKFZp686J1372
RPRD1A	EP400	PPP5C
ZNF428	GINS3	KIF4A
TTC1	XPO5	NASP
CNN2	NELFA	UBXN1
ARID3B	PDCD11	MCMBP
PUS7	VBP1	CHD1
CTDP1	NME1;NME2;NME1-NME2;NME2P1	UBA1
NCL	EIF4B	CBX3
RAD18	ZPR1	RPS12
SRCAP	CHERP	DNAJA1
GLMN	GLRX3	TCEA1
SMAP;C11orf58	TXN	HCFC1
ELL	PRDX2	AIP
RBM17	YWHAG	TMPO
NCOR1	CNBP	STIP1
RCC2	CNN3	U2SURP
TRIM33	SERBP1	ZRANB2
FTO	SH3GL1	USP5
BCLAF1	POLR1E	RBM26
TUBA1A;TUBA3E	CACYBP	IRF2BP1
PPAN-P2RY11;PPAN	AASDHPTT	HDLBP
GSTP1	PHF8	NPM1
PSMD9	IMPDH2	FLNA
CPSF7	TRIM24	PRDX1
RNF126	PRDX6	DNAJC7
GRB2	TXLNA	HNRNPA3
NR2C2AP	FOXK1	TLN1
SMARCC1	ANP32E	RNH1
POGK	PNN	FHL1
CARHSP1	BOLA2	KHSRP
PTBP1	ACIN1	SRRM2
CSTF2	CHD8	HSPH1
CDKN2A	PDLIM1	ZC3H14
RNGTT	TXNL1	CCT2
TOX4	FLNB	
JUN		

C277-dependent binding partners		
TLK2 ARNT C18orf25 PPP1R2;PPP1R2P3 UBXN7 RANBP3 COPS2 DCTPP1 TP53BP1 HDGFRP2 PCYT1A YWHAE SAFB MDM2;MDM2 isoform KB9;mdm2 SLC4A1AP YWHAZ PSME3 DFFA YWHAQ		





# *Chapter 5*

## **Evaluation and optimization of two thiol-labeling approaches**

Tao Shi<sup>1</sup>, Loes van Dam<sup>1</sup>, Paulien E. Polderman<sup>1</sup>, Robert van Es<sup>1</sup>, Harmjan R. Vos<sup>1</sup>, Boudewijn M.T. Burgering<sup>1,2</sup> and Tobias B. Dansen<sup>1,3</sup>

<sup>1</sup>Center for Molecular Medicine, Molecular Cancer Research and <sup>2</sup>Oncode Institute, University Medical Center Utrecht, Universiteitsweg 100 3584 CG Utrecht, The Netherlands.

<sup>3</sup>Correspondence to: [t.b.dansen@umcutrecht.nl](mailto:t.b.dansen@umcutrecht.nl).

## Abstract

Reversible cysteinyl thiol oxidation is one of the major mechanisms of how redox signaling controls target proteins. Identification of site-specific cysteine oxidation greatly aids in the identification of proteins sensitive to cysteine oxidation and therefore in better understanding of the role of redox signaling in biological processes. Multiple thiol-reactive chemical reagents combined with Mass spectrometry have been developed and are widely being used to quantitatively measure thiol oxidation in various biological systems. However, each of these has advantages and disadvantages. In this study, we aim to optimize a protocol for the identification and quantification of oxidized cysteines using two different thiol-labeling methods: BIAM and IAAyne-DADPS, that have successfully been used by other labs before. Although we observed reasonable labeling with both these compounds, we encountered low yields for both identified proteins and modified sites by MS, suggesting that more optimization is required to obtain robust results.

## Introduction

Owing to its intrinsically nucleophilic property, the cysteine residue is often modified by reactive oxygen species (ROS) (be it directly or indirectly) [1] to form a wide range of post-translational modifications (PTMs). Reversible cysteine oxidation (i.e. leading to Sulphur oxidation states that can be reduced by the cellular reduction systems) such as sulfenic acid (-SOH) and disulfide (-S-S-), has been shown to modulate protein function through several mechanisms, including regulation of protein stability [2], kinase activity [3, 4], and subcellular localization [5, 6] in both physiological and pathological processes [7].

In recent years, researchers have been able to quantitatively monitor cysteine reactivity or identify the bulk or organ-specific cysteine oxidation profile in a proteome-wide and site-specific manner in both physiological and challenged conditions using advanced thiol-reactive chemical probes and Mass spectrometry (MS)-based techniques [8-10]. So-called Oxidative isotope-coded affinity tags (OxICAT) have been widely used to quantitatively measure cysteine oxidation by isotopic labeling of reduced and reversibly oxidized cysteines in a proteome-wide manner [11]. However, the high price of the reagents limits their application as a routine technique in most labs. Alternatively, a biotinylated iodoacetamide (BIAM)-based approach has been used for redox proteomics analysis, which also involves differential alkylation of reduced and oxidized thiols within the same sample (known as BIAM-switch assay) [12, 13]. However, the strong interaction between biotin and Streptavidin can prevent the efficient elution of biotinylated proteins from Streptavidin beads. Biotinylated proteins can be on-bead digested with trypsin during the MS sample preparation, but this would still leave the biotinylated, cysteine-containing peptide trapped on the streptavidin beads, making it difficult to quantify site-specific thiol oxidation [14, 15]. Another approach makes use of Iodoacetamide Alkyne (IAAyne): a small thiol-reactive warhead and a cleavable biotin linker that has been widely used to label thiols in native conditions [8]. One of the cleavable biotin linkers is dialkoxydiphenylsilane (DADPS) [16]. The DADPS biotin

linker contains five parts: (i) a reactive azide handle capable of reacting with the alkyne introduced in the protein by the reaction with the IAAyne through a Copper-catalyzed azide-alkyne cycloaddition (CuAAC), (ii) a spacer between the reactive handle and the cleavable moiety, (iii) the cleavable moiety that allows for selective isolation of the labeled products, (iv) a spacer between the cleavable site and biotin, (v) a biotin group for enrichment (**Fig. 5A**). This DADPS linker has a high reaction specificity with IAAyne-labeled products through the azide-alkyne reaction and can be rapidly (30min) cleaved by formic acid to leave a small mass adduct (143 Da) on targeted sites. These features make DADPS applicable in a wide range of biochemical labeling strategies, including identification of glycosylation sites [17], profiling of deubiquitinase family of proteins [18], mapping the sites of small-molecule interactions [19, 20] and identifying site-specific thiol oxidation profile [21].

Our laboratory has experience in the identification of redox-dependent protein-protein interactions using a protein of interest and cysteine mutants as bait [5, 22, 23]. Using this approach many cysteine-dependent interactors of for instance FOXO, PRDXs, p53 and p16INK4A have been identified, but the used method does not give information on which cysteine in the identified binding partner is involved in the interaction. To complement this approach with the identification and quantification of redox-sensitive cysteines, we set out to introduce both the BIAM-switch assay and the cleavable DADPS methods to our laboratory, unfortunately with limited success. This chapter describes the optimization steps that were tried and discusses potential improvements for future work.

## Materials and methods

### Reagents and antibodies

Diamide(D3648), Hydrogen peroxide solution 30% (7722-84-1), N-Ethylmaleimide (NEM)(E3876), Biotin(D-)(B450) were from Sigma. Biotin-PEG3-Maleimide (BIAM, CLK-CSTM) was from Jena Bioscience. DADPS Biotin azide (JBS-CLK-1330-5) was from Enzo life sciences. IA-Alkyne (7015) was from Bio-Techne. Streptavidin Sepharose™ High Performance beads (17-5113-01) were from GE Healthcare.

Anti-p53 (Do-1) antibody was from Santa Cruz Technology. Anti-GAPDH (MAB374) antibody was from EMD Millipore. Anti- $\beta$ -catenin (BD610154) was from BD Biosciences.

### Cell culture

HEK293T cells were cultured in DMEM high-glucose (4,5 g/L) medium supplemented with 10% FBS, 2 mM L-glutamine, and 100 Units Penicillin-Streptomycin (All from Sigma Aldrich), at 37 °C and within the condition containing 6% CO<sub>2</sub>.

### BIAM-switch assay labeling of reversibly oxidized cysteines

The BIAM-switch assay contains three main steps: (i) Blocking: Free thiols are blocked by the alkylating agent N-ethylmaleimide (NEM); (ii) Reducing: Oxidized cysteines (e.g., -S-S-) are reduced by reducing agent DTT; (iii) Labeling: The new available free thiols (which were

reversibly oxidized prior to reduction) are labeled with Biotin-PEG3-iodoacetamide (BIAM) (Fig. 1).

HEK293T cells were treated with diamide or H<sub>2</sub>O<sub>2</sub>, followed by treatment with NEM to block free thiols and thereby fix the redox state. Cells were lysed in 20% Trichloroacetic acid (TCA) and centrifuged at 10,000 xg, 4 °C for 30 min, followed by washing with 10 % and 5% TCA. The pellets were then resuspended in 200 µl of NEM-buffer (50 mM NEM, 50 mM Tris-HCl, pH 8.5, 8 M urea, 5 mM EDTA, 1% SDS) on a shaker at 1000 rpm and 37 °C for 1h in the dark. The reaction was stopped by adding 1ml ice-cold Acetone. The excess NEM was removed by washing the sample with 1ml of ice-cold Acetone and centrifugation (at 10,000 g, 4 °C). The pellets were then incubated with 200 µl of reduction buffer (50 mM Tris-HCl, pH 8.5, 8 M urea, 5 mM EDTA, 1% SDS, 4 mM DTT) was added after the pellet was dissolved on a shaker at 850 rpm for 10 min. Before DTT was added, the protein concentration was measured using the Pierce™ BCA Protein Assay Kit. After reduction by DTT, 400 µg of protein was taken and washed with cold Acetone to remove the excess DTT, followed by labeling with 200 µl of BIAM buffer (0.2 or 2 mg/ml BIAM, 50 mM Tris-HCl, pH 8.5, 8 M urea, 5 mM EDTA, 1% SDS) on a shaker at 850 rpm, 37 °C for 1 h in the dark. Excess BIAM was removed by adding 1 ml ice-cold Acetone and washing the pellets three times.

#### **BIAM labeling of fully reduced cell lysates**

HEK293T cells were lysed by the TCA method as described in 2.3. The cell pellet was directly resuspended in 200 µl of DTT buffer (4 mM DTT, 50 mM Tris-HCl, pH 8.5, 8 M urea, 5 mM EDTA, 1% SDS), followed by labeling with BIAM at different concentrations (0.01, 0.1, 1, 5 and 10 mg/ml). The biotinylated proteins were enriched, eluted, and evaluated as described above (2.3). Additionally, BIAM labeling for specific proteins (e.g p53 and GAPDH) was examined.

#### **IAAyne labeling of reduced recombinant EGFP-β-Catenin**

10 µg of recombinant EGFP-β-Catenin (home-made) was taken and dissolved in 200 µl of DTT buffer (50 mM Tris-HCl, pH 8.5, 8 M urea, 5 mM EDTA and 2% SDS, 10 mM DTT) to reduce oxidized thiols. After incubation in DTT buffer for 30 min, the sample was precipitated with 400 µl of prechilled methanol and 100 µl of chloroform, followed by washing with 200 µl of methanol and 200 µl of chloroform three times to clear out the DTT. The protein pellet was then resuspended in 200 µl resolving buffer (50 mM Tris-HCl, pH 8.5, 8 M urea, 5 mM EDTA and 2% SDS), and incubated with IAAyne at a final concentration of 200 µM or 1 mM at 37 °C in the dark for 1h while rotating.

#### **IAAyne labeling of reduced cellular proteins**

HEK293T cells in 10 cm-dishes were lysed in 1ml ice-cold Trichloroacetic acid (TCA) as described in 2.3. The protein samples were resuspended in 400 µl of DTT buffer (10 mM DTT, 50 mM Tris-HCl, pH 8.5, 8 M urea, 5 mM EDTA and 2% SDS) to fully reduce oxidized cysteines. 1mg of protein was taken for IAAyne labeling. Before labeling, protein samples

were precipitated with methanol-chloroform as described above to remove excess DTT. IAAyne labeling was performed in 200  $\mu$ l of resolving buffer (50 mM Tris-HCl, pH 8.5, 8 M urea, 5 mM EDTA, and 2% SDS) containing IAAyne with a final concentration of 20, 50, 100, 200 or 500  $\mu$ M at 37 °C in the dark for 1h while rotating.

### **CuAAC reaction**

The IAAyne-labeled EGFP- $\beta$ -Catenin sample was precipitated again by the methanol-chloroform method as described above to remove excess IAAyne. The protein pellet was then resuspended in 50  $\mu$ l of 1% SDS-PBS buffer, and incubated with 50  $\mu$ l of a master mix of CuAAC reagents: Tris[(1-benzyl-1H-1,2,3,-triazol-4-yl)methyl] amine (TBTA) to a final concentration of 1 mM, CuSO<sub>4</sub> to a final concentration of 2 mM, Sodium ascorbate to a final concentration of 2 mM, and DADPS biotin azide to a final concentration of 200  $\mu$ M or 1 mM, at 37 °C in the dark for 1h. After that, 20  $\mu$ l of the sample was taken for evaluation by Western blotting and the reaction was stopped by adding 5x SDS-PAGE Laemmli sample buffer and boiling for 5 min at 95 °C. The rest of the sample was prepared for Mass spectrometry (MS).

The IAAyne-labeled whole lysate protein sample was also precipitated by the methanol-chloroform method as described above to remove excess IAAyne. The protein pellets were resolved in 168  $\mu$ l of 1% SDS-PBS buffer, and incubated with 32  $\mu$ l of a master mix of CuAAC reagents: tris[(1-benzyl-1H-1,2,3,-triazol-4-yl)methyl] amine (TBTA) to a final concentration of 500  $\mu$ M, CuSO<sub>4</sub> to a final concentration of 2 mM, Sodium ascorbate to a final concentration of 2 mM, and DADPS biotin azide to a final concentration of 500  $\mu$ M, at 37 °C in the dark for 1h. 20  $\mu$ l of the incubation was taken for detection by Western blotting and the reaction was stopped by adding 5x sample buffer and boiling for 5 min at 95 °C. The rest of the sample was prepared for MS examination.

### **Streptavidin enrichment of biotinylated proteins**

After BIAM labeling, the pellet was resuspended with 200  $\mu$ l of resolving buffer (50 mM Tris-HCl pH 8.5, 5 mM EDTA, 1% SDS, 10% Triton). The solution was diluted 10 times in PBS (0.1% SDS in final) and incubated with a certain amount of Streptavidin agarose beads (as indicated) at 4 °C for 30 min or overnight. Biotinylated proteins were eluted with 1x SDS-PAGE Laemmli sample buffer (or elution buffer) (2% SDS, 10 % glycerol, 6.25% Tris/HCl pH 6.8, 5% 2-mercaptoethanol, 0.002% bromophenol blue) or supplemented with 8 M urea or excess biotin (25 mM), and heating at 95 °C for 10 min. The sample was then analyzed by SDS-PAGE and Western blotting using an HRP-Streptavidin antibody.

After the CuAAC reaction, whole lysate protein samples were resuspended in 500  $\mu$ l of 1% SDS-PBS solution and transferred to a 15 ml tube. The solution was diluted by adding 4.5 ml PBS to get a final concentration of 0.1% SDS and incubated with 200  $\mu$ l of streptavidin beads overnight at 4 °C. After the incubation, the beads were washed with 1ml of 1 % SDS-PBS and PBS for 3 times respectively and were dried by aspirating the supernatant using an

insulin needle.

### **Trypsin digestion and formic acid cleavage for IAAyne-DADPS modified samples**

The IAAyne-DADPS labeled EGFP- $\beta$ -Catenin and cellular proteins on Streptavidin beads were incubated with 100  $\mu$ l of reduction and alkylation buffer: 1 M ammonium bicarbonate (ABC), 8 M urea, 10 mM TCEP, and 40 mM chloroacetamide (CAA), for 30 min at room temperature while rotating. After that, the solution was diluted by adding 300  $\mu$ l of ABC to get a final concentration of 2 M urea and the protein was digested by incubating with 5-10  $\mu$ g of the mix of Lyc-C/Trypsin at 37 °C overnight on an Eppendorf thermomixer. The next day the EGFP- $\beta$ -Catenin samples were directly incubated with a final concentration of 10% formic acid for 30 min at room temperature while rotating. The on-bead digested samples were first centrifuged at 10,000 xg for 5 min to remove the supernatant and the beads pellet was resuspended and incubated in 200  $\mu$ l of 10% formic acid at room temperature for 30 min, followed by centrifuging at 2000g for 5 min. The on-bead cleavage was repeated three times and the supernatant was combined as the final cleaved peptides.

### **Desalting**

Cleaved peptides were loaded onto 2 layers of C18 stagetips and washed twice with 0.1% formic acid (diluted in water). Peptides on C18 stagetips are stable and can be stored at 4 °C for up to a month. The peptides on C18 stagetips were eluted in 50  $\mu$ L of elution buffer (30% acetonitrile, 0.1% formic acid) and concentrated by speed-vacuum centrifugation. The concentrated peptides were then resuspended in 15  $\mu$ l of 0.1% formic acid and 10  $\mu$ l of the solution was loaded to a Mass spectrometry machine. The rest of the sample can be stored at -20 °C for backup.

### **Mass spectrometry**

Mass spectrometry was performed as described in chapter 4.

### **Mass spectrometry data analysis**

The raw Mass spectrometry data from the IAAyne-DADPS labeled EGFP- $\beta$ -Catenin samples were processed using Maxquant software (version 1.5.2.8) with Carbamidomethylation (+57.01Da) and DADPS (+238.29Da) on cysteines as the desired modifications. Data analysis regarding the identified EGFP- $\beta$ -catenin protein was further performed by R (version 3.6.1).

## **Results and discussion**

### **BIAM labels fully reduced proteins in whole cell lysate.**

To evaluate the labeling potential of the BIAM reagent, the TCA whole lysate was first reduced under denaturing conditions to enable labeling of oxidized and buried cysteines (**Fig. 2A**). The labeling of 200  $\mu$ g of whole cell lysate protein was saturated when 1 mg/ml of BIAM was used (**Fig. 2B**), suggesting that this concentration of BIAM would be more than sufficient

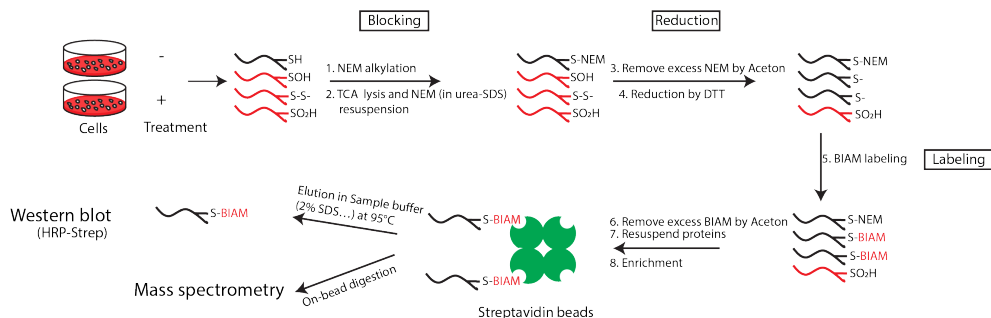


**Figure 1. A systematic scheme for labeling reversibly oxidized thiols by the BIAM-switch approach**

The BIAM-switch assay consists of three main steps: (i) Blocking of free thiols by N-ethylmaleimide (NEM). (ii) Reduction of oxidized thiols by DTT. (iii) Labeling of the newly available reduced thiols by BIAM. After BIAM labeling, the biotinylated proteins are enriched by pull-down with Streptavidin beads, followed by elution from the beads for Western blot detection or on-bead digestion for mass spectrometry identification.

to label a similar amount of lysate that was not fully denatured and reduced prior to labeling. Although total protein showed strong BIAM labeling, enrichment with Streptavidin beads only gave a low yield of biotinylated proteins (**Fig. 2B**). Because increasing amounts beads led to the progressive loss of BIAM signal we conclude that the low yield is likely caused by inefficient elution from the Streptavidin beads (**Fig. 2C**). The interaction between biotin and streptavidin is very strong [24], and we noted that especially big proteins which, in general contain more cysteine residues that can be targeted by BIAM, were lost upon increasing amounts of BIAM. When looking at specific proteins, for example p53, we noted a clear molecular weight shifting upon 1 mg/ml of BIAM labeling as compared to the unlabeled and 0.1 mg/ml BIAM labeled samples (**Fig. 2C**), suggesting that the p53 protein was effectively labeled by BIAM, which adds a molecular mass of (597.72Da) for each incorporated label to the p53 protein. However, p53 that was biotinylated using 1 mg/ml BIAM was barely eluted from Streptavidin beads regardless of how many beads were used (**Fig. 2C**), suggesting that multiple cysteines in reduced p53 protein might be labeled upon a higher concentration of BIAM (1 mg/m) and this resulted in high resistance to break the biotin-streptavidin bonds. Another example is GAPDH which was no longer recognized by a monoclonal antibody that only stains reduced GAPDH upon BIAM labeling, suggesting that most of GAPDH protein was modified by a low concentration of BIAM and a polyclonal antibody is required to recognize different versions of GAPDH (**Fig. 2C**). Collectively, these results indicate that increasing amounts of BIAM can more efficiently label proteins, but this also hampers the elution of these biotinylated proteins from Streptavidin beads, especially when multiple cysteine sites are targeted in one protein. These limitations interfere with the identification of

biotinylated proteins with a high yield and prohibit comprehensive site-specific thiol oxidation profiling.

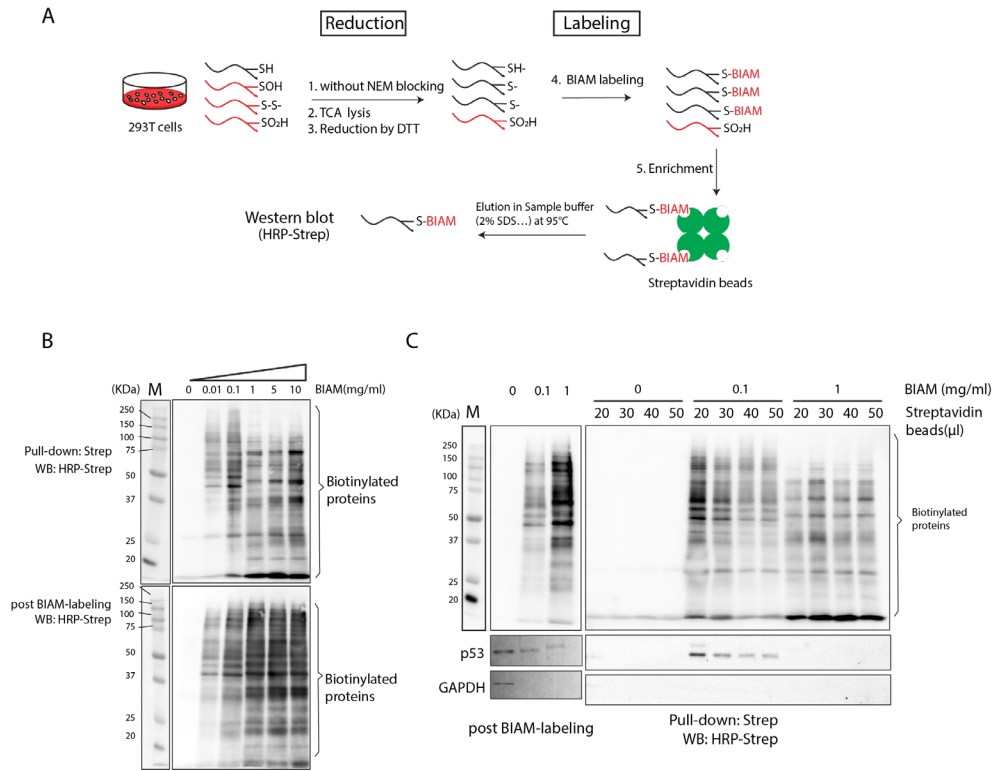


**Figure 2. Insufficient elution of BIAM-labeled proteins from Streptavidin beads**

(A) Scheme for BIAM labeling of fully-reduced whole cell lysate. 293T Cells were lysed in TCA and the pellets were resuspended in DTT buffer without pre-blocking by NEM. The samples were then labeled by BIAM, followed by enrichment, elution, and detection by Western blot. (B) 200 μg of reduced whole cell lysate was labeled with different amounts of BIAM (0.01, 0.1, 1, 5, and 10 mg/ml). Total lysate post BIAM labeling and Streptavidin pull-down samples were examined by WB using an HRP-conjugated streptavidin. (C) BIAM-labeling of p53 and GAPDH was evaluated upon treatment with the different amounts of BIAM compound and Streptavidin beads. Note that although total BIAM labeling increases when more BIAM is used, enrichment is progressively less efficient.

### BIAM labels the reversibly oxidized thiols upon H<sub>2</sub>O<sub>2</sub> and diamide

We suspected that one of the reasons for the insufficient elution could be the high stoichiometry of BIAM labeling to free thiols in the denaturing and fully reduced environment, whereas only oxidized thiols (after reduction) are available for BIAM labeling when samples are first alkylated by for instance NEM (Fig. 1). We therefore opted to monitor thiol oxidation in untreated, H<sub>2</sub>O<sub>2</sub> and diamide treated conditions and we found that indeed more proteins



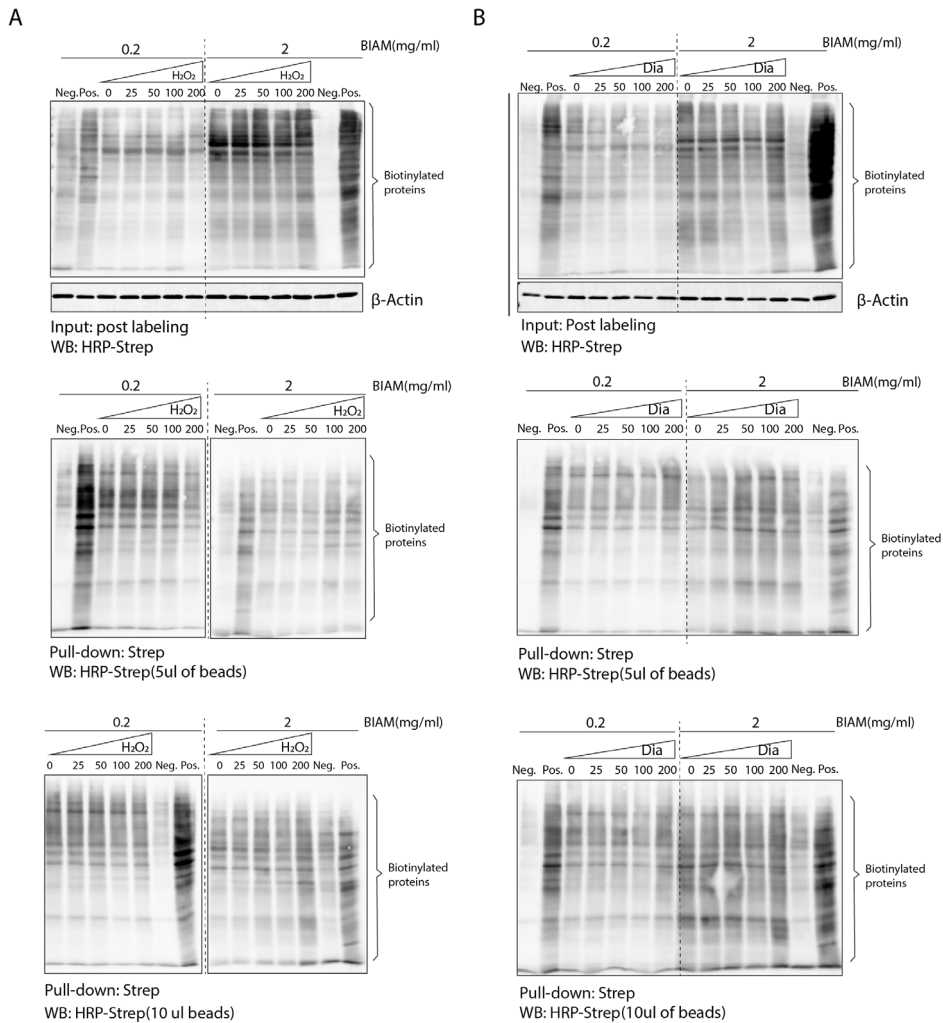


**Figure 3. The BIAM-switch assay labels reversibly oxidized thiols upon H<sub>2</sub>O<sub>2</sub> or diamide treatment**

(A) 400 µg of protein was respectively fully reduced (as a positive control), fully alkylated (as a negative control), left untreated or H<sub>2</sub>O<sub>2</sub> treated and subjected to the BIAM switch assay. Different amounts of BIAM (0.2 mg/ml and 2 mg/ml) were used for comparing labeling efficiency (top) and Streptavidin beads (5 µl and 10 µl) were taken for comparing elution efficiency (middle and bottom). (B) Same as in A, except that diamide rather than H<sub>2</sub>O<sub>2</sub> was used to induce cysteine oxidation.

were labeled in the fully reduced samples (Pos.) than those in the fully alkylated (Neg.), untreated or oxidized samples when either 0.2 or 2 mg/ml of BIAM was used (Fig. 3A, B). Additionally, 2 mg/ml of BIAM provided a higher labeling efficiency than 0.2 mg/ml BIAM for 400 µg of protein in both H<sub>2</sub>O<sub>2</sub> and diamide experiments (Fig. 3A, B). But also in these NEM-pretreated samples, biotinylated proteins in the 2 mg/ml BIAM groups were still not efficiently

eluted from Streptavidin beads particularly in the H<sub>2</sub>O<sub>2</sub> experiment (**Fig. 3A**). We observed a slight increase of BIAM modified proteins in samples with a higher concentration of H<sub>2</sub>O<sub>2</sub> and diamide compared to untreated samples, which suggests that only a small set of proteins is sensitive to H<sub>2</sub>O<sub>2</sub> or diamide and that the change in their oxidation states is not easily visible through Western blotting against the background of the total lysate, that also contains many structural disulfides that will be labeled by the procedure. Mass spectrometry could potentially aid in further evaluating H<sub>2</sub>O<sub>2</sub> and diamide-induced specific thiol oxidation.

To test whether the elution efficiency of biotinylated proteins from Streptavidin beads could be improved, we added excess biotin (25 mM) or 8 M urea on top of the original

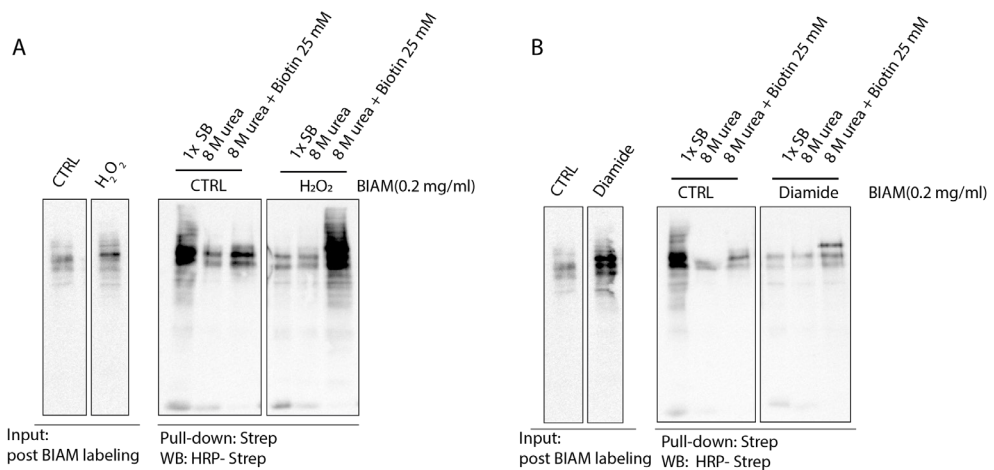


**Figure 4. Biotin addition increases the elution efficiency of biotinylated proteins from Streptavidin beads**

400 µg of protein from untreated (CTRL) and H<sub>2</sub>O<sub>2</sub> (**A**) or diamide (**B**) treated cells were labeled with 0.2 mg/ml BIAM (left). 1x SB, supplemented with either 8 M urea, or 8 M urea plus 25 mM Biotin buffers were used to elute biotinylated proteins from Streptavidin beads (right).

elution method (1x SDS-PAGE Laemmli sample buffer and heating at 95 °C). In principle, excess biotin will compete with biotinylated proteins to bind Streptavidin, resulting in the release of biotinylated proteins from the Streptavidin beads [15]. A high concentration of urea would facilitate protein denaturing including the Streptavidin protein, therefore weakening the interaction between biotin and Streptavidin. We found that the combination of urea and free biotin (25 mM) clearly increased the elution efficiency in both H<sub>2</sub>O<sub>2</sub> and diamide treated samples whereas the addition of urea (8 M) alone did not (**Fig. 4A, B**). Indeed, on-bead digestion of biotinylated proteins has been shown to yield less identified proteins as compared to when a cleavable biotin linker-based elution is used for Mass spectrometry sample preparation [25]. Importantly, since it is (most likely) the peptide containing the BIAM-

labeled cysteine that remains bound to the Streptavidin beads, information regarding the identity of the oxidized cysteine remains uncertain using a non-cleavable linker. Alternatively, even more harsh denaturing protocols (e.g. combining the high concentration of urea and SDS) could be tried, with the risk of generating potential drawbacks because the denaturing agent might not be compatible with the next steps in the MS sample preparation (e.g., SDS or material derived from the beads).

### **Cleavable DADPS linker labels purified EGFP- $\beta$ -Catenin**

Considering the drawbacks of the BIAM method, we opted to try another thiol-labeling probe: the iodoacetamide alkyne derivative (IAAyne), followed by conjugation with the cleavable biotin linker dialkoxydiphenylsilane (DADPS) (**Fig. 5A**). One big advantage of this biotin linker is that biotinylated proteins or peptides can be cleaved off from the Streptavidin beads by the addition of formic acid, bypassing the elution problems encountered using the BIAM approach (**Fig. 5A**). First of all, to test the efficiency of the IAAyne-DADPS labeling method, we took 10  $\mu\text{g}$  of purified recombinant EGFP- $\beta$ -Catenin protein as an example, which contains 13 cysteines (**Fig. S1**). As showed in **Fig. 5B**, the EGFP- $\beta$ -Catenin protein was firstly reduced using DTT under denaturing conditions (8 M urea) in order to maximize the amount of thiols available for labeling. After IAAyne labeling and the CuAAC reaction, samples were divided in two parts: one was used for SDS-PAGE and Western blot analysis and the rest was processed for Mass spectrometry (MS). Amounts of IAAyne, DADPS, and formic acid were titrated to optimize IAAyne labeling efficiency, CuAAC reaction specificity, and formic acid cleavage efficiency (**Fig. 5C**). The DADPS modification of EGFP- $\beta$ -Catenin was only observed when both IAAyne and DADPS reagents were present (**Fig. 5D**), suggesting that IAAyne successfully reached EGFP- $\beta$ -Catenin protein and that the CuAAC reaction between IAAyne and DADPS was indeed highly specific. However, biotinylation of EGFP- $\beta$ -Catenin was not further enhanced when a higher concentration (1000  $\mu\text{M}$ ) of IAAyne was used, suggesting that 200  $\mu\text{M}$  of IAAyne results in saturated labeling of 10  $\mu\text{g}$  of protein (**Fig. 5D**). EGFP- $\beta$ -Catenin showed various molecular weight shifts comparing unlabeled and biotinylated versions by gel electrophoresis, which is likely the consequence of one or more multiple IAAyne-DADPS conjugate adducts. The different biotinylated bands may represent variation in number or position of the cysteines that are targeted by IAAyne-DADPS. The molecular weight shift of biotinylated EGFP- $\beta$ -Catenin on SDS-PAGE may not be the exact addition of the IAAyne-DADPS mass because of for instance steric hindrance or changes in SDS binding.

After the CuAAC reaction, the samples used for MS analysis were reduced by TCEP and alkylated with Chloroacetamide which introduces a modification called Carbamidomethylation (CAM, +57Da) on reduced cysteines (**Fig. 5B** and **Fig. S2C**). Cleavage of biotinylated peptides through 10% formic acid results in an adduct with 238.29Da of mass weight on targeted cysteines (indicated as DADPS modification in this study) (**Fig. 5A** and **Fig. S2B**). The protein sequence of EGFP- $\beta$ -Catenin (**Fig. S1**) was used to searched peptides

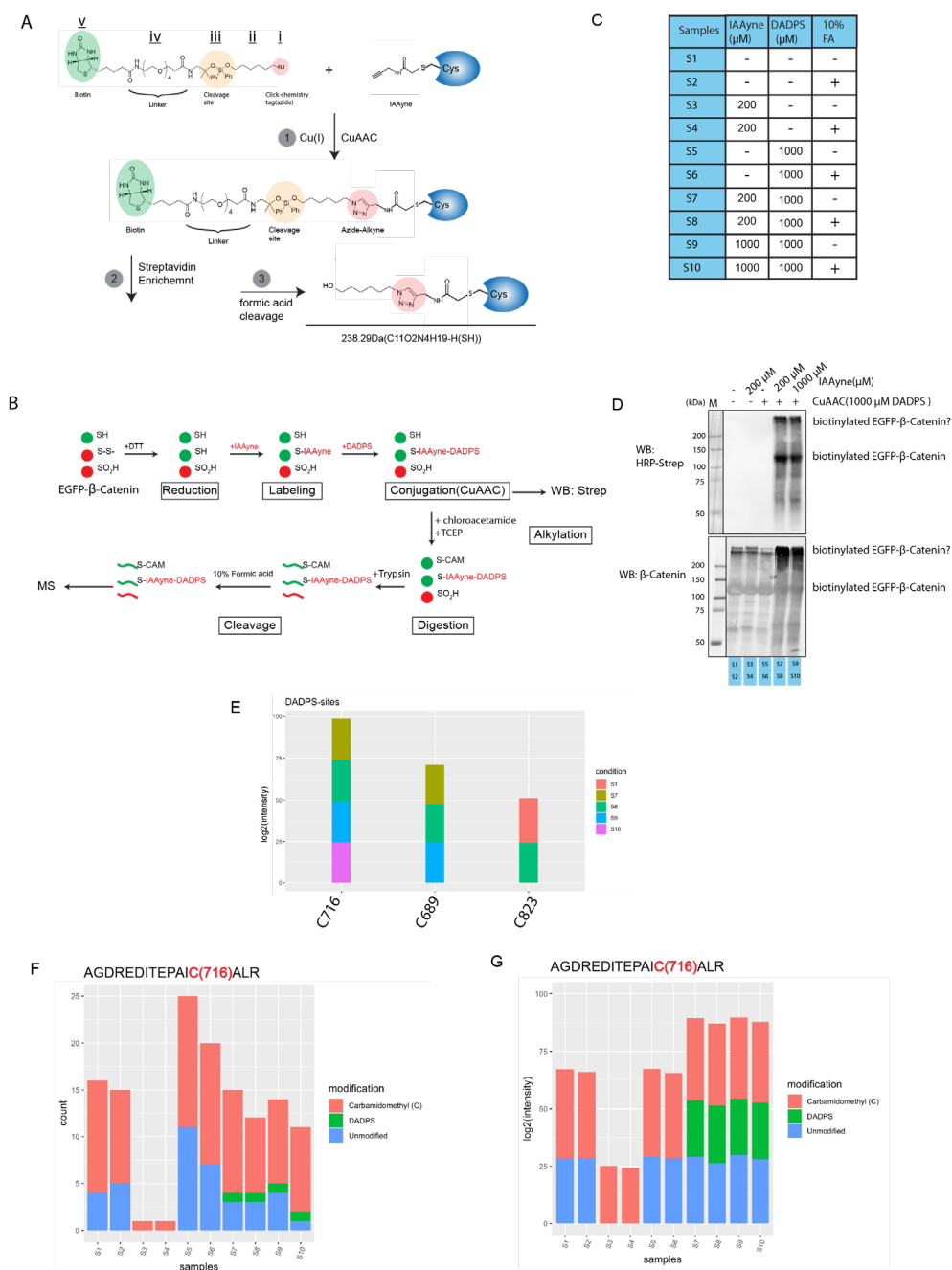


**Figure 5. IAAlkyne-DADPS labels purified EGFP-β-Catenin protein**

(A) The molecular formula of the DADPS linker: (i) the reactive handle (-azide) capable of reacting with an alkyne upon catalysis by Cuprous (CuAAC), (ii) a spacer between the reactive handle and the cleavable moiety, (iii) the moiety that can be cleaved by formic acid, (iv) a spacer between the cleavable site and biotin, (v) the biotin group required for Streptavidin-based enrichment. After final cleavage, the

whole IAAyne-DADPS conjugate leaves a small mass adduct (238.29 Da) on the cysteine of targeted proteins. **(B)** Scheme for labeling the reduced EGFP- $\beta$ -Catenin protein by the IAAyne-DADPS method. **(C)** Overview of processed samples. **(D)** 10  $\mu$ g of purified EGFP- $\beta$ -Catenin was taken for IAAyne-DADPS labeling. Samples subjected to the CuAAC reaction were detected by Western blotting using an HRP-Streptavidin or an anti- $\beta$ -Catenin antibody. Sample S1 and S2, S3 and S4, S5 and S6, S7 and S8, S9 and S10 were respectively from same CuAAC reaction sample, but incubated with or without 10% formic acid afterwards. **(E)** DADPS sites identified on EGFP- $\beta$ -Catenin. **(F)** Comparison of the counts of Carbamidomethylation (CAM), DADPS, and unmodified peptide for the C716 site. **(G)** Comparison of the intensity (log<sub>2</sub> transformed) of Carbamidomethylation (CAM), DADPS, and unmodified peptides for the C716 site.

identified from Mass spectrometry raw files by MaxQuant. About 150 total EGFP- $\beta$ -Catenin peptides were identified in all samples except in S3 and S4, which could be due to some technical issues (**Fig. S3A**). Multiple cysteine-containing peptides were also identified with both reasonable count and intensity (**Fig. S3B, C**). However, only one reasonable DADPS modified site (C716) was identified in samples S7, S8, S9, and S10 (**Fig. 5E**). The observation that the DADPS modification is detected in sample S7 and S9 indicates that the DADPS linker might also be cleaved in the absence of 10% formic acid or by a lower concentration of formic acid (0.1%) which is a routinely used in MS sample preparation. This can be further tested by taking a negative control that is not incubated with formic acid or another acidic solvent. When comparing the extent of DADPS and CAM modification on the C716 site, we found that only a small fraction of C716 site-containing peptides were labeled by DADPS, and most were labeled by CAM (**Fig. 5F, G**), suggesting the first step of the IAAyne labeling might not be efficient, leaving free thiols available for CAM labeling. Nevertheless, a higher amount of IAAyne (1000  $\mu$ M) did not increase the DADPS labeling, suggesting that the low DADPS labeling could be due to substantial oxidation of C716 prior to IAAyne treatment. Additionally, more extensive washing procedures (e.g. increased number or prolonged washes with Methanol-Chloroform), or for instance using Size Exclusion Spin Columns for cleanup) could be tried to remove excess reagents like DTT or IAAyne in order to prevent unwanted side-reactions.

### IAAyne-DADPS labels cell lysate

We showed above that the IAAyne-DADPS method could in principle successfully label cysteines in purified protein although with relatively low efficiency. Next, we tested whether IAAyne-DADPS can also label protein in a whole cell lysate. 1000  $\mu$ g of proteins from a cleared cell lysate were denatured and reduced with DTT and then labeled with IAAyne in different concentrations (**Fig. 6A, B**). Western blot analysis showed that 20  $\mu$ M of IAAyne was enough to label a wide range of proteins and the labeling was slightly increased when more IAAyne was used (**Fig. 6B**). Similar to the BIAM labeling, DADPS labeled GAPDH was also not recognized by the monoclonal antibody, which suggests that the endogenous GAPDH was efficiently labeled on the same cysteine (**Fig. 6B**). However, it was difficult to conclude whether p53 is labeled or not from the blot since no clear difference in molecular

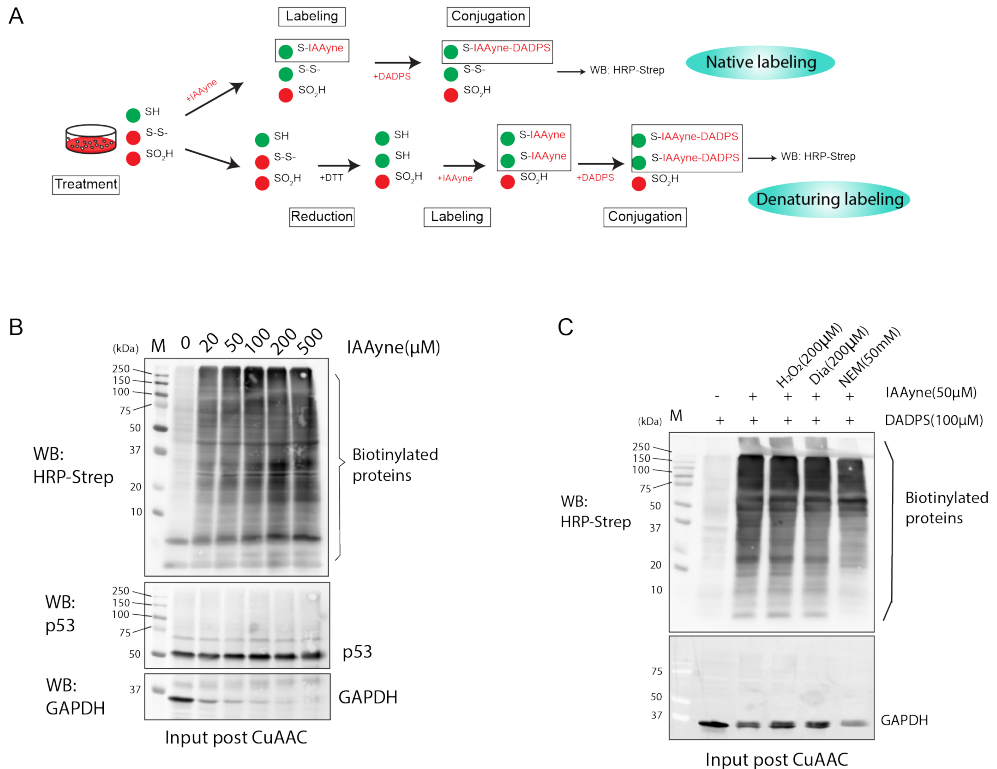


**Figure 6. IAAyne-DADPS labels cell lysate**

**(A)** Scheme for IAAyne-DADPS labeling of cellular protein in a native or denaturing environment. **(B)** 1000  $\mu\text{g}$  of denatured and reduced cellular protein was subjected to IAAyne labeling at different concentrations as indicated. Biotinylated proteins were exposed to the CuAAC reaction and evaluated by HRP-Streptavidin. p53 and GAPDH labeling were evaluated by their specific antibodies. **(C)** 250  $\mu\text{g}$  of native proteins from untreated,  $\text{H}_2\text{O}_2$ , diamide, or NEM treated cells were labeled with different amounts of IAAyne as indicated. The IAAyne-DADPS labeling efficiency was evaluated by HRP-Streptavidin and GAPDH labeling was also evaluated.

weight was observed, in contrast to our experiment using BIAM labeling (**Fig. 2C** and **Fig. 6B**). It is possible that IAAyne-DADPS labeling does not have a large effect on p53 protein migration, although with a mass of around 1KDa (uncleaved) this seems somewhat unlikely. Further identification by Mass spectrometry is required (ongoing).

The small structure of IAAyne enables it to access structurally partially buried cysteines and therefore IAAyne has been used to evaluate cysteine reactivity in native conditions (**Fig. 6A**) [8, 9]. In this case, thiol oxidation would lead to a decreased labeling by IAAyne. To evaluate the labeling efficiency of IAAyne in native conditions, we took 250  $\mu\text{g}$  of lysate treated with  $\text{H}_2\text{O}_2$ , diamide, or NEM and incubated with 50  $\mu\text{M}$  of IAAyne, followed by

the CuAAC reaction in the presence of 100  $\mu\text{M}$  DADPS. In the untreated condition, a big smear of biotinylated proteins was observed, indicating that IAAyne efficiently labeled thiols in native conditions. Pre-treatment with NEM significantly blocked the IAAyne labeling, which, however, was not notably affected by the treatment with  $\text{H}_2\text{O}_2$  or diamide (**Fig. 6C**). This could be because  $\text{H}_2\text{O}_2$  and diamide induce no extensive thiol oxidation post lysis, or oxidizes only a subset of specific proteins that can only be identified by targeted approaches or by MS. Furthermore, treatment with  $\text{H}_2\text{O}_2$  and diamide could be optimized regarding concentration and time course.

In the labeling experiments using reduced and denatured lysate (**Fig. 2C** and **Fig. 6B**) we observed that labeled GAPDH is no longer recognized by the used monoclonal antibody on Western blot. Likewise, we observed that GAPDH displayed slightly less intensity in the groups incubated with IAAyne (**Fig. 6C**), suggesting that IAAyne could capture the same thiol(s) in GAPDH in its native structure.

In conclusion, we evaluated two thiol-labeling methods: the BIAM-switch assay and IAAyne-DADPS conjugation, both of which did label thiols under certain conditions, whereas the methods need to be further optimized to be used in a proteome-wide fashion. BIAM labeling did work efficiently, but inefficient elution from Streptavidin beads resulted in a low yield of proteins or sites identified by MS. The cleavable IAAyne-DADPS method circumvented this problem and showed robust labeling for both recombinant and whole cell lysate in both denaturing and native conditions.

Indeed, others have used the IAAyne-DADPS method successfully and identified over 10,000 unique cysteine residues in cell lysate [21], suggesting that further optimization in our laboratory would certainly be worth the effort. Variables including the amount of material used to label (protein), freshness and concentration of reagents and buffers, alternative washing and elution procedures could be tried to further increase the labeling specificity and efficiency, eventually allowing us to precisely monitor thiol redox state in multiple biological systems.

## Reference

1. Stocker S., Van Laer K., Mijuskovic A., et al. The Conundrum of Hydrogen Peroxide Signaling and the Emerging Role of Peroxiredoxins as Redox Relay Hubs. *Antioxid Redox Signal*, 2018. 28(7): 558-573.
2. Kumar A., Wu H., Collier-Hyams L.S., et al. Commensal bacteria modulate cullin-dependent signaling via generation of reactive oxygen species. *EMBO J.*, 2007. 26(21): 4457-4466.
3. Meng T.C., Fukada T., Tonks N.K. Reversible oxidation and inactivation of protein tyrosine phosphatases in vivo. *Mol. Cell*, 2002. 9(2): 387-399.
4. Heppner D.E., Dustin C.M., Liao C., et al. Direct cysteine sulfenylation drives activation of the Src kinase. *Nature Communications*, 2018. 9(1): 4522.
5. Putker M., Madl T., Vos H.R., et al. Redox-dependent control of FOXO/DAF-16 by transportin-1. *Mol. Cell*, 2013. 49(4): 730-742.

6. Taguchi K., Motohashi H., Yamamoto M. Molecular mechanisms of the Keap1–Nrf2 pathway in stress response and cancer evolution. *Genes Cells*, 2011. 16(2): 123-140.
7. Sies H., Jones D.P. Reactive oxygen species (ROS) as pleiotropic physiological signalling agents. *Nat. Rev. Mol. Cell Biol.*, 2020. 21(7): 363-383.
8. Weerapana E., Wang C., Simon G.M., et al. Quantitative reactivity profiling predicts functional cysteines in proteomes. *Nature*, 2010. 468(7325): 790-795.
9. Fu L., Li Z., Liu K., et al. A quantitative thiol reactivity profiling platform to analyze redox and electrophile reactive cysteine proteomes. *Nat. Protoc.*, 2020. 15(9): 2891-2919.
10. Xiao H., Jedrychowski M.P., Schweppe D.K., et al. A Quantitative Tissue-Specific Landscape of Protein Redox Regulation during Aging. *Cell*, 2020. 180(5): 968-983.e924.
11. Leichert L.I., Gehrke F., Gudiseva H.V., et al. Quantifying changes in the thiol redox proteome upon oxidative stress in vivo. *Proc. Natl. Acad. Sci. U. S. A.*, 2008. 105(24): 8197-8202.
12. Löwe O., Rezende F., Heidler J., et al. BIAM switch assay coupled to mass spectrometry identifies novel redox targets of NADPH oxidase 4. *Redox Biol*, 2019. 21: 101125.
13. Fuhrmann D.C., Wittig I., Brüne B. TMEM126B deficiency reduces mitochondrial SDH oxidation by LPS, attenuating HIF-1 $\alpha$  stabilization and IL-1 $\beta$  expression. *Redox Biol*, 2019. 20: 204-216.
14. Rybak J.N., Scheurer S.B., Neri D., et al. Purification of biotinylated proteins on streptavidin resin: a protocol for quantitative elution. *Proteomics*, 2004. 4(8): 2296-2299.
15. Cheah J.S., Yamada S. A simple elution strategy for biotinylated proteins bound to streptavidin conjugated beads using excess biotin and heat. *Biochem. Biophys. Res. Commun.*, 2017. 493(4): 1522-1527.
16. Szychowski J., Mahdavi A., Hodas J.J., et al. Cleavable biotin probes for labeling of biomolecules via azide-alkyne cycloaddition. *J. Am. Chem. Soc.*, 2010. 132(51): 18351-18360.
17. Woo C.M., Iavarone A.T., Spiciarich D.R., et al. Isotope-targeted glycoproteomics (IsoTaG): a mass-independent platform for intact N- and O-glycopeptide discovery and analysis. *Nat Methods*, 2015. 12(6): 561-567.
18. Hewings D.S., Flygare J.A., Bogyo M., et al. Activity-based probes for the ubiquitin conjugation-deconjugation machinery: new chemistries, new tools, and new insights. *Febs j*, 2017. 284(10): 1555-1576.
19. Li W., Zhou Y., Tang G., et al. Characterization of the Artemisinin Binding Site for Translationally Controlled Tumor Protein (TCTP) by Bioorthogonal Click Chemistry. *Bioconjug. Chem.*, 2016. 27(12): 2828-2833.
20. Gao J., Mfuh A., Amako Y., et al. Small Molecule Interactome Mapping by Photoaffinity Labeling Reveals Binding Site Hotspots for the NSAIDs. *J. Am. Chem. Soc.*, 2018. 140(12): 4259-4268.
21. Rabalski A.J., Bogdan A.R., Baranczak A. Evaluation of Chemically-Cleavable Linkers for Quantitative Mapping of Small Molecule-Cysteine Reactivity. *ACS Chem. Biol.*, 2019. 14(9): 1940-1950.
22. Putker M., Vos H.R., van Dorenmalen K., et al. Evolutionary acquisition of cysteines determines FOXO paralog-specific redox signaling. *Antioxid Redox Signal*, 2015. 22(1): 15-28.
23. van Dam L., Pagès-Gallego M., Polderman P.E., et al. The Human 2-Cys Peroxiredoxins form Widespread, Cysteine-Dependent- and Isoform-Specific Protein-Protein Interactions. *Antioxidants*, 2021. 10(4): 627.
24. Weber P., Ohlendorf D., Wendoloski J., et al. Structural origins of high-affinity biotin binding to



streptavidin. Science, 1989. 243(4887): 85-88.

25. Scheurer S.B., Roesli C., Neri D., et al. A comparison of different biotinylation reagents, tryptic digestion procedures, and mass spectrometric techniques for 2-D peptide mapping of membrane proteins. Proteomics, 2005. 5(12): 3035-3039.

## Supplementary Figures

```
> EGFP-beta-Catenin (protein) (1031 aa)
MYSKGEELFTGVVPILVELDGDVNGHKFSVRGEGEGDATNGKLTTLKFIC[49]TTGKLPVPWPTLVTTLTYGV
QC[71]FSRYPDHMKQHDFFKSAMPEGYVQERTISFKDDGTYKTRAEVVKFEGDTLVNRIELKGIDFKEDGNIL
GHKLEYNFNSHNVYITADKQKNGIKANFKIRHNVEDGSVQLADHYQQNTPIGDGPVLLPDNHYLSTQSKLSKD
PNEKRDHMVLLEFVTAAGITLGMDELYRLQPKKKRKVEDPATQADLMELDMAMEPDRKAAVSHWQQQSYLDSG
IHSGATTTAPSLSGKGNPEEEDVDTSQVLYEWEQGFSQSFTQEQVADIDGQYAMTRAQRVRAAMFPETLDEGM
QIPSTQFDAAHPTNVQRLAEPSQMLKHAVVNLINYQDDAELATRAIPELTKLNDEDQVVVNKAAVMVHQLSK
KEASRHAIMRSPQMVSAIVRTMQNTNDVETARC[463]TAGTLHNLSHHREGLLAIFKSGGIPALVKMLASPV
DSVLFYAITTLHNLLHQEGAKMAVRLAGGLQKMVALLNKTNVKFLAITDC[550]LQILAYGNQESKLIL
ASGGPQALVNIMRTYTYEKLLWTSRVLKVLSVC[600]SNKPAIVEAGGMQALGLHLTDPSQRLVQNC[63
1]LWTLRNLSDAATKQEGMEGLLGTLVQLLGSDDINVVTC[669]AAGILSNLTC[679]NNYKNMMVC[68
9]QVGGIEALVRTVLRAGDREDITEPAIC[716]ALRHLTSRHQEAEMAQNAVRLHYGLPVVKLLHPPSHP
LIKATVGLIRNLALC[770]PANHAPLREQGAIPRLVQLLVRAHQDTQRRTSMGGTQQFVEGVRMEIVEGC
[823]TGALHILARDVHNRIVRIRGLNTIPLFBVQLLYSPIENIQRVAAGVLC[869]ELAQDKEAAEAIEAEGA
TAPLTELLHSRNEGVATYAAVLFRMSEDKPQDYKRLSVELTSSLFRTEPMAWNETADLGLDIGAQGEPLGY
RQDDPSYRSFHSGGYGQDALGMDPMEHEMGGHPGADYPVDGLPDLGHAQDLMDGLPPGDSNQLAWFDTDL*
```

### Cysteine sites

C49

C71

C463

C550

C600

C631

C669

C679

C689

C716

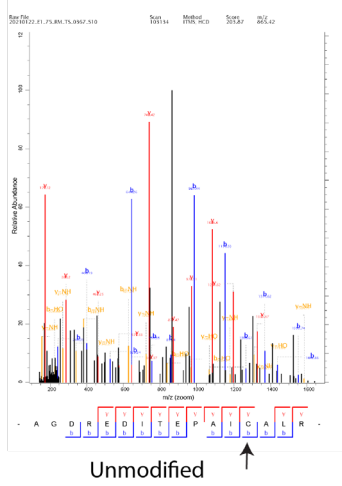
C770

C823

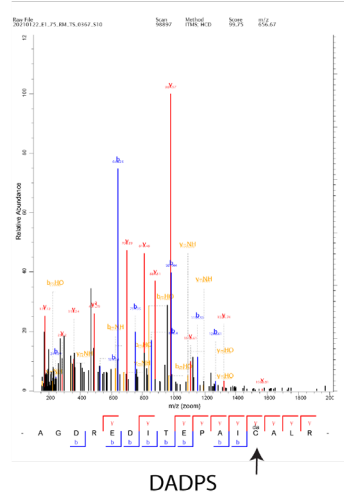
### Supplementary Figure 1. Protein FASTA sequences of EGFP-β-Catenin

(A) EGFP sequence is marked in green, and β-Catenin in grey, referring to the NCBI protein sequence NP\_001091679.1. All cysteine residues in the fused protein are bold and indicated with exact positions based on the full length of the fused protein (1031 aa).

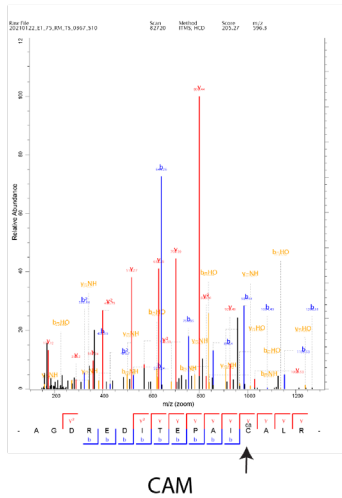
A



B

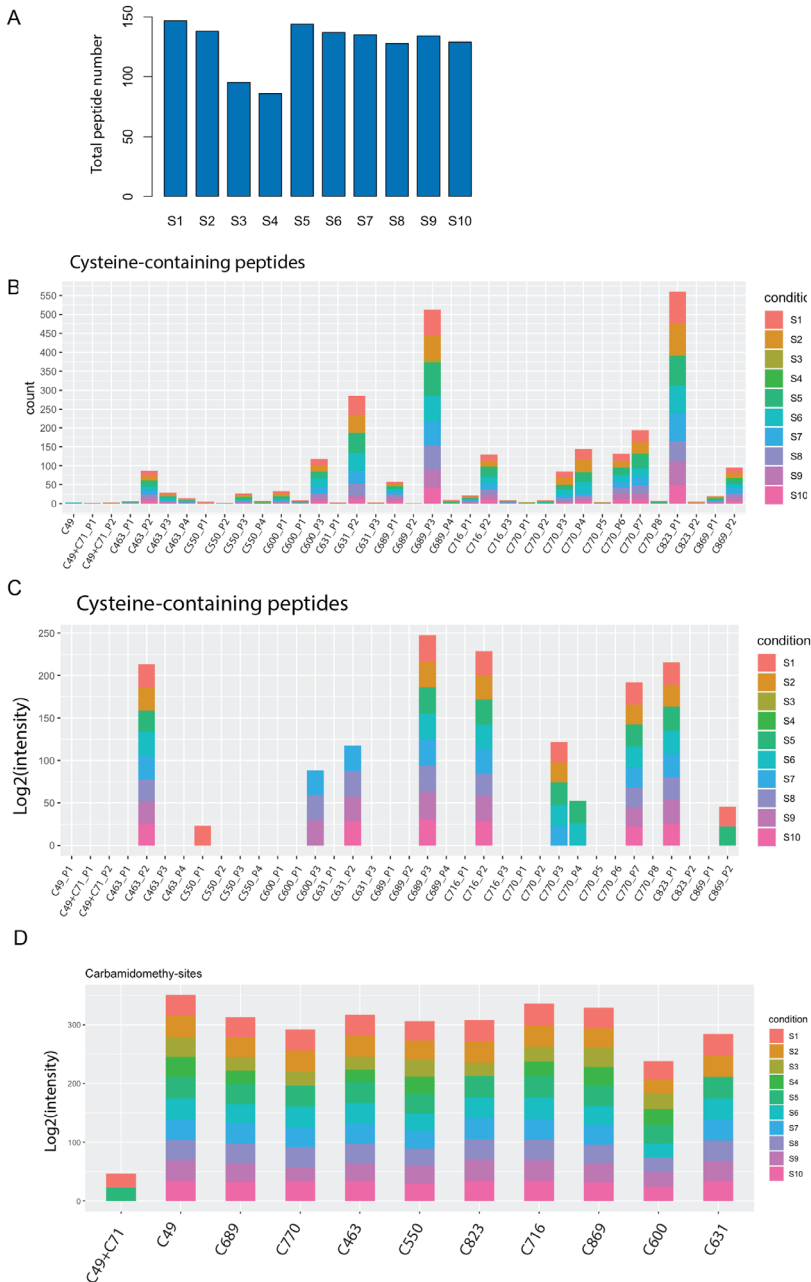


C



**Supplementary Figure 2. Mass spectra of the C716-containing peptide(AGDREDITEPAICALP) with different modification on the cysteine site.**

DADPS, IAAyne-DADPS(+238.29Da); CAM, Carbamidomethylation (+57.01Da)



**Supplementary Figure 3. Identified EGFP-β-Catenin peptides upon the IAAyne-DADPS labeling .** (A) Total EGFP-β-Catenin peptides identified in each sample. (B) Count and (C) Intensity of EGFP-β-Catenin cysteine-containing peptides identified in each sample. Multiple peptide sequences were identified for same cysteine site, for example 3 peptide sequences (P1, P2 and P3) were identified containing C716. (D) Carbamidomethylation sites identified in EGFP-β-Catenin.



# *Chapter 6*

## **Monitoring the activity of multiple transcription factors simultaneously through fluorescence-based transcriptional reporters**

Tao Shi<sup>1</sup>, Paulien E. Polderman<sup>1</sup>, TianShu Gui<sup>1,2</sup>, Gillian Schuurman<sup>1</sup>, Boudewijn M.T. Burgering<sup>1,2</sup>, Tobias B. Dansen<sup>1,3</sup> and Sasha De Henau<sup>1</sup>

<sup>1</sup>Center for Molecular Medicine, Molecular Cancer Research and <sup>2</sup>Oncode Institute, University Medical Center Utrecht, Universiteitsweg 100 3584 CG Utrecht, The Netherlands.

<sup>3</sup>Correspondence to: [t.b.dansen@umcutrecht.nl](mailto:t.b.dansen@umcutrecht.nl).

## Abstract

Transcription factors are of great importance in controlling many biological processes and their dysregulation is associated with many pathological conditions, including cancer. Myc and T cell factor (TCF) downstream of WNT signaling support cell proliferation and are frequently hyperactive in cancer. Tumor suppressor p53, the Forkhead box O proteins (FOXOs), nuclear factor E2-related factor 2 (NRF2) and hypoxia-inducible factor (HIF) are all activated in response to various cellular stresses and play roles in tumor suppression but also in tumor adaptation and survival. Understanding which of these transcription factors is activated during cancer initiation, progression and treatment in a spatiotemporal manner within the same cellular context has not been studied in detail. Here we describe the construction of two fluorescence-based reporters using the BSHA (BsmBI and SapI-mediated Hierarchical Assembly) platform for the simultaneous and dynamic measurement of up to 6 transcription factor activities at the single-cell level. Transient expression of these reporters in HEK293T cells showed that these reporters are indeed functional upon ectopic expression of specific transcription factors or exposure to certain stimuli. Further testing is needed to assess the applicability of these reporters under more endogenous conditions. Collectively, our fluorescence-based reporters will make it possible to simultaneously monitor the activity of key transcription factors involved in cancer biology in a live setting and in various model systems.

## Introduction

Transcription factors (TFs) are a class of proteins that bind to specific DNA motifs (Response Elements, RE) in the promoter or other regulatory regions (e.g., UTRs and introns) of genes and subsequently activate or suppress the expression of those genes. TFs are the endpoint of specific regulatory networks and are critical in controlling cellular identity and the response to external stimuli [1]. Dysregulation of TF activities is associated with many pathological outcomes, such as aging-related diseases and cancer. Aberrant TF activation results in perturbed cellular homeostasis and alters key cellular processes such as cell growth, death, stress response and metabolism [2]. TFs like Myc and WNT/TCF are vital regulators in promoting cell growth in physiological conditions, but their persistent increased activities lead to cell overgrowth and tumor formation [3] [4]. Tumor suppressor p53 and the FOXOs are induced by a variety of stresses, including DNA damage, oxidative and metabolic challenges. These TFs then trigger DNA damage repair, cell cycle arrest, anti-oxidation function or cell death, to prevent over-proliferation, genomic instability and tumor development [5] [6]. NRF2 is activated in response to oxidative stress and is essential for maintaining redox homeostasis by upregulating several anti-oxidant genes [7] [8], but has also been shown to be crucial for the outgrowth of certain tumors [9]. HIF-1 $\alpha$  is activated in response to hypoxia to promote lymphangiogenesis and as such sustains the oxygen and metabolite supply in growing solid tumors and paves the way for cancer cell dissemination and metastasis [10]. The activity of individual TFs has extensively been evaluated in various

cellular stages, primarily by assessing the expression of their target genes using static measurements like qPCR or (single) cell RNA sequencing. However, little is known about how multiple TFs are dynamically and simultaneously regulated at the single cells level within populations of cells, in a quasi-real-time manner. Approaches like qPCR and RNA sequencing only provide a fixed state of activity of TFs, and require elaborate and time-consuming sample preparation if multiple time points are included. In the present research project, we established fluorescence-based transcriptional reporters that will enable us to simultaneously track the activity of two sets of 3 TFs in real-time. These reporters can in principle be combined to dynamically measure the activity of up to 6 TFs simultaneously and connect the observations with cell fate.

Conventional approaches to create large expression vectors involve the elaborate design and cloning of suitable restriction enzyme recognition sites in both inserts and vector backbones, extensive PCRs for the generation of desired products, multiple ligation reactions, and tedious validation by diagnostic cutting followed by sequencing. Troubleshooting and optimization can be time-consuming and costly. Alternatively, the EMMA (Extensible Mammalian Modular Assembly) cloning kit established by Martella et al. [11], enables rapid and efficient modular assembly of mammalian expression vectors by using a standardized library of compatible genetic parts with unique biological functions, through a one-tube, one-step Golden Gate (GG) reaction. This method has been verified for the assembly of multiple DNA parts ranging from 9 to 25 in a single GG reaction, but with variable assembly efficiency depending on the number, size, nucleotide composition, and quality of the genetic parts that are included. Combined, these uncertain factors limit the application of EMMA to establish complex vectors involving a large number (over 20) of genetic parts. Here we developed a new BsmBI and SapI-mediated Hierarchical Assembly (BSHA) system based on the EMMA design. The hierarchical, 2-step approach of BSHA reduces the number of components in a single reaction to maintain a high assembly efficiency, and still allows to create large, complex vectors in a modular fashion. By using this BSHA system, we successfully established two fluorescence-based transcriptional reporter constructs, each allowing the assessment of the activity of three TFs (**Fig. 1B**): one construct for p53, Myc, and FOXO that makes use of fluorophores fused to a Nuclear Localization Signal (p53/Myc/FOXO<sup>NLS</sup>); and the other one for TCF, HIF, and NRF2 that expresses fluorophores (TCF/HIF/NRF2<sup>NES</sup>) equipped with a Nuclear Export Signal and hence are localized to the cytoplasm. The use of a single expression vector to express three TF reporters at once overcomes variations in transfection and expression rates as compared to when separate vectors are introduced. This approach also leaves more options for combining resistance-based selection. A combination of these two reporters will enable us to simultaneously measure the activity of 6 transcription factors.

## Materials and methods

### Bacteria

*E. coli DH5α* competent cells and One Shot ccdB Survival 2 T1R Competent cells (Fisher scientific) were incubated at 37 °C for plasmid amplification. Kanamycin (25 µg/ml) (Life Technologies) and Ampicillin (100 µg/ml) (Sigma) were used for positive clone selection.

### **Generation of Domestication vectors**

Each DNA fragment of interest was standardized by introducing two different fusion sites of BsaI through PCR using the primers designed by EMMA [11] (**Table S1**), followed by cloning into a compatible Part-entry vector (RFP-KanR-pSMART cassette, EMMA) through a BsaI Golden Gate (GG) reaction. This adaption process is termed 'domestication' and generates a product named 'Domestication vector', which is ready for a BsmBI GG reaction. The PCR template sources and primers for generating Part-entry vectors are listed in **Table S1**.

### **Construction of 4 mini-receiver vectors and expression cassettes**

Four gBlock fragments were ordered, each comprised of a ccdB gene sequence flanked by two pairs of BsmBI (for level-I GG) and SapI (for level-II GG) sites, followed by an EcoRI and XbaI site on either side. Using double digestion with EcoRI and XbaI (NEB) and following the T4 ligation method, four gBlock fragments were cloned into a receiver backbone (ccdB-AmpR cassette, EMMA), forming Four mini-receiver backbone vectors (1-6, 7-12, 13-18, and 19-15 ccdB-AmpR cassettes). Four mini expression cassettes (mini reporters) were constructed through a BsmBI GG reaction by mixing Domestication vectors with their separate compatible mini-receiver backbone vector (**Fig. 2**).

### **Generation of the Final SapI-ccdB-KanR receiver**

The Final SapI-ccdB-KanR receiver (**Fig. 2**) was obtained by adapting one of the part-entry backbone vectors (YCe1502 HC\_Kan\_RFP-p3, EMMA), where the RFP gene was replaced by a ccdB gene sequence flanking by two SapI cutting sites. Briefly, the ccdB gene sequence was obtained from the 19-25 mini-receiver backbone by PCR using the primers containing SapI sites (lowercase) (Forward: 5'-TAGAGAATTCGtgccgaagagcTAGGAGAG ACGCAATACGCAAAC-3'; Reverse: 5'-GATATCTAGAttacgaagagcTCGTTGAGACGGCC GCTACTAGT-3'), and then inserted into the part-entry vector through a double digestion with EcoRI and XbaI and T4 ligation. The ligation product was transformed into One Shot ccdB Survival 2 T1R Competent cells, and Kanamycin resistant colonies were selected and validated by EcoRI-XbaI digestion and sequencing.

### **BsaI, BsmBI, and SapI GG reaction**

Golden Gate (GG) reactions were performed as described previously [11]. Briefly, 10 µl of GG mixture was prepared as follows: 25 ng of each vector (Genetic parts and receiver), 5 U of BsaI-HF@v2 (R3733L, NEB), FastDigest Esp3I (BsmBI, FD0454, Thermo Scientific), or SapI (R0569S, NEB), 100 U of T4 DNA Ligase (M0202L, NEB) and 1x T4 ligation buffer (final). The reaction was performed according to the following program: step 1, 37 °C for 5



min; step 2, 37 °C for 5 min; step 3, 16 °C for 10 min; repeat steps 2 and 3 for 20 cycles; step 4, 16 °C for 20 min; step 5, 37 °C for 30 min; step 6, 75 °C for 6 min; step 7, 4 °C; hold. Subsequently, 0.25 μL of Plasmidsafe nuclease (Epicenter), and 0.5 μL of 25 mM ATP was added to the reaction and incubated further at 37 °C for 15 min. 2 μL of the resulting reaction was transformed into *E. coli* DH5α competent cells.

### Cell culture, transient transfection, and treatment

HEK293T cells were cultured in 8-well Nunc™ Lab-Tek™ II Chambered Coverglass (155409) (VWR) with 200 μL of DMEM high-glucose (4,5 g/L) supplemented with 10% FBS, 2 mM L-glutamine and 100 Units Penicillin-Streptomycin (All from Sigma Aldrich), at 37 °C, under 6% CO<sub>2</sub>, and 20% or 3% O<sub>2</sub> conditions. Transient transfections were performed using the polyethylenimine (PEI) (Sigma Aldrich) transfection reagent using 3 μl of PEI/ μg DNA.

After 24 or 48 h of transfection, cells were treated with different compounds: Nutlin-3 (Sanbio, 10004372), Hydrogen peroxide solution 30% (Sigma, 7722-84-1), Auranofin (AFN) (Sigma, A6733), CHIR (Bio Connect, 99021), or Human Epidermal Growth Factor (hEGF) (Peprotech, #100-15) to a final concentration as indicated in the Results section.

### Microscopy and image analysis

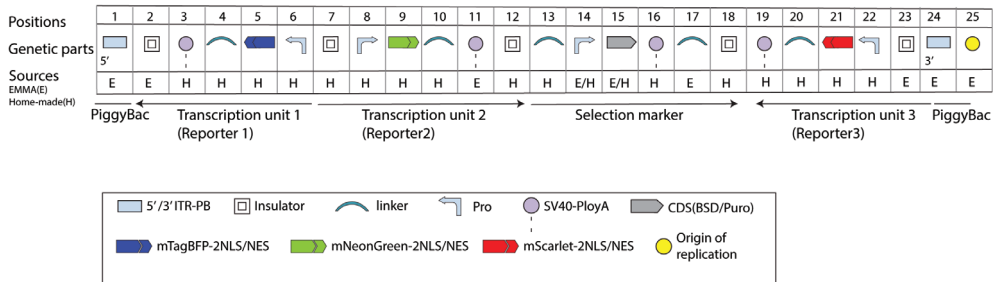
Live HEK293T cells in the 8-well Nunc™ Lab-Tek™ II Chambered Coverglass were imaged on a ZEISS confocal microscope LSM880 or LSM510 with a 20, 40, or 63x Objective. The laser setup λEx405nm/λEm410-475nm was used for the detection of mTagBFP2 protein, λEx488nm/λEm493-561nm for mNeonGreen and λEx561nm/λEx580-645nm for mScarlet. Microscope images were further processed using Fiji (Image J) software.

## Results

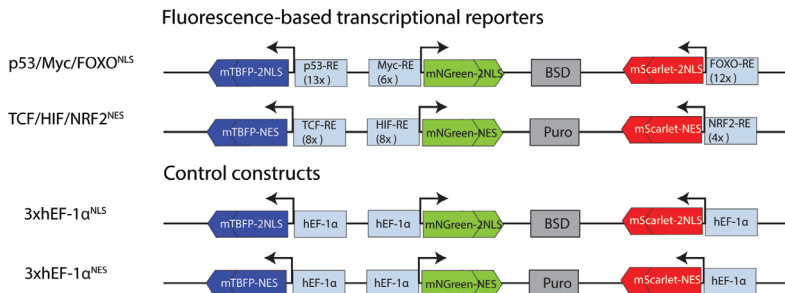
### Vector design

Inspired by the design of the EMMA toolkit that enables the rapid and efficient assembly of 25 compatible DNA parts into one single vector using a BsmBI Golden Gate (GG) reaction, we establish a new library of 25 standardized compatible genetic parts of our interest, utilizing the optimal BsmBI fusion sites designed by EMMA for each DNA part [11] (**Fig. 1A**) (**Table S1**). All 25 parts are assigned to specific positions depending on their biological function. These 25 parts were designed to create three Transcription Units and one Selection marker within a single expression construct (**Fig. 1A**). We used this design to make four expression constructs: two functional reporters that express nuclear-localized fluorophores driven by p53/Myc/FOXO (p53/Myc/FOXO<sup>NLS</sup>) and cytosolic localized fluorophores driven by TCF/HIF/NRF2 (TCF/HIF/NRF2<sup>NES</sup>), respectively. Note that multiple copies of canonical REs for each TF have been incorporated in the reporter vector in order to increase the responsiveness to these TFs (**Fig. 1C**). The two remaining constructs, 3xhEF-1α<sup>NLS</sup> and 3xhEF-1α<sup>NES</sup>, serve as positive controls for the construct design of p53/Myc/FOXO<sup>NLS</sup> and

A



B



C

Mini promoter	Sequence	Source
(13x) p53-RE	(13x) CCAGGCAAGTCCAGGCAGG	PG13-luc (Addgene plasmid # 16442) [23]
(8x) TCF-RE	(8x) GATCAAAGG	pGL4.10-luc2-TATA-8x TCF
(6x) Myc-RE	(6x) CCCACCAGTGGTGCCT	pGL3-6xMyc-RE-Luc2-AmpR
(8x) HIF-RE	(8x) GATCGCCCTACGTGCTGTCTCA	pGL3-8xHIF-RE-Luc2-AmpR
(12x) FOXO-RE	(12x) GTAAACAA	6xDBE-luciferase [24]
(4x) NRF2-RE	(4x) TGCAAAATCGAGTCACAGTGA CTCAGCAGAATCTGAGCCTAGG	pGL3-RE-NRF2-AmpR

### Figure 1. Design of fluorescence-based transcriptional reporter constructs

(A) Design of a single fluorescence-based transcriptional reporter. Each genetic part is assigned to a specific position (1-25) depending on their biological function, and flanked by compatible fusion sites optimized for the EMMA kit. Genetic parts annotated with an 'E' are adopted from the original EMMA kit, and ones with an 'H' are standardized by ourself (homemade) using fusion site-containing primers provided by the EMMA kit. The final construct will have three Transcription units, one Selection marker, and two PiggyBac transposon elements. The lower panel shows the key for the schematic symbols representing the functional classifications. ITR-PB, PiggyBac inverted terminal repeat; Pro, promoter; CDS, coding sequence. (B) Scheme of two fluorescence-based transcriptional reporters and two control constructs. In the transcriptional reporter for p53/Myc/FOXO (p53/Myc/FOXO<sup>NLS</sup>), 13 copies of p53-RE (response element) were introduced as a mini promoter for a nuclear-localized mTagBFP2 fluorophore,

6x Myc-RE for an mNGreen (nuclear) and 12 x FOXO-RE for an mScarlet (nuclear). The transcriptional reporter for TCF/HIF/NRF2 (TCF/HIF/NRF2<sup>NES</sup>) contains 8x TCF-RE with a cytosolic mTagBFP2, 8x HIF-RE with a cytosolic mNGreen, and 4x NRF2-RE with a cytosolic mScarlet. Two control constructs, 3xhEF-1 $\alpha$ <sup>NLS</sup> and 3xhEF-1 $\alpha$ <sup>NES</sup>, are positive controls for testing the expression of different fluorophores through a constitutively activate hEF-1 $\alpha$  promoter. NLS nuclear localization signal; NES, nuclear export signal. BSD, Blastidicin; Puro, Puromycin; hEF-1 $\alpha$ , human elongation factor 1 $\alpha$ . **(C)** The canonical response element (RE) sequence for each transcription factor and the number of repeats for each RE in the final mini promoters. RE sequences and number of repeats were copied from published plasmids or homemade luciferase reporters as shown in the 'Source'.

TCF/HIF1/NRF2<sup>NES</sup> by driving fluorophore expression through a constitutively active hEF-1 $\alpha$  promoter (**Fig. 1B**). Because the assembly efficiency of a one-step BsmBI GG reaction decreases considerably when more EMMA toolkit parts are involved, we established a BsmBI and SapI-mediated Hierarchical Assembly (BSHA) method. This approach provides high assembly efficiency of 25 parts by splitting the reaction in two steps. Practically, the BSHA involves two levels of GG reaction where the level-I (BsmBI) mediates the assembly of 6 or 7 DNA parts, resulting in 4 mini-cassette expression vectors (cassette 1-6, 7-12, 13-18, and 19-20). The level-II GG reaction (SapI) connects these 4 mini-cassette expression vectors into a final receiver backbone (Sap1-KanR-receiver) and yields the final expression vector (**Fig. 2**). Furthermore, we designed BSHA so that the mini-cassettes generated by the level-I BsmBI GG reaction are by themselves already functional reporter constructs that could be used for functional analysis in cells through transient transfection.

### Functional test of the 3xhEF-1 $\alpha$ <sup>NLS</sup> and 3xhEF-1 $\alpha$ <sup>NES</sup> vectors

To evaluate whether the BSHA method gives rise to the correct vector assembly, we first tested the constructs with the separate fluorophores under control of the constitutively active hEF-1 $\alpha$  promoter. Each mini-cassette successfully expressed a fluorescent protein (FP) with the desired nuclear or cytoplasmic localization upon transient transfection (**Fig. 3A-C**), confirming that the design for the mini-cassette expression vectors is correct. Next, the final expression vectors 3xhEF-1 $\alpha$ <sup>NLS</sup> and 3xhEF-1 $\alpha$ <sup>NES</sup>, expressing the three fluorophores simultaneously, were tested by transient expression in HEK293T cells. Both 3xhEF-1 $\alpha$ <sup>NLS</sup> and 3xhEF-1 $\alpha$ <sup>NES</sup> vectors brightly expressed the fluorophores (mTagBFP2, mNGreen, and mScarlet) in every cell in the nucleus or cytoplasm respectively (**Fig. 3D, E**). Thus, our newly designed BSHA system provides an effective tool to generate large and functional mammalian expression vectors. However, note that the mNGreen-NES protein was not exclusively localized in the cytoplasm (**Fig. 3B**), which would make the interpretation problematic when both the 3xhEF-1 $\alpha$ <sup>NLS</sup> and 3xhEF-1 $\alpha$ <sup>NES</sup> constructs are used within the same system. Therefore, some optimization still needs to be done, for instance by moving the NES or adding an extra NES signal, or by replacing the mNGreen protein with another compatible FP.

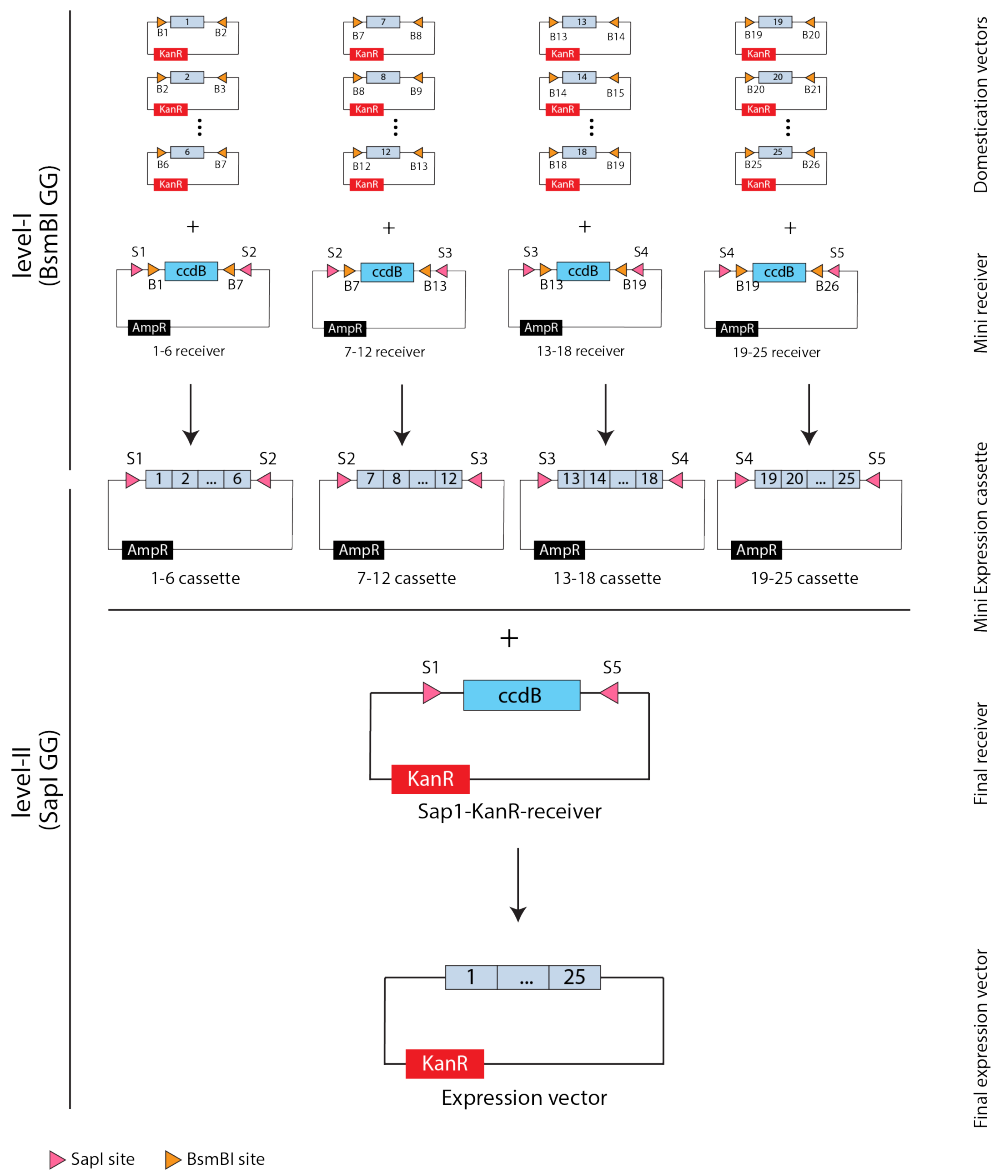


**Figure 2. Scheme for the BSHA (BsmBI and Sapl-mediated hierarchical assembly) procedure**  
 The BSHA method involves two levels of Golden Gate (GG) reactions. The level-I depends on a BsmBI (orange triangle) GG reaction which assembles 6 or 7 out of the 25 EMMA parts (from Domestication vectors) into compatible mini receivers, resulting in 4 mini expression cassettes: 1-6, 7-12, 13-18, and 19-25. The level-II Sapl (pink triangle) mediated GG reaction connects these 4 mini expression cassettes into a final receiver vector, forming the final expression construct covering 25 parts

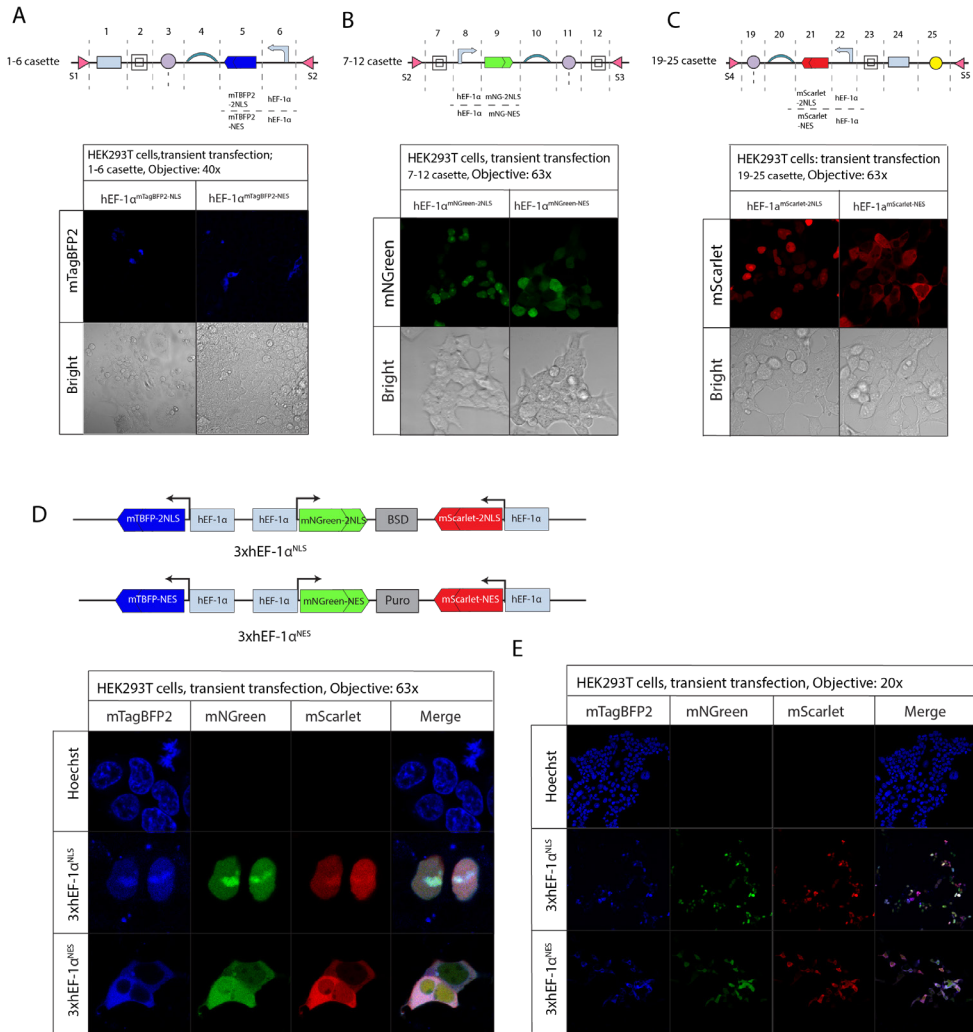


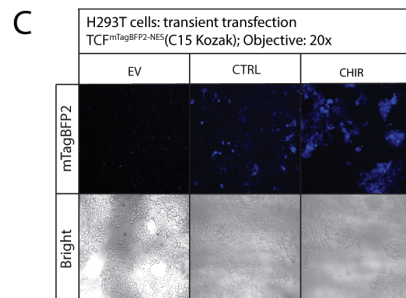
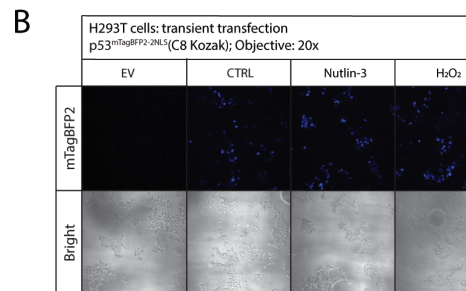
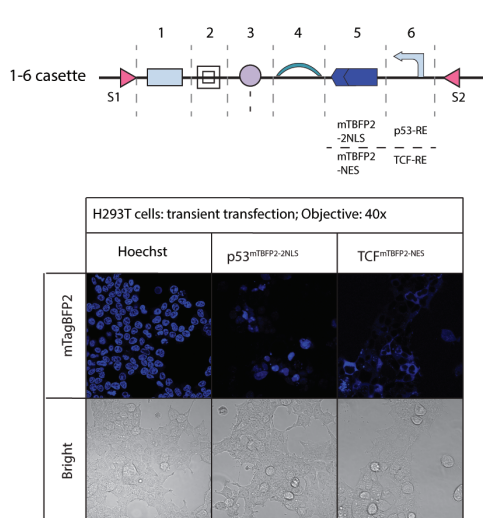
**Figure 3. Functional validation of the mini expression cassettes and final constructs 3xhEF-1 $\alpha$ <sup>NLS</sup> and 3xhEF-1 $\alpha$ <sup>NES</sup>**

(A) Nuclear or cytoplasmic localized 1-6 expression cassette hEF-1 $\alpha$ <sup>mTagBFP2-2NLS</sup> or hEF-1 $\alpha$ <sup>mTagBFP2-NES</sup> upon transient expression in HEK293T cells. Microscopy images were taken from live cells in the mTagBFP2 ( $\lambda$ Ex405nm/ $\lambda$ Em410-475nm) and Bright field channels with a 40x Objective. (B) Nuclear or cytoplasmic localized 7-12 expression cassette hEF-1 $\alpha$ <sup>mNGreen-2NLS</sup> or hEF-1 $\alpha$ <sup>mNGreen-NES</sup> upon transient expression in HEK293T cells. Microscopy images were taken from the live cells in the mNGreen ( $\lambda$ Ex488nm/ $\lambda$ Em493-561nm) and Bright field channels with a 63x Objective. (C) Nuclear or cytoplasmic localized 19-25 expression cassette hEF-1 $\alpha$ <sup>mScarlet-2NLS</sup> or hEF-1 $\alpha$ <sup>mScarlet-NES</sup> upon transient expression in HEK293T cells. Microscopy images were taken from the live cells under mScarlet ( $\lambda$ Ex561nm/ $\lambda$ Ex580-645nm) and Bright field channels with a 63x Objective.

Microscopy images were acquired from live HEK293T cells transiently expressing 3xhEF-1 $\alpha$ <sup>NLS</sup> or 3xhEF-1 $\alpha$ <sup>NES</sup> using a 60x Objective (D) or a 20x Objective (E). The constructs 3xhEF-1 $\alpha$ <sup>NLS</sup> and 3xhEF-1 $\alpha$ <sup>NES</sup> successfully express all fluorescent proteins with the desired localization.

## Validation of mini-cassette expression vectors

Mini-cassette expression vectors covering positions 1-6 (p53 or TCF reporter), 7-12 (Myc or HIF reporter) or 19-25 (FOXO or NRF2 reporter) were tested by transient transfection in HEK293T cells. Overexpression of specific TFs or addition of compounds known to activate TFs was used to stimulate reporter activation (Fig. 4). Each mini-cassette vector successfully expressed the desired fluorescent signal at the appropriate localization (Fig. A, D and G). Note that mNGreen driven by HIF showed a better cytoplasmic localization than the one downstream of hEF-1 $\alpha$  (Fig. 3D, E), suggesting that the rate of nuclear protein export could be limiting at high FP concentration. The p53-driven mTagBFP2 signal was slightly increased upon Nutlin-3 and H<sub>2</sub>O<sub>2</sub> treatments, suggesting that this expression vector indeed acts as a reporter for p53 transcriptional activity (Fig. 4B). However, more validation is needed in cells with functional p53 signaling (p53 activity is partially inhibited in HEK293T cells through SV40 large T antigen expression [12]). Note that TCF-dependent mTagBFP2 intensity was indeed dramatically augmented upon the addition of an WNT activator CHIR 99021 [13, 14] (Fig. 4C). Nuclear or cytoplasmic localized mNGreen proteins were extensively expressed when (HA-) Myc or (Myc-) HIF-1 $\alpha$  constructs were simultaneously expressed (Fig. 4E, F). Similarly, (Flag-) FOXO4 expression significantly induced the expression of FOXO-driven mScarlet (nucleus). FOXO-driven mScarlet was also slightly increased upon the addition of H<sub>2</sub>O<sub>2</sub> (Fig. 4H). H<sub>2</sub>O<sub>2</sub> has been shown to transcriptionally activate FOXO through redox signaling [15]. Finally, the redox-sensitive, NRF2-dependent mScarlet (cytoplasm) signal was strongly enhanced upon AFN treatment (Fig. 4I). Taken together, our results show that these mini-cassette expression vectors are properly expressed and can function as reporters for specific TFs.



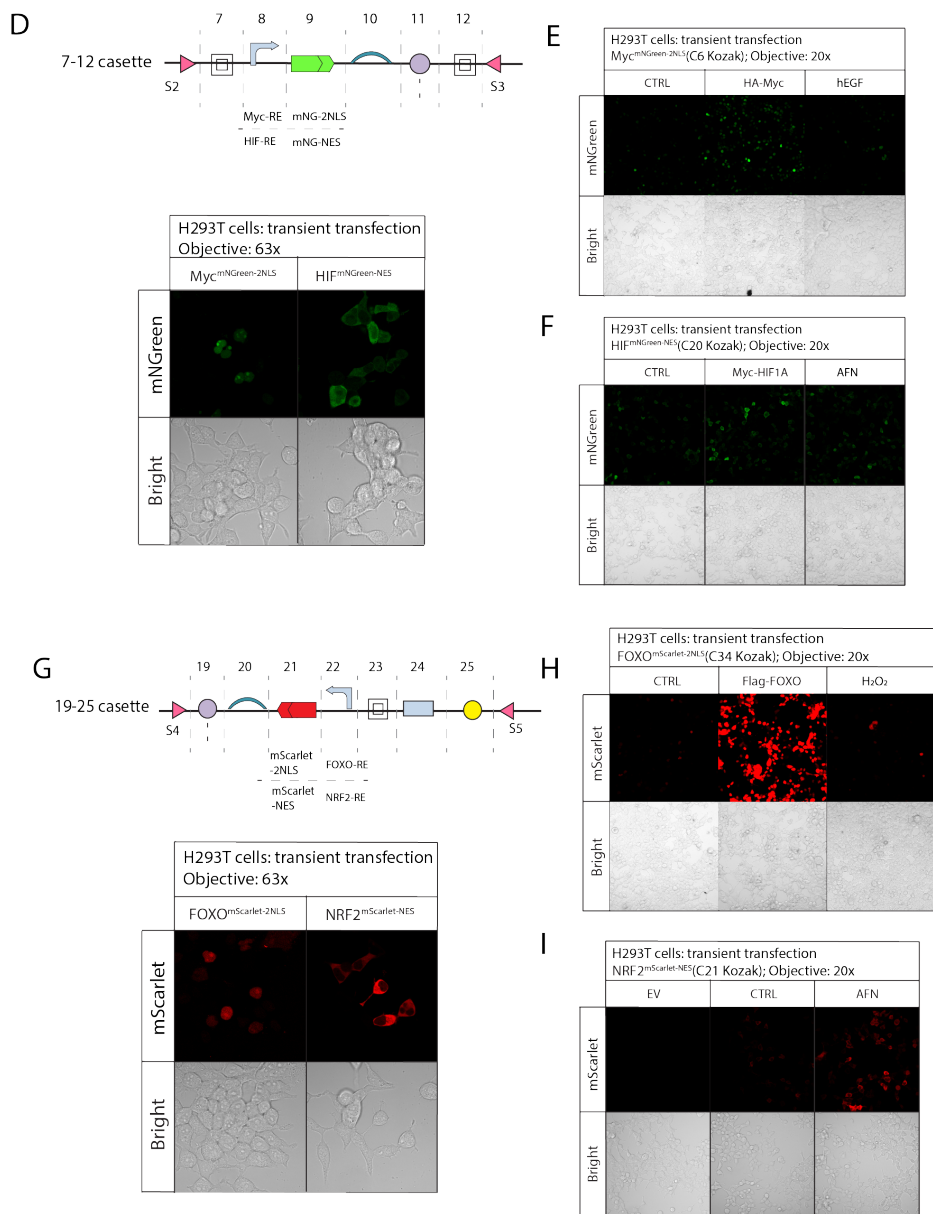


**Figure 4. Functional test of mini reporter cassettes**

(A) Microscopy images showing the nuclear or cytoplasmic expression of p53<sup>mTagBFP2-2NLS</sup> or TCF<sup>mTagBFP2-NES</sup> in HEK293T cells. (B) The fluorescent signal of mini reporter p53<sup>mTagBFP2-2NLS</sup> is slightly increased when cells were treated with Nutlin-3 (10  $\mu$ M) or H<sub>2</sub>O<sub>2</sub> (100  $\mu$ M). (C) The fluorescence intensity of mini reporter TCF<sup>mTagBFP2-NES</sup> is enhanced upon the treatment with CHIR (99021, 30  $\mu$ M). (D) Microscopy images showing the nuclear or cytoplasmic expression of Myc<sup>mNGreen-2NLS</sup> or HIF<sup>mNGreen-NES</sup> in HEK293T cells. (E) The mNGreen intensity of MycmNGreen-2NLS is increased upon ectopic expression of (HA-) Myc protein or addition of human epidermal growth factor (hEGF) (50 ng/ml). (F) The mNGreen intensity of HIF<sup>mNGreen-</sup>

<sup>NES</sup> is augmented when cells were transiently co-transfected with (Myc) HIF1A or treated with Auranofin (AFN, 1  $\mu$ M). **(G)** Transient expression of mini reporter FOXO<sup>mScarlet-2NLS</sup> or NRF2<sup>mScarlet-NES</sup> in HEK293T cells with the desired nuclear or cytoplasmic localized fluorophore. **(H)** The FOXOmScarlet-2NLS reporter exhibits an extensive fluorescence signal upon expression of (Flag-) FOXO or shows a slightly increased signal when cells were challenged with H<sub>2</sub>O<sub>2</sub> (100  $\mu$ M). **(I)** The NRF2<sup>mScarlet-NES</sup> reporter exhibits an increased fluorescence signal upon NRF2 activation by Auranofin (AFN, 1  $\mu$ M) treatment.

## Validation of final reporter constructs

After each mini-cassette expression vector was tested and showed an effective response to activation of specific TFs, the final assembly for the two reporter constructs- p53/Myc/FOXO<sup>NLS</sup> and TCF/HIF/NRF2<sup>NES</sup> - was performed using the SapI GG reaction (**Fig. 5A, B**). The p53/Myc/FOXO<sup>NLS</sup> reporter was successfully expressed in HEK293T cells 48h after transient transfection, and displayed a relatively lower intensity for each fluorophore as compared to the 3xhEF-1 $\alpha$ <sup>NLS</sup> construct. Co-expression of (Flag-) p53, (HA-) Myc and (Flag-) FOXO significantly induced the expression of the corresponding fluorophore, suggesting that each reporter in the larger vector can function as effectively as when expressed as a mini-cassette reporter vector (**Fig. 5A**). Similarly, the TCF/HIF/NRF2<sup>NES</sup> reporter showed detectable signal of mNGreen (HIF) and mScarlet (NRF2) under basal conditions, which were enhanced upon the expression of HIF-1 $\alpha$  or AFN addition respectively. However, the mTagBFP2 signal was hardly visible in both basal and CHIR-treated conditions, which was not the case for the mini-cassette reporter (**Fig. 4C, Fig.5B**). The lower transfection and expression rates of transient transfection of larger constructs could be a possible explanation for this observation. Surprisingly, the mTagBFP2 signal was increased when cells were incubated under 3% Oxygen and was further enhanced upon treatment with CHIR, AFN, or both (**Fig. 5C**). This preliminary result could mean that WNT/TCF activity is upregulated under hypoxic conditions, as previously suggested to occur in tumor cells [16, 17]. However, the reduced mNGreen and mScarlet signals in the low oxygen conditions suggests that HIF (and also NRF2) was unexpectedly less active. Perhaps more severe hypoxia (O<sub>2</sub> < 1%, or 0.5%) is needed to sufficiently activate HIF. Taken together, the constructed TF reporters seem largely functional and can be further tested in various biological settings. The low expression level of the mTagBFP2 fluorophore might be solved by making stable-expression clones followed by FACS sorting for cells with the highest reporter expression.

## Discussion

Transcription factors (TFs) are major effectors of signal transduction networks that control gene expression, and thereby play essential roles in determination of cell fate. Understanding which TFs are activated under what circumstances is important to study fundamental cell biology, but can also help to uncover vulnerabilities of tumor cells at various stages of tumor initiation and progression. While techniques like single cell RNAseq offer detailed information regarding which genes are transcribed, they lack the possibility to connect the timing and dynamics of certain TF activation to cell fate. In the present study,



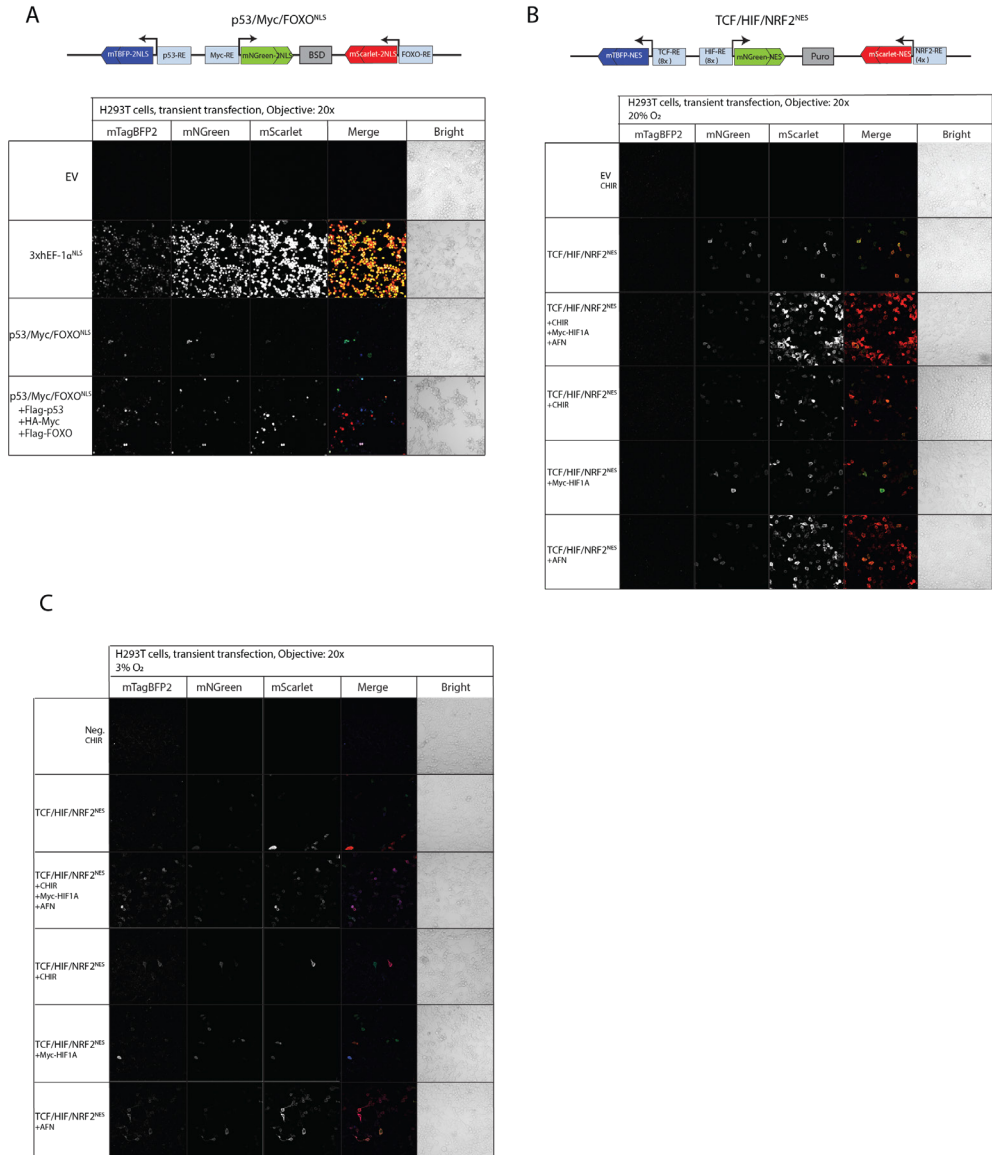


**Figure 5. Functional validation of the p53/Myc/FOXO<sup>NLS</sup> and TCF/HIF/NRF2<sup>NES</sup> reporters.**

**(A)** Microscopy images showing the transient expression of 3x hEF-1 $\alpha^{NLS}$  (a positive control), p53/Myc/FOXO $^{NLS}$  or p53/Myc/FOXO $^{NLS}$  upon co-expression of Flag-p53, HA-Myc and Flag-FOXO proteins in HEK293T cells. Each reporter in the larger vector can function as effectively as when expressed as a mini-cassette reporter vector. Microscopy images showing the transient expression of TCF/HIF/NRF2 $^{NES}$  in HEK293T cells treated with CHIR (30  $\mu$ M), AFN (1  $\mu$ M), co-expressed HA-HIF-1 $\alpha$  protein, or the combined stimuli, under an either 20% O<sub>2</sub> **(B)** or 3% O<sub>2</sub> **(C)** culturing condition. HIF and NRF2 reporters in the larger vector are effectively functional under a 20% O<sub>2</sub> condition, but TCF reporter shows a better expression in a 3% O<sub>2</sub> than 20% O<sub>2</sub> condition.

we developed two fluorescence-based reporters that each can simultaneously determine the activity of 3 key TFs (p53/Myc/FOXO<sup>NLS</sup> or TCF/HIF/NRF2<sup>NES</sup>) in live cells. With this tool we aim to understand the timing and potential crosstalk in response to various stimuli at both the single cell and population level.

To construct these reporters, we established the BSHA system, which enabled us to efficiently generate complex functional mammalian expression vectors. Compared with the one-step GG reaction in EMMA, the two-step GG reaction in the BSHA method takes a few more days, but presents a very high efficiency of assembly in each step (>60%), and a more robust and practical protocol to construct larger and more complex vectors. Similar to EMMA, the BSHA platform can generate diverse functional mammalian expression vectors by replacing interchangeable parts of interest like fluorophores and regulatory sequences. This allows for the rapid expansion and further optimization of our TF reporter toolbox.

So far, we observed that each of the tested TF reporters either in the mini (individual TF reporter) or final (multiple TF reporters) vectors was induced by activation of their respective transcription factor, suggesting that they are in principle functional. Future work is required to test whether all the reporters are also responsive to endogenous TFs. In some cases, crosstalk was observed, for instance we observed the induction of the p53 reporter upon Myc expression. It needs to be established whether this stems from aberrant reporter activation or whether it is an example of the type of crosstalk (p53 activation by an oncogene) we hope to uncover with the novel reporter constructs. Crosstalk between NRF2 and HIF has been reported before [18], in line with this, we observed HIF reporter induction by AFN treatment, which could be the consequence of NRF2 activation or HIF activation by oxidative stress [19]. Further strategies like genetic knockouts for specific TFs would facilitate determination of specific signaling pathways that contribute to the observed transcriptional responses.

Potential optimization for the reporters in order to improve their functionality (e.g., sensitivity and accuracy) might be required when they are used to answer specific research questions. For instance, the mTagBFP2 is a relatively dim fluorophore compared to mNGreen and mScarlet, and therefore a brighter fluorophore could be needed in order to better visualize, for instance, basal p53 activity or p53 activity upon mild cellular stress. To be able to detect the dynamic changes of reporter activities within a short time, a rapid turnover for fluorescent proteins is required, which can be achieved by including a degradation signal like the PEST sequence to the fluorophore [20, 21]. As mentioned above, in order to simultaneously measure the activity of 6 transcription factors upon a combination of reporters p53/Myc/FOXO<sup>NLS</sup> and TCF/HIF/NRF2<sup>NES</sup>, an extra fluorophore that is compatible with the three currently used fluorophores (e.g., LSS mOrange) fused to a nuclear localized protein (e.g., H2B) could be included to discriminate the nucleus and cytoplasm. Furthermore, in the current design, nuclear-localized FPs depend on a Nuclear Localization Sequence (NLS) which targets a protein for import over the nuclear envelope. However, the nuclear envelope breaks down at the beginning of mitosis, making the cytoplasm and the nucleus a continuum.

This prohibits the discrimination of TF activity during mitosis (although TF activity in mitosis is largely absent [22]). Alternatively, fusing the fluorophores to H2B could be a way to fix the fluorophore to the nucleosome, allowing discrimination from the cytoplasmic reporter.

Although our reporters do have some advantages over other methods as discussed above, we see also some potential limitations. For instance, we will lack information on the activation of specific target genes and downstream signaling pathways induced by TFs as compared to RNA sequencing. Another limitation is that only 6 TF activities can be determined simultaneously due to the chromatic overlap when more fluorophores are added. Furthermore, the integration of a large PiggyBac transposon carrying the TF reporters into random genomic positions could generate potential genotoxic effects, or may lead to the natural selection for cells with specific features in a long-term culture. These potential side effects, of course, need to be evaluated in every system to be studied.

Overall, visualizing gene expression in dynamic processes make this reporter system widely applicable for various biological studies. A few applications could be: (i) Track TF dynamics during cell proliferation, differentiation, and death in cell lines, organoids, or in vivo (mouse) models; (ii) Follow TF activities in the process of tumor development using a mouse model by intravital imaging; (iii) Understand drug action and resistance development in medium-throughput drug screens of, for instance, chemo and redox-dependent therapeutics. The regulation of TF activity is complex and many questions have remained unanswered. By showing when, where, and how much a TF is activated our reporters will be valuable tools to better understand the mechanistic regulation in normal cellular behaviors, disease and therapy.

## References

1. Latchman D.S. Transcription factors: an overview. *Int. J. Exp. Pathol.*, 1993. 74(5): 417-422.
2. Lee T.I., Young R.A. Transcriptional regulation and its misregulation in disease. *Cell*, 2013. 152(6): 1237-1251.
3. Kelly K., Siebenlist U. The role of c-myc in the proliferation of normal and neoplastic cells. *J. Clin. Immunol.*, 1985. 5(2): 65-77.
4. Brantjes H., Barker N., van Es J., et al. TCF: Lady Justice casting the final verdict on the outcome of Wnt signalling. *Biol. Chem.*, 2002. 383(2): 255-261.
5. Dansen T.B., Burgering B.M. Unravelling the tumor-suppressive functions of FOXO proteins. *Trends Cell Biol.*, 2008. 18(9): 421-429.
6. Vousden K.H., Lane D.P. p53 in health and disease. *Nat. Rev. Mol. Cell Biol.*, 2007. 8(4): 275-283.
7. Brigelius-Flohé R., Flohé L. Basic principles and emerging concepts in the redox control of transcription factors. *Antioxid Redox Signal*, 2011. 15(8): 2335-2381.
8. Chan S.Y., Zhang Y.Y., Hemann C., et al. MicroRNA-210 controls mitochondrial metabolism during hypoxia by repressing the iron-sulfur cluster assembly proteins ISCU1/2. *Cell Metab.*, 2009. 10(4): 273-284.

9. Kerr E.M., Gaude E., Turrell F.K., et al. Mutant Kras copy number defines metabolic reprogramming and therapeutic susceptibilities. *Nature*, 2016. 531(7592): 110-113.
10. Balamurugan K. HIF-1 at the crossroads of hypoxia, inflammation, and cancer. *Int. J. Cancer*, 2016. 138(5): 1058-1066.
11. Martella A., Matjusaitis M., Auxillos J., et al. EMMA: An Extensible Mammalian Modular Assembly Toolkit for the Rapid Design and Production of Diverse Expression Vectors. *ACS Synth Biol*, 2017. 6(7): 1380-1392.
12. Ahuja D., Sáenz-Robles M.T., Pipas J.M. SV40 large T antigen targets multiple cellular pathways to elicit cellular transformation. *Oncogene*, 2005. 24(52): 7729-7745.
13. Murray J.T., Campbell D.G., Morrice N., et al. Exploitation of KESTREL to identify NDRG family members as physiological substrates for SGK1 and GSK3. *Biochem. J.*, 2004. 384(Pt 3): 477-488.
14. Bain J., Plater L., Elliott M., et al. The selectivity of protein kinase inhibitors: a further update. *Biochem. J.*, 2007. 408(3): 297-315.
15. Dansen T.B. Forkhead Box O transcription factors: key players in redox signaling. *Antioxid Redox Signal*, 2011. 14(4): 559-561.
16. Mazumdar J., O'Brien W.T., Johnson R.S., et al. O<sub>2</sub> regulates stem cells through Wnt/ $\beta$ -catenin signalling. *Nat. Cell Biol.*, 2010. 12(10): 1007-1013.
17. Choi H., Chun Y.S., Kim T.Y., et al. HIF-2 $\alpha$  enhances beta-catenin/TCF-driven transcription by interacting with beta-catenin. *Cancer Res.*, 2010. 70(24): 10101-10111.
18. Lacher S.E., Levings D.C., Freeman S., et al. Identification of a functional antioxidant response element at the HIF1A locus. *Redox Biology*, 2018. 19: 401-411.
19. Bell E.L., Klimova T.A., Eisenbart J., et al. Mitochondrial reactive oxygen species trigger hypoxia-inducible factor-dependent extension of the replicative life span during hypoxia. *Mol. Cell. Biol.*, 2007. 27(16): 5737-5745.
20. Reverte C.G., Ahearn M.D., Hake L.E. CPEB degradation during *Xenopus* oocyte maturation requires a PEST domain and the 26S proteasome. *Dev. Biol.*, 2001. 231(2): 447-458.
21. Spencer M.L., Theodosiou M., Noonan D.J. NPDC-1, a novel regulator of neuronal proliferation, is degraded by the ubiquitin/proteasome system through a PEST degradation motif. *J. Biol. Chem.*, 2004. 279(35): 37069-37078.
22. Kadauke S., Blobel G.A. Mitotic bookmarking by transcription factors. *Epigenetics Chromatin*, 2013. 6(1): 6.
23. El-Deiry W.S., Tokino T., Velculescu V.E., et al. WAF1, a potential mediator of p53 tumor suppression. 1993. 75(4): 817-825.
24. Furuyama T., Nakazawa T., Nakano I., et al. Identification of the differential distribution patterns of mRNAs and consensus binding sequences for mouse DAF-16 homologues. *Biochem. J.*, 2000. 349(Pt 2): 629-634.

## Supplementary Materials

**Table S1 Primers used to establish the standardized library of some genetic parts**

Primer	Sequence(5'→3')	Templet
p3 PolyA F	acgtggctctcg <b>GAC</b> Taactgtttattgcagctta	SV40-polyA(EMMA) [11]
p3 PolyA R	acgtggctctcg <b>GTCC</b> cctaagatacattgatgagttgga	
p4 connector F	acgtggctctcg <b>GGAC</b> Ttaataacagcttccggactc	H-K linker(EMMA) [11]
p4 connector R	acgtggctctcg <b>CGG</b> Agacgaggatcacctgtagg	
p5 mTagBFP2-NES F	acgtggctctcg <b>TCCG</b> ccctgtacgagtcagatccaac	mTagBFP2
p5 mTagBFP2-2NLS F	acgtggctctcg <b>TCCG</b> ccaacttttcgcttctcttggtc	
p5 mTagBFP2 R	acgtggctctcg <b>CTG</b> Gatggtgcttaagggcgaag	
P6 p53-RE F	acgtggctctcg <b>CCAG</b> Tttaccaacagtagccgaat	PG13-luc [23]
P6 p53-RE R	acgtggctctcg <b>GCTG</b> gacggtatcgataagcttga	
p6 TCF-RE F	acgtggctctcg <b>CCAG</b> Ggtggctttaccaacagtagccg	pGL4.10-luc2-TATA-8X TCF
p6 TCF-RE R	acgtggctctcg <b>GCTG</b> ggtaccgagctcttacgcg	
p7 Ins F	acgtggctctcg <b>CAGC</b> ggccgcgaattctgaaagacc	Insulator-FB(EMMA) [11]
p7 Ins R	acgtggctctcg <b>GCC</b> Tgacggatgcgctagc	
p8 Myc-RE F	acgtggctctcg <b>AGG</b> Cggtaccgagctcttacgcg	pGL3-6xMyc-RE-Luc2-AmpR
p8 Myc-RE R	acgtggctctcg <b>ACGC</b> ggtgctttaccaacagtagccg	
p8 HIF-RE F	acgtggctctcg <b>AGG</b> Cggtaccgagctcttacgcg	pGL3-8xMyc-RE-Luc2-AmpR
p8 HIF-RE R	acgtggctctcg <b>ACGC</b> ggtgctttaccaacagtagccg	
p9 mNG- F	acgtggctctcg <b>GCG</b> Tatggtgagcaagggcga	mNeonGreen
p9 mNG-NLS R	acgtggctctcg <b>AGC</b> Accaacttttcgcttctcttggtc	
p9 mNG-NES R	acgtggctctcg <b>AGC</b> Accctgtacgagtcagatccaac	
p10 connector F	acgtggctctcg <b>TGC</b> Tctcaggatcacctgtagg	H-K linker(EMMA) [11]
p10 connector R	acgtggctctcg <b>TACC</b> cctaataacagcttccggactc	
p12 Ins F	acgtggctctcg <b>CGT</b> Gggccgcgaattctgaaagacc	Insulator-FB(EMMA) [11]
p12 Ins R	acgtggctctcg <b>GTA</b> Gtcaggcatgcgctagc	
p13 Connector F	acgtggctctcg <b>TAC</b> Gacataatccaccatcaacatg	M-R linker(EMMA) [11]
p13 Connector R	acgtggctctcg <b>GTA</b> Ggctgttctgggctagg	
p14 hEF-1α Pro F	acgtggctctcg <b>CATC</b> ggctccggtcccgcagtg	hEF-1α promoter sequence
p14 hEF-1α Pro R	acgtggctctcg <b>TTG</b> Ctaccgacacctgaaatggaagaaaaaact	
p15 BSD F	acgtggctctcg <b>GCAA</b> atggccaagcctttgtctc	Blasticidin sequence
p15 BSD R	acgtggctctcg <b>AGGG</b> Ttagccctcccacacataacc	
p16 SV40 PolyA F	acgtggctctcg <b>CCCT</b> Taagatacattgatgagttgg	SV40-polyA(EMMA) [11]
p16 SV40 PolyA R	acgtggctctcg <b>GAGC</b> Aaactgtttattgcagcttata	
p18 Ins F	acgtggctctcg <b>CGGT</b> ggccgcgaattctgaaagacc	Insulator-FB(EMMA) [11]
p18 Ins R	acgtggctctcg <b>GCA</b> Tgcaggcatgcgctagc	
p19 SV40 PolyA F	acgtggctctcg <b>GTG</b> Caactgtttattgcagctt	SV40-polyA(EMMA) [11]
p19 SV40 PolyA R	acgtggctctcg <b>GGC</b> Gcttaagatacattgatgagttgga	
p20 connector F	acgtggctctcg <b>AGCG</b> cctaataacagcttccggactc	M-R linker(EMMA) [11]
p20 connector R	acgtggctctcg <b>TCC</b> Agccgaggatcacctgtagg	
P21 mScarlet-NLS F	acgtggctctcg <b>TGGA</b> gaaacttttcgcttctcttggtc	mScarlet
p21 mScarlet-NES F	acgtggctctcg <b>TGGA</b> gactgtacgagtcagatccaac	
p21 mScarlet - R	acgtggctctcg <b>CAAC</b> atggtgagcaagggcgag	
p22 FOXO/NRF2-RE F	acgtggctctcg <b>GTTG</b> ggtgctttaccaacagtagccg	6xDBE-luciferase [24]/
p22 FOXO/NRF2-RE R	acgtggctctcg <b>TTCG</b> ggtaccgagctcttacgcg	pGL3-RE-NRF2-AmpR
p23 Ins F	acgtggctctcg <b>CGAA</b> ggccgcgaattctgaaagacc	Insulator-FB(EMMA) [11]
p23 Ins R	acgtggctctcg <b>CGT</b> Gtcaggcatgcgctagc	

Note: The name of Primer contains information of specific genetic parts and their corresponding positions in final vectors as shown in Fig. 1A. For example, 'p3 PolyA F' means forward primer (F) for generating the 'PolyA' part assigned to position 3. In the sequence of each primer, the BsaI site is highlighted in bold, where the 4 bp fusion sites (also for BsmBI) are in uppercases. Templates for PCRs are DNA parts from the EMMA kit, published plasmids, or home-modified constructs as indicated in the 'Templet' column.



# ***Chapter 7***

## **Summarizing discussion**

## Dissecting DNA damage and redox signaling upstream of p53

The tumor suppressor p53 is activated in response to various cellular stresses, including DNA damage and ROS. ROS, for instance hydrogen peroxide ( $H_2O_2$ ) derived from mitochondrial oxidative phosphorylation, is frequently cited as a major source of oxidative DNA damage [1, 2]. Indeed, exogenously-added  $H_2O_2$  induces both single-strand and double-strand DNA breaks and downstream DNA damage response (DDR) and p53 activation [3]. Therefore, p53 activation in response to ROS (e.g.,  $H_2O_2$ ) is often considered to be a result of DNA damage signaling. However,  $H_2O_2$ , as a second messenger in redox signaling, can also regulate protein activity directly through cysteine oxidation [4], and therefore independent of the DNA damage response (DDR). The engagement of multiple signaling pathways (e.g., redox signaling and the DDR) downstream of oxidants like  $H_2O_2$  makes it challenging to pinpoint by which of these mechanisms p53 activation is being achieved in response to an oxidative challenge that elevates cellular oxidants like  $H_2O_2$ . Furthermore, several DNA damaging agents that are widely used as chemotherapeutics in cancer, like Doxorubicin and Cisplatin, are associated with enhanced ROS generation and hence redox signaling [5, 6]. Redox signaling may actually contribute to their therapeutic effect, but because these compounds also trigger the DDR this is challenging to study. In **Chapter 3**, we show that it is possible to dissect the DDR and redox signaling downstream of  $H_2O_2$ , using carefully titrated Neocarzinostatin (NCS) (a DNA damaging agent) and diamide (a thiol oxidizing agent). Phosphorylation downstream of ATM/ATR is used as a readout for activation of the DDR, and redox signaling can be assessed by oxidation of the ultrasensitive HyPer7  $H_2O_2$  sensor and activation of the Stress Activated Protein Kinases (SAPKs) JNK and p38MAPK. Diamide treatment at a relatively low concentration only induces redox (oxidative) signaling without activation of the DDR, whereas NCS only induces the DDR without activation of redox signaling.  $H_2O_2$  indeed induces both the DDR and redox signaling.

Using this setup, we found that both DNA damage (NCS and  $H_2O_2$ ) and redox signaling (diamide and  $H_2O_2$ ) stabilized and activated p53, but through differential upstream kinases. As shown before ATM was indeed essential for p53 activation in response to NCS and  $H_2O_2$ -induced DNA damage signaling, whereas it was not involved in redox signaling-induced p53 activation. Redox signaling triggered by both diamide and  $H_2O_2$  activated JNK as well as p38MAPK. p38MAPK was required for diamide, but not  $H_2O_2$ , -induced p53 stabilization and activation. The simultaneous induction of ATM-dependent p53 activation by  $H_2O_2$  likely circumvents the requirement for p38MAPK. However, JNK inhibition did (partially) block  $H_2O_2$  induced p53 activation, similar to ATM inhibition. NCS induced DNA damage and subsequent p53 stabilization on the other hand is mediated by ATM only, without the requirement for JNK. This indicates that there is potential crosstalk between the ATM and JNK pathways to activate p53, specifically in response to oxidants, which needs to be further explored.

ATM has been reported to be activated through disulfide-dependent homodimerization upon oxidant treatment (i.e.,  $H_2O_2$  and diamide) in the absence of DNA damage [7]. In our



study, however, we found no evidence of diamide-induced ATM activation as judged by CHK2, H2AX and p53 phosphorylation in all cell lines tested. Still, we cannot exclude that oxidation-induced ATM activation depends on a specific cellular context.

## p53 regulation by redox signaling at multiple levels

Redox-regulated intermolecular disulfides can temporarily stabilize protein-protein interactions, and play key roles in redox signaling [8]. The p53 protein had been found to be a redox-sensitive protein that can be reversibly oxidized on cysteines such as C182 and C277 both in vitro and in cells upon specific oxidant treatment [9, 10]. Due to the nature of the differential alkylation-based protocol for the detection of reversibly oxidized cysteines, it was unclear whether p53 undergoes disulfide-dependent redox regulation and whether and how this would control p53 activity. In **Chapter 4**, we discover that p53 forms several intermolecular disulfide-dependent complexes with several regulatory proteins depending on C277.

The proteins that p53 forms intermolecular disulfides with include several of its well-known binding partners such as 14-3-3 $\theta$  and 53BP1, but previous studies did not assess the redox sensitivity of these interactions. We show that these proteins indeed also bind in a non-covalent manner, and that the disulfide greatly enhances the amount of these proteins pulled down in immunoprecipitation. This observation suggests that also in physiological situations the disulfide will stabilize these interactions. One could think of three possible outcomes of the disulfide-stabilized protein-protein interaction. (i) the disulfide strengthens the normal, electrostatic interaction and the regulatory protein has a prolonged or stronger effect on p53. (ii) the disulfide changes the conformation of the electrostatic interaction and temporarily blocks the regulatory effect of the binding partner on p53. (iii) the disulfide changes the conformation of the electrostatic interaction and provides an alternative regulatory function for p53, for instance by inducing a conformational change that leads to alternative transcriptional target selection. For example, 14-3-3 $\theta$  and 53BP1 have been shown to interact with p53 and positively regulate p53 transcriptional activity [11, 12]. The disulfide-dependent interactions between these proteins and p53 could possibly add an extra mechanistic regulation for selective transcriptional activation, for instance, by fine-tuning the p53 conformation so that it could recognize certain response element variants better than others. Indeed, C277 oxidation has been suggested to be implicated in selective transcriptional activation of specific response elements in the genes represented by p21 and GADD45a, depending on two distinct mechanisms [13, 14].

Even upon diamide treatment a large fraction of p53 does not partake in intermolecular disulfides and if these were absolutely required for the p53 regulation in response to oxidation, one would have expected more changes in transcriptional activity comparing p53 WT and the p53 C277S mutant. On the other hand, if these intermolecular disulfides would hamper p53 regulation, be it positive or negative, one would expect that this would result in evolutionary pressure to lose C277 [15]. The strong conservation of C277 among both

paralogs and vertebrate orthologs of human p53 that we observed therefore suggests that the intermolecular disulfides do fulfill a biological function.

Another explanation for a clear effect of the p53 C277S mutant could lie in the observations described in **Chapter 3**. The redox-dependent upstream activation of p53 by the ASK1/p38MAPK axis in response to diamide does not depend on (surface exposed and non-Zinc-binding) cysteines in p53 and hence could obscure any regulatory effects of intermolecular disulfide-dependent binding partners. Therefore, it would be interesting to examine whether blocking the p38MAPK pathway would expose potential consequences of p53 cysteine oxidation. The use of p53 overexpression in our studies facilitates immunoprecipitation and identification of binding partners by MS/MS, but certainly has limitations: the amount of p53 expressed may be exceeding the amount of binding partners present and obscures their regulatory effects. Introducing the C227S mutation in endogenous p53 by the CRISPR/Cas9 knock-in technique will allow us to study p53 protein regulation by redox signaling in a more robust and biologically related way than using a p53 overexpression platform. A comprehensive evaluation of gene expression profiling of p53 and the endogenous C277S mutant under oxidizing conditions, combined with the genetic knockout of specific binding partners would be a way to determine unequivocally whether and how redox regulation fine-tunes the p53 activity. The combined observations in **Chapter 3** and **Chapter 4** suggest that p53 can be regulated by redox signaling at multiple levels, including upstream redox signaling through the ASK1/p38MAPK axis and direct cysteine oxidation.

## **Reactivating p53 through redox signaling as a potential cancer therapy?**

In **Chapter 3**, we observed that redox signaling (i.e., diamide)-activated p53 induces significant cell death, suggesting that reactivating p53 by redox signaling in cancer cells would be a potential strategy for cancer therapy. As mentioned, several primary cancer therapies including chemotherapeutic drugs and irradiation induce DNA damage and one of their modes of action is the induction of p53-dependent cell death.

Some chemotherapeutic drugs like Doxorubicin and Cisplatin induce both the DDR and ROS. The data presented in **Chapter 3** provides evidence that redox signaling activates p53 and triggers p53-dependent cell death without causing collateral DNA damage, which would therefore limit mutation generation and consequent adverse effects in both healthy and tumor tissues. In line with our observations, several compounds with the aim to reactive p53 have been developed and exhibit promising effects against cancer outgrowth, and clinical trials are ongoing. Nultin-3 and its analogs stabilize p53 through inhibition of MDM2-dependent p53 degradation. APR-246, another p53-targeted drug, restores wild-type p53 function in misfolded p53. Interestingly, in light of **Chapter 4**, APR-246 binds covalently to p53 cysteines, partially Cys277 [16]. APR-246 also targets selenocysteine in thioredoxin reductase (TrxR) and impairs reductive power. It has been suggested that its anti-cancer potential can be attributed to the synergetic effects of reactivated p53 and redox stress.

Nevertheless, it remains to be addressed whether p38MAPK-p53 dependent cell death in response to oxidants is functional in various wild-type p53 expressing cancer cells and tumor models.

Chemotherapeutics like Doxorubicin and Cisplatin are obviously also used in p53 negative cancer: the lack of p53 impairs DNA damage repair and cell cycle arrest and cells proceed through cell cycle with severely damaged DNA and eventually die [17]. Since p53 is also involved in the cellular antioxidant response, it is not unthinkable that redox signaling/oxidant stress can function in a somewhat similar way: oxidant levels may rise further or be sustained in the absence of p53 and trigger cell death through other potential mechanisms. This is consistent with our observation in **Chapter 3** that diamide induces both p53-dependent and -independent cell death. It remains to be seen whether oxidants like diamide can also trigger cell death in the absence of DNA damage in p53 null tumors.

### Importance of monitoring the thiol redox state

In line with the previous finding that reversible oxidation of p53 was more induced by diamide than by  $H_2O_2$  [10], in **Chapter 4** we demonstrate that p53 forms intermolecular disulfide bonds in response to diamide, not  $H_2O_2$ , suggesting that diamide and  $H_2O_2$  have different targets. How oxidants find specific cysteines is one of the big questions in redox biology. The reactivity of most cysteines to for instance  $H_2O_2$  is not that high, and can be up to 5-6 orders of magnitude lower than that of cysteines in dedicated  $H_2O_2$  scavengers like peroxidases. This notion has led to the idea that oxidation of intrinsically unreactive cysteines by  $H_2O_2$  could be indirect and mediated by the transfer of oxidizing equivalents to target proteins in the so-called PRDX-relay mechanisms [18, 19]. A similar mechanism may be proposed for the action of diamide. The reactivity of cysteines with alkylating agents (nucleophilicity) correlates well with their redox sensitivity [20], meaning that at the concentrations used in our studies, it might be unlikely that diamide reacts directly with cysteines in p53 in the presence of highly abundant more reactive thiols. Indeed, Held et al.[10] observed that higher concentrations of diamide were needed to oxidize p53 in vitro as compared to in live cells. The thiol oxidizing agent diamide most likely targets GSH and peroxidases using GSH as a cofactor, or oxidized GSH (GSSG) itself could also act to oxidize cysteines in a redox relay-like manner. Diamide also targets the Trx system and thereby inhibits disulfide reduction, resulting in the accumulation of oxidized proteins [21]. Consistently, inhibition of the Trx system by Auranofin (AFN) also leads to p53 disulfide-dependent protein interactions, indicating that p53 oxidation occurs upon inhibition of the reductive system. Our observation also implies that different oxidants induce differential thiol oxidation profiles in a proteome-wide manner. Evaluation of the thiol redox state downstream of various oxidants is essential to understand the biological consequences of redox signaling. The development of advanced thiol-reactive chemical probes and combined Mass spectrometry techniques has enabled researchers to quantitatively monitor cysteinyl thiol redox state in a proteome-wide and site-specific manner in oxidant-challenged conditions as well as in fundamental

biological processes [20] [22, 23]. In **Chapter 5**, we evaluated two thiol-labeling methods: the BIAM-switch assay and the IAAyne-DADPS probe, both of which showed reasonable thiol-labeling results under certain conditions. Still, both labeling methods need to be further improved in order to be used successfully in our laboratory. For example, the IAAyne-DADPS method in our hands showed robust labeling for thiols in both recombinant proteins and cell lysates in both denaturing and native conditions, but with a relatively low labeling efficiency as compared to other studies [24]. More optimization of variables like labeling input, reagent concentrations and labeling specificity, etc., would certainly be worth the effort, eventually allowing us to precisely monitor thiol redox state in multiple biological systems. Within the context of this thesis, this method would not only aid in understanding how redox signaling is mediated downstream of specific oxidants, but also in finding which cysteines in the redox-dependent binding partners of p53 partake in the intermolecular disulfide. This knowledge will make it possible to design cysteine mutants of these binding partners to study the functional consequences of the redox-dependent interaction with p53.

### **Simultaneous visualization of multiple transcription factor activities**

p53 triggers various biological processes such as cell cycle arrest and apoptosis through transcriptionally activating target genes involved in these processes. In **Chapter 3**, we observe that both DNA damage and oxidative stress-induced p53 transcriptionally activate genes like p21, GADD45a and PIG3, and induces cell cycle arrest and cell death. However, the information on the timing and dynamics of p53 activation in response to these different signaling is lacking. The transduction of sensed extracellular stimuli and the translation into a specific cellular response activity is complex and could involve multiple TF activation in different timing and dynamics. Understanding which TFs are activated under what circumstances is important to uncover mechanistic regulation behind tumor initiation and progression and therapy response, but also to study fundamental cell biology. For example, similar to p53, FOXOs also exhibit tumor-suppressive functions by protecting cells from over-proliferation and genomic instability in response to stresses like DNA damage [25]. NRF2 is activated by oxidative stress and is essential for both maintaining redox homeostasis and supporting tumor cell survival by upregulating several antioxidant genes [26, 27]. HIF-1 $\alpha$  is activated in response to hypoxia and is essential to sustain the oxygen and metabolite supply, and its activation is triggered in growing tumors [28]. TFs like Myc and WNT/TCF are key regulators in promoting cell growth in physiological conditions, but their persistent increased activities lead to cell overgrowth and tumor formation [29, 30].

In **Chapter 6**, we describe the development of two fluorescence-based reporters that each can simultaneously determine the activity of 3 key transcription factors (TFs) (p53/Myc/FOXO<sup>NLS</sup> or TCF/HIF/NRF2<sup>NES</sup>). The reporters have been preliminarily assessed by transient expression in HEK293T cells and showed reasonable responsiveness to stimulating conditions or overexpression of the respective TF. More functional studies will be conducted in various systems by stably expressing the reporters through the PiggyBac transposon-

mediated genome integration. The different localization signals for each fluorophore potentially enable one to combine the two reporters and simultaneously monitor the activity of 6 TFs in a single cell. Notably, compared with techniques like single-cell RNAseq that only provides a fixed state of TF activity, our reporters will allow us to track the activity of TFs in live cells over time and possibly connect the observation to cell fate.

In conclusion, the work presented in this thesis mainly focuses on how redox signaling controls the tumor suppressor p53. Several observations were made that give credence to an important role for redox signaling in regulating p53 function. We uncovered that oxidants could activate p53 independent of, but also in synergy with DNA damage signaling. Importantly, our observation that redox signaling can activate p53 without inducing DNA damage and the downstream DDR, challenges the dogma that ROS-induced p53 activation is an indirect effect of oxidative DNA damage and emphasizes the importance of redox signaling in controlling p53 activity. We provide evidence that p53 can be regulated by redox signaling through multiple levels: upstream redox signaling that induces SAPK activation and oxidation of cysteines in p53 itself. For the first time, we show that p53 cysteine oxidation leads to the formation of intermolecular disulfide-dependent protein complexes with other regulatory proteins. It has been challenging to show a clear or distinct phenotype of redox-regulated p53. This may have several reasons. Redox signaling is not one pathway but controls, similar to kinase signaling, a myriad of protein activities downstream of H<sub>2</sub>O<sub>2</sub>. Exogenous oxidant treatment may be a good way to discover redox-sensitive proteins, but studying the phenotypic outcome of oxidation of a specific protein (e.g., p53) is hampered in this setup by the many signaling cascades that fire simultaneously. It is a bit as if one tries to study the effect of specific phosphorylation downstream of kinase signaling by activating all kinases simultaneously. Future experiments using induced and localized, low levels of H<sub>2</sub>O<sub>2</sub> like that has been done using the D-amino acid oxidase system [31] as well as CRISPR/Cas mediated construction of p53 cysteine mutants in the endogenous locus will likely give more insights on the biological roles of the here identified redox regulation of p53 tumor suppressor. It is definitely worth pursuing these experiments. Understanding redox control of p53 like described in this thesis and beyond helps to understand fundamental processes in cancer biology that may lead to new ideas for cysteine-directed anti-cancer therapies.

## References

1. Jackson S.P., Bartek J. The DNA-damage response in human biology and disease. *Nature*, 2009. 461(7267): 1071-1078.
2. Cadet J., Davies K.J.A., Medeiros M.H., et al. Formation and repair of oxidatively generated damage in cellular DNA. *Free Radic. Biol. Med.*, 2017. 107: 13-34.
3. Driessens N., Versteyhe S., Ghadhab C., et al. Hydrogen peroxide induces DNA single- and double-strand breaks in thyroid cells and is therefore a potential mutagen for this organ. *Endocr. Relat. Cancer*, 2009. 16(3): 845-856.
4. Sies H., Jones D.P. Reactive oxygen species (ROS) as pleiotropic physiological signalling agents. *Nature Reviews Molecular Cell Biology*, 2020. 21(7): 363-383.

5. Chen Y., Jungsuwadee P., Vore M., et al. Collateral damage in cancer chemotherapy: oxidative stress in nontargeted tissues. *Mol. Interv.*, 2007. 7(3): 147-156.
6. Yokoyama C., Sueyoshi Y., Ema M., et al. Induction of oxidative stress by anticancer drugs in the presence and absence of cells. *Oncol. Lett.*, 2017. 14(5): 6066-6070.
7. Guo Z., Kozlov S., Lavin M.F., et al. ATM activation by oxidative stress. *Science*, 2010. 330(6003): 517-521.
8. Putker M., Vos H.R., Dansen T.B. Intermolecular disulfide-dependent redox signalling. *Biochem. Soc. Trans.*, 2014. 42(4): 971-978.
9. Scotcher J., Clarke D.J., Weidt S.K., et al. Identification of Two Reactive Cysteine Residues in the Tumor Suppressor Protein p53 Using Top-Down FTICR Mass Spectrometry. *J. Am. Soc. Mass Spectrom.*, 2011. 22(5): 888-897.
10. Held J.M., Danielson S.R., Behring J.B., et al. Targeted quantitation of site-specific cysteine oxidation in endogenous proteins using a differential alkylation and multiple reaction monitoring mass spectrometry approach. *Mol. Cell. Proteomics*, 2010. 9(7): 1400-1410.
11. Falcicchio M., Ward J.A., Macip S., et al. Regulation of p53 by the 14-3-3 protein interaction network: new opportunities for drug discovery in cancer. *Cell Death Discovery*, 2020. 6(1): 126.
12. Cuella-Martin R., Oliveira C., Lockstone H.E., et al. 53BP1 Integrates DNA Repair and p53-Dependent Cell Fate Decisions via Distinct Mechanisms. *Mol. Cell*, 2016. 64(1): 51-64.
13. Buzek J., Latonen L., Kurki S., et al. Redox state of tumor suppressor p53 regulates its sequence-specific DNA binding in DNA-damaged cells by cysteine 277. *Nucleic Acids Res.*, 2002. 30(11): 2340-2348.
14. Augustyn K.E., Merino E.J., Barton J.K. A role for DNA-mediated charge transport in regulating p53: Oxidation of the DNA-bound protein from a distance. *Proc. Natl. Acad. Sci. U. S. A.*, 2007. 104(48): 18907-18912.
15. Marino S.M., Gladyshev V.N. Cysteine function governs its conservation and degeneration and restricts its utilization on protein surfaces. *J. Mol. Biol.*, 2010. 404(5): 902-916.
16. Zhang Q., Bykov V.J.N., Wiman K.G., et al. APR-246 reactivates mutant p53 by targeting cysteines 124 and 277. *Cell Death Dis.*, 2018. 9(5): 439.
17. Pestell K.E., Hobbs S.M., Titley J.C., et al. Effect of p53 status on sensitivity to platinum complexes in a human ovarian cancer cell line. *Mol. Pharmacol.*, 2000. 57(3): 503-511.
18. van Dam L., Pagès-Gallego M., Polderman P.E., et al. The Human 2-Cys Peroxiredoxins form Widespread, Cysteine-Dependent- and Isoform-Specific Protein-Protein Interactions. *Antioxidants*, 2021. 10(4): 627.
19. Stocker S., Maurer M., Ruppert T., et al. A role for 2-Cys peroxiredoxins in facilitating cytosolic protein thiol oxidation. *Nat. Chem. Biol.*, 2018. 14(2): 148-155.
20. Weerapana E., Wang C., Simon G.M., et al. Quantitative reactivity profiling predicts functional cysteines in proteomes. *Nature*, 2010. 468(7325): 790-795.
21. Pocsí I., Miskei M., Karanyi Z., et al. Comparison of gene expression signatures of diamide, H<sub>2</sub>O<sub>2</sub> and menadione exposed *Aspergillus nidulans* cultures—linking genome-wide transcriptional changes to cellular physiology. *BMC Genomics*, 2005. 6: 182.
22. Fu L., Li Z., Liu K., et al. A quantitative thiol reactivity profiling platform to analyze redox and electrophile reactive cysteine proteomes. *Nat. Protoc.*, 2020. 15(9): 2891-2919.
23. Xiao H., Jedrychowski M.P., Schweppe D.K., et al. A Quantitative Tissue-Specific Landscape of

Protein Redox Regulation during Aging. *Cell*, 2020. 180(5): 968-983.e924.

24. Rabalski A.J., Bogdan A.R., Baranczak A. Evaluation of Chemically-Cleavable Linkers for Quantitative Mapping of Small Molecule-Cysteine Reactivity. *ACS Chem. Biol.*, 2019. 14(9): 1940-1950.

25. Dansen T.B., Burgering B.M. Unravelling the tumor-suppressive functions of FOXO proteins. *Trends Cell Biol.*, 2008. 18(9): 421-429.

26. Brigelius-Flohé R., Flohé L. Basic principles and emerging concepts in the redox control of transcription factors. *Antioxid Redox Signal*, 2011. 15(8): 2335-2381.

27. Chan S.Y., Zhang Y.Y., Hemann C., et al. MicroRNA-210 controls mitochondrial metabolism during hypoxia by repressing the iron-sulfur cluster assembly proteins ISCU1/2. *Cell Metab.*, 2009. 10(4): 273-284.

28. Balamurugan K. HIF-1 at the crossroads of hypoxia, inflammation, and cancer. *Int. J. Cancer*, 2016. 138(5): 1058-1066.

29. Kelly K., Siebenlist U. The role of c-myc in the proliferation of normal and neoplastic cells. *J. Clin. Immunol.*, 1985. 5(2): 65-77.

30. Brantjes H., Barker N., van Es J., et al. TCF: Lady Justice casting the final verdict on the outcome of Wnt signalling. *Biol. Chem.*, 2002. 383(2): 255-261.

31. Bogdanova Y.A., Schultz C., Belousov V.V. Local Generation and Imaging of Hydrogen Peroxide in Living Cells. *Curr. Protoc. Chem. Biol.*, 2017. 9(2): 117-127.





# Appendices

## Nederlandse samenvatting

Dit proefschrift behandelt twee belangrijke aspecten: een literatuuroverzicht en twee mechanistische studies naar de redoxregulatie van p53 (**hoofdstukken 2, 3 en 4**) en technologische innovaties om redoxbiologie te bestuderen (**hoofdstukken 5 en 6**). Beide aspecten kunnen bijdragen aan het ontrafelen van de moleculaire mechanismen die ten grondslag liggen aan het behoud van homeostase, het ontstaan van de ziekten en de respons op therapie.

In **Hoofdstuk 2** geven we een overzicht van de literatuur over de regulatie van p53 door de DNA-schade en door redox-signalering. Vaak wordt aangenomen dat deze signaleringsroutes altijd gelijktijdig actief zijn. Wij bieden een perspectief op hoe deze routes zouden kunnen werken als afzonderlijke manieren om de activiteit van p53 te reguleren in termen van upstream kinase-activering (ATM, JNK of p38 MAPK), post-translationele modificaties (fosforylering of oxidatie) en de downstream transcriptionele respons (celoverleving of celdood).

In **Hoofdstuk 3** laten we zien dat het mogelijk is om de DNA-schaderespons (DDR)- en redox-signalering als reactie op  $H_2O_2$  te ontleden met behulp van zorgvuldig getitreerde Neocarzinostatine (NCS) (een DNA-beschadigend middel) en diamide (een thiol-oxidatiemiddel). Fosforylering door de kinases ATM/ATR wordt gebruikt om de activering van de DDR uit te lezen, en redox-signalering kan worden bestudeerd door middel van uitlezing van de oxidatie van de ultrasensitieve HyPer7  $H_2O_2$ -sensor en activering van de stressgeactiveerde proteïnekinasen (SAPK's) JNK en p38MAPK. Behandeling met diamide in een relatief lage concentratie induceert alleen redox (oxidatieve) signalering zonder activering van de DDR, terwijl NCS alleen de DDR induceert zonder activering van redox-signalering.  $H_2O_2$  induceert inderdaad zowel de DDR- als de redox-signalering. We demonstreren dat p53 wordt geactiveerd door redox- en DNA-schadesignalering via verschillende mechanismen. Redox-signalering activeert p53 voornamelijk via de p38MAPK-route, onafhankelijk van de ATM-afhankelijke DNA-schaderespons. Onze resultaten bieden een theoretische basis voor het idee dat inductie van oxiderende omstandigheden (waarschijnlijk door remming van reductievermogen) een strategie zou kunnen zijn om p53 te reactiveren als een behandeling voor typen kankercellen die wildtype p53 in verlaagde niveaus tot expressie brengen. Een voordeel in vergelijking met het gebruik van klassieke chemotherapeutica om DNA-schade te induceren als een trigger om p53 te reactiveren, is dat redoxafhankelijke activering geen DNA-schade veroorzaakt. Dit beperkt de opeenstapeling van mutaties in zowel gezond als tumorweefsel en voorkomt mogelijk de inductie van nieuwe oncogene laesies of

tumorprogressie en therapieresistentie.

Naast de regulatie van p53 door redox-signalering, is het al lang bekend dat cysteïnes in p53 zelf gevoelig zijn voor oxidatie. De protocollen die worden gebruikt om omkeerbare oxidatie in het algemeen te detecteren, kunnen het type oxidatieve modificatie niet identificeren. In **Hoofdstuk 4** beschrijven we dat p53 disulfide-afhankelijke interacties vormt met verschillende eiwitten in levende cellen, inclusief met bekende functionele regulatoren zoals 53BP1 en 14-3-3 $\theta$ . Deze interacties zijn afhankelijk van C277. Hoewel de C277-afhankelijke redox-modificaties geen dominante factoren zijn die bijdragen aan p53-activering, kunnen deze interacties mogelijk betrokken zijn bij het verfijnen van de transcriptionele activatie van p53 voor specifieke p53 doelgenen in reactie op redox-signalering zoals eerder voorgesteld. Een uitgebreide genexpressie-analyse in cellen die wildtype p53 of de endogene C277S-mutant tot expressie brengen onder oxiderende omstandigheden, gecombineerd met de genetische knock-out van specifieke bindingspartners, zou een manier zijn om te bepalen of en hoe redox-regulatie de p53-activiteit verfijnt. De gecombineerde waarnemingen in **Hoofdstuk 3** en **Hoofdstuk 4** suggereren dat p53 kan worden gereguleerd door redox-signalering op meerdere niveaus, waaronder redox-signalering via de ASK1/p38MAPK-as en directe cysteïne-oxidatie van p53 zelf.

In de afgelopen jaren zijn onderzoekers in staat geweest om zowel de cysteïne-reactiviteit kwantitatief uit te lezen en om cysteïne-oxidatieprofielen te identificeren in zowel fysiologische omstandigheden of na verschillende behandelingen met behulp van geavanceerde thiol-reactieve chemische sensoren en massaspectrometrie (MS)-gebaseerde technieken. Deze technologische innovaties gaven een diepgaand overzicht van proteoombrede cysteïne-oxidatieprofieling in fysiologische- en ziekteprocessen en dragen bij aan een beter begrip van de mechanismen van redox-regulatie van specifieke eiwitten bij specifieke cysteïnes. In **Hoofdstuk 5** evalueerden we twee thiol-labeling methoden: de BIAM-switch assay en de IAAyne-DADPS probe, die beide redelijke thiol-labeling resultaten lieten zien onder bepaalde omstandigheden. Toch moeten beide methoden verder worden verbeterd om met succes in ons laboratorium te kunnen worden gebruikt. De IAAyne-DADPS-methode toonde in onze handen bijvoorbeeld robuuste markering voor thiolen in zowel recombinante eiwitten als cellysaten in zowel denaturerende als natuurlijke omstandigheden, maar relatief een klein aantal eiwitten was gemarkeerd in vergelijking met andere onderzoeken. Meer optimalisatie van variabelen zoals markeringsinput, concentraties van reagentia, markeringsspecificiteit, enz., zouden zeker de moeite waard zijn, waardoor we uiteindelijk de thiol-redoxtoestand in meerdere biologische systemen nauwkeurig zouden kunnen volgen. Binnen de context van dit proefschrift zou deze methode niet alleen bijdragen aan het begrip van hoe redox-signalering als gevolg van specifieke oxidanten wordt gemedieerd, maar ook om uit te vinden welke cysteïnes in de redox-afhankelijke bindingspartners van p53 deelnemen aan de intermoleculaire disulfidebrug. Deze kennis zal het mogelijk maken om cysteïnemutanten van deze bindingspartners te ontwerpen om de functionele gevolgen van

de redox-afhankelijke interactie met p53 te bestuderen.

De transductie van waargenomen extracellulaire stimuli en de vertaling naar een specifieke cellulaire responsactiviteit is complex en kan de activering van meerdere transcriptiefactoren met verschillende tijdschalen en dynamiek betreffen. Begrijpen welke transcriptiefactoren onder welke omstandigheden worden geactiveerd, is belangrijk om mechanistische regulatie achter tumorinitiatie en -progressie en therapierespons te ontdekken, maar ook om fundamentele celbiologie te bestuderen. Bijvoorbeeld, vergelijkbaar met p53, vertonen FOXO transcriptiefactoren ook tumoronderdrukkende functies door cellen te beschermen tegen overproliferatie en genomische instabiliteit als reactie op stress zoals DNA-schade. NRF2 wordt geactiveerd door oxidatieve stress en is essentieel voor zowel het handhaven van de redoxhomeostase als het ondersteunen van de overleving van tumorcellen door de activering van verschillende antioxidantgenen te reguleren. HIF-1 $\alpha$  wordt geactiveerd als reactie op hypoxie en is essentieel om de zuurstof- en metaboliettoevoer in stand te houden. Deze transcriptiefactor wordt vaak geactiveerd bij groeiende tumoren. Transcriptiefactoren zoals Myc en WNT/TCF zijn belangrijke regulatoren bij het bevorderen van celgroei in fysiologische omstandigheden, maar hun aanhoudende verhoogde activiteit leiden tot teveel celgroei en tumorvorming. In **Hoofdstuk 6** beschrijven we de ontwikkeling van twee op fluorescentie gebaseerde reporters die elk tegelijkertijd de activiteit van 3 belangrijke transcriptiefactoren (p53/Myc/FOXO<sup>NLS</sup> of TCF/HIF/NRF2<sup>NES</sup>) kunnen weergeven. De reporters zijn voorlopig getest door ze kortdurend tot expressie te brengen in HEK293T cellen en vertoonden een redelijke respons op stimulerende omstandigheden of overexpressie van de respectievelijke transcriptiefactor. Meer functionele studies zullen in verschillende systemen worden uitgevoerd door de reporters stabiel tot expressie te brengen via PiggyBac transposon-gemedieerde genoomintegratie. De verschillende lokalisatiesignalen voor elke fluorofoor maken het mogelijk om de twee reporters te combineren en tegelijkertijd de activiteit van 6 transcriptiefactoren in een enkele cel te volgen. Met name, vergeleken met technieken zoals single-cell RNA-sequencing waarmee alleen de activiteit van een transcriptiefactor op een bepaald moment uitgelezen kan worden, zullen onze reporters het mogelijk maken om de activiteit van transcriptiefactoren in levende cellen in de loop van de tijd te volgen en mogelijk de observatie te koppelen aan het gedrag van de cel.

# Acknowledgement

Time flies! I can't believe five years of my PhD journey are approaching the end. Look back to this journey, there were moments full of excitement, inspiration, and achievement, but also the moments with frustration, confusion and self-denial. I believe, because of all of these uncertainties and surprises, this journey has always been so special and unique. I am glad that I made it! I am so grateful that I could meet the most wonderful and cutest people in the world during this journey. From the bottom of my heart, I want to express sincere thanks to all of you who have helped, supported, believed, cared, and loved me in this journey.

**Tobias**, I am so lucky and grateful to have a supervisor like you during my PhD study. Endless thanks for your time, enthusiasm, motivation, and patience to help me process all research projects and revise papers and thesis. I could not have accomplished my PhD without your help. I truly appreciate that you give me complete independence to think and perform all research programs. Your rigorous academic attitude, immense knowledge, scientific brainstorming, critical thinking, self-discipline and hard-working have been deeply inspired me. I am also impressed by your cooking skills and sports spirits. It was definitely fun to play Ping pong and speak Chinese with you. Hope you will get better and better. In the end, I wish all the best for you, your family and the lab!

**Boudewijn**, an enormous gratitude for you and Tobias to adopt me after my previous lab left and provide me such a wonderful platform to continue my PhD study. Thanks for your critical questions and valuable input in work discussions and manuscript writing. It is such a big surprise but also an inspiration for me that scientists like you are still performing experiments in the lab. Best wishes for you!

**Paulien**, my roommate, team partner, and best friend all the time! I can't imagine what my PhD life would be like without you around. First of all, many manyyyyy thanks to you for being my guide not only for the labs but also for the whole Netherlands. It was absolutely a great experience to work with you especially later of my PhD. I truly appreciate all the help and efforts you put into the projects we have worked on. I could not have done all the work this fast without your help. Also, thanks for being my Paranymp and taking such good care of my thesis. I know having three jobs (mom of two boys, technician and firefighter) at the same time is definitely not easy, but you made everything perfectly organized and progressed. I am so proud of you. Best wishes for you and your family, always! **Nguyen**, tough girl! Thanks a lot for being my Paranymp. It was a lovely time to hang out with you to try some Chinese and Vietnamese food. I wish we could have done more! BTW, don't put so hard on yourself. You know you already did a terrific job. Good luck with your PhD.

**Group Dansen:** I am thankful that I didn't miss the time to be a colleague of you guy's. **Sasha**, it has been a wonderful time to work and talk with you. You are such a talented scientist and a wonderful person. Good luck with your career. I wish all the best for you. **Loes**, tough girl! How amazing it is to have a person like you in the group. You are smart, creative, and always bring brilliant ideas for your project and Theme borrels. I love them so much. Good luck with your career and life. **Marc**, best bioinformatician ever! Thank you so much for assisting me with R programming and many other computer stuff. I believe, your intelligence, coolness and hard-working will make you a successful PhD student as well as a scientist. **Daan**, I always appreciate the work you have done for our paper. It was a lovely time to have coffee, talk and joke around with you. I am looking forward to your big achievements. Good luck!

**Roommates: Marlies**, another tough girl! You always look happy, energized and motivated. Thanks for spreading your positive power to everyone around you. You deserve what you have gained and you will deserve more! Good luck with your thesis. I believe it will be a really good one. Many thanks for translating the dutch summary, you totally saved my life. And you are the best roommate ever! **Lieke**, So are you! it is really nice to meet you and have those deep talks with you. Good luck with your master's study and future.

**MS experts: Harmjan**, it was a great chance for me to learn the Mass spectrometry (MS) technique from you. Thank a lot for your hard thinking and pivotal advice for the proteomics projects, as well as for guiding me through the MS data analysis. It was a lot of fun to talk with you. Best wishes to you and your family. **Robert**, thanks a lot for conducting MS experiments for me. Also, it was super fun to joke around with you. You know you are a funny guy. Hope you will get your big house soon!

**PIs: Fried, Yvonne, Maria, Peter, Jurian**, I would like to express my true thankfulness to all of you for your hard questions and valuable comments during every work discussion and meeting, which greatly aided in improving my research to a higher level. **Cristina**, thanks a lot for arranging all the documents for the PhD program and my stay in the Netherlands as well as organizing all kinds of meetings and conferences for us. **Tianshu (天书)**, my first Chinese colleague in the Netherlands. It was a lot more comfortable to discuss experiments with you in Chinese. Congratulations on your publications. Good luck with your thesis writing and defense. **Lydia, Miranda, Ingrid and Livio**, thank you guys so much for taking such good care of lab materials and facilities, which ensures a pleasant working environment for us and dramatically improves our work efficiencies. **Mojtaba**, always been eager to learn Mass cytometry from you. **Sara, Susan and Denis**, really nice to meet your girls. Good luck with your work. **Marjoleine, Cheuk and Marcel**, thanks for arranging and distributing our lab orderings.

**Lisa**, congratulations on your defense. I have always enjoyed chatting with you in the coffee corner, tissue culture lab, all kinds of borrels, PhD retreats as well as Masterclasses. Good luck with your postdoc. **Diana**, I still remember the delicious deserts from your grandma. It was a great time to collaborate with you on the p53 project. Can't wait for the story out. Good luck with your publications and thesis. **Maria**, always remember the good times we spent together in retreats, classes and Spetses. Wish all the best for you. **Tom**, you are such a kind and caring person. I always admire your courage and optimism to move your life forward. Good luck with your job. **WJ**, you are a very interesting person who has very interesting ideas. I enjoyed a lot talking with you. Best wishes! **Mathijs and Stephen**, I really enjoyed talking with your guys. Good luck with your projects and PhD.

**Former labmates: Marten, Jose, Maaïke, and Bram**, it was nice to know you guys. Thank you all for helping me out with some experiments and data analysis.

**To all MCR fellows**, thank you all for creating a cheerful and comfortable working vibe. Thank for the people who have provided me practical assistance and theoretical input for my research. **ICT group**: Marc and Dik, I appreciate your skills and patience in solving all the wired problems I encountered for my laptop.

**Willem**, I am so grateful that you could pick up Xiaogang and me from the Schiphol airport very early in the morning on the day we just arrived in the Netherlands and gave us a little tour of Uithof while it was raining. I also would like to express my big thanks to you for thinking of and introducing me to Boudewijn after my previous lab moved. I always remember those lovely times you invited us for dinners, the museum tour as well as the light show with your family in Amsterdam. All in all, thank you for being so kind and caring for us. Wish all the best to you and your family. **Maya and Martijn**, you guys are very cute couple. Thanks for inviting us to Christmas dinners and other fun activities. I wish all the best for you guys!

**Hospital team**: happy to meet you guys in the Netherlands and learn more about Chinese medicine. **John( 闰 月 ) Huang**, so impressed by your open minds and social skills. **Maojie( 茂杰 )**, congrats for being a daddy! It was so much fun to work with you in the lab and playing Ping pong in the gym. Good luck with your publications. **Sophie( 艳 娟 )**, it was a relatively short time to work with you, but like your unordinary mindsets on science, politics and society. **Lily( 丽 )**, love your casual attitudes toward life and science. Enjoy shopping with you. **Lipeng( 丽 鹏 )**, it was a hard time to stay in the Netherlands upon the outbreak of Covid-19, but you made it. **Huanjie( 幻杰 )**, good luck with your PhD study in the Netherlands.

**To my Friends: Bohui ( 伯 会 ) and Weiyang ( 卫 阳 )**, I always admire the way how you

guys keep both work and life forward. I can imagine there are difficult times, but every time we see **Yichen** ( 意 诚 ) who is so lovely and cute, I just know everything you have done is worth it. Plenty of thanks for your kind and warm hospitality, chatting with you guys and commenting on the things of our interest is definitely one of the most wonderful times for us in the Netherlands. Hope everything goes well for you in China. See you guys soon. **Xin**( 欣 哥 ), the most fabulous mathematician I have ever seen. Looking forward to your success. **Linglei** ( 菱 蕾 师 姐 ), profoundly impressed by your positivity and motivation. Thanks for sharing information and news about work and life with us, which makes our life in the Netherlands a lot easier. Good luck with everything in the US. **Jingwen**( 静 文 姐 ), I will never forget your 酸菜鱼 , everything is excellent. I believe your PhD work will be just as excellent as your 酸菜鱼 . Wish you get your PhD very soon! **Juntao**( 俊 涛 ), **Qiangbing**( 强 兵 ) and **Yaobing**( 姚 冰 ), so nice to meet you guys. It was so much fun to play table games with you guys. You guys are smart and hard-working and I believe you all will end up your PhD with beautiful papers. Good luck! **Yingnan**( 颖 楠 ) and **Lijun**( 丽 君 ), so happy to be able to reunite with you guys in Europe. Wish everything goes following your own heart. We will see each other one day in China!

**Xiaogang**, my best friend. Thank you for always being there for me. Celebrate and share good news with me, support and encourage me during difficult times. You are one of the most incredible people in the world I have ever seen. You should and will gain what you have paid. I am so proud of you, so are you!

Thank China Scholarship Council (CSC) for providing financial support for my PhD study in the Netherlands.

Last but not least, I would like to give my tremendous thanks to my family. 感谢爸爸妈妈一直以来对我生活无微不至的照顾, 对我学业的支持和鼓励, 永远做着我坚强的后盾, 让我有机会走向更高更远的梦想境地。感谢哥哥嫂子对父母的悉心照顾, 让我能够在异国他乡追梦时, 勇往直前, 没有后顾之忧。感谢小侄儿石瑾一的到来, 给我们家带来独一无二的欢乐, 也让我们在压抑黑暗的疫情时期对生活依然充满希望, 感受生命的强大和美好。感谢爷爷奶奶和所有亲戚朋友一直以来对我的关爱与照顾。In the end, I wish all the people who I love and who love me healthy and happy all the time.

Utrecht Medical Center  
乌特勒支医学中心

Autumn in 2021  
秋

## Thesis related publications

**Shi, T.**, Polderman, P.E., Pagès-Gallego, M., van Es, R.M., Vos, H.R., Burgering, B.M.T., Dansen, T.B. p53 Forms Redox-Dependent Protein–protein Interactions through Cysteine 277. *Antioxidants* 2021, 10(10), 1578.

**Shi, T.**, van Soest, D., Polderman, P. E., Burgering, B., & Dansen, T. B. DNA damage and oxidant stress activate p53 through differential upstream signaling pathways. *Free radical biology & medicine*.2021, 172, 298–311.

**Shi, T.**, Dansen, T. B. Reactive Oxygen Species Induced p53 Activation: DNA Damage, Redox Signaling, or Both?. *Antioxidants & redox signaling*. 2020, 33(12), 839–859.



## *Curriculum Vitae*

Tao Shi was born on 22nd of April in 1992, Dingxi city, Gansu province, China. She was raised in China. From 2009 to 2013, she did her bachelor study in Northwest A&F University, China, majoring in Animal Science, where she was awarded three times of national scholarship and excellent undergraduate. In 2013, she was selected as an examination-free candidate to continue her study as a master student at the same university. From 2013 to 2016, she performed her master study in the lab of Pro. Dr. Hong Chen, where she did screenings on genetic variations (e.g, SNPs and CNVs) occurred within different populations of Chinese cattle and aimed to understand their association with growth traits. After that, she was fascinated by discovering new things in science and decided to presume a PhD degree in life science. From 2016 to 2021, she did her PhD research in the lab of Pro. Dr. Boudewijn Burgering and Dr. Tobais Dansen at the Department Molecular Cancer Research, University Medical Center Utrecht, the Netherlands, where she mainly focused on understanding how tumor suppressor p53 was regulated in response to different cellular signaling, such as DNA damage and redox signaling. This thesis covers all the research work she has done during her PhD.

If you don't play, you can't win.

— Judith McNaught